SERVICIO NACIONAL DE GEOLOGÍA Y MINERÍA - CHILE
BOLETIN No. 63 2009

LAGUNA DEL MAULE VOLCANIC FIELD: Eruptive history of a Quaternary basalt-to-rhyolite distributed volcanic field on the Andean rangecrest in central Chile

Wes Hildreth[1], Estanislao Godoy[2], Judy Fierstein[1], Brad Singer[3]

[1] U.S. Geological Survey, MS-910, Menlo Park, California 94025, USA.
hildreth@usgs.gov
jfierstn@usgs.gov
[2] SERNAGEOMIN, Santiago, CHILE. Now at Departamento de Proyectos de Riego, DOH, Ministerio de Obras Públicas.
estanislao.godoy@mop.gob.cl
[3] University of Wisconsin, Madison, Wisconsin 53706, USA.
bsinger@geology.wisc.edu

LAGUNA DEL MAULE VOLCANIC FIELD: ERUPTIVE HISTORY OF A QUATERNARY BASALT-TO-RHYOLITE DISTRIBUTED VOLCANIC FIELD ON THE ANDEAN RANGECREST IN CENTRAL CHILE

FALLAS CUATERNARIAS EN CHILE

BOLETÍN No. 63, 2009
Inscripción No. 187.200
ISSN 0020-3939

Director Nacional: Alejandro Vio G.
Subdirector Nacional de Geología (P): Waldo Vivallo S.

Jefe de Publicaciones: Manuel Suárez D.
Encargada de Publicaciones: Soraya Amar N.
Diagramación: Nancy Espinoza P.

Referencia Bibliográfica:
Hildreth, W.; Godoy, E.; Fierstein, J.; Singer, B. 2009. Laguna Del Maule Volcanic Field: Eruptive history of a Quaternary basalt-to-rhyolite distributed volcanic field on the Andean rangecrest in central Chile. *Servicio Nacional de Geología y Minería, Boletín,* 63: 143 p. Santiago.

Portada:

Fotografía:

Tiraje: 1.000 ejemplares

Impreso por:

CONTENT

FIGURES

TABLES

APPENDIXES

Laguna del Maule Volcanic Field: Eruptive history of a Quaternary basalt-to-rhyolite distributed volcanic field on the Andean rangecrest in central Chile

Wes Hildreth
Judy Fierstein
Estanislao Godoy
Brad Singer

ABSTRACT

The Laguna del Maule (LdM) volcanic field, which surrounds the 54-km² lake of that name, covers ~500 km² of rugged glaciated terrain with Quaternary lavas and tuffs that extend for 40 km westward from the Argentine frontier and 30 km north-south from the Río Campanario to Laguna Fea. The distributed rear-arc volcanic field is contiguous with the Tatara-San Pedro stratovolcano complex on the volcanic front of the Quaternary Andean arc. The LdM field has had few large edifices but at least 130 separate vents have been identified, from which >350 km³ of products have erupted since 1.5 Ma. Products of 14 ice-ravaged (early and middle Pleistocene) stratocones and shields, and of ~115 monogenetic cones, domes, and lava flows, were mapped on foot, studied petrographically, and chemically analyzed. More than 70 radiometric ages were determined to calibrate the eruptive sequence. A large welded ignimbrite erupted at 1.5 Ma and was followed by another at ~950 ka, producing a 12 x 8 km-wide caldera that underlies the north half of the lake basin and rugged highlands north of it; outside the caldera, the south half of the basin is an erosional feature cut on Tertiary andesites and dacites.

A ring of 36 postglacial rhyolite and rhyodacite coulees and domes that erupted from 24 separate vents (and together cover ~100 km²) encircles the lake. The large number of postglacial silicic vents surrounding the basin, a general progression from rhyodacites to rhyolites, narrow compositional arrays, and scarcity of mafic enclaves in the rhyolites are features that suggest growth of a latest Pleistocene to Holocene magma reservoir beneath the basin. One rhyolite coulee (23.3±0.4 ka) blocked the lake outlet, impounding a lake 200 m higher than today, resulting in a single sharp high strandline that rings the basin and, just downstream from the gorge reamed by the outbreak flood, radial boulder bars, plunge pools, and a scoured lava-plateau scabland. In addition to the many postglacial silicic units, glacially eroded silicic lavas yield ages of 3.7, 2.5, 2.4, 2.0, 1.6, and 1.35 Ma, and 924, 880, 712, 695, 680, 460, 335, 240, 203, 115, 97, 83, and ~38 ka, providing evidence of a prolonged history of potentially explosive silicic eruptions from vents scattered throughout the volcanic field.

For the LdM field, 425 analyses define an array continuous from 49% to 77.6% SiO_2, medium-K toward its mafic end (1.5% K_2O @ 55% SiO_2) but high-K at its silicic end (4.5% K_2O @ 75% SiO_2). Quaternary eruptive units include 4 basalts, 28 mafic andesites (52-57% SiO_2), 33 andesites, 11 dacites (63-68% SiO_2), 23 rhyodacites, 21 rhyolites (>72% SiO_2), and 6 ignimbrites (andesitic to rhyolitic). None of the basalts is primitive and, as for continental-arc magmas globally, virtually all the mafic rocks display petrographic and chemical evidence for diverse crustal contributions. Production of distributed rhyolites throughout the long history of the volcanic field makes this intensively true here. A range of parental magmas is inferred, but there is little evidence for enriched intraplate mantle contributions nor for an eastward decrease in mantle melt fraction across the 50-km-wide Quaternary arc-volcanic zone. All products, basalt-to-rhyolite, carry strong arc-type geochemical signatures. Numerous trace-element indicators exhibit wide ranges but no systematic across-arc trends, except Ba/Nb, which declines eastward, suggesting a slight weakening of the slab signature inboard.

Keywords:

RESUMEN

El campo volcánico Laguna del Maule (LdM) rodea al lago homónimo de 54-km², cubriendo un área de ~500 km² de accidentado terreno glaciado, compuesto por lavas y tobas cuaternarias que se extienden por 40 km al oeste de la frontera con Argentina y por 30 km en dirección N-S desde el Río Campanario hasta Laguna Fea. El extenso campo trasarco es contiguo al complejo estrato-volcánico Tatara-San Pedro del frente volcánico del arco Cuaternario Andino. El campo LdM ha tenido pocos edificios mayores pero >250 km³ de productos han hecho erupción en los últimos 1,5 Ma desde los al menos 130 centros de emisión aquí identificados. Se ha cartografiado a pie, estudiado petrográficamente y analizado químicamente los productos de 14 estratoconos y escudos del Pleistoceno temprano a medio, devastados por el hielo, junto a ~115 conos, domos y flujos de lava monogenéticos. La secuencia eruptiva fue calibrada mediante más de 70 dataciones radiométricas. A una gran ignimbrita soldada que hizo erupción hace 1,5 Ma siguió otra de ~950 ka asociada a una caldera de 12 x 8 km, la cual subyace a tanto la mitad norte del lago como a los escarpados cerros al norte de él; fuera de la caldera, la mitad sur de la cuenca es un rasgo erosivo inciso en andesitas y dacitas cenozoicas.

El lago está rodeado por un anillo de 36 'coulees' y domos post-glaciales tanto riolíticos como riodacíticos que hicieron erupción desde 24 centros de emisión separados y que cubren un área de ~100 km². El gran número de centros de emisión silícicos post-glaciales que rodea la cuenca, la progresión general desde riodacitas a riolitas, el angosto abanico composicional y los escasos enclaves máficos en las riolitas son rasgos que sugieren el crecimiento de un reservorio magmático Tardi-Pleistoceno a Holoceno bajo la cuenca. Una coulee riolítica (23,3±0,4 ka) obstruyó el desagüe del lago, represándolo 200 m más alto que hoy, la cual originó primero una marcada y única línea de costa que rodea todo el lago y luego, aguas debajo de la garganta escariada por inundación post-ruptura, barras radiales de bolones, piletas de desplome ('plunge pools') y una meseta de lava formada por chorros de agua abrasivos o 'scabland'. A las numerosas unidades silícicas post-glaciales se suman lavas silícicas con erosión glacial que dan edades de 3,7, 2,5, 2,4, 2,0, 1,6 y 1,35 Ma y 924, 880, 712, 695, 680, 460, 335, 240, 203, 115, 97, 83 y ~38 ka, lo cual pone en evidencia una prolongada historia de erupciones silícicas potencialmente explosivas desde centros de emisión dispersos a través del campo volcánico.

425 análisis de muestras en el campo LdM definen un abanico continuo desde 49% a 77,6% SiO_2, K-medio hacia su extremo máfico (1,5% K_2O @ 55% SiO_2) pero de alto K en su extremo silícico (4,5% K_2O @ 75% SiO_2). Las unidades eruptivas cuaternarias incluyen 4 basaltos, 28 andesitas máficas (52-57% SiO_2), 33 andesitas, 11 dacitas (63-68% SiO_2), 23 riodacitas, 21 riolitas (>72% SiO_2) y 6 ignimbritas (andesíticas a riolíticas). Ninguno de los basaltos es primitivo y, tal como ocurre globalmente en magmas de arcos continentales, virtualmente todas las rocas máficas muestran evidencias petrográficas y químicas de contribuciones corticales diversas. Esto es aún más claro en este caso, debido a la producción de riolitas distribuidas a lo largo de la larga historia del campo volcánico. Se infiere un rango de magmas parentales, pero hay escasa evidencia tanto de contribuciones de un manto intraplaca enriquecido como de una disminución hacia el oriente de fracción de fundido mantélico a través de los 50 km de ancho en esta sección del arco volcánico Cuaternario. Todos los productos, desde basaltos a riolitas, poseen una fuerte marca geoquímica de tipo arco. Numerosos indicadores de elementos traza muestran tendencias de amplio rango, pero no-sistemáticas, a través del arco, excepto la razón Ba/Nb, la cual disminuye hacia el oriente y sugiere un leve debilitamiento de la marca de placa subducida hacia el trasarco.

Palabras clave:

INTRODUCTION

Straddling the Andean rangecrest (Figs. 1, 2), the Laguna del Maule (LdM) volcanic field is the superlative site of postglacial silicic volcanism in the Andean Southern Volcanic Zone (SVZ). No fewer than 36 postglacial eruptions from 24 vents surrounding the 9-by-11-km lake basin have produced rhyolite and rhyodacite lava flows, most or all of them accompanied by pumice falls. Although silicic volcanism has been recurrent here throughout the entire Quaternary, the abundance and frequency of rhyolitic eruptions in the postglacial interval appears to be unprecedented.

This distributed rear-arc volcanic field has few large edifices but at least 130 independent Quaternary vents, from which more than 350 km^3 of products have erupted since 1.5 Ma. Blanketing ~500 km^2 of rugged glaciated terrain with Quaternary lavas and tuffs, the field **laps** slightly into Argentina and extends 40 km west of the border and 30 km south from the Río Campanario to beyond Laguna Fea (Fig. 1). Although its products range from basalt-to-rhyolite, the LdM area can be considered a coherent volcanic field on account of **(1)** the high spatial density of its distributed Quaternary vents, in abrupt contrast to vent-poor surrounding areas, **(2)** the scattering of numerous eruptive sites throughout the field persistently for at least 1.5 Myr, **(3)** unbroken continuity (from 49 to 77% SiO_2) of tight compositional arrays for its multi-vent eruptive products, and **(4)** recurrent eruption of rhyolite, restricted regionally to only a few centers but widespread throughout the LdM field.

This report is the first attempt to assemble a comprehensive chronological and compositional eruptive history of the Laguna del Maule Quaternary volcanic field. Previous geological work on the volcanic field is limited to reconnaissance maps by González and Vergara (1962), Drake (1976), and Muñoz and Niemeyer (1984) and petrological-chemical reconnaissance by Munizaga (1978) and Frey *et al.* (1984). Our work entailed 121 field days spread over ten summer seasons (1984-2000), largely on foot but twice using an inflatable zodiak to camp at the south shore of the lake. We consider this report to be a detailed reconnaissance, limited by our backcountry backpack and bivouac mode of operation; many multi-flow edifices warrant more intensive sampling. Contacts were mapped in the field on the 1:50,000 topographic sheets Baños Campanario, Laguna del Maule, Paso Pehuenche, and Río Melado, published by the Instituto Geográfico Militar. Aerial photographs were amusing and suggestive but seldom of value for detailed work in glaciated terrain. Grid references to site locations mentioned in the text are simplified to 100 m using the Universal Transverse Mercator (UTM) grid, which is shown on the IGM topographic maps of the area. The first three digits are easting, and the second three are northing. For example, the dam at the outlet of Laguna del Maule would be approximated as 599/135; *i.e.*; 59.9 km east, 13.5 km north.

In the following discussion, we take the base of the Quaternary to be 2.6 Ma (Morrison and Kukla, 1998; Ogg, 2004; Pillans, 2004; Gibbard *et al.*, 2009). The boundaries between early, middle, and late Pleistocene are now generally agreed to be ~780 ka and ~126 ka (Gradstein *et al.*, 2004). Volcanic-rock nomenclature in this paper is kept simple, based principally on SiO_2 contents. Basalt has 47-52% SiO_2, basaltic or mafic andesite 52-57%, andesite 57-63%, dacite 63-68%, rhyodacite 68-72%, and rhyolite >72% SiO_2. For reasons of convenience or uncertainty, we commonly use the terms mafic to lump basaltic andesite with basalt, intermediate for andesite-dacite, and silicic for rhyodacite and rhyolite. The common phenocryst minerals clinopyroxene and orthopyroxene are usually abbreviated as cpx and opx. All eruptive units discussed in this report are named and assigned a (generally 3-letter) unit label; these are listed alphabetically within five major age groupings in Appendix 1, which provides concise characterization of each unit. To determine $^{40}Ar/^{39}Ar$ ages, incremental heating experiments were done on 47 samples, resulting in 41 plateau ages; six samples failed to yield a plateau (Table 1). In addition, conventional K-Ar ages were determined for another 27 samples (Table 2).

FIG. 1. Location map showing setting of Laguna del Maule (LdM) study area, southeast of regional capital city Talca. Chile-Argentina border is continental divide and rangecrest of Andean Cordillera. Santiago, Rancagua, Curicó, Talca, and Chillán are cities along axis of Chilean Central Valley. Constitución lies at mouth of Río Maule, which drains from Laguna del Maule via Talca through Coastal Cordillera to Pacific Ocean. Malargüe is nearest city eastward, situated at transition from cordillera to pampas. Selected Quaternary stratovolcanoes are marked by Δ symbol. Four shaded fields indicate north-trending belt of Quaternary volcanic fields atypically enriched in silicic eruptive units. See figure 2 for sense of rugged, sparsely inhabited, mountainous terrain around Laguna del Maule.

REGIONAL SETTING

The rear-arc LdM volcanic field is centered ~330 km east of the trench axis, 200 km from the coast, ~130-150 km above the Benioff zone, and 40-50 km above the continental Moho (Campos *et al.,* 2002; Yuan *et al.,* 2006; Gilbert *et al.,* 2006; Heit *et al.,* 2008). The field just overlaps the continental divide, which is here the international border. The rugged terrain (Fig. 2) is treeless high desert with sparse shrubs and bunchgrass, snow-covered much of the year, and now largely ice-free, though it was ice-scoured during several Pleistocene glacial episodes. Elevations are generally 2,500-3,100 m around the rim of the Laguna del Maule basin, ~2,160 m at lake level, and up to 3,943 m at Cerro Campanario. Sparsity of vegetation reflects the elevation, dry summers, ubiquitous volcanic screes, and windscour by a veneer of sandy or pumiceous fallout constantly remobilized by the prevalent rangecrest winds.

A lone gravel road (open only in summer) follows the Río Maule (Fig. 1), skirts the north shore of the lake, and crosses Paso Pehuenche into Argentina. Although a few rural settlements intervene, the nearest cities are Talca to the west and Malargüe to the east, each ~140 km by road from the lake. Customs entry stations are at La Mina (Chile) and Las Loicas (Argentina), each ~40 km from the lake. At the outlet of the Río Maule, Laguna del Maule is today impounded by a small dam, which only slightly enlarges the 54-km^2 natural lake, regulates its level seasonally, and is cited as a point of reference throughout this paper. The volcanic field and a large surrounding region are otherwise roadless and lack year-round habitation. Valley floors support perennial streams and scattered wet vegas used for centuries by transhumant herdsmen for grazing livestock. Likewise only in summer (when the otherwise snowbound road is open), police and agricultural officers are stationed near the outlet of the lake, which today attracts modest numbers of fishermen and vehicular tourists. A small crew that manages the dam remains during the winter. Because there is only the single road in the whole map area, we commonly give location information with reference to 'the road'.

To its west, the LdM field adjoins the Tatara-San Pedro-Pellado stratovolcano complex, which lies on the Andean volcanic front (Figs. 1, 2) and contrasts with the distributed LdM field in consisting of a few long-lived central-vent compound edifices (studied in detail by Davidson *et al.* (1988), Singer *et al.* (1997), and Dungan *et al.* (2001)). In what follows, we occasionally refer to the volcanic-front group, but the mapping addressed in the present study extends only to the eastern margins of Volcán Pellado. To the south and east of the map area lie deeply eroded intermediate volcanic centers, poorly known but probably of Pliocene and early Quaternary age. To the north, most exposures are of deformed Tertiary volcanic rocks, overlain locally by middle Pleistocene rhyolite lavas of the Puelche volcanic field (Hildreth *et al.,* 1999) and by glaciated remnants of several Quaternary ignimbrite outflow sheets from sources farther north and east.

PRE-QUATERNARY ROCKS BENEATH THE VOLCANIC FIELD

The Quaternary arc-volcanic belt at the latitude of Laguna del Maule (36°S) is 60 km wide. The Andean mountain range (Cordillera Principal) is here ~160 km wide, extending 60 km west and 40 km east of the Quaternary volcanic belt. It should be noted that the shallowly subducting 'flat-slab' segment of the Andes terminates 300 km north of Laguna del Maule and that a 'normal' slab dips 20°-30° beneath this segment. Moreover, inboard components of the orogen that are prominent farther north (Sierras Pampeanas, Precordillera, and Cordillera Frontal) are not present at this latitude, where instead the eastern slope of the Cordillera Principal is part of the basement-cored thick-skinned Malargüe fold and thrust belt. Still farther east at this latitude, the Llancanelo and Payún Matru extensional volcanic fields (on the Argentine pampas, 70 to 220 km east of the continental divide) consist of Pliocene and Quaternary mafic-alkaline intraplate lavas (Bermúdez and Delpino, 1989; Muñoz *et al.,* 1989; Kay *et al.,* 2006).

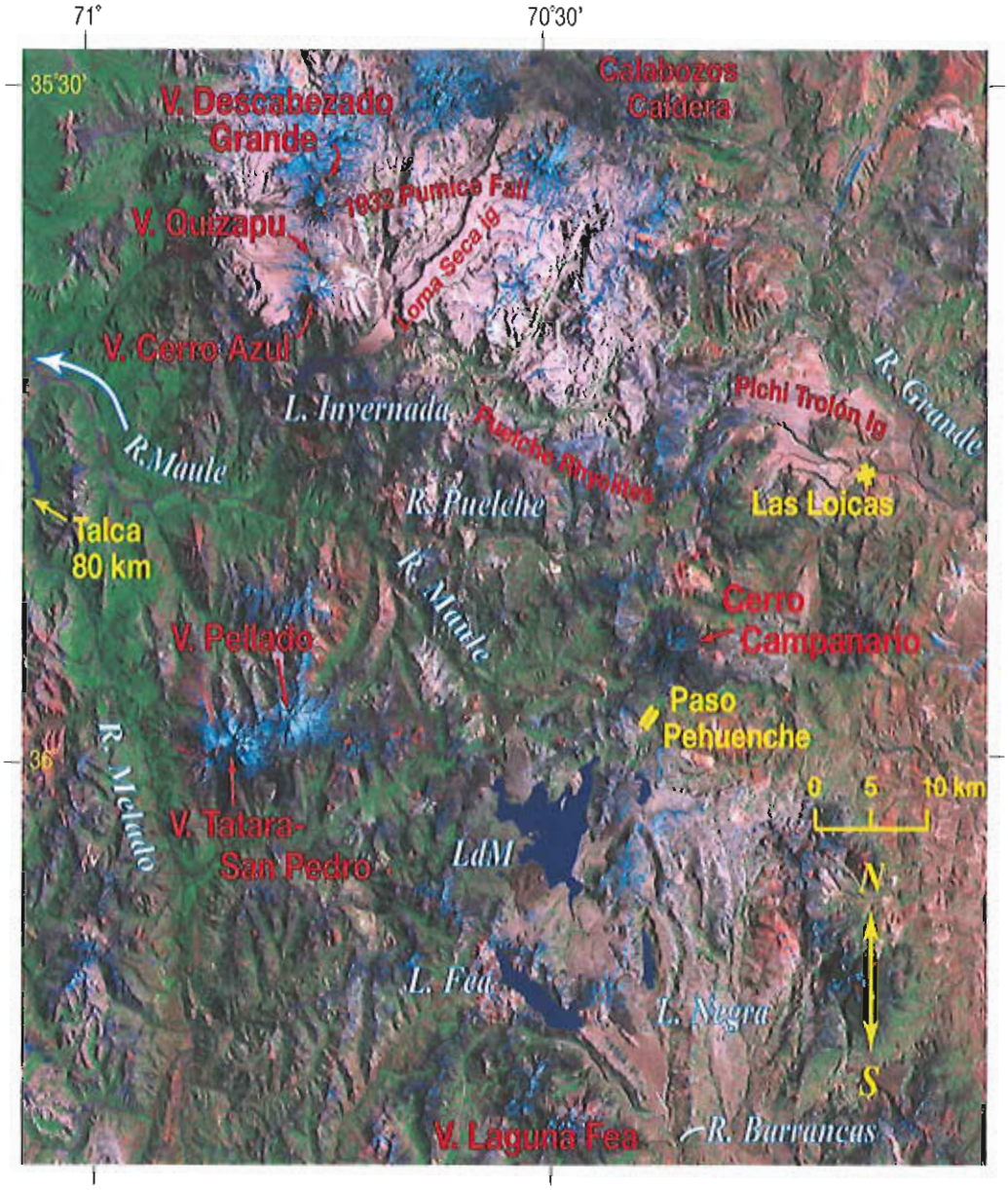

FIG. 2. Satellite photo of Andean study area (35.3°-36.2°S), about 100 km on a side and largely uninhabited, extending from Calabozos caldera (Hildreth *et al.*, 1984; Grunder and Mahood, 1988) southward beyond Laguna Fea. Laguna del Maule (LdM) is the large lake south of center. Volcán Descabezado Grande, Cerro Azul, and Volcán Tatara-San Pedro define Quaternary volcanic front of Andean Southern Volcanic Zone and lie about 50 km east of Chilean Central Valley. Calabozos, Puelche, and Laguna del Maule areas are rear-arc mafic-to-rhyolitic multi-vent distributed volcanic fields as far as 40 km behind volcanic front. Snow is (false color) blue. Large light-colored expanse north of center is plinian fallout sheet from April 1932 eruption of Volcán Quizapu (Hildreth and Drake, 1992). White plateaux at east center are rhyolite ignimbrite, probably of middle Pleistocene age, erupted at little-known Pichi Trolón caldera west of Las Loicas. Gravel roadway, lone trans-Andean road in region and open only in summer, ascends Río Maule, passes north shore of LdM to Paso Pehuenche on divide, and descends northeast to Las Loicas.

The Quaternary volcanic rocks of the LdM field (Fig. 3) principally overlie the following regional sets of Andean volcanogenic rocks of Tertiary age (Muñoz and Niemeyer, 1984; Jordan *et al.,* 2001; Burns *et al.,* 2006). **(1)** Folded nonmarine volcaniclastic sedimentary strata (principally epiclastic fluvial and lacustrine units, with minor lavas and pyroclastic units interfingering), grouped as the Cura-Mallín Formation, which is more than 2 km thick and of late Oligocene and early Miocene age. The extensive basin for these sediments was one of a chain of extenional intra-arc basins of that age along the Andean Cordillera between 33° and 42°S. The southernmost (Ñirihuao) includes minor marine sediments of Pacific provenance. **(2)** Andesitic and mafic lavas, stratified tuffs and breccias, and subordinate volcaniclastic sedimentary rocks, grouped as the Trapa-Trapa Formation, roughly 19-10 Ma, openly folded, and as thick as 1 km. **(3)** Ignimbrites and associated silicic and intermediate volcanic rocks assigned to the Campanario Formation, ranging from middle Miocene to Pliocene age, undeformed or moderately folded, and widely as thick as 500 m (or >1,000 m in a few intracaldera settings). **(4)** Undeformed mafic and intermediate lavas from many centers, lumped as the Cola de Zorro Formation of Pliocene and early Quaternary age (Vergara and Muñoz, 1982). These are generally apron-facies stacks as thick as 500 m that blanketed much of the preglacial relief and today form widespread subhorizontal rimrock lavas that conspicuously cap ridges between glacially incised valleys (see section 4, below). Associated proximal- and vent-facies complexes are thicker, structurally complex, intrinsically local, and not yet investigated.

A renewal of intense Andean arc magmatism began ~25 Ma, perhaps in response to a plate reorganization and an abrupt increase in convergence rate ~28 Ma (Jordan *et al.,* 2001). Although strict continuity is hard to demonstrate, it appears that such magmatism has persisted in this segment of the Andes ever since. The intra-arc extension inferred from subsidence of the Cura-Mallín and contemporaneous basins diachronously terminated at ~20 to 15 Ma with the close of such intra-arc sedimentation. Subsequent compressive deformation was probably intermittent and southward younging, but its timing is not well constrained here. The Cura-Mallín sedimentary package and overlying middle Miocene Trapa-Trapa arc-volcanic package were both deformed into broad north-trending folds by the end of the Miocene, probably principally during the interval 11-6 Ma (Melnick *et al.,* 2006). At the north edge of our map area, andesitic lavas and rhyodacite ignimbrite, both deformed, yield K-Ar ages of 12-14 Ma (Table 2) or perhaps as young as 7±1 Ma (Drake, 1976). K-Ar ages of 6.1±0.5 Ma and 3.4±0.8 Ma for apparently undeformed ignimbrites adjacent to the southwest margin of the LdM volcanic field were published by Muñoz and Niemeyer (1984).

Although the deformed Tertiary packages strike beneath the western and northern margins of the Laguna del Maule volcanic field (Muñoz and Niemeyer, 1984; Fig. 3), the Miocene folding is better known in well-exposed Mesozoic strata of the thick-skinned Malargüe fold-and-thrust belt on the Argentine slope of the Andes (Manceda and Figueroa, 1995; Ramos *et al.,* 1996; Ramos and Kay, 2006). Exposures of the folded Mesozoic rocks (Mzs in Figs. 3, 6) begin just beyond Paso Pehuenche, within 8 km of Laguna del Maule, yet none of the Pliocene and Quaternary volcanic rocks in our adjacent map area appear to be deformed; these include subhorizontal andesite lavas as old as 6.4±1.3 Ma on the east wall of the Laguna del Maule basin (Table 1). According to Ramos and Kay (2006), deformation in the foreland fold-and-thrust belt may have persisted from 15 to 5 Ma but peaked in the late Miocene. Investigation of synorogenic Miocene sediments and mafic lavas in syntectonic basins between anticlines to the east and northeast suggest secular eastward propagation of deformation from middle to latest Miocene (Silvestro *et al.,* 2005). The Mesozoic strata, nonmarine and mainly shallow marine sedimentary units of the Neuquén basin, are extensively exposed in the fold-and-thrust belt just east of the map area, where they overlie Permian to early Triassic silicic volcanics of the Choiyoi Group. They also crop out between La Mina and the El Indio granitoid pluton (80 Ma; Nelson *et al.,* 1999) northwest of the map area (Fig. 3). There are no Mesozoic exposures within the Laguna del Maule volcanic field and only two more small windows nearby-along Cajón de Troncoso 12 km southwest of the lake (Fig. 3) and at Río Invernada 25 km north of it (Hildreth *et al.,* 1999).

TABLE 1. SUMMARY OF $^{40}Ar/^{39}Ar$ INCREMENTAL-HEATING EXPERIMENTS ON 47 LAGUNA DEL MAULE SAMPLES.

					Age spectrum				Total	Isochron analysis		
Sample	Unit	% SiO_2	UTM Grid	Material	Age ± 2σ (ka)	^{39}Ar %	N*	MSWD	fusion age (ka)	$^{40}Ar/^{36}Ar$ ± 2σ intercept	$^{40}Ar/^{39}Ar$ Age ± 2σ (ka)	SUMS (N-2)
LdM-254	rcl	73 8	733/131	wr	17.3 ± 17.0	100 0	11 of 11	0 47	9 8 ± 14 1	no isochron, insufficient spread in data		
LdM-213	rdz	71 6	683/035	gm	21.1 ± 0.9	85 8	11 of 15	1 54	23 6 ± 1 1	295 6 ± 1 4	20 9 ± 1 5	1 96
LdM-6	rle	75 6	693/126	wr	23.3 ± 0 4	100 0	18 of 18	1 60	23 2 ± 0 5	293 5 ± 1 52	23 6 ± 0 5	1 28
LdM-222	dpj	58 8	612/077	wr	21 9 ± 4 2	100 0	5 of 5	0 43	22 6 ± 5 2	298 9 ± 17 8	19 3 ± 12 0	0 51
				wr	25 6 ± 2 5	73 7	6 of 7	1 38	24 3 ± 0 2	298 8 ± 8 7	22 2 ± 0 9	1 56
			Wtd. Means		24.6 ± 2.2			2 10		298 7 ± 7 8	22 2 ± 0 9	0 23
LdM-194	arm	58 8	591/112	wr	26 8 ± 0 8	59 8	5 of 10	2 57	29 8 ± 0 9	293 6 ± 5 5	27 8 ± 2 33	3 03
				wr	22 6 ± 4 0	100 0	5 of 5	1 19	24 1 ± 4 3	297 3 ± 3 9	20 1 ± 6 7	1 23
			Wtd. Means		26.6 ± 0.8			4 00*		296 1 ± 3 2	27 0 ± 4 2	4 60*
LdM 61	rep	73 5	602/137	plag	38.2 ± 29.0	85 6	4 of 7	0 76	40 8 ± 43 5	no isochron, insufficient spread in data		
LdM-44	mpn	52 2	553/136	wr	53.5 ± 21.0	100 0	4 of 4	0 76	46 7 ± 27 2	294 3 ± 1 6	67 1 ± 27 2	0 59
LdM-16	hbc	51.4	586/148	wr	62.2 ± 3.6	100 0	15 of 15	0 75	56 6 ± 8 7	293 8 ± 0 9	71 2 ± 6 0	0 88
LdM-94	rez	73 8	448/138	wr	82.5 ± 2.5	100 0	8 of 8	1 50	83 4 ± 2 2	298 0 ± 8 2	78 1 ± 14 2	1 63
LdM-407	meb	53 4	621/188	wr	85.6 ± 7.9	78 9	3 of 7	0 24	109 2 ± 11 9	298 3 ± 11 9	80 0 ± 24 6	0 36
LdM-102	rel	73 7	497/139	plag	96.7 ± 15.2	100 0	7 of 7	0 [illegible]	109 0 ± 23 3	297 0 ± 1 5	85 6 ± 19 2	0 47
LdM-139	mvp	58 8	415/123	wr	114.1 ± 5.9	94 1	4 of 6	3 25*	107 0 ± 3 1	296 0 ± 34 0	113 7 ± 33 0	5 6*
LdM-189	rddm	71 2	584/124	wr	114.5 ± 49.2	56 1	6 of 13	0 [illegible]	88 6 ± 12	296 3 ± 1 5	110 1 ± 27 4	1 21
LdM-427	avm	60 6	560/221	wr	115.9 ± 26.8	89 8	8 of 9	0 [illegible]	118 0 ± 3 2	303 0 ± 12 0	112 4 ± 5 7	0 77
LdM-240	mcc	54 1	760/222	wr	147.9 ± 4.1	47 2	4 of 13	2 48	146 6 ± 4 5	284 8 ± 8 6	158 1 ± 8 5	0 84
LdM-112	mvp	57.4	393/077	wr	150.7 ± 3.4	78 4	3 of 6	1 37	151 0 ± 2 6	291 0 ± 5 6	154 3 ± 5 3	2 81
LdM-354	mvc	56 1	713/046	wr	152.9 ± 6.5	49 5	4 of 9	1 31	140 4 ± 13 6	302 7 ± 40 2	150 7 ± 12 4	1 70
LdM-33	hbc	52 01	643/167	gm	154.0 ± 7.0	77 8	3 of 6	0 63	142 6 ± 7 8	289 4 ± 15 8	163 5 ± 25 2	0 63
LdM-335	rdct	67 9	585/033	wr	203.0 ± 40.9	94 2	11 of 12	0 08	179 5 ± 171 0	292 5 ± 16 6	339 1 ± 490 4	0 12
LdM-241	mcc	54 4	762/225	plag	215.3 ± 61.8	100 0	6 of 6	0 91	265 1 ± 272 4	297 5 ± 1 8	183 0 ± 93 2	3 25
LdM-161	rlm	73 2	463/226	wr	334.6 ± 2 4	100 0	9 of 9	0 92	334 7 ± 2 9	296 3 ± 8 9	334 4 ± 2 6	0 97
LdM-446	rlm	73 2	469/193	wr	340.6 ± 7.6	66 8	8 of 9	0 69	351 7 ± 17 3	297 9 ± 11 5	332 9 ± 42 2	0 16
LdM-420	aab	61 4	581/192	wr	371.5 ± 17.9	51 7	3 of 8	1 52	339 9 ± 76 8	260 3 ± 80 5	401 1 ± 93 0	3 81
LdM-429	asb	60.4	572/218	gm	374.1 ± 7.4	100 0	12 of 12	1 12	373 2 ± 8 2	295 0 ± 3 1	376 1 ± 12 0	1 47
LdM-430	ans	62 01	583/214	gm	429.1 ± 41.7	100 0	11 of 11	0 24	460 8 ± 71 9	299 6 ± 12 4	419 4 ± 44 3	0 42
LdM-350	rcn	75 3	700/010	wr	467.8 ± 5.6	100 0	11 of 11	0 91	465 5 ± 7 0	286 8 ± 14 2	476 6 ± 14 6	0 85
LdM-101	rdph	70 4	438/121	plag	679.8 ± 34.4	91 4	6 of 7	0 25	714 2 ± 22 6	290 8 ± 3 3	669 7 ± 43 1	0 64
VCE-1h	rdvc	~71	428/150	wr	694.9 ± 8.2	63 5	4 of 7	1 62	712 8 ± 6 8	300 0 ± 1 0	693 4 ± 7 4	0 92
LdM-415	rca	74 3	675/158	wr	711.6 ± 13.0	63 2	6 of 12	3 37*	724 6 ± 8 7	280 3 ± 20 9	715 2 ± 13 3	3 02*
LdM-278	mvm	54 7	708/187	wr	898.2 ± 20.0	59 2	6 of 11	8 64*	921 8 ± 10 8	283 7 ± 12 4	911 5 ± 22 7	6 37*
LdM-103	dab	65 1	498/138	plag	923.8 ± 37.4	100 0	7 of 7	0 39	891 6 ± 100 0	293 9 ± 1 4	954 5 ± 44 8	0 22
LdM-32	gcb	71 4	631/175	plag	950.0 ± 6.9	87 4	8 of 9	0 68	850 6 ± 9 8	295 1 ± 1 6	951 0 ± 7 9	0 84
LdM-255	alz	57 7	735/165	wr	1013 ± 28	47 8	4 of 9	0 62	1216 ± 18	298 8 ± 5 5	961 9 ± 91 8	0 43
LdM-166	mva	54 8	542/189	wr	1290 ± 13	61 3	3 of 7	2 89	1279 ± 13	280 1 ± 17 7	1308 ± 23	1 54
LdM-81	mvb	56 2	520/122	wr	1324 ± 20	60 3	3 of 6	1 26	1373 ± 24	299 2 ± 21 9	1295 ± 86	2 45
LdM-356	rif	72 7	651/974	bio	1351 ± 17	59 2	3 of 15	2 11	1369 ± 196	320 5 ± 23 4	1262 ± 86	0 38
LdM-46A	rgsp	65 7	562/141	plag	1484 ± 15	96 4	6 of 7	0 66	1445 ± 40	294 1 ± 2 7	1486 ± 23	0 87
LdM-198	dll	61 7	638/999	plag	1582 ± 9	92 8	8 of 9	0 37	1601 ± 16	298 3 ± 5 1	1576 ± 10	0 8
LdM-310	arp	61.9	553/027	wr	2010 ± 23	89 8	11 of 13	4 93*	2002 ± 21	309 4 ± 39	2001 ± 34	5 26*
LdM-78	Trcl	74 8	512/112	wr	2572 ± 9	71 8	5 of 9	0 48	2622 ± 9	283 7 ± 17 7	2586 ± 28	0 07
LdM-245	Tavm	57 2	725/091	plag	6365 ± 1286	80 7	6 of 9	0 13	7324 ± 2179	291 9 ± 7 6	6774 ± 991	4 29*
No plateau or discordant spectra												
LdM-en 01	gr-en		649/135	K-fsp					~1 1 Ma			
LdM-338	dll	65 1	589/007	wr					~1 5 Ma			
LdM-181	acs	54 1	561/103	wr					~2 0 Ma			
LdM-263	acs	62 2	568/093	wr					~2 1 Ma			
LdM-347	Tdcl	52 4	691/083	wr					~3 6 Ma			
LdM-250	Tarl	54 7	728/050	wr					~3 6 Ma			

Preferred ages are the plateau ages in **bold**. From results of replicate experiments on LdM-222 and LdM-194, inverse-variance weighted mean ages are preferred.
Samples irradiated either 60 or 20 minutes in CLICIT facility at Oregon State University Triga reactor.
Resistance furnace degassing and analyses using an MAP-216 spectrometer and techniques of Singer *et al.* (1999) and Jicha and Singer (2006).
N= number of plateau/isochron steps used in regression. Regression of data from plateau portions of experiments to calculate isochron ages reveals no significant departures from an atmospheric trapped component in any sample. Accordingly, plateau ages are preferred as slightly more precise than the isochron ages.
Ages calculated relative to Taylor Creek Rhyolite sanidine at 28.34 Ma or Alder Creek Rhyolite sanidine at 1.194 Ma (Renne *et al.* 1998).
*MSWD and/or SUMS/(N-2) are large and indicate scatter about the mean in excess of that due solely to analytical uncertainties.

TABLE 2. K-Ar AGES FOR LAGUNA DEL MAULE VOLCANIC FIELD.

Sample #	Label	UTM E/N	Material manalyzed	Unit SiO_2	Sample wt% K_2O	$^{40}Ar^*$ 10^{-12} mol/g	$\%^{40}Ar^*$	Age (ka)	Notes
USGS Menlo Park lab									
LdM-85	mcs	479/158	wr	50 8	1.07	3.95	6 09	256±20	Mafic lava, SW slope Cerro San Pedro
			wr		1.07	3.41	3.82	221±26	
							wtd mean=	243±16	
LdM-148	mcs	519/192	wr	55 1	0 75	2 63	3 51	243±43	Mafic lava, NE apron of Cerro San Pedro, thick basal flow supports fall on Estero Bahamondes
LdM-93	avz	446/155	wr	59 1	2 39	14 79	31 24	429±8	South face of Peak 2786; headwall of west cirque gutting Volcán El Zorro
LdM-49	rcn	692/120	wr	76 9	4.81	30 92	47 28	447±7	Biotite-rhyolite lava >900 m thick on NE wall of Laguna del Maule basin; near base at 2250 m
LdM-114	mvñ	425/111	wr	53 2	1 23	16 13	18 11	914±21	Mafic lava flow near top of Volcan Ñirales, 2,500 m on south nose
LdM-132	mvñ	431/148	wr	54 8	1 5	22 33	11 17	1037±36	Mafic lava at north end of Volcan Ñirales outcrop, underlies units **rdvc**, **avz**, and *rez*
U.C. Berkeley lab									
	KA-#								
GHC-451	2394	dcc	561/208	wr	63	2 13	3 101	5.01	100±10	Hornblende-dacite lava in roadcut at 1,750 m on Cuesta Los Condores grade
GHC-450	2387	dcc	561/208	wr	63	2.89	7.3	8 01	170±20	Ibid
C84-4	4714	rep	602/137	bi	73.6	7.452	25 09	3.6	240±55	Glaciated rhyolite lava at east end of Laguna del Maule dam (cf LdM-61 Table 2)
D1-3-19A	2405	mrb	566/227	wr	54	1 28	3.701	2.01	270±70	Mafic lava remnant northwest of Baños Campanario
D0-4-3D	2555	aeb	506/260	wr	59	2 29	9 301	8 01	276±20	Andesite lava flow capping rhyolite unit **rlm** atop Triangular Plateau
GHC-441	2419	igcc	565/218	obsidian	74	3 74	21 5	18.01	336±20	Pink nonwelded ignimbrite remnant banked on south face of Cordon de Constanza
D2-2-7A	2666	ava	656/187	wr	59	2 31	22.61	5	720±80	Andesite lava caps Peak 2753; overlies ignimbrite **igcb** on Bobadilla Chica-Grande divide
LdM-39	4998	rdla	572/191	pl	68.9	0 657	8 337	10 9	881±73	Rhyodacite dome of Lo Aguirre (through which road tunnel passes)
C84-3	4711	ava	633/135	wr	60 5	2 574	36.54	14.2	990±80	Crystal-poor andesite lava rests on ignimbrite **igcb** at N shore of LdM
D2-2-6A	2617	ava	671/217	wr	60	2.69	41 01	29	1060±30	Andesite lava caps Peak 2672 on Bobadilla-Campanario divide; overlies **igbc** and **igcb**
D2-1-4K	2643	ig1*	752/417	wr	~70	3 04	46 5	15	1060±40	Top ignimbrite on wall east of upper Río de la Invernada near continental divide
C84-2	4712	igcb	636/133	bi	70 6	8 195	128 6	9 6	1090±150	Large fiamma in welded zone at 2300 m just above north shoreline of Laguna del Maule
GHC-460	2390	alz	710/180	wr	62	2 53	42.5	14.01	1160±400	Andesite lava flow of widely altered center north of NE arm of Laguna del Maule
D2-2-8F	2675	mva	550/190	wr	54	1 241	20 8	12.01	1170±50	Mafic lava on east slope of Peak 2707 above Arroyo Arenas Blancas
LdM-18	5001	igsp	585/160	pl	66.0	1.049	21.33	8.3	1412±130	Large fiamma in densely welded ignimbrite on hill 2379, 3 km NW of Laguna del Maule dam
LdM-12	5004	Trea	590/183	wr	76 9	5.937	204 1	7 6	2388±100	Small rhyolite dome at roadside on west rim of Río Maule gorge, 5 km north of dam
LdM-27	5009	Trea	581/171	bi	72.2	8.236	443.2	37 1	3740±120	Rhyolite dome between forks of Estero Aguirre, 7 km NW of LdM dam
GHC-449	2411	Tad	557/224	pl	~55	0 169	31 3	3.01	12.5±4 5 Ma	Altered andesite lava beneath stack of 3 Pleistocene lavas on Maule-Campanario nose (Fig. 17)
LdM-21	5000	Tigh	600/166	pl	70.7	0.83	154.9	15.6	12 9±0.7 Ma	Fiamma in welded ignimbrite near river level on east wall of Río Maule gorge, 3 km north of dam
C84-13	4696	Tecg	625/264	pl	59	2 801	580 1	38.7	14 34±0 31 Ma	Brecciated andesite lava east of Cajon de la Galaz, deformed edifice north of Río del Campanario

Menlo Park determinations by Singer in lab then supervised by M.A Lanphere Berkeley determinations by R E. Drake in University of California lab then supervised by G.H. Curtis
Some of Drake's data were recalculated subsequent to publication in Drake (1976) Whole-rock (wr) % SiO_2 data by XRF in USGS laboratory at Lakewood, Colorado, rounded to nearest wt% where our sample was not a split of that dated by Drake All errors are 2-sigma. pl=plagioclase, bi=biotite Unit ig1* in Puelche volcanic field is described by Hildreth *et al.* (1999). UTM grid coordinates explained in text introduction

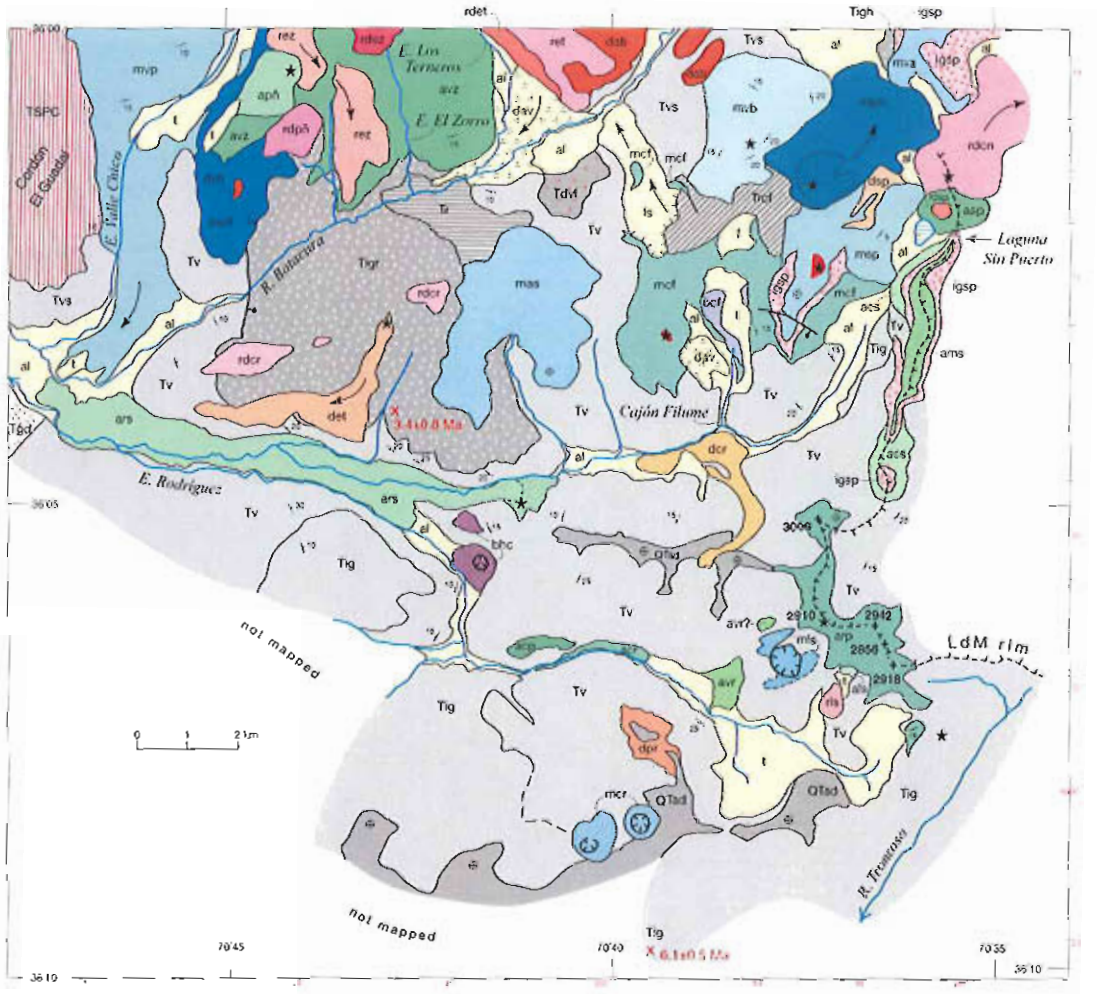

FIG. 8. Simplified map of southwestern quarter of LdM volcanic field, limited approximately by west of rim of lake basin (hachured), Volcán Pellado, Río Botacura, and Estero Rodríguez. All units are discussed in text and unit labels are identified alphabetically in Appendix 1. Colors and symbols as in figures 6, 7. Major streams in blue. Additionally, **Tv**=deformed lavas and tuffs; **Tvs**=same, where volcaniclastic sedimentary strata make up more than a trivial proportion; all are thought to be Miocene or older. **Tig**=extensive silicic ignimbrites; two ages indicated in red (from Muñoz and Niemeyer, 1984) are late Miocene and Pliocene. **Tgd**=late Miocene granitoid pluton (Nelson *et al.*, 1999). Cordón El Guadal at west edge consists of mafic to dacitic lavas (510-360 ka), a component of the Tatara-San Pedro Complex (**TSPC**) studied by Feeley and Dungan (1996) and Feeley *et al.* (1998). Marginal ticks are UTM grid in km east and north, as on IGM topographic maps.

above the floor of the nearby Río Campanario (Fig. 9). A patch of coarse scoria surviving at the uphill end of the lava bench suggests a local vent, and a small plug on the spur 300 m southeast may be related.

(4) Unit **acc** is a single andesite lava flow (62% SiO_2) as thick as 130 m that extends for 1.5 km along the crest of Cordón de Constanza, its base lying 300 m above the Río Maule and 400 m above the Río Campanario (Fig. 9). The lava carries abundant plagioclase phenocrysts, common opx, and subordinate cpx. It rests on deformed Miocene tuffs and lavas and is overlain by a lag of rounded fluvial cobbles and scattered erratic blocks, suggesting that it had been a valley-filling flow,

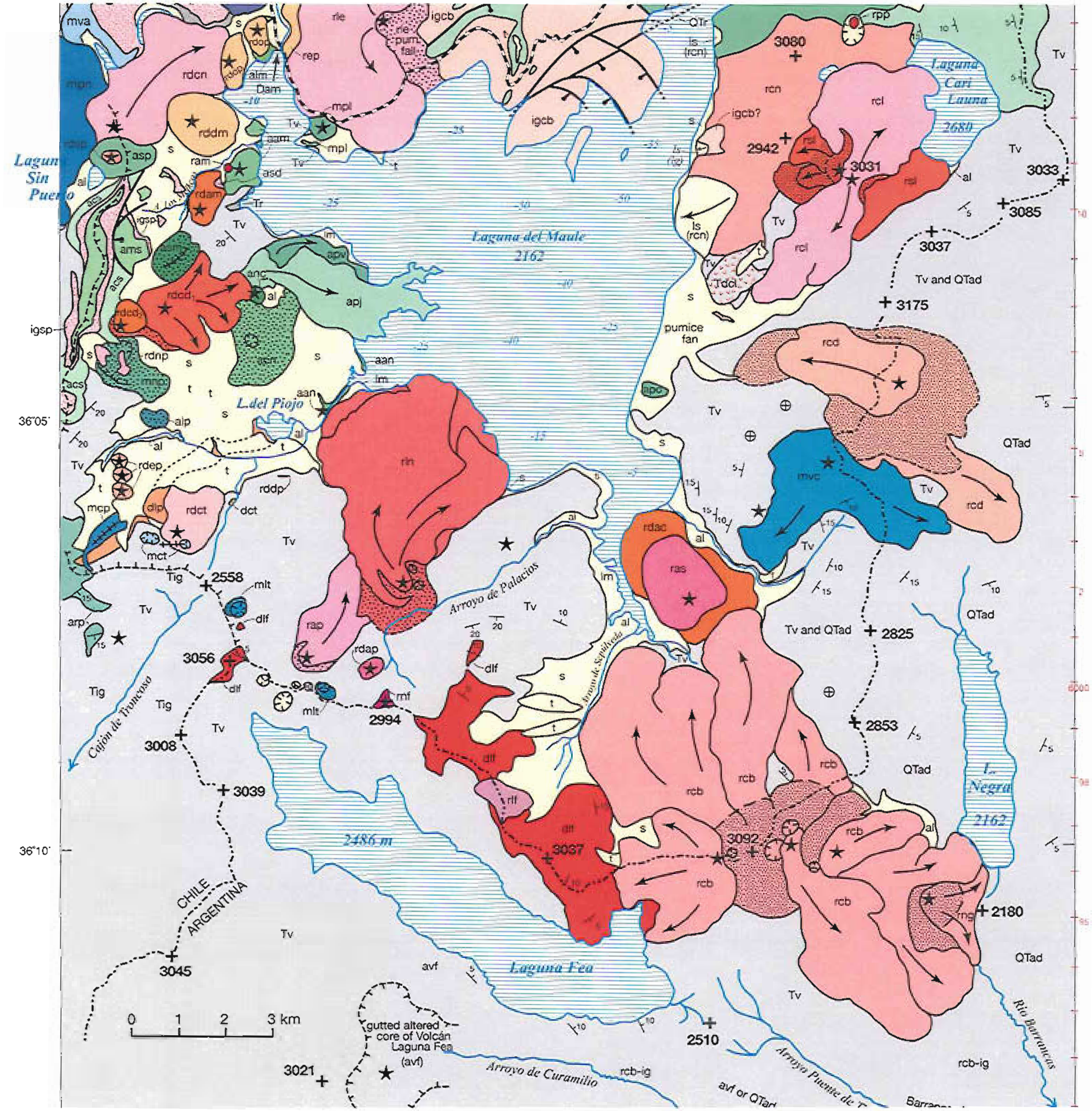
Laguna del Maule
2162
Laguna Cari Launa
2680
Laguna Sin Puerto
L. del Piojo
Laguna Fea
2486 m
L. Negra
2162
Arroyo de Palacios
Cajón de Troncoso
Arroyo de Curamilio
Arroyo Puente de T
Río Barrancas
CHILE
ARGENTINA
gutted altered core of Volcán Laguna Fea (avf)
pumice fan
Tv and QTad
36°05'
36°10'
0 1 2 3 km
3080
2942
3031
3033
3085
3037
3175
2825
2853
2180
3092
3037
2994
2558
3056
3008
3039
3045
3021
2510

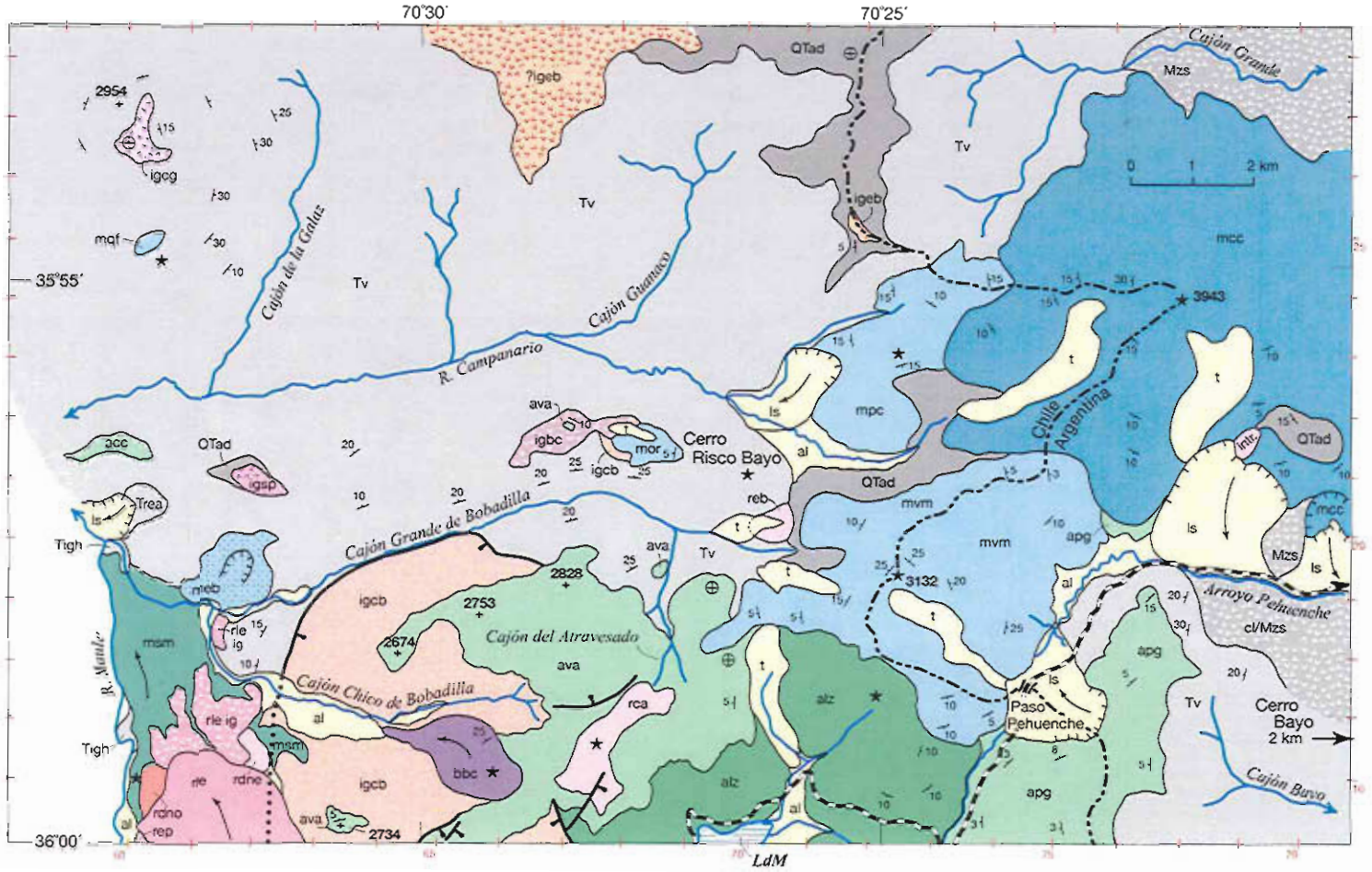

FIG. 6. Simplified map of northeastern sector of LdM volcanic field, north of lake, between Río Maule and Cerro Campanario. Lone road (CH 115) crosses international border at Paso Pehuenche. All units are discussed in text and unit labels are identified alphabetically in Appendix 1. In general, silicic units are in warm colors, andesites in greens, and mafic units in blues or purple. Additionally, Tv=deformed lavas, tuffs, and minor volcaniclastic sedimentary strata, undivided; mostly intermediate but including some silicic ignimbrites; all thought to be Miocene. Mzs=folded Mesozoic sedimentary rocks, undivided. Stars mark eruptive vents. Arrows indicate directions of lava flows and slumps. Major streams are in blue. Marginal ticks are UTM grid in km east and north, as on IGM topographic maps.

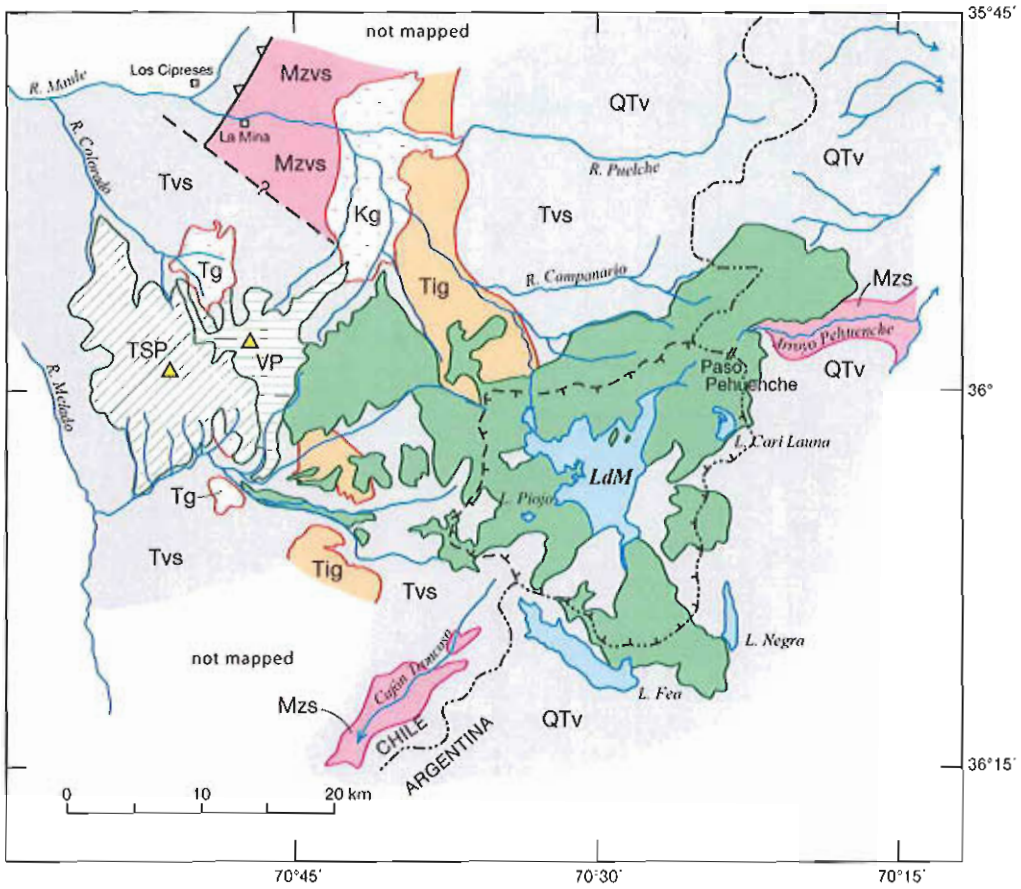

FIG. 3. Generalized map indicating sets of pre-Quaternary rocks exposed beneath and around the Quaternary volcanic field, which is shown in green. Long-lived Tatara-San Pedro (**TSP**) compound edifice on the volcanic front and adjacent Volcán Pellado (**VP**) (Singer *et al.*, 1997) are distinguished from the distributed Laguna del Maule volcanic field, the focus of this report. Basement includes Mesozoic sedimentary and metavolcanic rocks (**Mzs, Mzvs**), Cretaceous (**Kg**) and Tertiary (**Tg**) granitoid plutons, Tertiary ignimbrite sheets (**Tig**), deformed Tertiary volcanic and volcanogenic sedimentary rocks (**Tvs**), and undeformed flat-lying volcanic rocks (**QTv**) thought to be mostly early Quaternary or Pliocene in age. Villages of La Mina and Los Cipreses to northwest are the only permanent settlements in the map area. The basin that drains into Laguna del Maule (**LdM**) is outlined by the international boundary (continental divide) on the east and south and by a hachured line on the north and west. The lake drains through a small dam on its northwest arm into the Río Maule, one of Chile's major rivers.

OVERVIEW OF VENT DISTRIBUTION

Pliocene and Miocene lavas and tuffs are extensively represented in the ranges and canyons surrounding the LdM volcanic field and are exposed in several areas within it (Fig. 3). We devoted little attention to them, and most of those we attempted to date gave poor results that reflect mild secular alteration. Our understanding of the volcanic history is far better after than before 1.5 Ma, when a widespread sheet of pyroxene-dacite ignimbrite (unit **igsp**) was emplaced.

Sixteen mafic or andesitic Quaternary polygenetic stratovolcanoes and shields have been distinguished within or at the margins of the LdM volcanic field (Table 3; Fig. 4). The highest is Cerro

TABLE 3. POLYGENETIC EDIFICES WITHIN AND ADJACENT TO THE LDM VOLCANIC FIELD.*

Edifice	Unit	Age (ka)	%SiO_2	Max %MgO	Notes
Cerro Campanario	mcc	150	54.1-54.4	4.6	Mafic stratocone at northeast edge of volcanic field
V. de la Calle	mvc	150	53.5-56.1	5.1	Mafic shield at southeast edge of map area
V. Pellado	Mvp, avc	200-80	52.1-61.2	5.7	Stratocone at northwest edge of map area
Cerro San Pedro	mcs	240	49.3-58.2	7.2	Mafic shield centered 11 km west-northwest of LdM
V. El Zorro	avz	430	52.4-60.8	5.5	Complex stratocone centered 14 km west-northwest of LdM
V. Tatara-San Pedro	tsp	925-0	49.0-75.4	9.9	Compound edifice on volcanic front west of LdM; several vents and sequences, basalt-to-dacite, plus flank rhyolites
V. Munizaga	mvm	900	50.3-54.7	6.8	Mafic stratocone centered 2 km northwest of Paso Pehuenche
V. Atravesado	ava	950-720	53.5-64.6	5.0	Postcaldera intermediate edifice eroded from LdM basin; its north flank preserved along and beyond north wall of basin
V. Ñirales	mvñ	1,050-900	51.4-65.7	6.3	Mafic shield near west edge of map, 17 km west of LdM; severely eroded
V. La Zorra	alz	1,160-950	57.7-62.2	2.9	Stratocone centered 3 km SW of Paso Pehuenche, altered and severely eroded
V. Sin Puerto	msp	<1.5 Ma	53.2-56.7	4.9	Mafic cone with 300-m-wide plug centered 5 km west of LdM
V. Aguirre	mva	1,290-1170	51.4-56.1	4.4	Mafic stratocone centered 6 km northwest of LdM
V. Bolacura	mvb	1,320	53.4-56.2	4.8	Mafic stratocone centered 7 km west-northwest of LdM
V. Filume	mcf, mas	2.5-1.5 Ma	52.8-58.8	5.0	Eroded stratocone centered 10 km west of LdM
V. Fea	avf	2-1.3 Ma	-	-	Intermediate stratocone centered 2-3 km south of Laguna Fea; some outflow lavas preserved on north rim of lake
Cerro Bayo	apg	2-1 Ma?	-	-	Eroded altered edifice centered 7 km east of Paso Pehuenche; may be source of plateau-capping andesitic lavas on divide

* Edifices on figure 4. Unit labels in Appendix 1. V. Volcán; LdM. Laguna del Maule. Radiometric ages in Tables 1, 2.

Campanario (3,943 m; Hildreth *et al.*, 1998) on the continental divide, and the most voluminous is Volcán Tatara-San Pedro (Singer *et al.*, 1997; Dungan *et al.*, 2001) on the volcanic front. Only the latter has remained active into the Holocene, though, like all the others, that edifice too had been glacially dissected repeatedly during the Pleistocene. Of the 16, three might be as old as 2 Ma, eight others commenced activity about or before 900 ka, and five are younger than 500 ka (Tables 1-3). Six of the big centers lie east or northeast of the LdM lake basin, seven are within 15 km west of it, and two are on the volcanic front 20-25 km from the lake (Figs. 3, 4). One of the oldest (and poorest known) lies south of Laguna Fea (Figs. 2, 4).

Scattered across the volcanic field but more concentrated near the LdM lake basin are numerous lesser vents, mafic to silicic, the great majority monogenetic. Figure 4A locates 44 postglacial vents, of which 15 are basaltic-to-andesitic, 3 dacitic, and 26 rhyodacitic or rhyolitic; two of the postglacial vents are indicated on Volcán Tatara-San Pedro. Figure 4B shows all the glaciated vents identified, divided into late, middle, and early Pleistocene sets. The late Pleistocene set (younger than 126 ka) includes vents for 19 basaltic-to-andesitic units, two dacites, three rhyodacites, and four rhyolites, plus two vents on Volcán Tatara. Vents are covered or otherwise unrecognized for two additional late Pleistocene lavas, both andesitic (units **alc** and **avm**; Appendix 1). Middle Pleistocene vents (778-126 ka) shown in figure 4B represent 10 basaltic-to-andesitic units, two dacites, eight rhyodacites, and three rhyolites. Units with concealed or unknown vents

that erupted in this time interval include two poorly welded ignimbrites (units **igcc** and **igcg**) and one mafic and three andesitic lavas (units **mor**, **aeb**, **ans**, and **asb**; Appendix 1). Early Pleistocene vents represent three mafic, five dacitic, four rhyodacitic, and three rhyolitic units, plus the caldera sources of extensive welded ignimbrite units **igcb** and **igsp** (Appendix 1). Additional units of this age for which we have not located vents include five lava-flow remnants (units **acc**, **ams**, **apg**, **arp**, and **dlf**) and scraps of two regional sheets of welded ignimbrite (**igbc** and **igeb**; Appendix 1).

The distributed LdM volcanic field (not counting the large western edifices Tatara-San Pedro and Pellado; Fig. 3) thus embraces 121 exposed vents (Fig. 4), of which 14 built medium-sized polygenetic stratocones or shields, 46 produced basaltic-to-andesitic monogenetic cones and flows, and 61 issued dacitic-to-rhyolitic lavas and ejecta. A few of the silicic vents produced multi-lobate lava-flow complexes. There are altogether no fewer than 23 lava-flow map units and remnants of four ignimbrites for which vents are either buried or otherwise unlocated, as well as the two welded ignimbrites (units **igcb** and **igsp**) thought to have erupted within the LdM lake basin itself.

VENT DISTRIBUTION WITH TIME

Almost the full 50-km-wide east-west strip (Fig. 3) became volcanically active by the end of the early Pleistocene, with major centers established on the volcanic front and near Paso Pehuenche by 900 ka (Fig. 4). A thick sheet of welded pyroxene-dacite ignimbrite (unit **igsp**), preserved only within 15 km north and west of the LdM basin, is inferred to have erupted there close to 1.5 Ma. Like most of the early Quaternary volcanic rocks, the ignimbrite rests largely on deformed strata of presumed Miocene age. Remnants of flat-lying lava flows of Pliocene age, mostly andesitic or mafic, locally underlie the early Quaternary volcanic units, but they are principally confined to high present-day ridgecrests, owing to glacial canyon-cutting during the first million years of the Quaternary; *i.e.*; prior to emplacement of the 1.5-Ma ignimbrite, from which we date our more complete understanding of the volcanic field. Several Pliocene rhyolite domes are also preserved northwest of the LdM basin, possibly a harbinger of the major silicic center the basin was to become during the Quaternary. A second ignimbrite (unit **igcb**), this time biotite-rhyodacite, erupted about 950 ka, in part from what has since become the LdM basin. An andesitic successor stratocone soon grew atop the intracaldera ignimbrite just north of the present-day lake, adding to the nine early Pleistocene stratocones previously established, three to the northeast, one to the south, and five to the west of the basin (Fig. 4). The few monogenetic vents thought to be of early Pleistocene age are scattered either west of the basin or in the south where they may have been peripherally related to the major edifice south of Laguna Fea (Fig. 4b). More monogenetic vents are likely to have existed, now scoured down to dikes or buried by younger units, as suggested by the seven early Pleistocene units for which we failed to find a vent.

FIG. 4. Distribution of Quaternary vents exposed in map area. See figures 1-3 for regional setting. (**a**) Sixteen polygenetic shields and stratovolcanoes (Δ) of any Quaternary age or composition, and 44 *postglacial* monogenetic vents, of which 15 are mafic or andesitic (**o**) and 29 are silicic domes, coulees, or pumice cones (•). (**b**) Pleistocene vents; 16 polygenetic edifices (Δ) and other symbols are same as in panel A. Monogenetic vents are as follows: 31 late Pleistocene vents are indicated in black; 23 middle Pleistocene vents in *red*; and 14 early Pleistocene vents in green. Lakes are in blue. Polygenetic edifices are identified in panel A and their ages (in ka) noted in panel B: **CB**=Cerro Bayo; **CC**=Cerro Campanario; **CSP**=Cerro San Pedro; **TSP**= Volcán Tatara-San Pedro on volcanic front; **VA**=Volcán Aguirre; **VB**= Volcán Botacura; **VC**= Volcán de la Calle; **VEZ**= Volcán El Zorro; **VF**= Volcán Filume; **VLF**= Volcán Laguna Fea; **VLZ**=Volcán La Zorra; **VM**= Volcán Munizaga; **VÑ**= Volcán Ñirales; **VP**= Volcán Pellado; **VSP**= Volcán Sin Puerto; **VX**= Volcán Atravesado. North of LdM field, nearest Quaternary vents are middle Pleistocene field of Puelche rhyolites (and a nearby 1.4 Ma rhyodacite intrusion) and the Pichi Trolon (**P-T**) caldera, source of undated Pleistocene rhyolitic ignimbrite sheets that extend from near the Puelche field (Hildreth *et al.*, 1999) at least as far east as Las Loicas (Fig. 2).

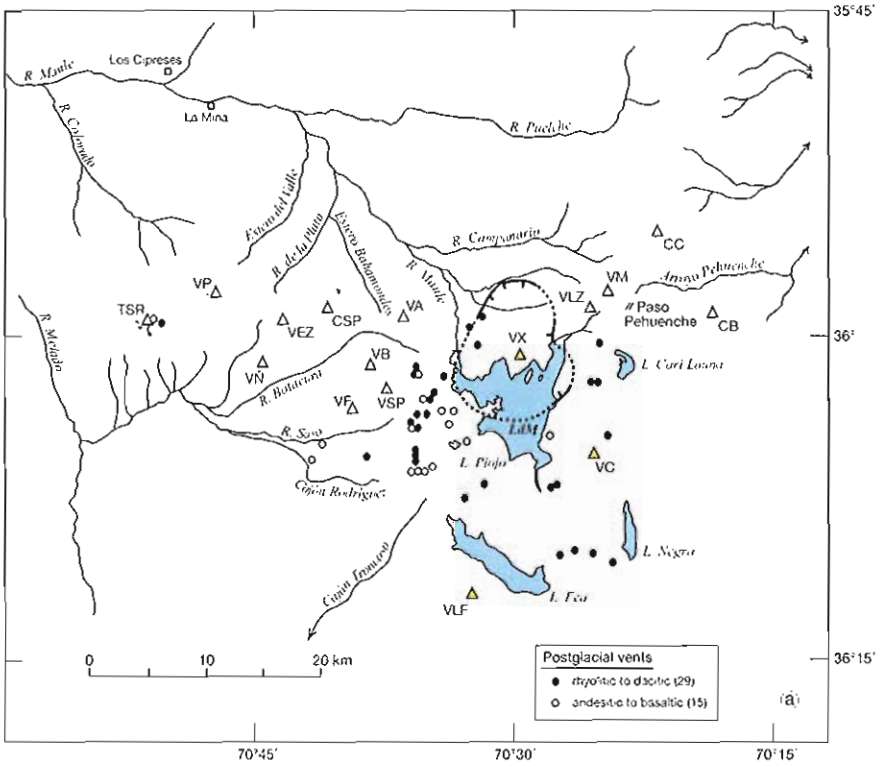
35°45'
36°
36°15'
70°45'
70°30'
70°15'
R. Maule
Los Cipreses
La Mina
R. Colorado
R. Puelche
Estero del Valle
R. de la Plata
Estero Babamendes
R. Campanario
R. Melado
R. Botalcura
R. Seco
Cajón Rodriguez
Cajón Amarillo
Arroyo Pehuenche
Paso Pehuenche
L. Cari Laufen
L. Piojo
L. Negra
L. Fea
VP
TSR
VEZ
CSP
VA
VN
VB
VF
VSP
VLZ
VM
CC
CB
VX
VC
VLF
0
10
20 km
Postglacial vents
rhyolitic to dacitic (29)
andesitic to basaltic (15)
(a)

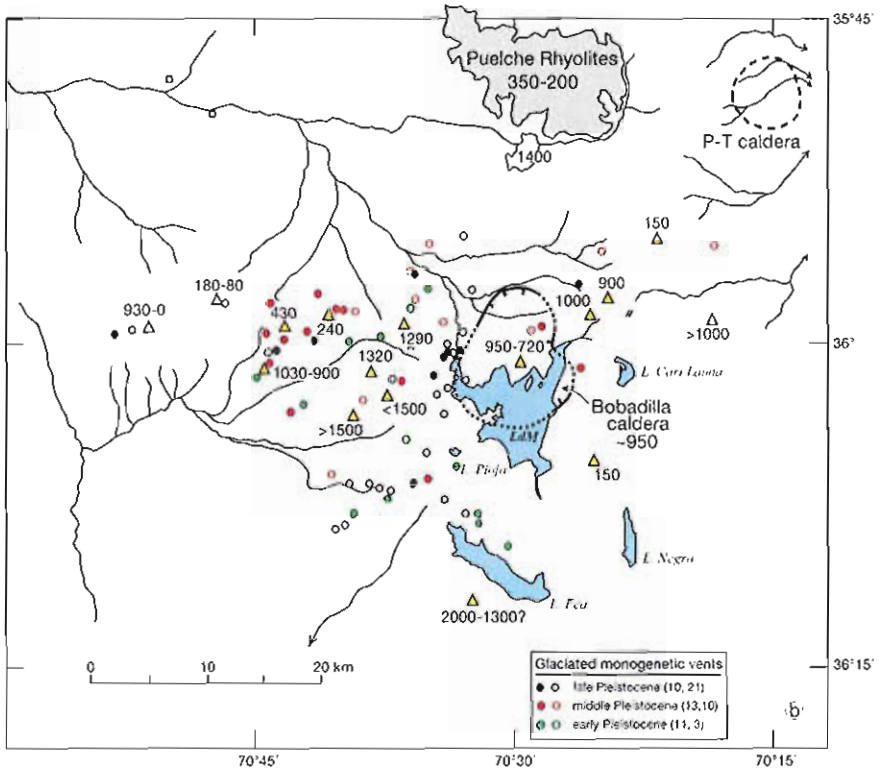
35°45'
36°
36°15'
70°45'
70°30'
70°15'
Puelche Rhyolites
350-200
1400
P-T caldera
150
180-80
930-0
430
240
1290
1320
1030-900
900
1000
>1000
950-720
<1500
>1500
L. Cari Laufen
Bobadilla
caldera
~950
150
L. Piojo
L. Negra
L. Fea
2000-1300?
0
10
20 km
Glaciated monogenetic vents
late Pleistocene (10, 21)
middle Pleistocene (13,10)
early Pleistocene (11, 3)
(b)

Middle Pleistocene vents were likewise distributed across the whole volcanic field, from Volcán Tatara on the volcanic front to Cerro Campanario on the rangecrest. Volcán Pellado and Volcán El Zorro, both andesitic, and the mafic shield Cerro San Pedro all developed in the west, while the mafic edifices Volcán de la Calle and Cerro Campanario were built in the east. Monogenetic vents that produced either scoria cones or silicic domes were scattered across the field but were most concentrated in the west, peripheral to Volcán El Zorro and Cerro San Pedro (Fig. 4b). To the north, separated from the LdM volcanic field, the extensive field of Puelche rhyolite lavas also developed in the middle Pleistocene (Hildreth *et al.*, 1999), as probably did the undated and poorly known Pichi-Trolon caldera (Fig. 4b), source of two sheets of biotite-rhyolite ignimbrite that extend eastward to Las Loicas (Fig. 2).

Late Pleistocene vents were slightly more numerous (noteworthy because the middle Pleistocene is six times as long as the late) as well as spatially more focussed, many being either near the outlet of the lake or at the southwest fringe of the volcanic field (Fig. 4b). The only stratovolcanoes remaining active in the late Pleistocene were Tatara-San Pedro and Pellado, just beyond the western edge of the distributed LdM volcanic field.

In postglacial time, however, the region around and southwest of the lake basin came to life magmatically. Postglacial silicic vents virtually surround the lake, while the mafic and andesitic ones are concentrated in a belt that extends 15 km west from the lakeshore (Fig. 4a). The only stratocone that remained active in the Holocene is Volcán San Pedro, far to the west on the volcanic front. Progressive concentration of vents toward the lake basin, already underway during the late Pleistocene, became pronounced after deglaciation. The number of silicic vents and the volume of postglacial silicic products increased strikingly around the periphery of Laguna del Maule, which thus became a focus of silicic magmatism unparalleled since the caldera-forming eruption at 950 ka.

PLIOCENE THROUGH EARLY PLEISTOCENE ERUPTIVE HISTORY

Subhorizontal to gently dipping stacks of lava flows, broadly andesitic (52-63% SiO_2) but not tied to known vents, are preserved as remnants capping ridgecrest divides between canyons in three broad areas within or near the LdM volcanic field: **(1)** along the narrow continental divide north of Cerro Campanario; **(2)** plateaux on the east rim of the LdM basin, extending south to both rims of Laguna Negra; and **(3)** the narrow divide west and southwest of Laguna del Maule, separating the LdM lake basin from the Saso drainage and continuous with lavas capping ridgecrests that wrap around the upper basin of Cajón Rodríguez. All these remnants are thought to have erupted in the Pliocene or earliest Pleistocene and, as undeformed intermediate lavas older than major canyon incision, they would conventionally be assigned to the Cola de Zorro Formation, a regional catch-all employed when individual undeformed eruptive centers remain unmapped. In area (3) just cited, packages of lava flows (units **arp** and **acs**; 53-62% SiO_2) that underlie the 1.5-Ma sheet of pyroxene ignimbrite (unit **igsp**) yield $^{40}Ar/^{39}Ar$ ages of ~2 Ma (Table 1). In area (2), the topmost andesitic lava gave a total-fusion age of 3.6 Ma, though the data were too erratic to yield a plateau age. In area (1), the divide-capping lavas extend northward beneath a thick pile of ignimbrites (northeast of the Puelche volcanic field; Figs. 1, 2), the top sheet of which gave Drake (1976) a K-Ar age of 1.06±0.04 Ma (Table 2); and 10 km farther north, Drake (1976) determined an age of 2.0±0.3 Ma for an undeformed pile of andesite lavas of similar topographic and stratigraphic position. All these undeformed remnants overlie folded or tilted volcanic (or subordinate volcanogenic sedimentary) rocks last deformed in the late Miocene.

There are several places in the LdM volcanic field where the older deformed, broadly andesitic, strata crop out-along the northwestern and southern shores of Laguna del Maule, on the walls

of the Saso and Rodríguez canyons to the west, and on the lowermost walls of upper Arroyo Botacura, where the strata are cut by an acid-altered 1.5-km² diorite stock. In all these areas, the volcanogenic strata dip 10-25° and are presumed to be Miocene. On the other hand, a stack of ~20 andesitic lavas and breccias (55-61% SiO_2) making up the southeastern wall of the LdM basin remains almost horizontal. The lowest (and thickest) flow exposed there yields a plateau age of 6.4±1.3 Ma, the topmost flow gives a total-fusion age of ~3.6 Ma, and a 1-km² diorite stock intruding the base of the wall yields a similar total-fusion age of ~3.6 Ma. The shallow magma-supply system for the extensive stack of lavas may have included elements now beneath the lake, the diorite stock itself, and dikes that cut lower flows of the stack.

PLIOCENE RHYOLITES

The only group of Pliocene rocks that we considered in any detail is a cluster of rhyolite lava domes northwest of Laguna del Maule that represent onset of the rhyolitic magmatism recurrent in the area ever since. Five discrete lava masses (lumped as unit **Trea**), 4 to 7 km north of the outlet dam, intrude and overlie Miocene rocks (Fig. 5). All five lavas are crystal-poor quartz-biotite-plagioclase high-silica rhyolite (75-77% SiO_2), and two of them yielded K-Ar ages of 3.74±0.12 Ma and 2.39±0.1 Ma (Table 2). All are extensively devitrified, having been glacially scoured of their glassy exterior facies, but local remnants of glassy vesicular margins, tiers of columnar joints, and variously oriented flow foliations show all of them to be independent extrusions rather than erosionally separated remnants. All five consist of cream-white to tan felsite, widely stained by rusty orange-brown films. The two rhyolite units exposed along the twin Aguirre canyons (Fig. 5) overlie and intrude a white nonwelded ignimbrite of similar composition and mineralogy that probably represents an early eruptive phase related to one or both of them. Those rhyolite lavas are overlain by a 1.5-Ma dacite ignimbrite (unit **igsp**, described next) and by mafic products of Volcán Aguirre (unit **mva**; 1.3 Ma), dikes of which also cut the rhyolites. Two additional rhyolites that crop out along the road rest on paleosols developed atop Miocene welded tuff, and the fifth rhyolite unit (northeast of the Río Maule) extends down into an exposed feeder that cuts stratified andesitic Miocene rocks.

Another Pliocene rhyolite (unit **Trcf**) forms the Botacura-Filume divide 6 to 9 km west of the outlet dam and 6 km southwest of the Aguirre rhyolite cluster just discussed. This 1.5 x 3-km lava flow has 250 m of relief and consists of biotite-plagioclase felsite (74.8% SiO_2), which is variously buff, cream, or pink and patchily iron-stained. Little glass is preserved except along a flow contact exposed in a northwest-facing landslide scarp, where the lava is also cut by an andesite dike probably related to one of the contiguous early Pleistocene mafic-to-andesitic edifices. The rhyolite overlies andesitic breccias and volcaniclastic sediments presumed to be Miocene, and it yields a $^{40}Ar/^{39}Ar$ age of 2.57±0.01 Ma (Table 1). The rhyolite lava is not itself hydrothermally altered, but rubble derived from it forms a major constituent of a landslide mass that extends 3 km northwest and is strongly acid-altered in its downstream half where it approaches the Arroyo de Botacura.

Another biotite-plagioclase rhyolite lava, undated but inferred to be Pliocene, crops out over an area of 1.5 x 2 km along both walls of Arroyo de Botacura at the confluence of Estero El Zorro. The deeply incised lava is white, in part hydrothermally altered, has 800 m of exposed relief on the south wall, and is in apparent fault contact with intracaldera biotite-rhyolite ignimbrite (unit **Tigr**), which was K-Ar dated at 3.4±0.8 Ma by Muñoz and Niemeyer (1982).

In addition, there are two small outcrops of Tertiary or early Quaternary rhyolite along the margins of Laguna del Maule. A 200-m-wide nose of hydrothermally altered, crystal-poor rhyolite crops out at the shoreline of the northeast arm of the lake (UTM grid 683/144). The poorly exposed white rhyolite is just outside the structural margin of the ignimbrite-filled 950 ka Bobadilla caldera, and it underlies or intrudes andesitic lavas and breccias assigned to early Quaternary unit **alz**. Still another rhyolite lava has limited exposure around a cove on the west shore of the northwest

arm of Laguna del Maule (590/102) and along the arroyo draining into it. The stony crystal-poor rhyolite crops out beneath west-dipping stratified andesitic lavas, tuffs, and breccias, which are altered, cut by several dikes, and presumed Miocene. If that age inference is correct, this rhyolite is significantly older than the Pliocene rhyolites 6 km north and northwest.

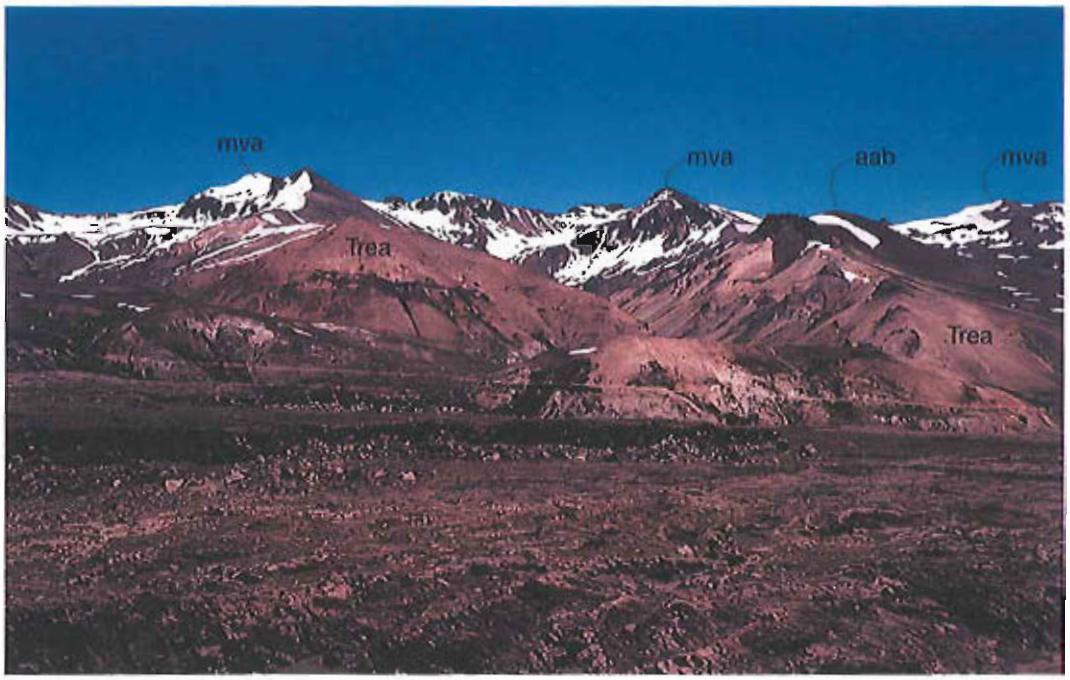

FIG. 5. View southwestward up twin Cajones Aguirre from flood-scoured scabland plateau of mafic lavas (unit **msm**) along Río Maule, 6 km downstream from Laguna del Maule dam. Just right of image center, roadway cuts through 2.4-Ma tan dome of high-silica rhyolite, which intrudes and rests on white 12.9-Ma biotite-rhyodacite ignimbrite. Canyon at center is flanked by two more tan masses of high-silica rhyolite, that on left yielding a K-Ar age of 3.7 Ma. Columnar jointing and lithologic zonation show all three rhyolites (unit **Trea**) to be separate extrusions. Ragged ridge along entire skyline consists of mafic lavas and breccias of erosionally ravaged edifice of 1.3-Ma Volcán Aguirre (unit **mva**). Snow-mantled ledges in upper canyons are 1.5-Ma welded pyroxene-dacite ignimbrite (unit **igsp**). Smooth red-brown scoria cone at upper right overlies all other units and is vent for andesitic lava flows (unit **aab**; 372±18 ka) that extend to road (to right of image). A 5-m-thick andesite dike that cuts rhyolite ridge at right is compositionally similar to unit **aab**, not **mva**.

PYROXENE-DACITE IGNIMBRITE OF LAGUNA SIN PUERTO (1.5 Ma)

Ridge-capping remnants of an extensive sheet of pyroxene-dacite ignimbrite (unit **igsp**) are conspicuous to the north and west of Laguna del Maule. The thickest exposure (300 m) lies 2 km northwest of the outlet dam, where it rests on the Pliocene rhyolites just described as well as on limited exposures of hornblende-dacite and mafic lavas of early Pleistocene age. Other remnants of the ignimbrite are 75-100 m thick atop Cordón de Constanza (7.5 km north of the dam); 100 m thick along the Filume-Saso divide southwest of Laguna Sin Puerto (8 km SW of the dam); 50-100 m thick along the western divide separating the LdM basin from the Río Saso; and 35 m thick on

the plateau east of the confluence of Estero Bahamondes and the Río de la Plata (15 km NW of the dam). In upper Arroyo Los Mellicos, 1 to 2 km southeast of Laguna Sin Puerto, a 1,200-m-long ledge of the ignimbrite (along with enclosing lavas) has slumped ~1 km downslope (~200 m vertically) from its *in situ* outcrop strip along the ridgecrest. Plagioclase separated from one large fiamma in the thick section above the dam yields a $^{40}Ar/^{39}Ar$ age of 1,484±15 ka (Table 1).

Most exposures are densely welded and cliff-forming, and, wherever exposed, the basal few meters consist of black vitrophyre. The rest is typically grey-brown, devitrified, eutaxitic, welded tuff rich in fiamme, which are generally strongly flattened, range in length from 1 to 40 cm, make up 15-30% of the rock, and tend to remain glassy throughout thick devitrified sections. Associated fallout and nonwelded ignimbrite zones have nowhere been recognized, though thin zones of lesser welding in the 300-m section close to the dam have eroded out as minor benches that divide the unit into as many as four conformable emplacement packages. Upper zones of vapor-phase alteration have been stripped except at the distal Bahamondes locality (UTM grid 496/250), where 10 m of buff to pale violet vapor-altered tuff caps the surviving remnant. Lithic inclusions are abundant, typically 5-10% but as much as 20% of the rock locally, and are mostly 1-5 cm but as big as 20 cm. By far the most abundant lithics are crystal-poor rhyolites, accompanied by a variety of crystal-richer intermediate lavas, scoriae, and hydrothermally altered clasts. Phenocrysts in the ignimbrite are predominantly plagioclase (1-2 mm) along with orthopyroxene and sparser clinopyroxene; hornblende, biotite, and quartz are absent. Fiamme have ~10% crystals, but the welded-tuff matrix ranges from 15% to 30%. Fourteen samples of individual fiamme from all sectors of the ignimbrite range in SiO_2 content from 64% to 70%.

The unit is not present on ridgetops or elsewhere around the eastern and southern sides of the LdM basin, though erratic blocks are common along valley floors in the southwest corner of the basin. All remnants are confined to a 120° northwesterly sector (240° to 360°) and lie within 8 km west, 15 km northwest, or 8 km north of the northwest arm of the present-day lake. Because pre-ignimbrite rhyolites, which dominate the lithic suite, are likewise confined to that sector, because the ignimbrite thins away from the area near the dam, and because no alternative source has been found in the surrounding region, we think the pyroxene-dacite ignimbrite erupted from the area now covered by the northwestern part of the lake. Since the same area underwent caldera collapse about 0.5 Myr later, during eruption of a sheet of biotite-rhyodacite ignimbrite (unit **igcb**), evidence for a 1.5-Ma caldera (or any alternative vent structure) has apparently been obliterated.

EARLY PLEISTOCENE ERUPTIVE UNITS YOUNGER THAN 1.5 Ma

Our knowledge of this interval (older than 0.78 Ma) is extensive but incomplete, owing to erosion and cover by younger eruptive units. We start by characterizing several deeply eroded polygenetic edifices, followed by a description of the caldera-forming biotite ignimbrite (unit **igcb**), an early postcaldera andesitic edifice, and a miscellaneous collection of monogenetic or orphan lavas known or inferred to be of early Pleistocene age.

NINE PRECALDERA POLYGENETIC EDIFICES

Two large intermediate volcanoes, Cerro Bayo and Volcán Laguna Fea (Fig. 4a), are each centered ~6 km into Argentina, beyond the limits of our mapping. What appear to be their apron lavas, however, extend across the border into the area investigated. The cores of both centers were hydrothermally altered and deeply eroded, while the flank lavas have been glacially ravaged, leaving ruggedly incised terrain in place of the former stratocones.

The narrow plateau that extends 7 km northward along the border from the cirque now occupied by Laguna Cari Launa (Fig. 7) consists of a package of at least nine pyroxene-andesite lava flows (55-62% SiO_2), widely platy and each 10-30 m thick. The plateau-capping package (unit **apg**) dips gently (3-5°) west or northwest away from the **Cerro Bayo** center 6 km farther east, but it steepens to 10-15° where it dips beneath the rhyolite of Cerro Negro (unit **rcn**; 460 ka) and the mafic edifice of Volcán Munizaga (unit **mvm**; 900 ka), apparently pitching into whatever paleodrainage was ancestral to the LdM basin.

South of Laguna Fea (Fig. 7), an edifice at least 12 km across is evident from its gutted core and its remnant ramparts that dip radially. The apron of lavas (unit **avf**) from what is here called **Volcán Laguna Fea** extends to the south shore of Laguna Fea, and some of the lavas are also preserved along the north rim of that lake-filled glacial trough, where they overlie southward-dipping Tertiary breccias and tuffs. At its eastern end, the north-rim remnant is a gently east-dipping package more than 250 m thick consisting of at least seven similar pyroxene-dacite lava flows (64% SiO_2). North of the central part of Laguna Fea, the rim package is more than 350 m thick and consists of four lava flows (63-65% SiO_2) that dip only 5°NE; the second and thickest of the flows yields a plagioclase $^{40}Ar/^{39}Ar$ plateau age of 1,582±9 ka (Table 1). These two (apparently related) packages (unit **dlf**) are intruded, physically separated, and overlain by a 1-km-wide dome of crystal-poor biotite rhyolite (unit **rlf**) more than 300 m thick, which gave a biotite $^{40}Ar/^{39}Ar$ age of 1,353±17 ka (Table 1). On Peak 3,104 the rhyolite is convolutely flow-foliated and craggily eroded, but its flat-topped north ridge appears to be a near-primary surface. Six kilometers northwest, on the rim above the northwest end of Laguna Fea, an isolated 1-km-long remnant of a hornblende-opx-plagioclase dacite lava flow (65% SiO_2; also assigned to unit **dlf**) caps Peak 3,056, is 100-m-thick, has striking columnar joints and flow foliation, rests on Tertiary tuffs and lavas, and dips gently northward away from its presumed source at Volcán Laguna Fea. Likewise on the north rim of Laguna Fea and 3 km east of Peak 3,056, a small plagioclase-poor hornblende-biotite rhyolite dome (unit **rnf**; 75% SiO_2) forms Peak 2,994, and 500 m north of it a plagioclase-rich opx-biotite rhyodacite knob (unit **rdap**; 69% SiO_2) with flaring sets of columns (either ice-contact or shallowly intrusive) is exposed on the northeast face of Peak 2,818. Whether these undated silicic units represent peripheral vents temporally related to the Volcán Laguna Fea center is unknown.

Another inadequately known intermediate volcano of early Pleistocene age, here called **Volcán Filume**, is centered 10 km west of Laguna del Maule (Fig. 8). A 450-m-thick stack (unit **mcf**) of at least 30 gently dipping, olivine- and pyroxene-bearing, andesitic lavas and breccia sheets is exposed on the eastern slope of Cordón Filume where it is cut by a columnar-jointed intrusive mass ~200 m in diameter. A few andesitic lava flows (53-59% SiO_2) extend to the north where they bank against the Pliocene rhyolite (unit **Trcf**; 2.57 Ma) and to the east where they underlie the pyroxene-dacite ignimbrite (unit **igsp**; 1.5 Ma). Just west of Cordón Filume, a more extensive (and inferred correlative) outflow apron of gently dipping olivine-andesite lava flows (unit **mas**; 53-54% SiO_2) thickens westward to ~300 m where it banks against a thick pile of (probably caldera-filling) biotite-rhyodacite ignimbrite, which was K-Ar dated by Muñoz and Niemeyer (1984) at 3.4±0.8 Ma. The undated eruptive products of Volcán Filume appear to be fairly well bracketed between ~2.5 and 1.5 Ma.

Eroded remains of three more mafic volcanoes are preserved 5-8 km west and northwest of the outlet arm of Laguna del Maule. Centrally, each has an extensive stratified fragmental facies, but their lava aprons and their preserved widths of 4-7 km indicate that each was a modest composite cone or steep shield rather than just a big scoria cone. All three have similar phenocryst assemblages, containing varied proportions of clinopyroxene, olivine, and plagioclase. Opposing dips indicate that the three were independent, although they are thought to be of roughly similar age.

Northernmost of the three is **Volcán Aguirre**, which caps the divide between Cajón Bahamondes and the Aguirre tributaries of the Río Maule (Figs. 5, 9). Products preserved (unit **mva**)

are dark-grey mafic lavas and breccias (51-56% SiO_2), which are 250-350 m thick on the eastern flank but probably thicker on the west where the base is widely concealed and a considerable fraction of the edifice was removed by glaciation along the valley of the Bahamondes. The mafic pile variously overlies Miocene ignimbrite (unit **Tigh**), Pliocene rhyolite lavas (unit **Trea**), and the pyroxene-dacite ignimbrite (unit **igsp**; 1.5 Ma). In a general way, the lower half of exposed sections consists dominantly of massive coarse breccia that grades up into stratified breccia; these are overlain by lava flows that now cap ridgecrests and appear to have extended slightly above the ice of successive glaciations. A thick lava flow that caps the section on Peak 2,707 yields a $^{40}Ar/^{39}Ar$ plateau age of 1,290±13 ka (Table 1). The breccias are thought to be proximal phreatomagmatic explosive deposits, rich in basement lithics and in both dense and scoriaceous juvenile clasts. The deposits are poorly sorted, with a range of angular to subrounded clasts as big as 1.5 m in a matrix of coarse ash. The lower part of the pile may include subglacial hyaloclastite, widely palagonitized, while the better stratified upper part includes block-and-ash flow deposits and subordinate scoria falls. The northern and southern ends of the outcrop belt consist dominantly of lava flows. The principal vent is eroded out as a 500-m-wide plug that stands 200 m high on Peak 2,784 and exhibits sets of inclined columns. Several mafic dikes nearby cut the underlying units, and remnants of a lesser flank vent on the north wall of Cajón Chico Lo Aguirre crops out as 200-m-wide crag with columns in several thick tiers. Most products have sparse plagioclase phenocrysts but carry abundant microphenocrysts of plagioclase, olivine, and subordinate cpx; a few flows differ in being rich in plagioclase phenocrysts.

A few kilometers southwest of Volcán Aguirre, a second deeply eroded mafic cone, here called **Volcán Botacura**, forms the divide between the Filume and Botacura drainages (Fig. 8) and is similarly dominated by fragmental deposits (53-56% SiO_2) that dip radially. The main pile (unit **mvb**), centered on Peak 2,920, consists of more than 500 m of dark-grey, poorly sorted, thick-bedded breccias interpreted as explosive phreatomagmatic deposits. Many layers are proximal fall deposits in beds 5 to 15 m thick. Enclosed in a coarse-ash matrix, larger clasts show a range of vesicularity, with scoria lapilli and bombs slightly outnumbering denser ejecta that include prismatically jointed blocks as big as 1 m. The 4-km-long edifice may have been in part fissure-fed. At its southwestern end, a subdued 1-km-wide shoulder strewn with brick-red scoria, which is compositionally identical but volcanologically in striking contrast to the main pile, was probably a flank scoria cone on strike with the main vent system. This red-scoria segment is rich in partially melted rhyolite xenoliths torn from the Pliocene rhyolite lava beneath it, whereas the main pile, which rests on andesitic Tertiary bedded tuffs and sediments, lacks such rhyolitic lithics. A few mafic lava-flow remnants are preserved atop the fragmental pile and along the southern flank where they overlap the rhyolite. All products are rich in plagioclase and olivine phenocrysts along with minor cpx. The massive devitrified interior of a 1-m block from high on the edifice gave a $^{40}Ar/^{39}Ar$ age of 1,324±20 ka (Table 1), only marginally older than neighboring Volcán Aguirre.

Centered 3 km southeast of Volcán Botacura lies a third deeply eroded mafic edifice (53-56% SiO_2), which is here called **Volcán Sin Puerto** after the lake just east of it (Fig. 8). Radial dips define a modest edifice 4 km wide, of which the surviving components (unit **msp**) include a 150-m-high twin-peaked plug ~400 m wide, an adjacent remnant of a stratified scoria and agglutinate cone (Peak 2,889), a peripheral apron of glaciated lava flows, and two ice-sculpted ridges consisting of a few thick flows that extend northeast and southwest from the plug. Most products are phenocryst-poor, containing sparse plagioclase, olivine, and cpx. The scoria-cone remnant includes bombs that exceed 1 m, and parts of its lower slopes are palagonitized. Lava flows to the southwest overlie the pyroxene-dacite ignimbrite (unit **igsp**; 1.5 Ma), and those to the northwest bank against the Pliocene rhyolite (unit **Trcf**). Two 100-m-thick mafic lava flows (54-56% SiO_2) each have columnar jointing suggestive of ice-contact emplacement; one is phenocryst-rich and forms a broad bench west of Laguna Sin Puerto while the other is crystal-poor and caps the adjacent northeast ridge. The two flows sandwich a 150-m-thick sheet of crudely stratified

dacite breccia (unit **dsp**; 65.6% SiO_2), unknown elsewhere and of uncertain origin. The glassy dacite clasts contain biotite, amphibole, opx, and abundant plagioclase phenocrysts. Products of the center have not been dated, but its degree of dissection is more severe than that of nearby Volcán Botacura (1.3 Ma) despite its much greater proportion of lavas to fragmental deposits. There is little doubt that Volcán Sin Puerto, too, is of early Pleistocene age.

At the western margin of the distributed volcanic field, the remains of another early Pleistocene mafic volcano (51-57% SiO_2) are strikingly exposed for 5 km along the steep north-south ridge called Puntilla Los Ñirales, though younger units cover much of its northern half. The products of what is here called **Volcán Ñirales** (unit **mvñ**) also crop out in tiny windows along the canyon of Estero El Zorro 2-3 km east, but best exposures are along the steep wall of the glaciated trough, Valle Chico (Fig. 8), where a 550-m stack of ~30 lavas (each 5-25 m thick) is exposed in the south and ~17 lavas form a 300-m section exposed farther north. All products examined contain olivine and subordinate cpx, but plagioclase phenocrysts range from sparse to abundant in different flows. A lava flow at the north limit of the exposures gave a K-Ar age of 1,037±36 ka, and one from the top of the section at the south end gave 914±21 ka (Table 2). The vent complex has been deeply eroded but was near Peak 2,623, the southeast face of which consists of numerous thin lavas and agglutinates, stratified red breccias, and red scoria falls, all cut by numerous near-vertical dikes of varied orientation. The dikes also cut the units exposed beneath the edifice, which are propylitized Tertiary andesitic lavas, tuffs, and sediments on the west and Pliocene biotite-rhyodacite ignimbrite (3.4±0.8 Ma) on the east, separated by a near-vertical segment of an apparent caldera wall that strikes south across Arroyo Botacura (Fig. 8). The highest point on the ravaged edifice of Volcán Ñirales (Peak 2,623) is a 350-m-long remnant of a phenocryst-rich dacite lava flow (unit **dvñ**; 65.6% SiO_2) ~50-m-thick, which may be related to a set of 5 m thick vertical dikes that strike N80°E across the mafic edifice ~100 m farther north. The dacite carries phenocrysts of amphibole, biotite, opx, and as much as 25-30% plagioclase.

Near the northeast margin of the LdM volcanic field (Fig. 6) are two additional deeply eroded centers: andesitic Volcán La Zorra, which lies adjacent to the northeast arm of Laguna del Maule, and Volcán Munizaga, a mafic stratovolcano near Paso Pehuenche and contiguous with the much younger edifice of Cerro Campanario. The apparent core of **Volcán La Zorra** (3 km WSW of Paso Pehuenche) consists of a lava dome and radially dipping stacks of lavas (unit **alz**), all hydrothermally altered. Stacks of fresher, gently dipping, andesitic apron lavas (58-62% SiO_2) crop out along both walls of the northeast arm of the lake and also extend several kilometers northward from Quebrada La Zorra into Estero Bobadilla. In the latter area, their contact with (similarly eroded) andesitic lava flows derived from a younger center to the west (Volcán Atravesado; unit **ava**) is inadequately defined, as both sets are nearly horizontal where they meet. An andesitic lava from the northern part of Volcán La Zorra was K-Ar dated by Drake (1976) at 1.16±0.04 Ma, and another near Paso Pehuenche gave us a $^{40}Ar/^{39}Ar$ age of 1013±28 ka (Table 1). The lavas carry opx, cpx, and abundant plagioclase phenocrysts, and a few flows also have subordinate opacitized amphibole.

In contrast, the products of **Volcán Munizaga** (which overlie those of Volcán La Zorra) are exclusively mafic (unit **mvm**; 50-55% SiO_2), containing 7-15% plagioclase phenocrysts, ~2% olivine, and sparse cpx. The remains of the edifice now cover a 4 x 7 km area, with relief of more than 600 m. The altered fragmental core of the edifice has been glacially gutted, and is now occupied by a southeast-facing cirque adjacent to the present-day high point at Peak 3,132. On the cirque headwall, as many as 10 dikes cut the stratified fragmental interior of the edifice. Thin flank lavas and agglutinates dip radially away from this central high and, on the north and west sides, extend to steeply eroded scarps that expose 20 or more flows in stacks 250-350 m thick. A sample from high on the western scarp of the west ridge gave a $^{40}Ar/^{39}Ar$ plateau age of 898±20 ka, consistent with its position overlying the lavas of adjacent Volcán La Zorra (unit **alz**).

BIOTITE-RHYODACITE IGNIMBRITE AND BOBADILLA CALDERA

The most voluminous eruption in the Quaternary history of the volcanic field resulted in collapse of an 80-km^2 elliptical caldera with dimensions of 12-13 km north-south and 8 km east-west (Figs. 6, 7, 10). The subsidence affected the northern half of the basin now occupied by Laguna del Maule, which has subsequently been enlarged by glacial erosion and modified by several postcaldera lava flows. The caldera-forming eruptive unit (**igcb**) is a biotite-plagioclase rhyodacite ignimbrite that is preserved only within the caldera, except for a small outflow remnant on its northeast rim. It is widely exposed along the north shore of the lake and in the Bobadilla canyons a few kilometers farther north; much more of the ignimbrite, no doubt, extends beneath the central part of the lake, which is 35-50 m deep. We previously reported a biotite K-Ar age of 1.09±0.1 Ma (Hildreth *et al.*, 1991), but we now prefer a plagioclase $^{40}Ar/^{39}Ar$ age of 950±7 ka (Table 1); both mineral separates were extracted from individual fiamme (collapsed pumice) from intracaldera welded tuff. Compositions of eight fiamme chemically analysed range from 66 to 72% SiO_2.

Surface exposures of the ignimbrite, everywhere glacially modified, range from densely to moderately welded or, if nonwelded, intensely vapor-phase altered and indurated. Most exposures are devitrified and crumbly or flaky, although fiamme remain glassy in many places and, where banked against the northwestern caldera margin, much of the tuff is vitric. In general, the degree of welding decreases upward, as vapor-phase alteration increases. Nowhere, however, is the base of the intracaldera ignimbrite exposed, even though the thickness exposed north of the lake exceeds 500 m. On the divide between the Bobadilla canyons, the 250-m-thick exposure consists of ~100 m of grey-brown welded tuff overlain by 150 m of pale grey vapor-altered tuff, proportions that suggest a far greater unexposed thickness for the unit. The islets and promontories at the north end of the lake (Fig. 10) are predominantly punky vapor-altered tuff with lithophysae and rotten pumices, but densely welded eutaxite crops out at beach level.

The ignimbrite contains 10-20% plagioclase, 2-5% biotite, and sparse quartz, orthopyroxene, clinopyroxene, and FeTi oxides. Fiamme also show a range of about 15±5% plagioclase phenocrysts. Pumice clasts in nonwelded vapor-phase zones range from granules up to 30 cm in diameter. Fiamme in welded zones range from tiny wisps to a measured maximum of 45 x 8 cm and typically make up 15-30% of the rock. Lithic fragments are notably abundant, widely constituting 10% of the rock and consisting principally of varied andesites along with subordinate felsite and hydrothermally altered clasts. Most lithics are smaller than 4 cm, but some are 10-15 cm. In several sections, the lithic abundance appears to decline upward from ~10% to less than 5%, and exposures on the islets may be the lithic-poorest of all, perhaps because farthest from the caldera walls. On the other hand, a few hundred meters inboard (south) of the northwestern wall, at least two 10 m thick sheets of coarse lithic wall-collapse breccia are intercalated within the ignimbrite.

Owing to glacial reduction of the surrounding landscape and protection of the tuff by postcaldera lavas, the northern half of the caldera is no longer a physiographic depression but, instead, a lava-capped rugged highland. Lacking such protective lavas, intracaldera ignimbrite of the southern half was glacially scoured, deepening the lake basin. Structural margins of the caldera are exposed only along the north and northwest sides, where the tuff banked against a truncated stack of 25 or more hydrothermally altered, Miocene andesitic lavas that dip ~25°N, away from the caldera. The northeastern margin is concealed by the postcaldera lavas, and the eastern margin was intruded by an enormous middle Pleistocene rhyolite dome complex (unit **rcn**) that now forms the steep wall of the lake basin (Fig. 10). The southern structural margin lies beneath the lake, probably at the south end of its deep central floor, and the western margin is concealed by a postglacial rhyolite coulee (unit **rle**), which may have flowed along a paleo-outlet trough that had been incised along the ring-fault zone. Stratified Miocene andesitic lavas, tuffs, and breccias are exposed on the northwest, north, and southeast walls of the caldera, as well as along the southern and northwestern shorelines of the lake (Fig. 7).

POSTCALDERA LAVAS OF VOLCÁN ATRAVESADO

A variety of intermediate lava flows (unit **ava**), glacially dissected, faulted, and largely andesitic, overlies the biotite-rhyodacite ignimbrite along the north rim of the LdM basin and around the Bobadilla canyons as far as 7 km north of the lake (Fig. 6). No central vent is preserved, but a preponderance of 5-15° northward dips and several intermediate dikes that cut the ignimbrite near the lakeshore suggest that the lavas erupted from within the intracaldera basin. If this is correct, then only the northern flank of this early postcaldera edifice is preserved, the main portion atop the ignimbrite within the basin having been glacially destroyed. The surviving package of lava flows is as thick as 350 m on the high divide north of the lake and 250 m on the ridges that separate the Bobadilla canyons and the Cajón del Atravesado (for which the assemblage is here named). Of 20 lava flows sampled, 18 are two-pyroxene plagioclase-rich andesites with 56 to 64% SiO_2, while a capping cpx-olivine-plagioclase flow has 53.5% and an outlying dome remnant (UTM grid 685/194) of hornblende-plagioclase dacite has 67%.

A phenocryst-poor, chunky jointed, partly glassy andesite lava flow (60.5% SiO_2) that rests on the gullied surface of the ignimbrite just above the road along the north shore of the lake gave a K-Ar age of 990±80 ka (Hildreth *et al.,* 1991; Table 2). Its ubiquitously intricate jointing and glassiness and its local brecciation suggest chilling by lakewater or ice. Atop this flow is a stack of at least six plagioclase-rich pyroxene-andesite lava flows and breccias, each 25-75 m thick, that thickens eastward, overruns the caldera margin, and **laps** east over precaldera andesitic lavas assigned to Volcán La Zorra. Crudely stratified breccias (57-62% SiO_2), thick, very coarse, and dark-brown-weathering, that make up the east part of the scarp just north of the lake (UTM grid 670/157) may be the most proximal surviving products.

A few kilometers north of the divide between the lake basin and the Bobadilla canyons, the andesite stack atop the ignimbrite still consists of 6-8 flows, each 25-100 m thick, but dips have diminished toward subhorizontal. The topmost flow of pyroxene andesite capping Peak 2,753 on the divide between the Bobadilla canyons gave a K-Ar age of 720±80 ka (Drake, 1976; Table 2). Overlying the andesite pile atop the drainage divide just north of the lake is a 2-km-long remnant of a plagioclase-rich biotite-rhyolite lava flow (unit **rca**), glacially stripped but still 120 to 180 m thick, that yields a $^{40}Ar/^{39}Ar$ plateau age of 712±13 ka (Table 1). The pale-grey lava is locally underlain by 10-20 m of white, massive, nonwelded, lithic-rich, biotite-rhyolite tuff that probably fills their common vent. The northeast end of the lava flow and subjacent andesites are affected by acid-sulfate alteration.

ISOLATED UNITS OF EARLY PLEISTOCENE AGE (MOSTLY MONOGENETIC)

A dozen map units fall into this catch-all collection of isolated monogenetic lavas and remnants of lava flows or ignimbrites for which vents have generally not been identified. Two are ridge-capping sets of subhorizontal andesitic lava flows on the western rim of the Laguna del Maule basin:

(1) Unit **ams** includes three or four pyroxene-andesite lava flows (61-63% SiO_2) that directly overlie the pyroxene-dacite ignimbrite (unit **igsp**; 1.5 Ma) along the crest of the divide between the Río Saso and the basin.

(2) unit **arp** consists of remnants of a set of three (older and compositionally unrelated to **ams**) pyroxene-andesite lavas (60.5-62% SiO_2) that cap Peaks 2,918, 2,856, and 2,942 on the high southwestern divide that separates the basin from headwaters of Cajón Rodríguez (Fig. 8). The top flow of the three has stout vertical columns, is more than 120 m thick, and yields a $^{40}Ar/^{39}Ar$ plateau age of 2,010±23 ka (Table 1).

Two more of the twelve are small lava-flow remnants near the northern edge of the volcanic field.

(3) Unit **mqf** is an olivine-cpx-plagioclase andesite lava flow (53.7% SiO_2) that forms an isolated 300-m-wide bench at the head of Quebrada Fiera, high on the south slope of Cerro Galaz, 600 m

now utterly inverted. The flow gave a K-Ar age of 1.04 Ma (R.E. Drake, Berkeley Geochronology Center, personal communication, 1990), but its source vent is unknown.

Two additional orphan units are ignimbrite remnants preserved on high divides in the northern part of the volcanic field.

(5) Unit **igbc** is an opx-plagioclase-rhyodacite (69% SiO_2) densely welded tuff, as thick as 150 m, that extends 2.5 km along the Bobadilla-Campanario divide, its base lying 300-400 m above the adjacent valley floors. It has a flat-lying vitrophyric base but is mostly devitrified and dark grey-brown with prominent subhorizontal and vertical jointing. Andesite-dacite lithics are ubiquitous but zonally distributed, ranging from abundant to sparse. The isolated ignimbrite remnant rests on Miocene strata that dip ~25°N, and it laps onto the vapor-phase zone of an outflow remnant of the biotite-rhyodacite ignimbrite unit **igcb** (950±7 ka). It is overlain by an andesite lava scrap on Peak 2,672 that was K-Ar dated at 1.06±0.03 Ma (Drake, 1976). The dating obviously requires refinement, but the unit is unequivocally early Pleistocene. Its source is unknown and no correlatives are present in the LdM volcanic field, although we think the unit is an outlier of a 650-m-thick stack of ignimbrites along the international border ~20 km NNE (Drake, 1976; Hildreth *et al.*, 1999).

(6) Unit **igeb** is a 50-m-thick ridgecrest remnant of weakly to densely welded pyroxene-andesite ignimbrite (61.5% SiO_2) that extends for 600 m along the continental divide about 5 km west of the summit of Cerro Campanario (Fig. 6). The tuff is pale-grey and devitrified but rich in black glassy discoid fiamme. It carries sparse plagioclase phenocrysts and sparser microphenocrysts of cpx and opx. The remnant rests on a subhorizontal stack of mafic and andesitic lavas that form most of the narrow, glacially sculpted ridgecrest. An ignimbrite plateau 5 km farther northwest may be correlative but was not investigated. Its source is unknown and the unit is undated, though its flat-lying position atop the high divide, more than 800 m above the floors of flanking canyons, virtually requires that it be early Pleistocene or older.

Two of the twelve isolated older units are dacite lavas.

(7) Unit **dab** is a grouping of convenience, a cluster of dacitic lavas poorly exposed along the upper Arroyo de Botacura (Fig. 9) that may include flows of various ages. Three cliff-forming flows (64.5-67.7% SiO_2), each 30-100 m thick, are exposed only as ledges at the foot of the northwest wall of the valley where they are overlain by much younger mafic and rhyolitic lavas, which probably also cover their vent areas to the north. Two are pyroxene dacites and the uppermost (and most silicic) a plagioclase-rich hornblende-hypersthene dacite. The thickest of the three yields a $^{40}Ar/^{39}Ar$ plateau age of 924±37 ka (Table 1). Facing these on the southeast side of the valley is a parallel pair of 1-km-long ridges, elongate downvalley, each a 300-m-wide remnant of pyroxene-dacite lava ~75-m-thick. They overlie bedded tuffs and volcaniclastic sediments (presumed Miocene), and the southerly one appears to bank against the base of the Volcán Botacura edifice (unit **mvb**; 1.3 Ma). On the north bank of Arroyo de Botacura, 1.5 km east of these, a coarsely blocky flow-breccia of glassy plagioclase-rich hypersthene rhyodacite (69.3% SiO_2) crops out poorly in vegas on the Bahamondes divide. Vents are covered and unknown for all these early Pleistocene lavas.

(8) Unit **dpr** is a convolutely flow-foliated, plagioclase-rich opx-hornblende dacite lava (63% SiO_2) more than 250 m thick that supports a prominent mesa called La Puerta de Rodríguez in the headwaters of Cajón Rodríguez (Fig. 8). Cliff-forming on most sides, the 1.7-km-long remnant is widely glassy, brecciated, and columnar with several tiers of columns, both internal and basal. It is overlain by two thin andesitic lava flows on the mesa top, and it rests on a thick pile of Miocene andesitic lavas and tuffs that dips ~25°S. Because its base lies 500 m above the modern valley floor and because it filled a broad depression (not a canyon), we infer the lava to be no younger than early Pleistocene. It may be a glacially modified dome rather than a flow, as no other remnants are preserved in any direction.

The final four isolated units are silicic, monogenetic, and appear to have erupted where preserved.

(9) The **Rhyodacite of Cordón Las Romazas** (unit **rdcr**) is a flow-foliated lava (71% SiO_2) as thick as 200 m that flowed more than 5 km gently westward (~5°) along what is now the Cordón

Las Romazas, the Saso-Botacura divide. Eroded into three separate remnants, all lying along the ridgecrest, the plagioclase-rich hornblende-biotite lava flow appears to have vented beneath the easternmost exposure (Peak 2,757). Crumbly crystal-rich vitrophyre is subordinate to sheared, massive, or spherulitic and vuggy felsite; basal columnar zones as thick as 50 m are developed locally. The base of the lava is ~800 m above the adjacent valley floors and rests directly on Pliocene biotite-rhyodacite ignimbrite (3.4±0.8 Ma; Muñoz and Niemeyer, 1984). Only 500 m northeast, the ignimbrite is in contact with a hydrothermally altered rhyolite mass that extends down to the valley floor (Fig. 8). We infer the rhyolite to be related to the caldera-forming Pliocene ignimbrite episode and the glassy undated rhyodacite lava (unit **rdcr**) to be much younger, though its position along the high divide suggests that it is no younger than early Pleistocene. Either the topography

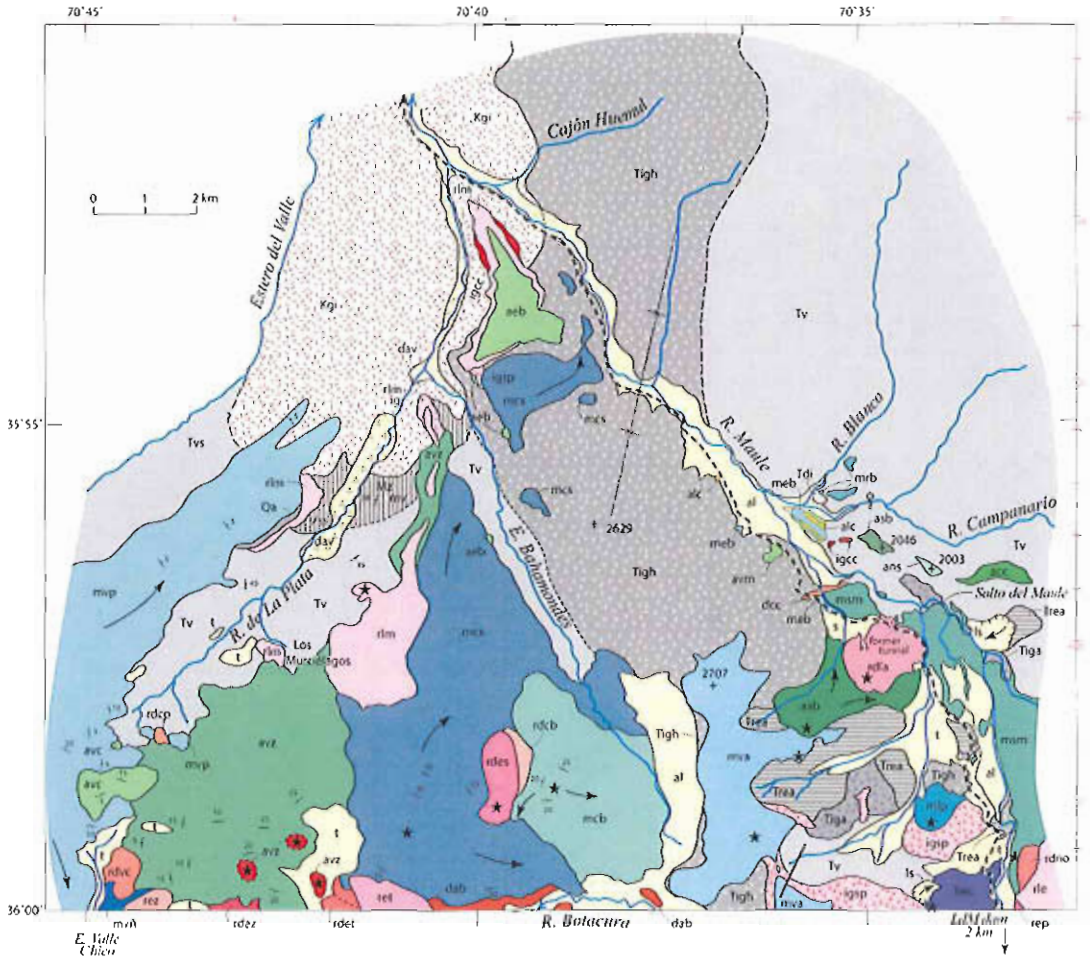

FIG. 9. Simplified map of northwestern quarter of LdM volcanic field, bounded approximately by Volcán Pellado, Río Botacura, and Río Maule. All units are discussed in text and unit labels identified alphabetically in Appendix 1. Colors and other symbols as in figures 6, 7, 8. Major streams in blue; lone road (CH 115) follows Río Maule. Additionally, **Kgi** = 80-Ma Los Indios granitoid pluton; **Mz mv** = metavolcanic wall rocks intruded by that pluton; **Tigh** = mid-Miocene synclinally deformed silicic ignimbrite of Cajón Huemul. Marginal ticks are UTM grid in km east and north, as on IGM topographic maps.

has since been very severely inverted or the glassy lava flowed westward along a groove then separating glaciers that filled the flanking valleys.

(10) The **Rhyolite of Las Salinas** (unit **rls**) is a cryptodome of biotite felsite (72.4% SiO_2), ovoid in plan, on the headwall of upper Cajón Rodríguez (Fig. 8). It intrudes deformed and dike-ridden andesitic lavas and tuffs (presumed Miocene), and its glacially scoured surface everywhere exhibits small-scale (~10 cm wide) columns, which are oriented vertically in the center but rotate toward horizontal at the peripheral contacts. The 450 x 700-m intrusion has ~250 m of exposed relief and consists of slightly glassy to finely crystalline felsite that contains ~10% plagioclase phenocrysts (1-2 mm), ~3% biotite, and minor hornblende. There is no significant alteration other than rusty orange or pink staining along columnar joint surfaces.

(11) Unit **rddp** is a rhyodacite dike (71% SiO_2), ~5 m thick, exposed 1 km south of Laguna del Piojo and 1 km west of the postglacial Las Nieblas rhyolite coulee (Fig. 7). Vertical and oriented east-west, the felsite dike cuts across a north-facing hillslope developed on a stack of andesitic lavas and fragmental-flow deposits more than 600 m thick. Presumed Pliocene or older, the stack is probably part of the erosionally receding southwest wall of the Bobadilla caldera (950 ka). The rhyodacite dike has several percent phenocrysts of plagioclase and biotite, along with minor hornblende and zeolite amygdules. Its age is unknown but likely to be precaldera, though its freshness suggests that it is younger than Miocene.

(12) Finally, the **Rhyodacite of Lo Aguirre** (unit **rdla**) is a 1.5 x 1-km-wide lava dome (67-69% SiO_2) on the south wall of the Río Maule where formerly penetrated by a tunnel (now a roadcut) at the top of the steep grade called Cuesta Los Cóndores (Fig. 9). The dome has as much as 450 m of exposed relief and is flow-foliated throughout and marginally strongly columnar. The cliffy exposures near and below road level may have originally been shallowly intrusive (or ice-contact) and those at higher levels extrusive. Most of the unit is at least partly glassy, although felsite is common on the ridgetop and oxidation and vapor-phase alteration are widespread. Remnants of brecciated carapace on top exhibit castellated erosion. Contacts with the Miocene ignimbrite (unit **Tigh**) it is inferred to intrude are nowhere exposed because the dome is surrounded by younger units. The rhyodacite contains 5-10% plagioclase phenocrysts and 1-2% each of biotite, hornblende, and opx, along with minor cpx and common mafic enclaves and blebs. Felsite from the summit of the dome yields a plagioclase K-Ar age of 881±73 ka (Table 2).

MIDDLE PLEISTOCENE ERUPTIVE UNITS (780-126 ka)

Numerous volcanic units of this age interval are scattered across the entire width of the LdM field, from the arc front to Argentina, and they are generally better known than older ones owing to better preservation and less cover. Within the map area, we recognize 33 eruptive units of middle Pleistocene age, including three stratovolcanoes; one large shield; six modest scoria, spatter, and lava cones; two ignimbrites; 12 discrete lava domes and flows; one dike; and eight remnants for which vents have not been identified.

THREE MIDDLE PLEISTOCENE STRATOVOLCANOES

The three polygenetic stratocones of middle Pleistocene age are compositionally varied, deeply eroded glacially, and well separated from each other. Oldest of the three is **Volcán El Zorro** (unit **avz**) centered on the divide between Estero Botacura and the Río de la Plata ~15 km WNW of the outlet dam (Fig. 9). Its lava-flow apron stretches 9 km north-south, but the edifice is exposed east-west for only 4 km between upper Valle Chico and the overlapping younger shield lavas of Cerro San Pedro. The southern half of the ice-ravaged stratocone is deeply gutted by Estero Ter-

neros and Estero El Zorro, at the head of which a 350-m-wide microdiorite plug (57.4%% SiO_2) is well exposed. A second former vent appears to be represented at the head of Estero Terneros by a coarse breccia mass, southwest-dipping stratified agglutinate, several dikes, and another plug. Walls of these south-opening cirque-headed canyons provide more than 600 m relief, revealing stacks of 5-12 mafic and andesitic lava flows (52-61% SiO_2) and many intercalated proximal scoria falls. Also exposed on the steep Zorro-Terneros divide are coarse proximal vent breccias, crudely stratified, very thick, and gray to orange-brown. The more gently sloping ice-scoured surface to the north is a beveled stairstep stack of lava-flow benches, proximally cut by dikes and locally mantled by intercalated remnants of brick-red agglutinate and scoria. Nearly all products of Volcán El Zorro carry phenocrysts of cpx, olivine, and abundant plagioclase in varied proportions, and some have opx as well. Some thin proximal lava flows grade into agglutinate and were probably fountain-fed; most flows, however, are 10-30 m thick and a few as thick as 100 m. Thick glassy zones with chunky or columnar jointing are common and suggest ice-contact emplacement. An andesite lava near the top of a stack exposed on the northwest cirque headwall of Estero El Zorro (just below Peak 2,786) gave a K-Ar age of 429±8 ka (Table 2).

On the continental divide at the northeast edge of the map area, **Cerro Campanario** (unit **mcc**) is a steeply ice-sculpted mafic stratocone 6-8 km in diameter (Fig. 11). Although the highest peak in the area at 3,943 m, it rests on Jurassic basement as high as 3,000 m, so its eruptive volume was probably no more than 10-15 km^3, of which about half is preserved today. Its dike-laced fragmental core, the radial ramparts eroded from its lava-flow apron, and its radiometric ages of ~150 ka were discussed in detail by Hildreth *et al.* (1998). Rich in phenocrysts of olivine and plagioclase along with sparse cpx, all eruptive products sampled are fairly uniform in composition (54.1-54.4% SiO_2). In common with many shields and stratocones worldwide that are monotonously mafic compositionally, Cerro Campanario may have grown during an eruptive lifetime no longer than 103 to 104 years (Hildreth *et al.,* 1998).

At the northwest edge of the map area, **Volcán Pellado** (unit **mvp**) is another large glacially eroded edifice, but, in contrast to Cerro Campanario, its products have a wide compositional range (52-62% SiO_2), and it had an eruptive lifetime (~188 to 83 ka) at least as long as 100 kyr (Singer *et al.,* 1997), continuing into the late Pleistocene. Its hydrothermally altered central-vent complex and its radially distributed apron lavas are summarized by Singer *et al.* (1997), who estimated a present-day volume of 12.5 km^3 for the ice-ravaged volcano, a value plausibly only half of what erupted. Two radial aprons of Volcán Pellado lavas frame the western margin of our map: one that extends 10 km south along Valle Chico and another that extends 10 km northeast along the crest of Cordón Loma Seca (Fig. 9). Recurrently glaciated, the floor of Valle Chico is a stairstep series of ice-scoured benches representing valley-confined lava flows (53-59% SiO_2), 30 to 100 m thick. The most distal and perhaps oldest of the Valle Chico flows yields a $^{40}Ar/^{39}Ar$ plateau age of 151±3 ka (Table 1). Largely overlying these lavas are remnant stacks of 5-10 thinner flows, each flow typically 8-20 m thick, preserved as sidewall veneers banked against older rocks on the east and west walls of the glacial valley. One such flow in mid-stack on the east wall gives a $^{40}Ar/^{39}Ar$ plateau age of 114±6 ka (Table 1). The stack of Pellado lavas capping Cordón Loma Seca, a 2-km-wide flat-topped ridge separating two glacial canyons, consists of as many as 13 flows proximally and only four distally. Many of these flows (55-59% SiO_2) are ~30 m thick and a few are as thick as 75-150 m, suggesting lateral confinement during outflow, plausibly by glaciers that then filled the adjacent parallel valleys (cf. Lescinsky and Sisson, 1998). A thick distal flow along Cordón Loma Seca is directly underlain on the wall of Río de la Plata by a rhyolite lava (unit **rlm**) with a $^{40}Ar/^{39}Ar$ plateau age of 335±2 ka (Table 1), and the topmost proximal flow on Cordón Loma Seca itself yields 83±2 ka (Singer *et al.,* 1997). In both areas, Pellado lavas are petrographically varied, individual flows carrying anywhere from ~1% to 25% phenocrysts, ubiquitously of plagioclase and olivine, commonly of sparse cpx, and additionally of opx in silicic andesites.

CERRO SAN PEDRO MAFIC SHIELD VOLCANO

One of the larger centers in the volcanic field is the glacially eroded mafic shield (unit **mcs**) called Cerro San Pedro (not to be confused with Volcán San Pedro, 15 km west, on the volcanic front). Centered midway between Laguna del Maule and Volcán Pellado (Fig. 9), Cerro San Pedro (Peak 2,879) is an ice-ravaged cinder-spatter-lava cone and plug, now 250 m high and ~1 km wide, representing the vent complex for the shield (Figs. 12, 13). Oxidized south-dipping scoria and agglutinate layers on adjacent Peak 2,750 (~700 m south) indicate that this, too, was part of the vent complex now gutted by a southeast-opening cirque between the peaks. Stacks of radially dipping olivine-rich lava flows extend west against Volcán El Zorro, south to the rim of Arroyo de Botacura, eastward (beneath peripheral shield Cerro Bahamondes) beyond Cajón Bahamondes, and 10 km northward as a broad ice-scoured till-mantled stairstep plateau. More than 20 lava flows, mostly 5-20 m thick, are exposed in sections along the wall of Cajón Bahamondes (Fig. 13). Distally, this northerly apron extends northeast beyond the Bahamondes, fills an east-trending paleovalley cut in Miocene ignimbrite and continues down the west bank of the Río Maule, where lava remnants now form benches 50-150 m above the present-day river. Lavas analyzed (n=13) range in SiO_2 from 49.3 to 58.2%, but nine are in the range 51-55%. The three most silicic flows have abundant plagioclase and rare cpx in addition to the olivine common to all; more mafic flows have abundant olivine and sparse or only microphenocrystic plagioclase. One flow (50.8% SiO_2) at the southwest extremity of the shield gave a K-Ar age of 243±16 ka, and a waterfall-supporting flow (55% SiO_2; 125 m thick, thickest flow of unit **mcs**) that boxes Cajón Bahamondes at 2,050 m yielded 243±43 ka (Table 2). The shield lavas overlie ignimbrite and andesitic strata of Tertiary age as well as the lava-flow apron of Volcán El Zorro (unit **avz**; 429±8 ka), the older silicic lavas along the Botacura (unit **dab**; 924±16 ka), and the rhyolite coulee of Los Murciélagos (unit **rlm**; 341±8 ka). They are overlain by the adjacent mafic shield of Cerro Bahamondes (unit **mcb**; undated but similarly eroded) and by two undated rhyodacite coulees (units **rdcb** and **rdes**), both ~1 km east of the Cerro San Pedro vent cone.

SIX SMALL MAFIC AND INTERMEDIATE CONES

Cerro Bahamondes (unit **mcb**), Peak 2,667, is a 500-m-wide brick-red scoria cone centered 3 km east of Cerro San Pedro (Figs. 9, 12, 13). Its radially dipping scoria and agglutinate are gutted by a SSE-facing cirque and cut by several exposed dikes. Its lava shield is 3 x 4 km wide and overlies the shield lavas of adjacent Cerro San Pedro. A meter-sized bomb at the vent has 53.5% SiO_2, but a shield lava ~1 km east has 59.3%; both are phenocryst-poor, carrying small amounts of plagioclase, cpx, and olivine. Although built on the flank of Cerro San Pedro and comparably eroded glacially, Cerro Bahamondes is wholly younger (though undated) and differs in both phenocryst content and bulk composition.

The **Andesite of Arroyo Arenas Blancas** (unit **aab**) built a 1-km-wide scoria cone at 2,500 m on the northeast slope of Volcán Aguirre (Fig. 9) and produced two lava lobes that straddled the rhyodacite dome of Lo Aguirre (unit **rdla**), each extending ~2 km northeast to elevations lower than 2,000 m. The cone is degraded but not deeply eroded; stratified agglutinate and scoria dip east off its east flank, but its smooth west and north slopes are sloughed red-cinder scree. The cone itself and its scoriaceous, blocky, leveed proximal lava flows are unglaciated above 2,200 m, whereas the lower reaches of both lava tongues are ice-scoured. The tongue down Arroyo Arenas Blancas is plucked and eroded into a stack of several lava-flow benches, each 5-20 m high. The snout of the eastern tongue encountered ice at Estero Aguirre, developing striking subhorizontal to vertical sets of long slender ice-contact glassy columns distally and sets of stouter columns farther upslope. All products are plagioclase-rich with varied proportions of olivine, cpx, and opx; two lava samples have 59.3% and 61.4% SiO_2, whereas a near-vent scoria bomb has only 55.0%

SiO_2. A devitrified sample from the stoutly columnar zone gave a $^{40}Ar/^{39}Ar$ plateau age of 372±18 ka. The lavas overlie Pliocene rhyolite of unit **Trea**, breccia sheets of Volcán Aguirre (unit **mva**; 1,290±13 ka), and the rhyodacite dome of Lo Aguirre (unit **rdla**; 881±73 ka).

The **Andesite of La Poza** (unit **mlp**) is a small scoria cone remnant ~6 km northwest of the dam impounding Laguna del Maule (Fig. 9). The brick-red 500-m-wide scoria mound has been severely glacially eroded, exposing dikes and a platy devitrified plug in the core. Products have 53.1% SiO_2, carry 5-8% plagioclase and 2-3% olivine phenocrysts (both as big as 2 mm), minor cpx, and abundant rhyolite xenoliths. The undated unit overlies Miocene biotite-rhyodacite ignimbrite and the 1.5-Ma pyroxene-dacite ignimbrite (unit **igsp**).

Volcán Bobadilla Chica (unit **bbc**) is a glacially eroded mafic spatter and lava cone (52.0-52.7% SiO_2) centered 4 km north of Laguna del Maule (Fig. 6). Peak 2,863 atop the 1.5-km-wide cone is a coarsely jointed plug and dike complex that intrudes stratified red scoria and agglutinate. A northwesterly dipslope of thin lava flows condenses distally into a narrow glaciated tongue preserved as low as 2,150 m along Cajón Chico de Bobadilla. Columnar jointing at the terminus ~2 km from the vent suggests ice-contact emplacement. Products contain abundant olivine and plagioclase phenocrysts. The cone was built atop the biotite-rhyodacite ignimbrite (unit **igcb**; 950±7 ka) and lavas of Volcán Atravesado (unit **ava**; >700 ka). The distal lava tongue gave a $^{40}Ar/^{39}Ar$ plateau age of 154±7 ka (Table 1).

The **Andesite of Paso Campanario** (unit **mpc**) is a stack of at least seven lava flows that dip radially away from a vent remnant at Crag 2,985, ~4.5 km west of the summit of Cerro Campanario. The crag lies midway along an ice-sculpted spur ridge that extends 3 km southwest from the eponymous pass at an elevation of 2,955 m on the continental divide. Monolithologic vent breccia consists of subangular to subrounded blocks (as big as 1 m) of plagioclase-rich olivine-bearing two-pyroxene andesite in a coarsely gritty lavender matrix, cut by dikes as thick as 4 m. The surrounding stack of lavas thickens southwestward, apparently filling a paleocanyon, but it is not known how much of the 500 m relief at the steep southwest end of the ridge represents its true thickness (as opposed to draping a paleocanyon wall). The undated stack of lavas overlies altered intermediate volcanic rocks, probably of Pliocene or early Quaternary age. It is overlain east of the pass by mafic lava flows from Cerro Campanario (unit **mcc**; ~150 ka). The top lava preserved on the ridgeline north of the vent crag has 54.0% SiO_2), whereas a block from the phenocryst-richer vent breccia gave 58.1%.

Volcán de la Calle (unit **mvc**) is a small glacially eroded mafic shield volcano centered along the continental divide ~3 km east of the southeast corner of Laguna del Maule (Fig. 7). Remnants of the ravaged vent complex are marked by red scoria and agglutinate that crop out around an ice-scoured upland bowl just southwest of Peak 2,954, which is a remnant of its east-dipping flank lavas that now line the divide. Aprons of numerous thin rubbly scoriaceous lava flows with massive zones 1-3 m thick extend 3 km southeast into Argentina and 3 km southwest, draping steeply down to as low as 2,350 m in Arroyo de la Calle. Three widely separated lava flows sampled are all rich in plagioclase and olivine, carry minor cpx, and contain 53.5-56.1% SiO_2. A near-vent flow gave a $^{40}Ar/^{39}Ar$ plateau age of 153±7 ka (Table 1), almost identical to the age of Volcán Bobadilla Chica (unit **bbc**) 12 km north. The shield rests on Tertiary andesitic rocks, subhorizontal or gently west- or east-dipping, that make up the southeast wall of the Laguna del Maule basin. The shield lavas are overlain by a discontinuous veneer of till and by a Holocene rhyolite coulee of unit **rcd** and its thick proximal pumice-fall deposits.

TWO MIDDLE PLEISTOCENE RHYOLITE IGNIMBRITES

Remnants of two different nonwelded to weakly welded ignimbrites of high-silica rhyolitic composition (>74% SiO_2 SiO_2) crop out north and northwest of Laguna del Maule at such high elevations above present-day canyon floors that we infer their eruptive ages to be no younger than middle

Pleistocene (*i.e.*, >126 ka). The **Ignimbrite of Cerro Galaz** (unit **igcg**) is recognized only as a 1-km-wide bench at 2,700-2,800 m elevation high on the southeast shoulder of Peak 2,954, ~5 km northeast of Baños Campanario and 12 km north of the dam impounding Laguna del Maule. The bench-forming sheet is nearly horizontal, as thick as 50 m, and is mostly white, contrasting with the subjacent dark gray-brown, radially dipping, mafic lavas and fragmental strata of a large dike-ridden Tertiary stratocone here called Cerro Galaz (after Cajón de la Galaz on its east side). The base of the undated ignimbrite is ~1,250 m higher than the confluence of the canyons of the Ríos Maule and Campanario (6 km southwest). The dominantly white to tan-weathering massive nonwelded tuff grades up into gray-brown zones that are lightly sintered to partially welded. All facies are eroded into ledges, knobs, spires, and hoodoos. Everywhere vitric, the ashy matrix carries sparse biotite and abundant plagioclase crystals, ~5% phenocryst-poor white pumice lapilli (mostly 1-3 cm), and ≤5% accidental lithic fragments (1-10 cm) of rhyolitic and intermediate lava. Analyses of two biotite-bearing pumice clasts yield 74.8 and 75.5% SiO_2. The source of the ignimbrite remnant is unknown. Thick sheets of Pleistocene biotite-rhyolite ignimbrite are known regionally (Figs. 1, 2) only in the Puelche volcanic field (12 km northeast; Hildreth *et al.,* 1999) and around a probable caldera in upper Arroyo Pichi Trolón (22-32 km northeast; west of Las Loicas; Figs. 2, 4). Pumice and fiamme sampled from both those areas, however, have ~74% SiO_2 SiO_2 and are geochemically somewhat less evolved than our two pumice clasts from unit **igcg**.

The **Ignimbrite of Cordón Constanza** (unit **igcc**) is recognized as three remnants of nonwelded to weakly sintered biotite-plagioclase rhyolite tuff, two of which are banked against the western nose of the eponymous ridge (cordón) that forms the steep divide between the Ríos Maule and Campanario, ~2 km east of their confluence. The lower of the two is ~100 m wide , 60 m high, and is weathered into tan to pinkish-brown spires as high as 30 m that are conspicuous from the road grade at Cuesta Los Cóndores across the Río Maule; its base lies at ~1,650 m elevation. The upper remnant is ~40 m thick, begins ~120 m higher than the top of the first, and caps the ridgecrest for ~250 m longitudinally between 1,830 and 1,870 m elevation. Bases of the two remnants are respectively ~150 m and 330 m higher than the nearby confluence of canyon floors; both are banked against Tertiary andesitic rocks and the difference in their elevations probably reflects paleocanyon topography against which they were concurrently banked, rather than different ages or an extraordinary combined original thickness. Both are largely nonwelded, though their upper parts grade into lightly sintered tuff with no flattening of pumice. Most outcrops have a case-hardened carapace, which spalls off in flakes as thick as 1 cm and generally 5-30 cm across. The tuff contains sparse biotite and plagioclase crystals and abundant white to buff, phenocryst-poor pumice lapilli, most of which are 1-5 cm in diameter, though pumice as big as 16 cm occurs in flow-top pumice-concentration zones. The ashy matrix remains vitric and is in many zones so coarse that 25-70% of the poorly indurated deposit consists of pumice grains 0.5-2 mm across. A subordinate but common kind of pumice is black to medium gray, fibrous, and 1-10 cm across. The two pumice types, as well as common clasts of black juvenile obsidian (mostly <1 cm), are compositionally identical at 74.0-74.4% SiO_2 (significantly less evolved than the lithologically similar ignimbrite unit **igcg** up on Cerro Galaz, only 5 km northeast but ~1,000 m higher). Lithic clasts are abundant (3-5%) but small (0.1-1 cm) and predominantly phenocryst-rich Tertiary intermediate lavas; sparse biotite-bearing felsite lithics may (like the obsidian) be cognate. No partings or internal scour suggestive of discontinuous deposition were observed, but at least four conformable flow units are distinguished by flow-top pumice-concentration zones. Plagioclase separated from the lower remnant gave a K-Ar age of 336±20 ka (Table 2).

A third remnant of unit **igcc** survives 8 km farther downstream, cropping out atop Cretaceous granodiorite high on both walls of the steep divide between the canyons of the Río de la Plata and Río Maule, ~1.5 km upstream from their confluence (Fig. 13). The base of the ignimbrite lies at 1,550-1,520 m elevation, ~100 m lower than the base of the upstream remnants but still ~250 m above the Río Maule. The pink nonwelded outcrop is 50-80 m thick, lithologically similar to those just

described, and overlain directly by a phenocryst-poor rhyolite lava flow of unit **rlm** (335±2 ka; 341±8 ka). The lava flow has only 73% SiO_2 and is correspondingly less evolved geochemically than the ignimbrite. Their distribution and indistinguishable ages nonetheless suggest that ignimbrite unit **igcc** might be an early explosive and slightly more evolved member of the Rhyolite of Los Murciélagos (unit **rlm**) complex, which is now deeply incised by the Río de la Plata tributary of the Río Maule.

TWELVE SILICIC LAVA FLOWS AND DOMES

Eruptive units of middle Pleistocene age further include 12 silicic coulees and lava domes, each of which extruded from its own vent, either peripheral to or independent of any pre-existing edifice. The dozen units include three rhyolites, two northeast of Laguna del Maule and an extensive complex along the Río de la Plata; eight rhyodacites, of which five lie between Arroyo de Botacura and upper Valle Chico, two just east of Cerro San Pedro, and one a few kilometers southwest of Laguna del Maule; and a single dacite coulee that extends along the north wall of the Río Saso.

(1) The **Rhyolite of Cajón del Atravesado** (unit **rca**) is a 2-km-long lava-flow remnant that caps a narrow ridge just north of the northeast arm of Laguna del Maule (Fig. 6). The ridge forms a triple divide separating the lake basin from Cajón del Atravesado and Cajón Chico de Bobadilla. The glaciated lava flow is 120-150 m thick and drapes the north wall of the lake basin from Peak 2,933 atop the divide to as low as 2,650 m on the wall, only ~1 km from the lakeshore. Rich in plagioclase and carrying sparse biotite phenocrysts, the lava is locally vitrophyric but dominantly white flow-foliated felsite, widely vuggy or spherulitic and at its northeast extremity acid-altered. Along the ridgecrest, the lava flow overlies 10-20 m of massive white nonwelded ignimbrite, also biotite rhyolite but rich in lithic fragments, presumably an explosive vent-clearing phase of the **rca** eruption. The unit rests on postcaldera intermediate lavas of Volcán Atravesado (unit **ava**; 990-720 ka) and might be considered a late product of that edifice. Three widely separated samples of the rhyolite contain 74.1-74.4% SiO_2 and one gave a $^{40}Ar/^{39}Ar$ plateau age of 712±13 ka (Table 1).

(2) The **Rhyolite of Cerro Negro** (unit **rcn**) is a lava dome complex of high-silica rhyolite (75.3-77.6% SiO_2) that forms most of the steep northeast wall of Laguna del Maule (Fig. 10). The complex extends 5 km north-south, 4 km east-west, and has >900 m of relief. Although predominantly flow-foliated white to pale-gray (gray-brown weathering) felsite, several black obsidian zones tens of meters thick define boundaries between at least four stacked extrusive lobes. The rock contains 1-3% plagioclase phenocrysts and sparse biotite. It is locally vuggy, lithophysal, or spherulitic, and is strikingly flow-foliated and deformed on scales ranging from 100-m folds to convolute lamination. So pervasive are thin flow laminae that the unit widely decays into thinly platy screes. A sample from the northwest scarp gave a K-Ar age of 447±7 ka (Table 2), and another from the southerly ridgecrest gave a $^{40}Ar/^{39}Ar$ age of 468±6 ka (Table 1). The rhyolite was extruded at the east margin of the Bobadilla caldera, locally overlies ignimbrite unit **igcb** at the base of the eastern wall of the Laguna del Maule basin, and was sheared off by ice that later filled the basin, producing the steep scarp observed today (Fig. 10). Several postglacial slumps now mark the toe of that scarp.

(3) The **Rhyolite of Los Murciélagos** (unit **rlm**) is a discontinuous chain of six glaciated remnants (Fig. 9), possibly of a single lava flow, that extends 11 km northeastward, from as high as 2,863 m above a vega called Los Murciélagos to an eroded terminus at 1,500 m, just above the confluence of the Río de la Plata and the Río Maule. At the 1.5-km-wide rhyolite plateau above Los Murciélagos, the flow is >200 m thick, and it remains as thick as 150 m at the most distal remnant, a 1-km-wide triangular plateau near the confluence (Fig. 13). Other remnants are smaller and only 50-100 m thick, but all six have thick basal obsidian zones, which are in places columnar. Most exposures, however, are flow-banded felsite, locally vuggy or spherulitic. Two medial lava remnants rest upon white nonwelded rhyolitic ignimbrite as thick as 30 m, probably coeruptive, rich in lithics and phenocryst-poor pumice lapilli. Relative elevations suggest that the vent was beneath or near the high plateau above Los Murciélagos. Just off the north edge of the

FIG. 10. View eastward from central peninsula at north shore of Laguna del Maule toward Cerro Negro atop steep northeast wall of basin. Entire high skyline and most of wall consists of pale felsite and dark obsidian of extensive high-silica rhyolite complex of Cerro Negro (unit **rcn**), which yields ages of 447±7 ka and 468±6 ka (Tables 1, 2). Reddish brown promontories and both islands (at right) consist of intracaldera biotite-rhyodacite welded ignimbrite (unit **igcb**; 950±7 ka). Ignimbrite also crops out near far shoreline as brown ledge just right of center, but three ledges at far right are slump masses of rhyolite lava. At upper left, rhyolite lava has steep intrusive contact with gently dipping andesite-dacite lavas assigned to Volcán La Zorra (unit **alz**; 1.0 to 1.1 Ma). Beyond are Paso Pehuenche and clouds in Argentina.

plateau, a 500-m-wide glaciated buttress with coarse vertical jointing and upward-flaring obsidian margins may be an exposed part of the vent structure (UTM grid 475/207). The phenocryst-poor rhyolite carries sparse 1-mm plagioclase phenocrysts as well as tiny opx and biotite. Eight widely distributed samples yield a narrow range of bulk composition: 72.6-73.2% SiO_2 and 3.9-4.0% K_2O. One sample from the plateau rim above Los Murciélagos gave a $^{40}Ar/^{39}Ar$ age of 341±8 ka and another from a 100-m-high rhyolite cliff on the opposite (northwest) wall of the canyon of the Río de la Plata gave 335±2 ka (Table 1). The unit rests principally on deformed Tertiary andesitic strata and Cretaceous granodiorite, but it also overlies andesitic lavas from Volcán El Zorro (unit **avz**) proximally and remnants of pink rhyolitic ignimbrite (unit **igcc**) distally. It is overlain by mafic lavas from Cerro San Pedro (unit **mcs**; ~243 ka) and Volcán Pellado (unit **mvp**) and, atop the distal plateau (Fig. 13), by a phenocryst-rich pyroxene-andesite lava flow (unit **aeb**).

(4) The **Rhyodacite of Arroyo Cabeceras de Troncoso** (unit **rdct**) is a 1-km-wide coulee (just west of the eponymous arroyo) that erupted ~5 km southwest of the southwestern corner of Laguna del Maule (Fig. 7) and flowed 1.5 km toward the lake from a vent near the divide between the lake basin and Cajón de Troncoso. As thick as 50 m, the flow is rich in plagioclase, biotite, and amphibole along with sparse opx. Its exposures are flow-foliated and, although somewhat degraded, still blocky and glassy: mostly dense vitrophyre with subordinate scoriaceous interlayering. Fine-grained, mafic magmatic enclaves (1-10 cm) are abundant. Three samples range in SiO_2 content from 67.1 to 68.6%, and one yielded a $^{40}Ar/^{39}Ar$ plateau age of 203±41 ka (Table 1). The coulee overlies Tertiary andesitic lavas and breccias and Miocene silicic ignimbrite; it is heavily mantled by scoria falls of units **mcp** and **mct**, and a hornblende-dacite lava flow of unit **dlp** banks against its west margin. The snout of the coulee was notched by a wave-cut bench during the postglacial highstand of Laguna del Maule.

FIG. 11. Cerro Campanario, 150 ka mafic stratovolcano on continental divide, 11 km northeast of Laguna del Maule. View is northeastward from 8 km southwest of its 3,943 m high summit, which consists of fragmental and agglutinated core facies, laced with dikes. Three black buttresses, at left, right, and toward viewer, are radially dipping stacks of thin mafic lavas, now glacially sculpted. Pale-gray crag at right is intrusive core of an undated older volcanic edifice. Middle ridge at left edge of image is southeast rampart of mafic Volcán Munizaga (unit **mvm**; 900 ka). Low sunlit divide near center of photo is 2,553 m Paso Pehuenche, crossed by international roadway.

FIG. 12. Glaciated mafic shield, 243-ka Cerro San Pedro (unit **mcs**), viewed northward across confluence of Estero Los Terneros (left) and Arroyo de Botacura (right). Its 2,879-m summit stands 950 m higher than confluence. Snow-patched knob at right is Cerro Bahamondes (peak 2,667), vent cone for a smaller mafic shield (unit **mcb**). Snowy shelf between peaks is south end of glaciated rhyodacite coulee (unit **rdes**). These three units are all of middle Pleistocene age. Bifurcating rimrock lava at center of image is late Pleistocene rhyolite coulee (unit **ret**; 97±15 ka). Snowclad pyramid on left skyline is Volcán Azufre, part of Peteroa cluster, 80 km north. On valley floor at confluence is postglacial debris-avalanche deposit (**dav**) from Estero Terneros.

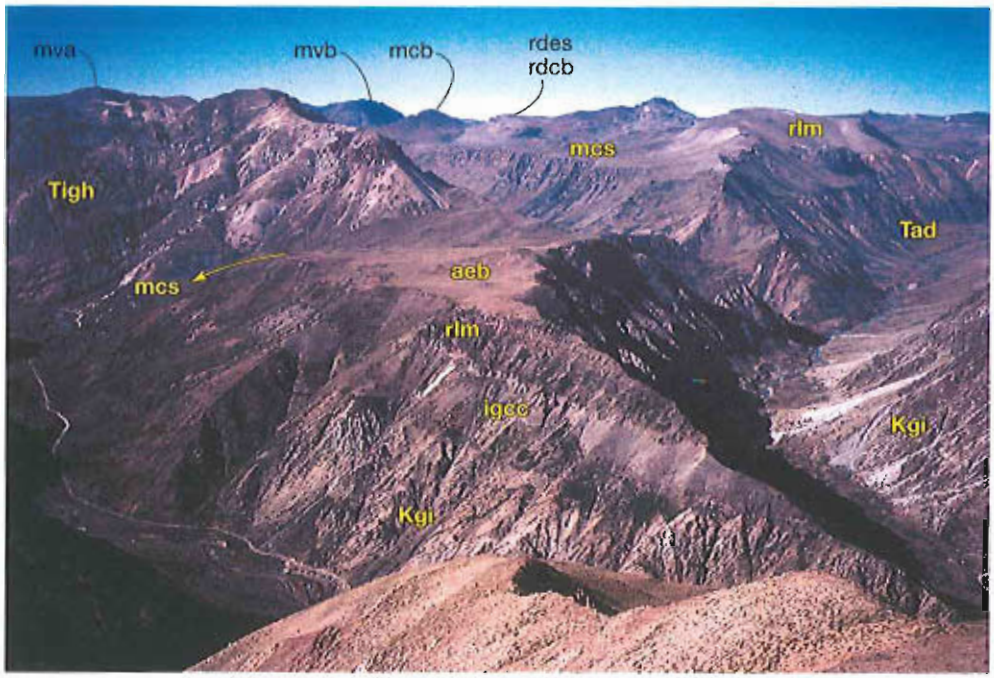

FIG. 13. Convergence of valleys of Río Maule (at left with road) and Río de la Plata (right). View is southward to Cerro San Pedro on right skyline, 12 km south of confluence. Just above center of image, stack of at least 20 olivine-rich shield lavas from Cerro San Pedro (unit **mcs**) forms glaciated west wall of Estero Bahamondes, which joins Río de la Plata at right center. Triangular Plateau (Drake, 1976) at center is capped principally by 100-m-thick rhyolite lava flow (unit **rlm**; 335±2 ka), remnants of which are also preserved high along wall of Río de la Plata for 7 km farther upstream. Atop plateau, rhyolite is overlain by scoured remnant of andesite lava unit **aeb** (276 ka). Rugged wall at left, light-colored and stratified, is Miocene ignimbrite (unit **Tigh**), here synclinally deformed (cf. Fig. 18). Between rhyolite plateau and ignimbrite ridge, subdued gray-brown swale is paleovalley filled by 243 ka mafic shield lavas from Cerro San Pedro that flowed into Río Maule valley prior to cutting of Estero Bahamondes. Beneath plateau, rugged lower slopes are 80-Ma granodiorite (unit **Kgi**), as is foreground ridge. White gully at center of image reveals (elsewhere scree-covered) nonwelded rhyolitic ignimbrite (unit **igcc**; 336±20 ka) sandwiched between granodiorite and rhyolite lava flow. On central skyline, red-brown knob is Cerro Bahamondes cone (unit **mcb**; cf. Fig. 12), and tan skyline bench to its right is superimposed pair of rhyodacite coulees, units **rdcb** and **rdes**. On skyline just left of Cerro Bahamondes is ravaged stratified remnant of Volcán Botacura (unit **mvb**), and on far left skyline are comparably eroded dark-gray remnants of Volcán Aguirre (unit **mva**), each ~1.3 Ma and both mafic.

(5) The **Rhyodacite east of Cerro San Pedro** (unit **rdes**) and **(6)** the **Rhyodacite west of Cajón Bahamondes** (unit **rdcb**) are a pair of overlapping coulees that together form a prominent glacially scoured ridge between the mafic centers Cerro San Pedro and Cerro Bahamondes (Figs. 9, 13). The upper coulee (**rdes**; 69.7% SiO_2) is >1,00 m thick, ~600 m wide, and flowed nearly 2 km northward to a sloping flow front that has ~150 m relief. Most of the flow is strongly flow-foliated, mixed felsite and vitrophyre, and carries ~10% plagioclase phenocrysts along with ~1% amphibole, minor biotite, and sparse opx microphenocrysts, in contrast to the lower coulee (**rdcb**; 68.9% SiO_2), which instead contains ~15% plagioclase and abundant opx. The lower coulee is ~50 m thick, likewise partly glassy, and is exposed for only ~1 km as a bench underlying the northeast margin of the upper. Both are presumed to have erupted from a southerly vent concealed beneath them near knoll 2,648. They overlie the mafic-lava apron of unit **mcs** (~243 ka), and both coulees appear to have andesitic lavas of Cerro Bahamondes (unit **mcb**) banked against them.

(7) The **Rhyodacite of Estero Terneros** (unit **rdet**) is the easternmost of five independent rhyodacite units of middle Pleistocene age distributed 2-6 km west and southwest of the summit of Cerro San Pedro, between Arroyo de Botacura and Valle Chico (Figs. 8, 9). Along the Botacura tributary called Estero Terneros, a pair of thick rhyodacite lava flows forms much of the canyon's steep northeast wall, extending 2.5 km from the rim of its alluviated cirque bowl nearly down to the Botacura. Both flows are strongly flow-foliated and rich in plagioclase; the lower has biotite and hornblende, while the upper carries opx and sparse opacitized biotite phenocrysts. Both flows range from partly glassy to devitrified and thinly platy, and both weather dark brown. The lower flow (69.6% SiO_2) is as thick as 200 m and has a columnar base; the upper (70.0% SiO_2) forms a 150-m-high scarp near the head of the canyon. The lower flow banks against a mafic plug associated with the gutted core of Volcán El Zorro (429±8 ka), and the upper flow is overlain by mafic lavas from Cerro San Pedro (~243 ka); both of the undated flows are overlain directly by a thick coulee of biotite rhyolite (unit **ret**; 97±8 ka).

(8) The **Rhyodacite of Estero El Zorro** (unit **rdez**) is a 1 km wide lava dome only 1.5 km west of Estero Terneros, on the floor of the cirque bowl at the head of Estero El Zorro (Fig. 9), where it is directly overlain by andesitic lavas in the gutted core of Volcán El Zorro (429±8 ka), to which it is likely to be related. With about 200 m of exposed relief, the rhyodacite (69.9% SiO_2) is glacially scoured into cliffy benches and ledges, and its base is concealed by till and scree. Because the lava is exceptionally rich in plagioclase phenocrysts and subordinate opx, many exposures crumble into grus. Parts of the dome are platy and much of it is slightly altered, weathering yellow-brown.

(9) The **Rhyodacite of Puntilla Los Ñirales** (unit **rdpñ**) is another glacially modified dome of pyroxene rhyodacite, lying only 1.5 km southwest of the unit **rdez** dome and 1.5 km north of Arroyo de Botacura (Figs. 8, 14). The 900 x 1,400-m-wide dome (knoll 2603) forms the middle reach of a steep narrow ridge called Puntilla Los Ñirales; incised by a glacial canyon tributary to the Botacura, the sheer southeast face of the dome has >300 m of relief, its toe buried in its own coarse talus. The face is entirely felsite and much of it is marked by a single set of slender (~1 m thick) columns >150 m high. Vitrophyre is locally preserved on top and along the gentler western margin. The rhyodacite carries ~5% plagioclase phenocrysts as big as 4 mm, small amounts of opx, amphibole, and biotite, and sparse fine-grained, relatively mafic enclaves (mostly <1 cm; some to 5 cm). Samples from top and bottom both contain 70.4% SiO_2; the latter gave a $^{40}Ar/^{39}Ar$ plateau age of 680±34 ka (Table 1).

(10) The **Rhyodacite of Valle Chico** (unit **rdvc**) is a composite flow-dome complex that crops out steeply along the east wall of upper Valle Chico (Fig. 9). It lies only 2 km north of the unit **rdpñ** dome just described and is of similar age (695±8 ka (Table 1), but it consists of pyroxene-plagioclase rhyodacite. The complex consists of two superimposed extrusive subunits, which altogether crop out for 1 km north-south and 700 m east-west. The upper unit (70.3% SiO_2) is the more extensive, is strongly flow-foliated, has >200 m of cliffy relief, and is phenocryst-rich, containing >20% plagioclase (up to 3 mm), common cpx and opx microphenocryts, and scattered mafic blebs. Its steep west face is marked by a vertically jointed central domain, flanked by flow lobes with moderately dipping foliations that ramp upward distally both north and south. The lava is mostly devitrified, pale gray, and vuggy but weathers gray-brown; medium gray domains of crumbly vitrophyre are preserved locally. It is cut by at least two olivine-plagioclase mafic dikes, which may be related to nearby Volcán El Zorro. The lower unit (71.2% SiO_2) is a discrete lava dome or flow that directly underlies the central part of the upper one along the vega margin at Valle Chico. Although its base is not exposed, it has ~150 m of cliffy relief and crops out for 400 m north-south. Distinctively less phenocryst-rich than the upper unit, the lava has only ~3% plagioclase (as big as 1.5 mm) and sparse opx and cpx, but it too carries fine-grained mafic enclaves (1-5 mm across). The rhyodacite pair overlies a stack of thin mafic lavas of unit **mvñ**. Banked against the northwest toe (poorly exposed at the vega) are mafic and andesitic lavas from Volcán Pellado (unit **mvp**), and banked against the upper flow on the east are lavas from Volcán El Zorro (unit **avz**; 4,29±8 ka).

(11) At the head of the Río de la Plata (Fig. 9), only 1 km north of its divide with Valle Chico and 2 km north of the unit **rdvc** rhyodacite just described, the **Rhyodacite of Cabeceras de la Plata** (unit **rdcp**) is yet another small rhyodacite dome of middle Pleistocene age. The equant dome is ~300 m across and has ~70 m relief on its steep north side. Glacially scoured, the dome is flow-foliated pale-gray felsite (71.0% SiO_2) that weathers buff to pinkish tan and carries 3-5% plagioclase phenocrysts, ~1% amphibole, and sparse opx and biotite. It is cut by a 5-m-thick vertical mafic dike that strikes northwest, probably related to Volcán El Zorro. The undated dome is overlapped by the apron of olivine-plagioclase mafic andesite lavas from Volcán El Zorro (unit **avz**; 4,29±8 ka) and by outliers of plagioclase-rich pyroxene-andesite lava, probably from Volcán Pellado (unit **mvp**).

(12) Last to be described of the dozen silicic lavas of (known or inferred) middle Pleistocene age is the undated **Dacite of Estero Tapia** (unit **det**), a single thick lava flow that erupted at ~2,600 m elevation high on the south slope of Cordón Las Romazas (the Botacura-Saso divide; Fig. 8). The flow drapes down the north wall of the Río Saso, descending steeply for 2.5 km (just west of a Saso tributary called Estero Tapia) as a 300-m-wide tongue that doubles in width lower on the slope, then at 1,900 m elevation turns west, forming a 100 m-thick-cliffy ledge that dips gently westward for 3 km downstream. Its base is now ~150 m above the floor of the present-day Río Saso, perched on a 700-m-wide ledge that was evidently the floor of the Saso paleovalley at the time of its emplacement. Much of the glacially scoured surface of the ledge is devitrified felsite, block-jointed or slabby, but the lower half of its scarp is strikingly columnar and partly glassy. The dacite (63.9-65.5% SiO_2) is flow-foliated and contains 5-10% plagioclase phenocrysts (as big as 2 mm), sparse amphibole, and rare opx and opacitized biotite. It erupted through and overlies a major biotite-rhyodacite ignimbrite (3.4±0.8 Ma; Muñoz and Niemeyer, 1984) and, along the lower wall of the Río Saso, it rests on still-older Tertiary andesitic lavas and tuffs that dip ~20° NE.

ANDESITE DIKE OF CUESTA LOS CÓNDORES

A heterogeneous intermediate dike (unit **mlc**), near-vertical and 1-10 m thick, strikes northeast across the road at an elevation of 1,770 m along the precipitous road grade called Cuesta los Cóndores (UTM grid 560/208), ~8 km northwest of the dam impounding Laguna del Maule. From above the road, the dike descends the cliff below for at least 100 m, toward the base of the waterfall of Arroyo Arenas Blancas. Alternating massive and vesicular zones define a crude vertical foliation within the dike, which generally splits platy. The dike contains ~10% plagioclase phenocrysts (1-2 mm), common olivine, and sparse pyroxenes. Two samples from near the road gave contrasting compositions: 53.4% SiO_2 at 1.19% K_2O and 59.5% SiO_2 at 2.01% K_2O. The (fresh, nonhydrated) dike cuts only Miocene biotite-rhyodacite ignimbrite and is clearly distinguishable from altered Tertiary dikes nearby. It is not known to be related to any of the several mafic and intermediate lava flows that crop out along the adjacent canyon. We infer the dike to be of middle Pleistocene age, principally by comparison of its topographic situation and degree of weathering relative to many nearby Pleistocene lavas, but we cannot exclude that it could be early Pleistocene.

EIGHT ORPHAN REMNANTS OF MIDDLE PLEISTOCENE LAVA FLOWS

In addition to the 25 middle Pleistocene units just described, there are eight glaciated remnants of lava flows known or inferred to be of this age, for which vents have not been identified. The eight range from basalt to dacite, are scattered widely across the volcanic field, and are generally isolated scraps without clear stratigraphic context.

Two of the eight cap the Cordón de Constanza, the Maule-Campanario divide, forming narrow ridgecrest remnants (Fig. 9) ~8 km north of Laguna del Maule and ~300 m above the nearby canyon floors. The **Andesite north of Salto del Maule** (unit **ans**) is a 600-m-long remnant of a single lava flow as thick as 120 m, centered on knoll 2,003. Slender glassy columns, probably reflecting ice-

contact emplacement, make up its lower 80 m cliff, and only its ice-stripped upper part is devitrified and platy. The flow has 62.0% SiO_2 and carries 10-15% plagioclase phenocrysts (1-3 mm) and sparse opx and cpx. It yields a $^{40}Ar/^{39}Ar$ plateau age of 429±42 ka (Table 1). Less than 1 km west and capping the same ridgecrest, the **Andesite south of Baños Campanario** (unit **asb**) forms a narrow 750-m-long remnant of another lava flow, as thick as 130 m and centered on knoll 2,046 (Fig. 9). Its lower half consists of black glassy columns, including a basal colonnade of stout vertical columns 10-25 m thick and an overlying 50-m-thick zone of slender columns variably oriented. The upper half is devitrified, platy to block-jointed, and pale gray, weathering tan to orange-brown. The flow has 60.4% SiO_2 and carries abundant plagioclase phenocrysts along with sparse opx and cpx. It yields a $^{40}Ar/^{39}Ar$ plateau age of 374±7 ka (Table 1). Both remnants rest on deformed Tertiary volcanic rocks that include white biotite-rhyodacite ignimbrite.

Across the canyon northwest of Cordón de Constanza (Fig. 9), three remnants of mafic lava and ejecta, the **Andesite of Río Blanco** (unit **mrb**; 54.1-54.4% SiO_2) are preserved within 1 km of Baños Campanario, on the nose separating the Río Campanario from its Río Blanco tributary. The upper remnant, ~300 m wide, lies 1 km northeast of the confluence, up at 1,650 to 1,750 m elevation, and consists principally of a 100-m-thick lava flow banked against the west side of the nose. Most of the cliff-forming lava has hackly or irregularly spaced vertical joints, but its basal 25 m is columnar, some columns inclined at 45°. At the lower southeast end of the outcrop are exposed several meters of brick-red breccia, agglutinate, and scoria bombs as large as 1 m, suggesting a nearby vent, possibly concealed by the thick lava itself. Two lower remnants of similar lava are banked against the same nose down at 1,600 to 1,650 m elevation and, taken together, are ~750 m long and 200 m wide. Their partly glassy chunky-columnar aspect suggests ice-or-river-contact emplacement. Products contain 3-5% plagioclase phenocrysts (1-4 mm) and ~1% each of cpx and olivine (≤1 mm). The undated remnants rest against Tertiary andesitic lavas and tuffs and a small mass of pyroxene diorite; their bases lie 80 to 130 m above the nearby confluence of the Ríos Campanario and Blanco. Just south of the confluence, only 500 m from the lower remnants of unit **mrb**, an intracanyon lava flow of unit **avm** (lowest lava on the Campanario-Maule nose) rests virtually at river level (~1,550 m) and yields a $^{40}Ar/^{39}Ar$ plateau age of 116±27 ka (Table 1). On this basis we infer the remnants of unit **mrb** to be still older, and in fact Drake (1976) determined a K-Ar age of 270±70 ka for one of them (Table 2).

A glacially eroded stack of three phenocryst-poor mafic lava flows, the **Andesite west of Cerro Risco Bayo** (unit **mor**), caps the Campanario-Bobadilla divide, ~6 km north of Laguna del Maule and 7 km northwest of Paso Pehuenche (Fig. 6). Each of the three is 6-8 m thick, with scoriaceous rubble separating block-jointed to slabby massive interior zones 4-5 m thick. Together they form a till-strewn plateau 600 m wide and 1,200 m long. The lavas have 53.7-54.2% SiO_2 and carry very sparse phenocrysts of olivine, cpx, and plagioclase. They are compositionally unlike any other mafic lavas in the area nearby (*e.g.*, units **alz**, **ava**, **mcc**, **mpc**, and **mvm**), and their source vent remains unidentified. The stack overlies unit **igcb** (950±7 ka) as well as Tertiary andesitic strata that dip 25°N; it also banks against unit **igbc** to the west and an altered Tertiary dome called Cerro Risco Bayo to the east.

The **Andesite of Estero Bahamondes** (unit **aeb**) consists of four remnants of (variously one or two) lava flows of plagioclase-rich pyroxene andesite (59.4-61.6% SiO_2) that flowed northward down a paleo-Bahamondes valley from an unidentified source. The southernmost is a columnar-jointed ledge only 100 m long but also 100 m thick, banked against unit **mcs** high on the west wall of the Bahamondes gorge at 1,850 to 1,950 m elevation (UTM grid 499/218). Downstream 2 km on the opposite (east) rim at 1,800 to 1,900 m elevation is another glassy columnar remnant (502/238) of similar dimensions, also banked against lavas of unit **mcs** as well as against Miocene ignimbrite beneath them. Above the confluence of Estero Bahamondes with the Río de la Plata, ~1 km farther downstream, another east-rim ledge at ~1,750 m elevation (495/248) is 30 m thick, 200 m long, and mostly glassy and chunky-columnar, with subhorizontal columns where it banks against a wall

consisting of both Miocene biotite-rhyodacite ignimbrite and 1.5-Ma pyroxene-dacite ignimbrite (unit **igsp**). By far the largest remnant is 2.7 km long and as wide as 1.5 km, capping what Drake (1976) called the 'Triangular Plateau', a mesa that tapers to a point above the confluence of the Río de la Plata with the Río Maule (Fig. 13). The ice-scoured lava that caps the plateau is at least 70 m thick and locally overlies what may be an earlier related flow unit; its till-mantled surface is rich in erratics of unit **mcs**, fewer of units **rlm** and **avz**, and few or none of unit **mvp**. The capping lava contains ~15% plagioclase phenocrysts (1-3 mm) and sparse cpx and opx. It overlies units **rlm** (~335 ka) and **mcs** (~243 ka) as well as the older ignimbrites, and gave Drake (1976) a K-Ar age of 276±20 ka (Table 2). The andesites are compositionally unlike Pellado-derived lavas of unit **mvp** and richer in phenocrysts than andesites of unit **mcb**. Because no andesites younger than ~243 ka are exposed farther upstream, we speculate that Cerro San Pedro itself may have been the source of unit **aeb**; while most are more mafic, the most evolved lavas of unit **mcs** are similar (though not identical) to those of unit **aeb**.

The **Basalt of Cajón Filume** (unit **bcf**) is an intracanyon unit that extends ~1.5 km southward down the floor of a valley cut into the early Pleistocene andesitic edifice of Volcán Filume (unit **mcf**), ~8 km west of Laguna del Maule (Fig. 8). At its eroded terminus at ~2,200 m elevation, a single ice-scoured bench-forming flow is 30-50 m thick and may well have originally extended the additional 1.5 km to the Río Saso. Upstream benches of the same lithology at 2,350 m elevation on both walls of the canyon may be the same or a higher flow unit, but the intervening area is concealed by till. A 200-m-long remnant only 20 m thick is also preserved ~1.5 km farther northeast atop a Pliocene rhyolite dome (unit **Trcf**) at 2,625 m elevation. The lavas have 51.2-52.4% SiO_2 and carry abundant olivine and plagioclase phenocrysts. All outcrops are glaciated and most are block-jointed to slabby, though the base of the terminal scarp is stoutly columnar. The source vent is unidentified but might have been one of several dikes that cut the rhyolite dome. Assignment of this undated unit to the middle Pleistocene is tenuous and poorly constrained.

The **Dacite of Arroyo Cabeceras de Troncoso** (unit **dct**) is a remnant of phenocryst-rich vitrophyre (63.2% SiO_2) banked against Tertiary andesitic rocks at 2,300 m elevation on the west wall of the eponymous arroyo, 4 km southwest of Laguna del Maule, 1.5 km southwest of Laguna del Piojo, and 100 m east of the coulee of unit **rdct** (Fig. 7). The black glassy remnant (UTM grid 589/039) is <100 m long, slightly vesicular, and disintegrates blocky. It is apparently a marginal facies of a plagioclase-rich opx-dacite lava flow that once filled the arroyo and was largely removed by glacial erosion. Its source vent is unknown and its age is poorly constrained.

The **Andesite of Casa de Piedra** (unit **acp**) is an extensively glassy mass of columnar jointed and convolutely flow-foliated lava banked against the north wall of Cajón Rodríguez (Fig. 8) ~15 km west of the south end of Laguna del Maule. More than 200 m thick, the cliff-forming unit extends 1.3 km east-west and consists internally of several discrete columnar zones (variously inclined or vertical) separated by thin shear planes. The undated lava contains 59.0-59.6% SiO_2, and it carries 10-15% plagioclase phenocrysts (1-5 mm), 2-3% pyroxenes (0.5-2 mm), and rare opacitized amphibole. Its stoutly columnar base is 150 m above the present-day stream, banked against a wall of altered and dike-ridden Tertiary andesitic strata. The source vent is uncertain; it may well be at a glaciated spur at the top of the outcrop, but this has not been verified. The unit may have been emplaced against the margin of a canyon-filling glacier and need not ever have occupied the entire valley.

LATE PLEISTOCENE ERUPTIVE UNITS (126-25 ka)

Within the area mapped, we have delineated 28 units that erupted in this age interval, including four rhyolites, two rhyodacites, two dacites, 12 silicic andesites, seven mafic andesites, and

one true basalt. We ignore the conventional end of the Pleistocene as poorly applicable here and instead consider (as discussed in section 9, below) units younger than 25 ka as 'postglacial'. Nonglaciated lavas that yield $^{40}Ar/^{39}Ar$ ages as old as 24.6±2.2 ka occupy the floor of the glacially excavated, ice-scoured, and till-strewn basin of Laguna del Maule (Singer *et al.*, 2000). Glacially modified eruptive units of the late Pleistocene are scattered widely across the whole volcanic field, just as during the middle and early Pleistocene. In discussing the 28 units, we group them as follows: one stratovolcano, two rhyolite coulees, three silicic domes, six small mafic centers, five small andesitic centers, five components of the Río Maule intracanyon assemblage, and six orphan units for which vents have not been identified.

LATE PLEISTOCENE COMPONENTS OF VOLCÁN PELLADO

As discussed earlier, **Volcán Pellado** (unit **mvp**) is a glacially eroded stratovolcano that frames the northwest edge of our map (Fig. 9). We have addressed only its margins, but Singer *et al.* (1997) found its eruptive products to have 52-62% SiO_2 and its eruptive lifetime to extend from ~188 ka to at least as young as 83 ka, thus well into the late Pleistocene. Many of the youngest lavas of Volcán Pellado are andesitic (57.3-61.0% SiO_2; n=6 in our data set); some of these are shown as unit **Qpmy** on the map of Singer *et al.* (1997). Such lavas have yielded $^{40}Ar/^{39}Ar$ ages of 114±6 ka, 110±3 ka, and 103±4 ka, all in upper Valle Chico; and 83±2 ka atop the proximal end of Cordón Loma Seca (Table 1 and Singer *et al.*, 1997). A Pellado-derived phenocryst-poor andesite lava flow (unit **avc**; 58.6% SiO_2) as thick as 130 m that caps ridge 2,630 (the Valle Chico-Río de la Plata divide) may be younger still.

TWO RHYOLITE COULEES

Compositionally similar rhyolite lava flows were extruded in the late Pleistocene near the headwaters of two adjacent tributaries of the Arroyo de Botacura, Esteros Terneros and El Zorro, one phenocryst-bearing, the other aphyric. The **Rhyolite of Estero Terneros** (unit **ret**) is a cliff-forming glaciated coulee (Fig. 12) as wide as 1 km and as thick as 150 m that flowed 3 km southward to a now-eroded terminus where its base stands >100 m above the floor of the Botacura. Its vent is revealed on the east wall of the cirque heading Estero Terneros by a zone of near-vertical flow foliation. Much of the lava is at least partly glassy, and its basal zone is dense black vitrophyre. It contains 73.7% SiO_2 and carries 2-3% plagioclase phenocrysts and ~1% biotite as well as abundant mafic blebs. The flow overlies units **dab**, **rdet**, and **mcs** (~243 ka), and a sample from its distal scarp yields a $^{40}Ar/^{39}Ar$ plateau age of 97±15 ka (Table 1).

Four kilometers west, the **Rhyolite of Estero El Zorro** (unit **rez**) is an obsidian flow (Fig. 14) that extruded on the divide between Valle Chico and Estero El Zorro and flowed both 1 km north and 3 km south. As wide as 1 km and as thick as 170 m, the glacially scoured coulee is subtly flow-foliated and largely glassy, although felsitic and mixed interior zones are exposed on cliff faces. Despite an erosional gap near its center of distribution, samples from its north and south ends are compositionally identical at 73.8% and are strictly aphyric. The rhyolite overlies units **mvñ** and **avz**, and it is overlapped by the scoria cone of unit **apñ**. It yields a $^{40}Ar/^{39}Ar$ plateau age of 83±3 ka (Table 1).

SILICIC LAVA DOMES

During the late Pleistocene, silicic domes (71-75% SiO_2) were extruded in three places, two near the outlet of Laguna del Maule and another 13 km northeast. The latter, the **Rhyolite of Estero de Bobadilla** (unit **reb**), is an ice-scoured ovoid dome (knoll 2667), 500 x 700 m across and 150 m high, that erupted in the headwaters of Cajón Grande de Bobadilla (UTM grid 705/202), 5 km north of the northeast arm of the lake (Fig. 6). The till-strewn felsitic dome

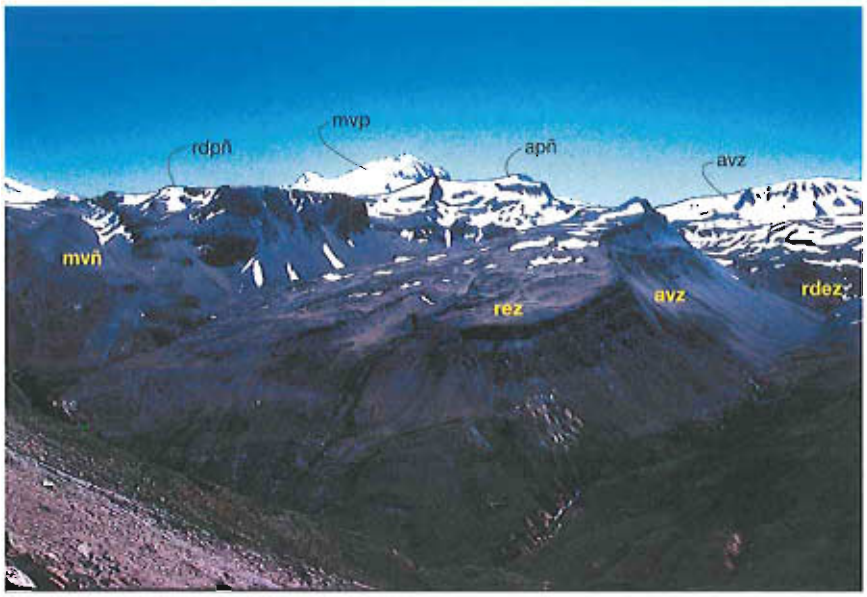

FIG. 14. View northwestward across confluence of Estero El Zorro (right) and Arroyo de Botacura (left foreground). Dip-slope lava flow with 50-m rimrock ledge that caps ridge at center of image is aphyric rhyolite obsidian (unit **rez**; 83±3 ka). It overlies a stack of mafic and andesitic lava flows from Volcán El Zorro (unit **avz**; 429±8 ka), part of which also forms snowy ridge at right skyline. On central skyline, swayback ridge (with ice hollow) is andesite scoria cone (unit **apñ**) that overlies the obsidian flow. At left, flat-topped lava with 300-m-high face is pyroxene rhyodacite of unit **rdpñ**, a 680 ka dome that rests on ravaged remnants of early Pleistocene Volcán Ñirales (unit **mvñ**). Snowclad double peak on far central skyline (10 km from camera) is Volcán Pellado (unit **mvp**; 188-83 ka). Snowy slope of Volcán San Pedro (on volcanic front) is visible at far upper left.

is largely devitrified or spherulitic and locally oxidized red-brown or silicified white. Fresh felsite has 74.8% SiO_2 and contains 10% plagioclase, sparse biotite, and rare amphibole. The dome extruded through altered andesitic strata of Tertiary or early Quaternary age, and it banks against a large, highly altered, Tertiary lava dome called Cerro Risco Bayo (hill 2,729). Although stripped of much of its glassy carapace, the undated rhyolite dome is inferred to be of late Pleistocene age because it remains compactly ovoid, domical, and unfaceted.

Centered 2 km southwest of the dam impounding the lake, the **Rhyodacite of Domo del Maule** (unit **rddm**) is a glassy 200 m high lava dome, 1 km wide and subcircular in plan view, that rises above a comagmatic lava-flow platform ~100 m thick that slopes gently eastward for ~600 m, ending in a 50-m-high scarp above the lakeshore (Figs. 7, 15). The uneroded dome retains a pale-gray micropumiceous carapace that is subtly flow-foliated but texturally quite uniform, weathers tan, and disintegrates slabby to blocky. The transition from dome to platform is weakly marked by the wave-cut highstand bench at 2,350 m elevation that encircles Laguna del Maule, but the lava-flow platform had earlier been glacially eroded. Its lakeside cliff exposes felsitic, spherulitic, and glassy micropumiceous zones but neither dense vitrophyre nor vuggy to scoriaceous facies; the lower half is strongly flow-foliated but the rim of the eroded shelf is block-jointed. Samples from both dome and platform have 70.6-71.6% SiO_2 and contain ~10-15% plagioclase phenocrysts, 3-5% biotite, sparse amphibole, and rare opx. The base is nowhere exposed, as the unit is surrounded by its own pumice-fall deposits, both primary and reworked, and the north side of the dome is wrapped by the postglacial rhyodacite coulee of unit **rdcn**. A moraine along the north side of Arroyo Los Mellicos consists predominantly of material eroded from unit **rddm**, not from nearby rhyodacite unit **rdam**. A felsite sample from the lakeside scarp yields a $^{40}Ar/^{39}Ar$ plateau age of 115±49 ka.

FIG. 15. View southwestward of rhyodacitic Domo del Maule (unit **rddm**; 115±49 ka), ~1 km in diameter, which rises 400 m above northwest arm of Laguna del Maule. Little-eroded glassy dome and glacially eroded 100-m-thick lava flow in foreground are compositionally identical and presumed to be comagmatic. Postglacial high strandline at 2,350 m coincides with break-in-slope from shelf to dome, where it is mantled by talus from dome. Dark-gray post-highstand lava at right is rhyodacitic Northwest Coulee (unit **rdcn**), which just reaches present lakeshore between glaciated shelf of unit **rddm** and toe of glaciated outlet dome (unit **rdop**). Ridge on left skyline is narrow divide between lake basin and Río Saso, consisting of 1.5-Ma pyroxene-dacite ignimbrite (unit **lgsp**) and andesitic lava flows both below and above it; slump masses of ridgecrest lavas and ignimbrite protrude through pumice-fall deposits at toe of scarp.

The **Rhyodacite west of Presa Laguna del Maule** (unit **rdop**) is a pair of lithologically and compositionally identical lava domes that lie immediately west of the dam (Figs. 7, 16). Each is 200 m high, only 500 m wide, and somewhat elongate north-south, owing to glacial erosion concentrated at the basin outlet. A paleo-outlet channel separates them narrowly, and the present outlet channel for the Río Maule lies just to the east. Both domes retain parts of their glassy pumiceous carapace, but glacial erosion has exposed internal felsite on their steep channel-facing margins. Each dome contains 71.3-71.6% SiO_2 and carries ~10% plagioclase phenocrysts as well as ~3% biotite and rare amphibole. The east dome overlies unit **alm**, and the west one is abutted by postglacial unit **rdcn**. Magmas of units **alm** and **rdop** apparently mingled during extrusion, as best observed on the northeast spur of the eastern dome, and are thus inferred to have been approximately contemporaneous. An attempt to date the eastern dome failed to yield measurable radiogenic Ar.

SIX SMALL MAFIC VOLCANOES

Among the 28 late Pleistocene eruptive units mapped are three modest scoria cones near the outlet of Laguna del Maule and three shallow scoria-ringed craters well southwest of the lake. The **Basalt of El Candado** (unit **bec**) forms an erosively ravaged scoria-and-spatter cone ~1.5-km-wide

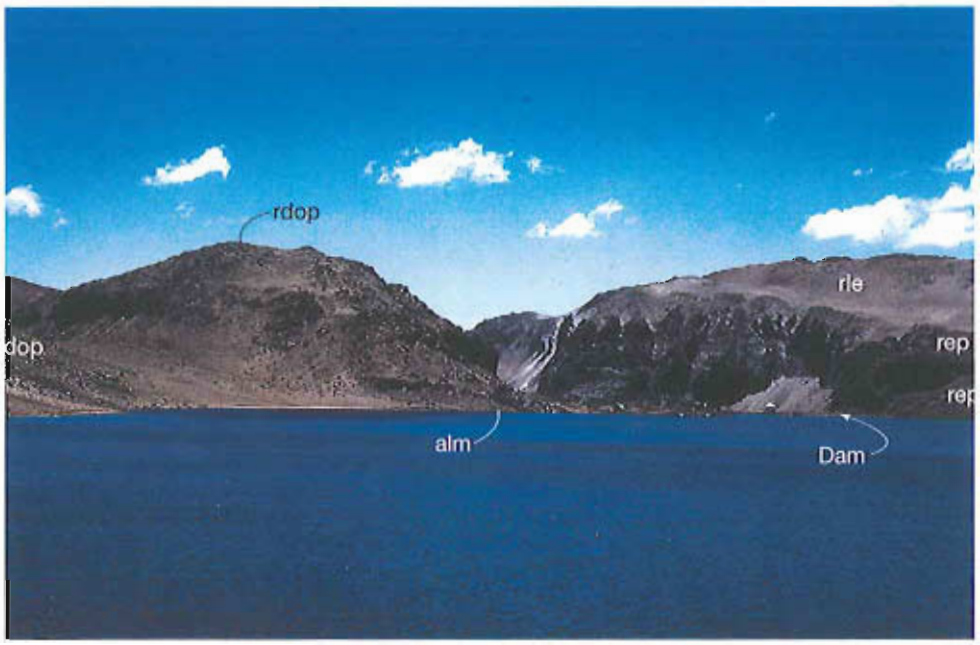

FIG. 16. Outlet of Laguna del Maule viewed northward, illustrating three different silicic units and one andesite. At right, 100-m-long dam regulates lake level and controls Río Maule outflow through 200 m deep outlet gorge. At right, cliff is late Pleistocene rhyolite lava (unit **rep**), of which two flow units are visible at right end of dam. This is overlain by lighter brown, rubbly postglacial coulee of high-silica rhyolite, Loma de Los Espejos (unit **rle**). Dome to left of dam is late Pleistocene rhyodacite of unit **rdop**, which is separated from its twin dome (toe at left edge of image) by a glaciated paleo-outlet channel. Beneath the dome and between it and the dam, the ragged lakeside shelf consists of hybrid andesitic lava unit **alm**, which may have issued from same vent as overlying dome. Wavecut bench at 2,350 m elevation, ~200 m above current lake level, is visible on all three silicic units on both sides of dam. This postglacial high strandline rings the lake basin, formed in response to damming of the outlet by emplacement of Loma de Los Espejos coulee, and here illustrates the threshhold of overflow prior to catastrophic outbreak and deepening of the gorge. Visible in distance on right (east) wall 2 km down gorge is sheared-off cliff of unit **rle** (above scree) where blockage collapsed.

on the west bank of the Río Maule, ~1 km downstream from the dam (Figs. 7, 9). The edifice is a 350 m high half-cone banked against the steep western sidewall (of welded ignimbrite **igsp**) of the outlet gorge. Stratified scoria-fall deposits dip 10°-30° radially down the southeast, east, and northeast flanks, away from the remains of a devastated summit crater where the strata roll over to dip 10-35° inward, are capped by remnants of an effusive lava flow, and are locally fused at the margins of a crater-filling massive intrusive complex. Extensively black but proximally brick-red and locally palagonitized orange, most scoria layers are 0.3-2 m thick, either nonindurated or tack-welded and strongly agglutinated only in and near the crater. The massive composite lava intruding and overspilling the crater is ~200 m wide and exposed for >100 m vertically. Extending southwest from the crater, several vertical dikes, 1-2 m thick and glacially striated, cut and locally fuse the layered scoria. The ejecta are predominantly scoria lapilli, though some layers are rich in coarse ash, and scoria bombs are commonly as big as 30 cm on the flanks and as big as 2 m around the crater. Sparse lithic ejecta include clasts of Tertiary andesite and pyroxene-dacite ignimbrite (unit **igsp**), both shallowly subjacent. All juvenile products are rich in phenocrysts of plagioclase (1-3 mm) and olivine (1 mm), with or without sparse cpx. Five samples range in SiO_2 from 51.4 to 52.9%, and one yielded a $^{40}Ar/^{39}Ar$ plateau age of 62±4 ka (Table 1).

Erosive undercutting along the outlet gorge has promoted failure of numerous slide masses down the east and northeast dipslopes, such that the lower half of the fragmental mafic edifice (below ~2,270 m elevation) now consists of displaced material. Eruption of El Candado at ~62 ka apparently postdated the last advance of a major glacier from the LdM basin into the outlet gorge, because the toe of the edifice overlies gorge-floor till rich in clasts of basin-derived lithologies but devoid of Candado material. Thin diamicts rich in Candado material overlie the till along the river-bank and probably represent local debris-flow deposits. The wavecut high strandline that surrounds Laguna del Maule at ~2,350 m elevation (~200 m higher than present-day lake level) is preserved as a pebble-strewn bench on the south shoulder of the Candado cone. A small moraine deposited by a local slope glacier from the ridge above is rich in blocks of pyroxene-dacite ignimbrite (unit **igsp**), overlies Candado scoria, and ends abruptly at the strandline bench. White diatomite as thick as 2.6 m, apparently deposited during the highstand, overlies the toe of Candado deposits near river level along the road as far as 1.1 km north of the dam. Instability of the fragmental Candado strata contributed to the breaching that catastrophically drained the highstand lake, as interpreted in section 16, below. Undercutting by the outbreak flood in turn promoted recurrent slumping and sliding of the Candado edifice.

The **Andesite of Volcán Puente de la Laguna** (unit **mpl**) forms a 600-m-wide scoria cone on the east shore of the northwest arm of Laguna del Maule, 2 km south of the dam (Fig. 7). The badly degraded cone has been glacially scoured and further eroded during the highstand of the lake. Although it has only ~70 m of surviving relief, the cone still has a shallow central crater, 150 m wide, rimmed by a lag of disrupted lava blocks and scoria bombs (presumed to have been depleted of scoria lapilli by wave action). Most of the cone consists of layered scoria lapilli and agglutinate, largely brick-red, strewn with spindle bombs and capped by a few spatter-fed lava flows only 1-2 m thick. All products have abundant plagioclase phenocrysts, sparse cpx, and rare tiny olivine. Two bombs sampled have 56.3% and 57.2% SiO_2. The undated unit overlies glacial deposits and is overlain by scattered erratics of rhyolitic and intermediate lavas. The postglacial pre-highstand high-silica-rhyolite coulee called the Loma de Los Espejos (unit **rle**) banks against the glaciated cone (Fig. 17).

Five kilometers west of the northwest arm of Laguna del Maule, a broad divide between the headwaters of Cajón Filume and Arroyo de Botacura (Figs. 8, 9) consists of a lava plateau and an associated overlying scoria cone, together assigned to the **Andesite of Vega Piedras Negras** (unit **mpn**). The glacially scoured till-strewn plateau, 2 x 3.5 km across, appears to be a single lava flow as thick as 100 m. The lava is generally massive, though locally streaky or slightly vesicular, and its block-jointed terminal scarp is 50 to 100 m high, facing northward above Vega Piedras Negras. The 1-km-wide scoria cone atop the southeast end of the lava plateau is only ~50 m high but extends northeastward into a parallel pair of fissure-fed ridges of variably oxidized scoria. Most products carry 10-15% plagioclase phenocrysts (1-2 mm), varied proportions of opx and olivine, and sparse cpx; scoriae are apparently poorer in phenocrysts. Four lava samples contain 52.2-53.4% SiO_2, and a scoria bomb has 54.1%. The lava overlies units **Trcf**, **mva**, **mvb**, **msp**, and **dsp**, and its east margin is overrun by the postglacial coulee of unit **rdcn**. A sample from the steep north-central scarp yields a $^{40}Ar/^{39}Ar$ plateau age of 54±21 ka.

The **Andesite south of Cajón Rodríguez** (unit **mcr**) consists of two low-volume spatter-rimmed craters at 2,550-2,750 m elevation, just below the south rim of Cajón Rodríguez (Fig. 8), ~14 km southwest of Laguna del Maule (at the limit of our mapping). The glaciated craters are centered ~1 km apart, and each is ~300 m wide and surrounded by ejecta aprons 1,000 m and 700 m in diameter, respectively. Mafic scoriae on the subdued rims of the shallow craters are widely agglutinated and locally grade into thin spatter-fed dense lava flows. A dense agglutinate sample from the west crater has 54.2% SiO_2, and a lava rimming the east crater has 52.6%. Thicker proximal accumulations of ejecta and broader aprons may well have been substantially reduced by glacial erosion. Products contain 15-20% plagioclase phenocrysts and 1-2% each of opx and cpx. The deposits overlie ignimbrite and stratified andesitic rocks, both of some undetermined Tertiary age.

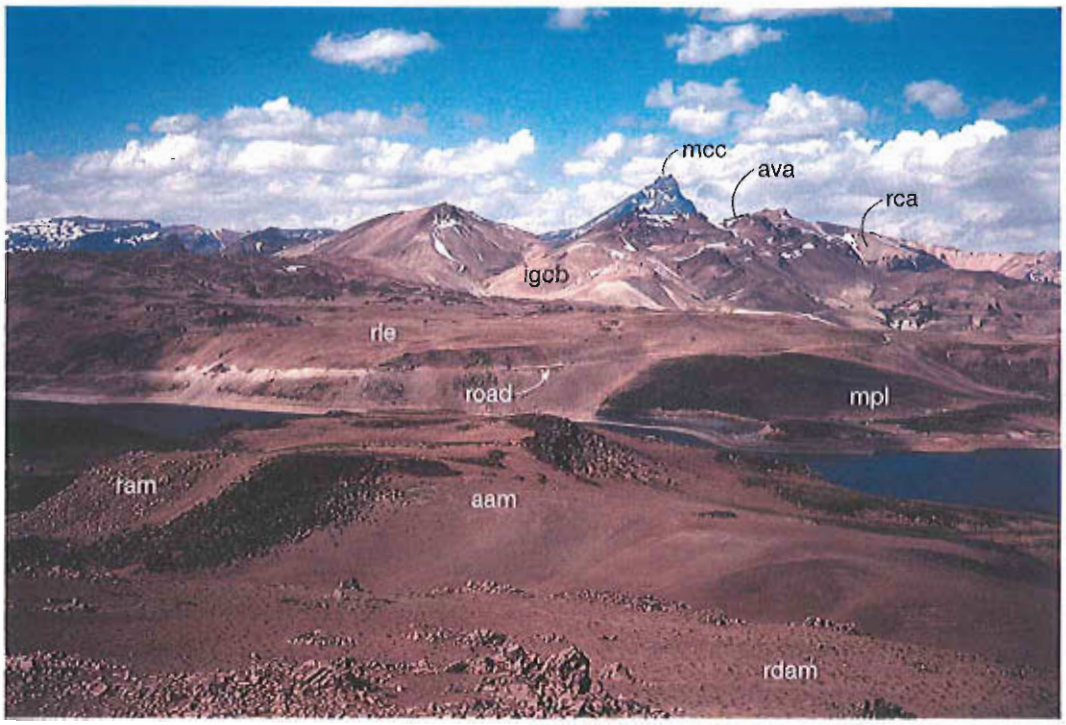

FIG. 17. View northeastward across northwest arm of Laguna del Maule, from Mellicos postglacial rhyodacite coulee (unit **rdam**, near foreground) to 150-ka Cerro Campanario (unit **mcc**; 3,943 m), 23 km away on continental divide. Glacially scoured andesitic vents flank both sides of lake's outlet channel: Volcán Puente de la Laguna (unit **mpl**) with subdued crater on far shore, and sediment-filled brick-red spatter ring of Andesite of Arroyo Los Mellicos (unit **aam**) in foreground. Latter yields $^{40}Ar/^{39}Ar$ age of 26.6±0.8 ka and is intruded at left by postglacial rhyolite minidome (unit **ram**), which is far more evolved than foreground rhyodacite **rdam**. Roadway beyond lake is cut on high-silica rhyolite coulee, Loma de Los Espejos (unit **rle**), which partly overruns andesite cone **mpl** and has itself been smoothed by wave action and lake sedimentation up to elevation 2,350 m during highstand. Transition at left to dark-gray, sediment-free, blocky vesicular carapace is attended by several parallel beach berms. The postglacial Espejos coulee, dated at 23.3±0.4 ka, blocked a paleo-outlet and raised lake level temporarily by 200 m. Serrate ridge beyond Espejos coulee consists of intracaldera Bobadilla biotite-rhyodacite ignimbrite (unit **igcb**; 950±7 ka), more than 500 m thick, overlain by north-dipping andesite-dacite lavas and breccias of Volcán Atravesado (unit **ava**; 900 to 700 ka) and rhyolitic lava and tuff of unit **rca** (712±13 ka).

Because the undated craters remain well-formed despite glaciation, we speculate that they erupted in the late Pleistocene, but they might well be older.

The **Andesite of Crater Las Salinas** (unit **mls**) is a low-volume deposit of phenocryst-poor ejecta around the rim of a 600-m-wide crater atop a ridgecrest in the headwaters of Cajón Rodríguez, 9 km southwest of Laguna del Maule and 1 km north of Puesto Las Salinas (Fig. 8). A thin sheet of black scoria lapilli, including sparse bombs as big as 35 cm, mantles the east and south rims, and a brick-red agglutinate sheet mantles the northwest rim, but each deposit extends outward no more than 300 m from the rim, and the ejecta are wholly missing on the southwest and northeast rims. Juvenile ejecta contain 56.0% SiO_2 and carry 3-5% plagioclase phenocrysts, minor opx, rare amphibole, and abundant tiny white lithics. Walls of the crater, which is floored by an ephemeral pond, consist entirely of Tertiary andesitic strata and are as high as 50 m, though as low as 20 m below the west rim. Lithic ejecta as coarse as 1 m torn from the Tertiary strata are abundant around

the rim, suggesting a major phreatic component in the crater-excavating eruption; the volume of lithic and juvenile ejecta, taken together, however, is far from matching the crater volume. The volumetric budget can be satisfied only if a large fraction of the ejecta has been eroded away, but the fragile material of the steep upper crater walls does not appear to have been glaciated. The crater and its deposits are undated, but preservation of its steep walls and partial preservation of the sheet of loose scoria suggest a late Pleistocene age rather than one still greater.

The sixth of the small mafic eruptive units is the **Andesite of Laguna Turbia** (unit **mlt**), ridge-mantling scoria-fall deposits ejected from two craters on and near the triple divide between Laguna Fea, Laguna del Maule, and the Cajón de Troncoso (Fig. 7). Altogether, six small shallow craters lie within 2.5 km of each other, but only the northwesternmost (Laguna Turbia) and easternmost produced juvenile ejecta, while the four between were exclusively phreatic. The crater of Laguna Turbia is ~250 m in diameter, enclosing a sediment-filled floor and small green lake; its walls consist of andesitic lavas and buff ignimbrite (both probably Tertiary), blocks of which dominate the wind-deflated ejecta sheet surrounding the crater. The ejecta also include subordinate scoriaceous to dense blocks (as big as 1.5 m) of fresh, juvenile phenocryst-poor mafic andesite (52.8% SiO_2). Along the north and west rims, a scoria-fall sheet as thick as 10 m has survived wind scour and drapes the upper inner wall of the crater. In other sectors the sheet has been deflated to a lag of larger blocks. The scoriae contain ~1% plagioclase phenocrysts (≤1 mm), sparser olivine, and scattered white xenoliths, probably altered tuff, angular to rounded, and as big as 3 cm. The easternmost crater (UTM grid 608/999) is ~150 m in diameter, likewise blown out through Tertiary basement, and surrounded by a scoria-fall deposit 5-10 m thick that dips back into the crater on its south rim. The lower half of the ejecta sheet is brick-red near the rim but black above and elsewhere, where the scoria fall is preserved on ridges for 2 km eastward as well as within a narrow sector for 1.5 km WNW of the crater. Scoria bombs from the eastern crater are nearly aphyric but contain abundant cream-white frothy xenoliths of partially melted granitoid or crystal-rich tuff. The ejecta resemble those around Laguna Turbia in lithology, situation, and degree of preservation, but grainsize clearly decays away from two discrete centers of emission. A bomb from the eastern crater yields 54.3% SiO_2 (1.5% more than in a bomb from Laguna Turbia); the difference might be attributable to contamination by the molten xenoliths. Around neither of the craters is a liberally reconstructed volume of juvenile ejecta sufficient to account for crater volume. Phreatic explosions evidently contributed to crater excavation, in part for these two and entirely for the four craters between them. The degraded craters and scoria-fall remnants are inferred to be of latest Pleistocene age (~25-10 ka) but they apparently postdate local deglaciation.

FIVE SMALL INTERMEDIATE VOLCANOES

Among the 28 late Pleistocene eruptive units identified, there are also five small volcanoes of silicic andesite. Two lie at the northwest shore of Laguna del Maule, two are well southwest of the lake, and one is atop the ridge east of Valle Chico, 15 km west of the lake.

The **Andesite of Presa Laguna del Maule** (unit **alm**) is a conspicuously heterogeneous lava flow that extends from the dam that impounds the lake for 600 m westward as a raggedly glaciated lakeshore bench (Figs. 7, 16). Directly overlain there by rhyodacite dome 2,367 (unit **rdop**), the lava flow also crops out ~500 m north as an ice-scoured spur beneath the northeast edge of the dome. The andesite lava is widely glassy or partly so and generally massive, although its scoriaceous surface is preserved locally near the south toe of the overlying dome; horizontal and inclined columnar joints are preserved locally. Streaky heterogeneity is broadly discernible, and intimately mingled, relatively mafic and silicic lenses, sheets, and blebs are conspicuous at the northeastern outcrop. Discrete chilled enclaves, fine-grained and finely vesicular, are abundant and ubiquitous; most are smaller than 2 cm, a few as large as 10 cm, and all contain sparse olivine and plagioclase. The host lava itself is variably phenocryst-rich, carrying 5-12% plagio-

clase, common opx, and sparse biotite and amphibole (both opacitized), and (locally) sparse olivine and cpx, both probably disaggregated from enclaves. Relatively homogeneous-appearing samples from the south and northeast outcrops contain 61.8% and 61.2% SiO_2, respectively. The base of the undated unit is not exposed, but Tertiary ignimbrite crops out 800 m downstream on the east bank of the Rio Maule. The silicic magma with which the andesite mingled is probably that of the overlying glaciated rhyodacite dome (unit **rdop**), which is also thought to be of late Pleistocene age.

The **Andesite of Arroyo Los Mellicos** (unit **aam**) is a glacially scoured lava-flow platform that extends (in three remnants) for 1.8 km along the west shore of the northwest arm of Laguna del Maule (Figs. 6, 17). What appears to be a single flow has up to 100 m relief near the lakeshore, and its low-relief surface is capped locally by degraded remnants of a 150-m-wide crater now defined by a low ring of brick-red spatter and sheeted agglutinate. The shallow crater depression is largely filled with pumice and lake sediments, which also infill most of the modest surface relief on the lava plateau, outcrops of which are strongly marked by glacial striae that strike northeast toward the lake outlet. The medium-gray lava is largely block-jointed, locally platy, and is generally stripped of any glassy exterior. It contains 57.9-58.8% SiO_2 and carries 3-5% plagioclase phenocrysts (1-2 mm) as well as sparse cpx and olivine (both <1 mm). A sample from the striated surface of the principal plateau yields a $^{40}Ar/^{39}Ar$ age of 26.6±0.8 ka, making this the youngest glaciated unit in the Laguna del Maule basin. The unit overlies deformed Tertiary andesitic and rhyolitic lavas and tuffs, is intruded by a postglacial rhyolite minidome (unit **ram**), and is overlain by the postglacial rhyodacite coulee of unit **rdam**. With its high point at 2,278 m elevation, the unit was wholly submerged during the 2,350 m highstand of Laguna del Maule.

The **Andesite west of Laguna del Piojo** (unit **alp**) is an ice-scoured red scoria cone on the valley floor 4 km west of Laguna del Maule and 2 km west of the eponymous lake (Fig. 7). Thinned by glaciation and later planated by wave action during the highstand of Laguna del Maule, the pile is partly mantled by till, lake sediment, and aeolian sand, leaving no evidence of a former crater or other vent structure. Also surrounded by surficial deposits, its base is nowhere exposed. The 500-m-wide mound has ~30 m relief and consists of stratified scoria and agglutinate, mostly oxidized, capped by a 5-m-thick lava flow that extends along the east rim for ~150 m. Probably spatter-fed, the lava is streaky to flow-foliated and locally preserves ghost blobs 1-5 cm across. Many scoria bombs are fairly dense and as big as 1 m. They contain 8-10% plagioclase phenocrysts (1-3 mm), sparse amphibole and minor opx; one such bomb analyzed has 60.7% SiO_2. The unit contrasts with a postglacial scoria complex just 200 m north (unit **mnp**), products of which are phenocryst-poor and considerably less silicic.

The **Andesite of Cajón Rodríguez** (unit **acr**) is an intracanyon lava flow 25-30 m thick that extends for 3 km along Cajón Rodríguez from a vent ~12 km southwest of Laguna del Maule (Fig. 8). The vent cone is largely eroded away and covered by till, but many remnants of interstratified lapilli falls and agglutinate drape the lava flow at 2,120 m elevation on the canyon floor. For 2 km downstream the lava flow floors the canyon, and for an additional 1 km to its eroded terminus down at 1,870 m, remnants on both walls form ledges as high as 25 m above the river. The lava is widely vesicular, glacially striated, has 61.1% SiO_2, and carries 5-8% plagioclase phenocrysts, sparse opx and cpx, and opacitized amphibole. It rests exclusively on Tertiary andesitic strata. Although undated, its good state of preservation on the canyon floor indicates an age no older than late Pleistocene.

The **Andesite of Puntilla Los Ñirales** (unit **apñ**) is a scoria cone atop the ridge just east of Valle Chico, 15 km west of Laguna del Maule (Figs. 8, 14). Actually a half-cone, in part because originally built on a slope and in part because its east side has been glaciated away, the stratified scoria and agglutinate that make up the 1.5 x 1-km-wide edifice dip ~25° to the west and southwest. The south and west sides of the edifice, which has ~200 m of surviving relief, are also glacially eroded and strewn with varied erratics, and only its top ~70 m remained above the ice. The slopes

are mostly stratified or sloughed scoria lapilli, along with scattered bombs as big as 1 m, but a 20-m-thick gray lava flow, probably spatter-fed, is exposed on the southwest slope, enclosed by layers of red scoria. All products are phenocryst-poor, containing sparse plagioclase, olivine, and cpx. Two bombs analyzed contain 56.2% and 57.9% SiO_2. The undated cone overlies units **mvñ**, **rdpñ**, **avz**, and obsidian flow **rez** (83±3 ka).

RÍO MAULE INTRACANYON ASSEMBLAGE

Along the Río Maule, from a point 2 km below its origin at the lake, a scoured plateau (Fig. 9) of mafic and andesitic lava flows extends ~6 km to an abrupt erosional scarp over which the river falls nearly 100 m as the Salto del Maule (Fig. 18). Below the scarp, several intracanyon lava remnants are preserved on both sides of the Río Maule for another 5 km downstream. The various remnants are complexly stacked and distributed, but, on the basis of composition and petrography, they have been subdivided into five eruptive units: two mafic andesites, two silicic andesites, and a dacite. The lowermost, unit **avm**, yields a $^{40}Ar/^{39}Ar$ plateau age of 116±27 ka, so all the others are thought likewise to be of late Pleistocene age.

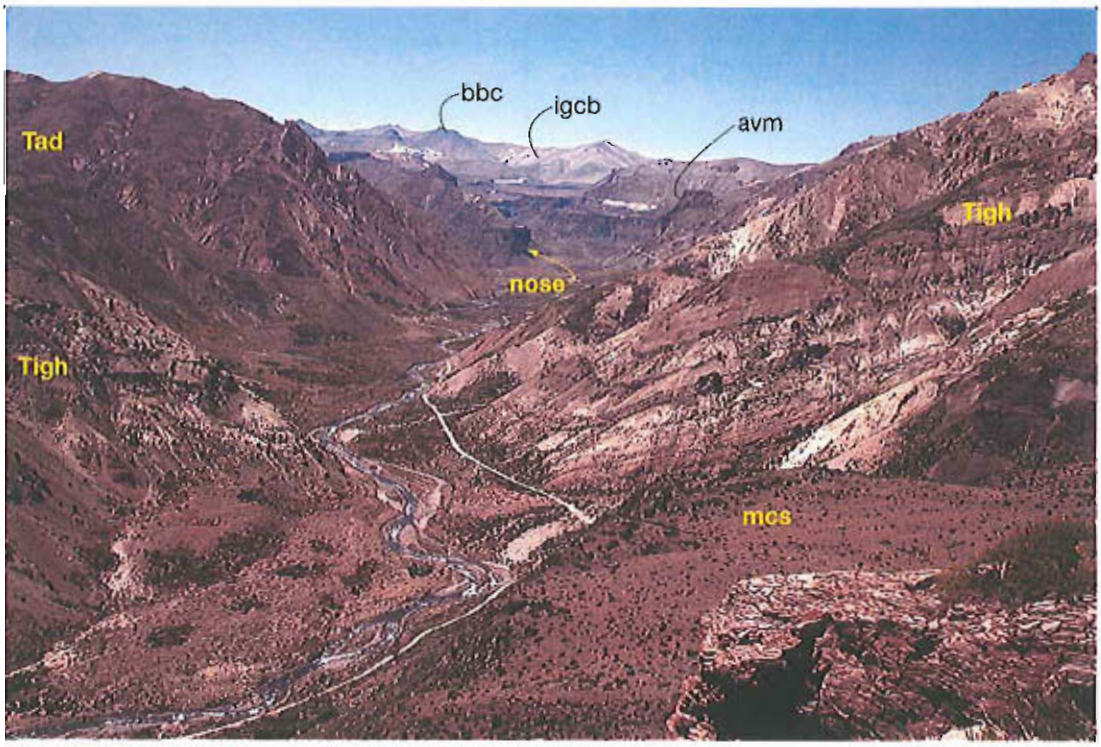

FIG. 18. View southeastward up canyon of the Río Maule from rim of Triangular Plateau (Fig. 13), 400 m above deeply alluviated valley floor and area's only road. Middleground walls are synclinally folded Miocene ignimbrite (unit **Tigh**) and stratified Miocene andesites (**Tad**). Upvalley 7 km, alluvial floor ends abuptly at 150-m-high scarp cut on stack of late Pleistocene lava flows over which Salto del Maule falls. Above scarp rim is scabland plateau seen in figures 5, 20, and 38. Downstream 1 km from scarp (toward viewer), dark cliff left of valley floor is stack of three lavas on Maule-Campanario **nose** seen in figure 19, and dark lava remnant higher on opposite (right) wall is Vacas Muertas (unit **avm**). On skyline, black crag is eroded basaltic cone of unit **bbc** (154±7 ka) and pale-gray peak to its right consists of intracaldera rhyodacite ignimbrite of unit **igcb** (950±7 ka).

The **Andesite of Vacas Muertas** (unit **avm**) includes two separate remnants, one forming the lowest of three lava flows that form the cliffy nose between the Ríos Campanario and Maule just east of their confluence (Fig. 19) and the second a precipitous remnant ~225 m thick on the south wall of the Río Maule ~1 km south of the confluence. The basal flow is exposed on both sides of the nose, is 40-50 m thick, rests on Tertiary andesitic rocks, and is pervasively columnar and partly glassy. It has a basal colonnade of stout (0.5 to 1 m thick) vertical columns 5-8 m high, overlain by a 40 m thick zone of slender (10-20 cm-thick) sweeping columns that locally bend over to inclinations of 45°. We infer ice-contact emplacement, probably along a trough between converging glaciers of the Maule and Campanario valleys. On the south wall of the Maule canyon, the lava remnant forming the great cliff called Vacas Muertas (Fig. 18) is a single flow, its lower 150 m strikingly columnar and its upper 75 m displaying widely spaced vertical (non-columnar) joints. The lower part was probably emplaced between the Maule glacier and the steep sidewall of Tertiary ignimbrite, while the upper part was supraglacial. The lavas have 60.6-62.0% SiO_2 and carry ~10% plagioclase phenocrysts (0.5-1.5 mm), as much as 5% olivine (≤1 mm), and minor cpx. The basal flow on the south face of the nose 1 km east of the confluence yields a $^{40}Ar/^{39}Ar$ age of 116±27 ka (Table 1).

FIG. 19. Stack of three late Pleistocene lava flows on nose dividing glacial valleys of Río Campanario and Río Maule (foreground at 1,540 m elevation), 600 m southeast of their confluence. Lowest flow (unit **avm**; 60.6% SiO_2), pervasively columnar, partly glassy, and 50 m thick, rests on Tertiary andesite and yields a $^{40}Ar/^{39}Ar$ age of 116±27 ka. Middle flow (unit **alc**; 59.3% SiO_2) is platy or block-jointed, largely devitrified, and 12-15 m thick. Top flow (unit **meb**; 53.9% SiO_2) has several tiers of partly glassy, variously oriented columns, and thickens at the nose from 50 m to 100 m where it drapes down over the lower pair. View is northeastward to Cerro Galaz (peak 2,954), a deformed and dike-laced Miocene mafic-to-andesitic center on skyline 6 km away; banked high against its right side, white-rimmed skyline bench is undated Pleistocene ignimbrite unit **lgcg**, nonwelded biotite-bearing high-silica rhyolite. In upper right distance, patch of red scoria and nearby knob are remnants of olivine-bearing phenocryst-poor unit **mqf** (53.7% SiO_2), probably early Pleistocene.

The **Dacite of Cuesta Los Cóndores** (unit **dcc**) is a single thick flow of hornblende-bearing dacite lava exposed on the north-facing scarp over which Arroyo Arenas Blancas pitches in a high waterfall ~600 m south of its confluence with the Río Maule (Fig. 9). At a distance, the dark-gray

flow is easily confused with the set of cliff-forming mafic lava flows that overlie it. Lowest flow of the stack exposed on the scarp, the dacite is largely glassy, widely vesicular, 50-80 m thick, and marked by slender near-vertical columnar joints. At the southwest sidewall of the canyon, however, where banked against a cliff of Miocene ignimbrite, the glassy dacite margin extends ~100 m higher than its own top surface on the adjacent north-facing scarp and also 50 m higher than the mafic lavas that overlie it on the scarp. It can be inferred either that during emplacement the upper half of the flow drained away after marginally chilling against its sidewall or that a flat-floored canyon was eroded into the dacite prior to emplacement of the overlying mafic lavas. The high sidewall remnant of the dacite crosses the road that ascends Cuesta Los Cóndores at an elevation ~170 m above the valley floor; the remnant is ~10 m thick at road level and extends for ~25 m above the road as three upward-thinning glassy, flow-foliated, locally brecciated veneers banked against baked colluvium. The flow contains ~10% plagioclase phenocrysts (1-2 mm), ~2% each of opx and hornblende, and rare cpx and olivine, as well as common fine-grained, relatively mafic enclaves, which are typically crenulate, chilled, and finely vesicular. Disaggregation of enclave material may be the source of the rare cpx and olivine in the host dacite. Three samples have 63.4-65.5% SiO_2 and 2.54-2.78% K_2O. Drake (1976) reported K-Ar ages of 100±10 ka and 170±20 ka for the dacite (Table 2).

The **Andesite of Cuesta Los Cóndores** (unit **alc**) consists of three glaciated remnants, -one a plateau-rim roadcut at 1760 m elevation on the Cuesta Los Cóndores road grade (UTM grid 562/207), another the middle flow of the stack of three on the narrow nose (Fig. 19) separating the Ríos Maule and Campanario just above their confluence, and distally a rôche moutonée <100 m long beside the road ~1 km WNW of that confluence (543/230). The first is locally the top flow on the westerly rim, overlying thick dacite unit **dcc**. On the nose, the middle flow is 10-12 m thick, largely devitrified with platy to blocky non-columnar jointing, and sandwiched by thicker, glassier, columnar flows of units **avm** and **meb**. The small distal remnant is banked against Tertiary basement. The three outcrops are virtually identical chemically at 59.2-59.6% SiO_2 and 2.00-2.05% K_2O. They carry 10-15% plagioclase phenocrysts (1-5 mm, some shattered), common opx, and scattered cpx-olivine-plagioclase clots but few free cpx or olivine crystals.

The **Andesite of Salto del Maule** (unit **msm**) is the principal plateau-capping set of glaciated mafic lava flows that extends 6 km along the Río Maule from beneath the Loma de los Espejos rhyolite coulee to the eroded scarps near Salto del Maule (Figs. 9, 20). The stairstep plateau consists of several lava flows, each 5-15 m thick, striated, scoured, and plucked into a series of ledges and polished knobs and ribs, massive to vesicular, and only locally platy or rubbly. Till is preserved in a few pockets, but the plateau surface near the Maule gorge is a scabland scoured clean by the breakout flood that culminated the Laguna del Maule highstand (see section 16, below). Evidence for vents is preserved in two areas: **(1)** On the steep east wall of the Maule gorge (601/158), stratified red scoria and agglutinate >25 m thick are intercalated near the middle of a stack of ~10 thin lava flows (each 0.5-5 m thick) that may represent the edge of an adjacent vent concealed beneath silicic coulees of units **rdno** and **rle**; and **(2)** on the 2,250-m-nose (625/165) just northeast of the unit **rle** flow front, two blocky 10 m thick lava flows sandwich a 50-m-section of stratified red scoria, likewise probably a remnant of a glaciated vent complex. Separated by only 2 km, they may be parts of the same vent system, perhaps fissural, now largely covered by the Loma de Los Espejos coulee (unit **rle**) and its rhyodacite satellites (units **rdno** and **rdne**). Some of the flows have only a few percent phenocrysts, but most have 5-10% plagioclase and 1-3% olivine and cpx. Flows become fewer and thicker downvalley, such that the distal northwest scarp (570/210) consists of only three flows, together nearly 100 m thick; the lowest is ~50 m thick, rests on Tertiary andesites and tuffs, and pinches out southward over the thick dacite lava flow of unit **dcc**. From vents near or above 2,250 m elevation, the package of flows descends downvalley to 1,800 m at the Salto del Maule rim, and (2 km farther northwest) its base is as low as 1,650 m below its terminal scarp. A dozen samples analyzed range in SiO_2 from 51.8% to 57.0%, but nine of them have 53.3-55.6%. The least silicic is a thin spatter-fed flow at the westerly vent, the most silicic a

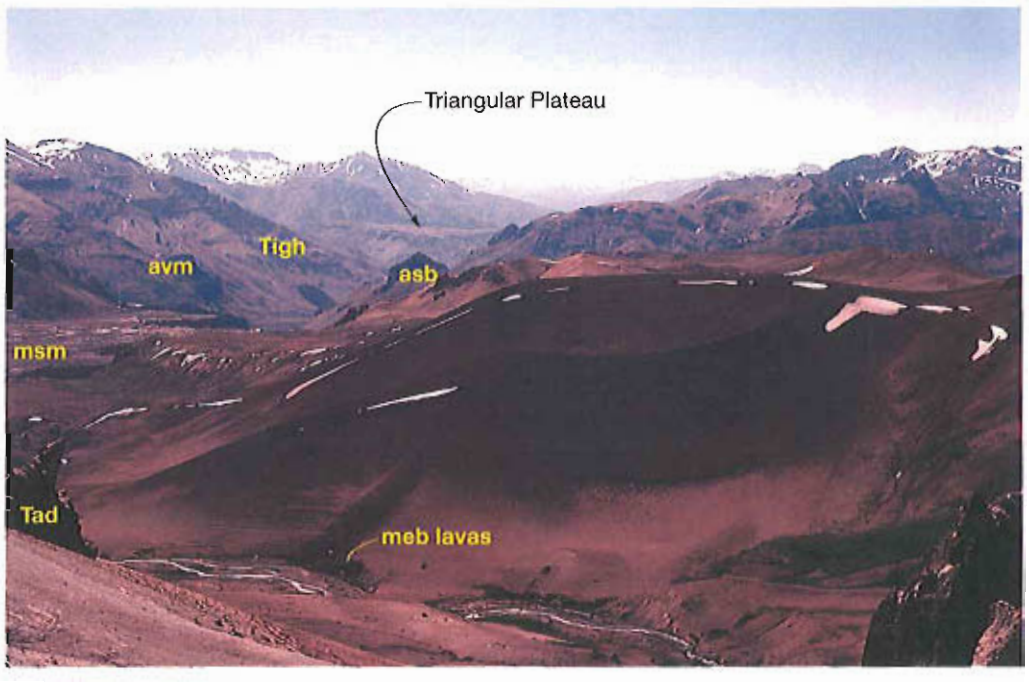

FIG. 20. Crater Bobadilla (unit **meb**), latest Pleistocene scoria cone, 200 m high and 1 km wide, of mafic andesite. Cone itself stood aside of glaciers, but fountain-fed lavas issuing from its base become glacially modified within 2 km of cone where they merge onto flood-scoured scabland lava plateau (left center) along Río Maule. Plateau ends in 150-m-high scarp over which river falls at Salto del Maule. Steep black buttress on left bank ~1 km beyond scarp is Vacas Muertas, a 250-m-thick remnant of andesite unit **avm** (116±27 ka) banked against wall of Miocene ignimbrite. Black pyramid opposite Vacas Muertas on right side of Maule valley is 130-m-thick remnant of andesite unit **asb** (374±7 ka; see Fig. 37). Skyline ridges and walls of Maule canyon downstream to northwest consist of deformed Tertiary and Mesozoic volcanic and sedimentary strata and an 80-Ma granodiorite pluton. In middle distance at medial elevation, Triangular Plateau, 13 km downstream from scoria cone and 500 m above present canyon floor, is capped by 335-ka rhyolite lava unit **rlm**, which issued from Río de la Plata tributary (cf. Fig. 13) and indicates elevation of valley-floor confluence at that time.

rubbly flow at the easterly vent; otherwise, no simple compositional correlation with emplacement sequence has been discerned. It may need emphasizing that none of the three units (**avm**, **alc**, and **meb**) preserved on the Maule-Campanario nose (Figs. 6, 19) are represented on the plateau-terminating scarp over which Salto del Maule plunges just 3 km upstream (Figs. 18, 20).

The **Andesite of Estero Bobadilla** (unit **meb**) is the youngest of the five compositionally distinguishable units making up the glaciated assemblage of lava flows above and below the scarp at Salto del Maule. It is preserved as remnants in four separate areas: **(1)** Along both banks of Estero Bobadilla at the foot of the scoria cone called Crater Bobadilla (Fig. 20); **(2)** a flow remnant overlying the dacite (unit **dcc**) near the northwest end of the plateau, along the road and adjacent Arroyo Arenas Blancas (UTM grid 564/206); **(3)** the top flow of the stack of three on the narrow nose (Fig. 19) separating the Ríos Maule and Campanario just upstream of their confluence; and **(4)** a 200-m-long remnant at 1,600-1,650 m elevation banked against Miocene ignimbrite at the base of the west wall of the Maule valley, 800 m southwest of the confluence (548/220). Although the other outcrops are clearly glaciated, those along Estero Bobadilla include rubbly scoriaceous surfaces on lava-flow terraces adjacent to the stream gorge, which cuts down into a platy devitrified interior.

At the upstream end of the Crater Bobadilla scoria cone, a 10-m-high lava-flow ledge (621/188) that grades up into stratified agglutinate and red scoria of the unglaciated cone (Fig. 20) gives a $^{40}Ar/^{39}Ar$ plateau age of 86±8 ka (Table 1). Because there are no lava outcrops farther upstream, we infer that the scoria cone conceals the source of the lava and that an ice-free window separated the Maule and upper Bobadilla glaciers during and subsequent to eruption of the cone and its lavas.

The other outcrops are strongly eroded, although part of the glassy rubbly top of the flow survives at the Arroyo Arenas Blancas location, where a columnar basal zone and massive interior are also exposed along the creek. The top flow on the Maule-Campanario nose thickens from 50 m to nearly 100 m distally where it drapes down over the two flows beneath it (Fig. 19); several tiers of vertical, inclined, and subhorizontal glassy columns strikingly exposed on both of its sidewalls suggest that the flow was emplaced against ice. Lavas at all four locations contain 10-15% plagioclase phenocrysts (1-3 mm), 1-3% olivine (0.5-1 mm, commonly in clusters), and sparse cpx. Seven lava samples are chemically similar, containing 53.0-53.9% SiO_2, 1.14-1.31% K_2O, and unusually high Al_2O_3 (18.7-19.7%). By comparison, a scoria bomb from the crater of the vent cone, which intimately overlies the most proximal lava, has fewer phenocrysts and is slightly more evolved at 54.9% SiO_2. The scoria cone is banked against a ridge of Tertiary lavas and tuffs, has ~200 m relief, and is degraded but not glaciated. Its shallow crater is open to the south, and its red and black cinder-scree slopes are marked locally by thin ledges of tack-welded to dense agglutinate. The crater rim is armored by a deflation lag of scoria bombs, many as coarse as 1 m. Rare partially melted granitoid blocks are present, but (overall) accidental lithics are remarkably sparse, indicating open-vent strombolian activity.

SIX ORPHAN REMNANTS OF LATE PLEISTOCENE LAVA FLOWS

Of the 27 late Pleistocene units delineated, six are isolated lava flows for which vents are buried or otherwise unlocated. These include two units in Cajón Rodríguez, three units just west of Laguna del Maule, and a glaciated rhyolite coulee that forms the east wall of the lake's outlet gorge.

The **Andesite of Vega Rodríguez** (unit **avr**) is a glaciated intracanyon lava flow that floors the upper Cajón Rodríguez for ~1 km (Fig. 8), ending in an eroded flow front at 2,250 m elevation. Resting on deeply eroded Tertiary andesitic strata, the flow is at least 30 m thick, and parts of its striated surface remain glassy and block-jointed. The undated lava contains 61.9% SiO_2 and carries 10-15% plagioclase phenocrysts as well as sparse amphibole and opx. Phenocryst-poor ejecta around the nearby crater of unit **mls** (~1 km east) are far more mafic and evidently unrelated. Possible sites of a source vent (not visited in this investigation) include another glaciated remnant that floors a cirque ~1.5 km to the northeast and red to black scoria and spatter-fed lavas draping the 2,750-m south-trending spur ridge ~1 km to the north.

The **Andesite northeast of Las Salinas** (unit **als**) is an isolated remnant of a blocky lava flow at 2,600 m elevation that floors the upper northeast cirque in the headwaters of Cajón Rodríguez, 8 km southwest of Laguna del Maule (Fig. 8). Covering an area of only 200 x 400 m, the bench-forming flow is horizontal and as thick as 40 m. Although lightly glaciated and with till overlapping its south margin, much of its surface remains partly glassy, vesicular, and blocky. The flow-foliated lava has 59.6% SiO_2 and carries ~5% plagioclase phenocrysts (1-2 mm), sparse opx and cpx, and abundant pale-gray crystal-poor mafic enclaves (1-10 cm). The remnant overlaps the contact between deformed Tertiary andesites and subhorizontal ridge-capping andesitic lavas of early Quaternary age (unit **arp**; 2,010±23 ka). It is unrelated to the phenocryst-poor mafic andesite of Crater Las Salinas (unit **mls**), ~1 km to the west.

The **Dacite of Laguna del Piojo** (unit **dlp**) is a single lava flow from a largely concealed vent at ~2600 m elevation in the southwest corner of the Laguna del Maule basin (Fig. 7). It extends 4 km northeast as a series of windows through younger deposits to a terminus on the southwest shoreline of Laguna del Piojo at 2,200 m. Less than 500 m wide, the flow is everywhere black, glassy,

block-jointed, and massive to vesicular. Distally, it is widely overlain by till, highstand lake deposits, aeolian sand, and pumice scree. Medially, it banks against the coulee of unit **rdct** (203±41 ka). Proximally, the flow is mantled by agglutinate and scoria-fall deposits of fissure-fed mafic units **mcp** and **mct**. At its most proximal exposures (UTM grid 562/030), along the northeast-trending gulch that parallels the southeast slope of scoria ridge 2,657, the glaciated glassy dacite forms both the floor and the 30-m-high sidewall; at the head of that gulch, the flow grades into layers of dense agglutinate as thick as 5 m, probably marginal to its concealed vent. The undated lava contains 5-10% plagioclase phenocrysts (1-3 mm), ~2% slender prisms of amphibole, and minor biotite and opx. Four samples yield 63.0-64.1% SiO_2 (with no obvious spatial systematics).

The **Older Andesite of West Peninsula** (unit **apv**) is a single glacially scoured lava flow that crops out for ~2 km along the northwest side of the major peninsula on the west shoreline of Laguna del Maule (Figs. 7, 21). Its exposure is 300-600 m wide with 50-80 m total relief, and it rests on altered and deformed Tertiary intermediate lavas and tuffs. The ice-scoured lava shelf is widely covered by highstand lake sediments and overlapped on the south by a postglacial lava flow of andesitic unit **apj**. The flow is partly devitrified, platy to block-jointed, has 57.9% SiO_2 and carries ~5% plagioclase phenocrysts, sparse olivine, and rare cpx microphenocrysts. Its vent is covered by the postglacial rhyodacite coulee of unit **rdcd**, which also overlies the source of younger andesitic unit **apj**.

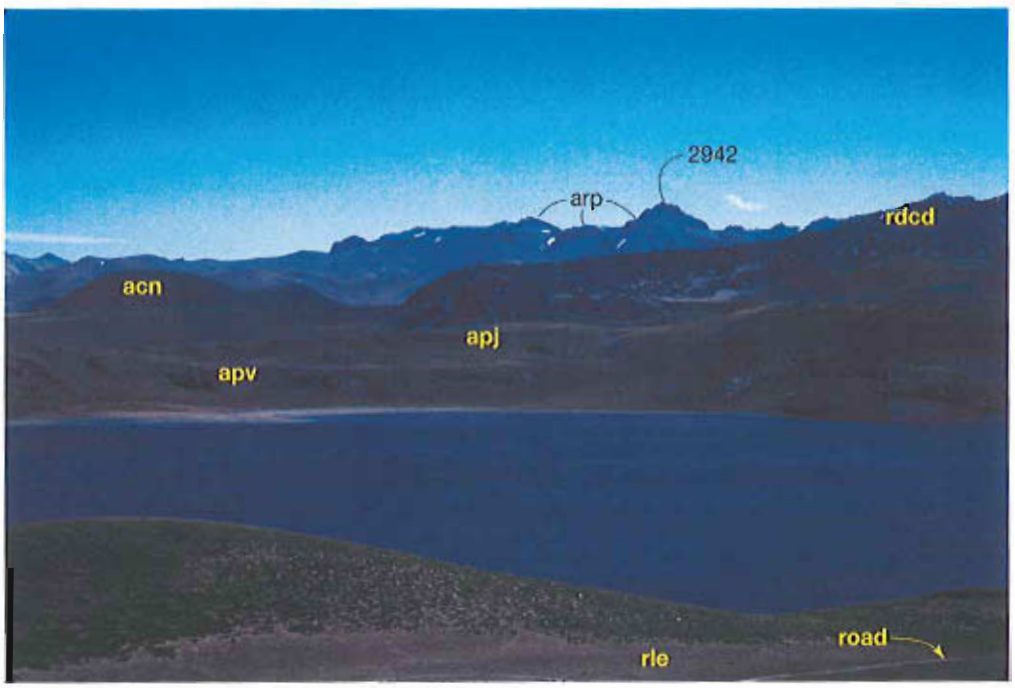

FIG. 21. High strandline cut at 2,350 m on postglacial Crater Negro scoria cone (unit **acn**) and Colada Dendriforme (unit **rdcd**), as viewed toward southwest across northwest arm of Laguna del Maule from lake-smoothed surface of Loma de Los Espejos coulee (unit **rle**); international roadway in foreground. Major gravel bar, rich in rounded clasts from both units, follows strandline between cone and coulee. Two ledges at left center are andesite lava flows of West Peninsula, the lower one glaciated (unit **apv**), the upper postglacial (unit **apj**), but both subdued by wave action and lake sedimentation during the highstand. Hills at right center consist of Tertiary andesitic lavas and tuffs. Crags on skyline frame snow-floored pass toward Cajón Rodríguez; subhorizontal stack of thick silicic pyroxene-andesite lavas (unit **arp**) capping divide rests on deformed Tertiary intermediate lavas and tuffs; topmost lava flow on highest peak 2,942 yields $^{40}Ar/^{39}Ar$ age of 2.0 Ma.

The **Andesite south of Domo del Maule** (unit **asd**) is a small window of glassy glaciated lava exposed locally beneath the northeast snout of the postglacial rhyodacite coulee of unit **rdam**, just south of Arroyo Los Mellicos and 600 m from the west shore of Laguna del Maule (Fig. 7). Cropping out over an area of 150 x 200 m, the lava has total exposed relief of only 30 m. Its base is covered and thus its relationship with adjacent glaciated unit **aam** (26.6±0.8 ka) remains uncertain. Its lower part is massive vitrophyre, and its upper part is slightly vesicular and striated but only lightly ice-scoured, as illustrated by preservation of prismatic and jigsaw jointing on its glassy surface. The undated unit may be a small lava dome rather than a flow front. It has 62.5% SiO_2 and carries ~10% plagioclase phenocrysts, 1-2% each of amphibole and opx, rare biotite, tiny cpx, and sparse small mafic enclaves.

Last of the orphan lavas is the **Rhyolite east of Presa Laguna del Maule** (unit **rep**), which forms the steep east wall of the outlet gorge downstream from the dam that impounds the lake (Fig. 16). With ~150 m of relief, the unit crops out from the lakeshore near the dam for ~1.5 km northward as a great cliff, the rim of which is draped by the postglacial coulee of unit **rle**. Just east of the dam, a sheared contact divides the unit into a lower shelf and the main cliffy wall, but the two subunits are compositionally and petrographically identical. They have 73.5% SiO_2 and carry 5-7% plagioclase phenocrysts, 3-5% biotite, and rare amphibole. Glassy surfaces are preserved locally on both subunits, but their spherulitic to felsitic interior zones are deeply exposed on the walls of the outlet gorge. The unit is unequivocally different from three other biotite-bearing silicic lavas nearby (Fig. 7): glaciated unit **rdop** (71.6% SiO_2) which forms the domes west of the dam, postglacial unit **rdno** (69% SiO_2) which forms the east wall of the outlet gorge 2-3 km below the dam, and postglacial unit **rle** (76% SiO_2) which drapes both units **rdno** and **rep**. The rhyolite is directly overlain by high-silica- rhyolite coulee unit **rle** (23.3±0.4 ka). An attempt to date plagioclase from unit **rep** itself yielded a $^{40}Ar/^{39}Ar$ plateau age of 38±29 ka (Table 1).

POSTGLACIAL ERUPTIVE UNITS (<25 ka)

Of ~135 eruptive units distinguished within the map area, 34 are unmodified by glacial erosion. These include eleven rhyolites, nine rhyodacites, two dacites, eight silicic andesites, three mafic andesites, and one true basalt. Morphologically, they include two scoria cones, six small mafic or intermediate pyroclastic rings or fissure vents, four substantial flows of intermediate lava, two small lavas for which vents are not exposed, and 20 silicic units consisting of domes, coulees, or radial arrays of flows with or without pumice rings or cones. In many parts of the world (including the Chilean lake district only 400 km south of here), the Last Glacial Maximum took place around 21-18 ka, and at middle latitudes many mountain glaciers readvanced or remained in advanced positions for several thousand years after that. In the Laguna del Maule basin, however, on the 36th parallel, with its floor at ~2150 m and its narrow surrounding divides at ~3,000 m, glaciers had withdrawn from the basin floor by ~25 ka (Singer *et al.*, 2000). Glaciated andesitic unit **aam**, at the lakeshore 2 km south of the outlet, yields a $^{40}Ar/^{39}Ar$ plateau age of 26.6±0.8 ka. Three non-glaciated lavas, all also at lake level, yield plateau ages only slightly younger: Unit **ajp** on the west peninsula gives 24.6±2.2 ka; unit **rdac** at the southeast corner of the lake gives 21.1±0.9 ka; and unit **rle**, the coulee that dammed the outlet of the lake, gives 23.3±0.4 ka (Table 1; Fig. 7).

TWO SCORIA CONES

The **Basalt of Cerro Hoyo Colorado** (unit **bhc**) is a 200-m-high scoria cone ~900 m in diameter located on the northeast bank of Estero Rodríguez, a few kilometers upstream from its convergence with the Río Saso and 14 km west of Laguna del Maule (Fig. 8). The cone has a

200-m-wide summit crater, and, from a mid-slope bocca on its west side, there emerges a 350 m long bilobate package of very thin (1-2 m) effusive lava flows. The lavas are pervasively vesicular, as are scoria bombs as big as 50 cm. Through the scoria scree that mantles the cone, dipslopes of thin agglutinate are exposed locally. Additionally, a 10 m thick accumulation of several thin oxidized agglutinate sheets mantles a basement ridge 500 m north of the cone, and a layer of black ashfall drapes steep topography for ~2 km southeast of the cone. Products have 50.0-51.3% SiO_2 and contain 15-20% plagioclase phenocrysts (1-3 mm), ~5% olivine (few >1 mm), <1% cpx, and rare plagioclase megacrysts as big as 10 mm.

The **Andesite of Crater Negro** (unit **acn**) is a 200-m-high scoria cone, elongate southwest-northeast, that covers a 1.3 x 2 km area, its summit located only 2 km from the west shore of Laguna del Maule (Fig. 7). Its upper 100 m is a steep cone 600 m in diameter, dominantly of scoria lapilli, smoothed and bevelled by the wind but otherwise little eroded. Below 2,350 m elevation, its lower 100 m was surficially reworked by wave action, which cut a prominent bench around the cone during the brief highstand of the lake (Fig. 21). A beach bar of rounded scoria and lithic pebbles extends north from the toe of the upper cone for 600 m along the wave-cut bench. A shallow crater 300 m across tops the cone; on its rim are sparse juvenile bombs, some fusiform or breadcrusted, as well as ballistic ejecta as big as 50 cm from the vent of younger rhyodacite unit **rdcd**, ~2 km to the west. Sloughed sheets of pale-gray pumice-fall lapilli from unit **rdcd** mantle the indigenous black scoria on the inner walls of the crater. On the west rim of the crater, an enigmatic patch of andesite lava only 6 m wide, polygonally jointed but only 20 to 50 cm thick, rests directly on the loose scoria; it may be an agglutinate remnant but, if so, it was strongly homogenized. Lavas and scoria alike have 57.1-57.7% SiO_2 and contain 2-5% plagioclase phenocrysts (1-2 mm), sparse opx and cpx, and rare olivine. At its south toe, the scoria cone overlies concealed hillocks presumed to be till. It is abutted on the east by rhyodacite lobes of unit **rdcd**, and its north toe is apparently overrun by the west peninsula andesite lavas of unit **apj**. The cone is almost surrounded by surficial deposits reworked during the lake highstand; a few tiny outcrops of lava that protrude through such deposits are compositionally and petrographically like those of Crater Negro. Attempts to date lava and scoria samples failed to yield measurable radiogenic Ar.

SIX SMALL LINEAR VENTS AND EJECTA RINGS

Independent postglacial vents for six small, exclusively pyroclastic, units of mafic to silicic andesite are scattered (without alignment) within an 8-km-long north-south belt that lies 2-6 km west of Laguna del Maule (Fig. 7). There are few constraints on their relative ages, so we describe them from north to south.

The **Andesite of Laguna Sin Puerto** (unit **asp**) is a low ejecta ring of phenocryst-poor scoria that thinly covers an area of 900 x 1,400 m, centered 3 km west of the northwest arm of Laguna del Maule. Although the sheet of ejecta is nowhere thicker than 30 m, it has total relief of ~140 m because it drapes a steep ridgecrest divide and the northeast wall of the Laguna Sin Puerto depression. The northern part of the ring drapes the rugged margin of the postglacial rhyodacite coulee of unit **rdcn**. The scoriaceous ejecta are crudely stratified, red or black, and largely non-indurated, except on the north rim where thin agglutinate sheets dip back into the shallow crater; scoria bombs as big as 50-150 cm are abundant. The crater is centrally intruded by a lava dome of biotite-hornblende rhyodacite (unit **rdsp**), which is 400 m in diameter, surrounded by a narrow shallow moat. With 40 m of relief, the dome is as high as parts of the encircling scoria ring. Neither soil nor colluvium was observed at contacts between the scoria deposit and the older or younger rhyodacites; all three are younger than the highstand of Laguna del Maule. The inner wall of the scoria ring has locally suffered fumarolic alteration. Scoriae contain <1% plagioclase phenocrysts (~1 mm) and only traces of olivine and cpx, but some have streaks and blobs of partially melted rhyodacite. An apparently uncontaminated bomb contains 59.1% SiO_2.

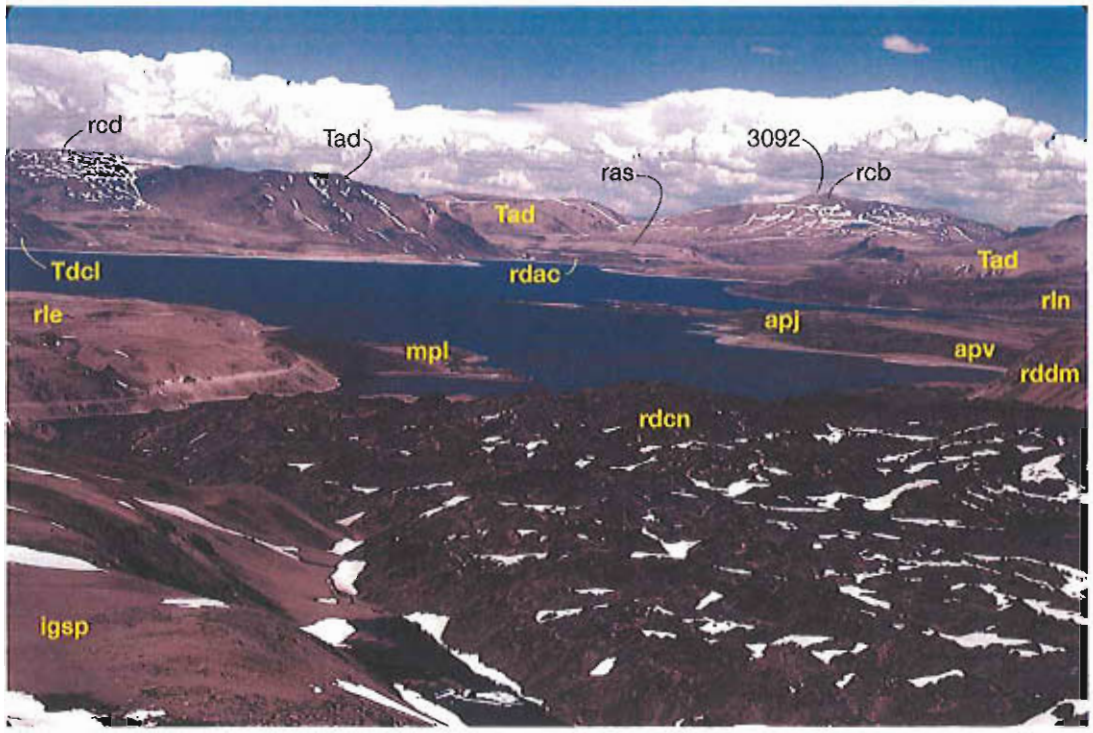

FIG. 22. View southeastward across Laguna del Maule. On right skyline, Cerro Barrancas, a postglacial rhyolite complex (unit **rcb**), rises 930 m above lake level, 23 km from camera. Image includes seven more postglacial units, clockwise as labelled: Colada Las Nieblas (**rln**), West Peninsula andesite (**apj**), Northwest Coulee (**rdcn**, foreground), Loma de Los Espejos (**rle**), Colada Divisoria (**rcd**), and two superimposed pumice-mantled coulees at southeast edge of lake: units **rdac** and **ras**. Three late Pleistocene, glacially modified units are also labelled: Older andesite of West Peninsula (**apv**), Domo del Maule (**rddm**), and Volcán Puente de la Laguna (**mpl**). Shelf in left foreground consists of 1.5 Ma welded ignimbrite (**igsp**), inferred to have erupted from the lake basin. Foreground pond was impounded by **rdcn** coulee, through which it drains to vigorous springs at lakeside snout of lava flow. Basin walls are pre-Quaternary lavas, breccias, and tuffs (**Tad**), predominantly andesitic, probably all Pliocene and late Miocene, but including a 3.6 Ma diorite pluton at far left lakeshore (**Tdcl**).

The **Andesite south of Arroyo Los Mellicos** (unit **asm**) is a small-volume fissure-fed field of phenocryst-poor scoria, centered 2 km southeast of Laguna Sin Puerto and 2 km west of Laguna del Maule. Parallel northeast-trending low-relief ridges of coarse ejecta merge to the southwest, forming a thin sheet altogether ~1 km long and 700 m wide that slopes gently northeastward to as low as 2,350 m. Nearly central to the field, a tiny window (20 x 30 m wide) of fumarolically altered hornblende dacite (unit **dsm**) has been stripped clean of the overlying scoria on the north slope of cerrillo 2484 (UTM grid 577/091). Accidental fragments of this dacite, including abundant 0.5-2 m angular blocks, make up 10-15% of the entire ejecta sheet and are also common as angular or partially melted inclusions within juvenile andesite scoria. A clean scoria bomb sampled has 61.3% SiO_2 and is almost aphyric, carrying only rare plagioclase crystals. The ejecta overlie glacial deposits and Tertiary andesitic lavas and tuffs; some of the relief on the scoria-mantled ridges may be inherited from pre-eruptive topography formed by these units. The scoria deposit is not itself glaciated, but a small proportion of the accidental lithic ejecta (lavas and granitoids) appear to be derived from underlying till. Along its south margin, the scoria deposit is overrun by a rhyodacite coulee of unit **rdcd**, which predates the highstand of Laguna del Maule.

The **Andesite north of Crater Negro** (unit **anc**) is a small-volume ejecta ring only 300 m wide that surrounds a shallow alluvium-filled depression next to the snout of a rhyodacite coulee of unit **rdcd**, ~1.5 km southwest of the northwest arm of Laguna del Maule. The low ring includes thin agglutinate sheets and abundant scoria bombs as big as 30-50 cm (many with dense glassy polygonally jointed rinds), but much of the ring is concealed by lake sediments and aeolian drifts of sand and pumice. A bomb contains 59.5% SiO_2 and carries ~10% plagioclase phenocrysts and 1-2% each of cpx and olivine (far more abundant mafic phenocrysts than in comparably young andesitic units **acn** and **apj** nearby). The unit erupted through the north toe of Crater Negro (**acn**) and was almost overrun by the coulee of unit **rdcd**; it appears to be marginally overrun by the postglacial west peninsula andesite lava flows of unit **apj**. The ring is postglacial but predates the highstand of the lake.

The **Andesite north of Estero Piojo** (unit **mnp**) is a small field of phenocryst-poor scoria and agglutinate centered 5 km west of Laguna del Maule at the base of the steep narrow divide separating the lake basin from the Cajón del Saso. Apparently fed from a 1.5-km-long southeast-trending fissure vent, its upper (northwest) half is a scoria ring draping the headwall and sidewalls of a small cirque. Its southeastern third is a 700-m-wide pile of scoria and agglutinate sheets that locally enclose at least one 15 m thick zone of massive andesitic lava. The medial part of the unit has transverse ridges that suggest outflow and rafting of scoria from the upper bowl, but the distal pile, more than 50 m high, was probably a discrete focus of emission. Intruding and obscuring much of the andesitic fissure vent are two 500 m wide low-relief domes of glassy micropumiceous hornblende-biotite rhyodacite (unit **rdnp**). The upper dome clearly postdates the scoria ring, but the lower (southeasterly) dome occupies the floor of the ring, has only a few meters of relief, and may be overlapped marginally by agglutinate at the southeast end of the ring. Contemporaneous or alternating eruption is suggested but not proven. The scoria bombs have 57.6-60.3% SiO_2 and carry 1-2% plagioclase phenocrysts (≤1 mm), sparse olivine and cpx, and numerous partially melted silicic inclusions and streaks. Scoriae are black or brick-red, mostly lapilli but including bombs as big as 50 cm. The unit overlies deformed Tertiary andesitic strata, and on the glaciated headwall it drapes mafic andesite lavas that underlie the welded pyroxene ignimbrite (unit **igsp**; 1.5 Ma). Distally, the unit laps onto hillocks of till, just at the 2,350-m strandline bench cut during the highstand of Laguna del Maule; rounded clasts of both scoria and varied stones from the till are prominent in the beach deposit.

The **Andesite of Arroyo Cabeceras de Troncoso** (unit **mct**) is a pair of spatter-rimmed craters in the southwest corner of the Laguna del Maule basin (UTM grid 572/030), 6 km southwest of the lake and 1.5 km west of the eponymous arroyo. The adjacent craters are each 80 m in diameter and surrounded by a joint ejecta apron only 300 m across. Agglutinate sheets and red and black spatter and scoria bombs as big as 1 m ring the craters, but none are larger than 25 cm on the surrounding apron, showing that coarser scoria mantling nearby plateaux to the west, southwest, and northeast are from other vents. The scoriae have 53.6-53.8% SiO_2 and carry 2-3% plagioclase phenocrysts, sparse olivine, abundant microphenocrysts of cpx and plagioclase, and abundant partially melted silicic inclusions. Another scoria-ringed crater (578/030), ~150 m in diameter and 600 m east of the pair, is included in this map unit, for reasons of convenience and compositional identity, although its ejecta may have somewhat fewer phenocrysts. It lies at the east end of a 400-m-long fissure, which is (like the crater rim and walls) locally draped with agglutinate and sprinkled with scoria bombs. In addition to sparse olivine and plagioclase phenocrsyts, the scoriae of this crater also carry abundant partially melted silicic inclusions, probably from the underlying coulee of unit **rdct**, through which the eruption issued.

The **Andesite of Crater 2657** (unit **mcp**) is the complex spatter-and-scoria fall deposit of a northeast-striking fissure vent in the southwest corner of the Laguna del Maule basin, 6 km from the lakeshore at the base of the steep divide separating the lake basin from Cajón Rodríguez. A shallow 200-m-wide crater marks the northeast end of the 1.3-km-long linear vent, which principally built a 60 m high ridge of stratified scoria and agglutinate. An outlier of compositionally similar

agglutinate ~700 m northeast of the crater (UTM grid 567/040) mantles a rhyodacite dome (unit **rdep**) and appears to represent a continuation of the fissure vent, isolated beyond a Neoglacial terminal moraine. Scoria-fall deposits up to 10 m thick (including thin agglutinated layers) extend 1 km south and 2 km southwest of vent, draping the high divide, as well as mantling a rhyodacite coulee (unit **rdct**) as far as 2 km northeast. Deposits are rich in spatter and scoria bombs, which are as big as 1 m and widely oxidized brick-red, although densely agglutinated layers tend to remain black and glassy or, if as thick as 3-5 m, internally pale gray and devitrified. Products contain 53.5-55.8% SiO_2 and carry <1% plagioclase phenocrysts and rare microphenocrysts of cpx and opx, as well as common partially melted silicic inclusions as big as 5 cm. At the southwest end of the fissure-fed ridge, the stratified andesitic deposit overlies superficially similar ledges of agglutinate and scoria (individually as thick as 5 m) that contain 61.8% SiO_2 and traces of hornblende and biotite; these apparently represent contamination or mixing with dacite magma of unit **dlp**, which had erupted from a vent now largely or wholly concealed by the ridge of unit **mcp**. Proximal deposits of the andesite rest on units **dlp** and **rdep** and on both Pleistocene and early Neoglacial till; a small Neoglacial terminal moraine, however, overlies the northeast part of the unit, presumably reflecting a post-eruptive glacial readvance. The associated scoria-fall sheet rests on Tertiary lavas and ignimbrite and on units **arp** and **rdct**; it appears not to overlie the nearby ejecta of unit **mct**, to which its most mafic material is compositionally similar.

FOUR POSTGLACIAL INTERMEDIATE LAVA FLOWS

Four unglaciated andesite-dacite lava flows that erupted effusively and failed to build substantial vent cones are distributed west of Laguna del Maule, two near the lakeshore and two that erupted on the south wall of the Cajón de Saso, respectively 10 km and 13 km west of the lake.

The **Younger Andesite of West Peninsula** (unit **apj**) is the prominent multi-flow complex that extends 4 km eastward into the lake basin from a vent concealed beneath the rhyodacite coulee of unit **rdcd** (Figs. 7, 21, 22). As wide as 1.5 km, the flow field is dominated by the final lava flow, as thick as 50 m, which overrode preceding lobes, both proximally and distally. Rugged flow margins and local levees are blocky and glassy, typically with scoriaceous surfaces oxidized red-brown, but locally they are more finely brecciated and rubbly. Ridges and hillocks on the flow top are also blocky but were somewhat subdued by wave action and patchy deposition of lake sediment during the highstand. Four samples analyzed yield 58.1-58.8% SiO_2, and one on the south-central margin gives a $^{40}Ar/^{39}Ar$ plateau age of 24.6±2.2 ka (Table 1). All samples have ~10% plagioclase phenocrysts (1-3 mm), sparse cpx, and rare olivine. The unit overlies postglacial units **acn** and **anc**, glaciated unit **apv**, and deformed Tertiary andesitic lavas and tuffs.

The **Andesite of Arroyo Las Nieblas** (unit **aan**) consists of blocky, vesicular to scoriaceous lava flows that are exposed in two separate reaches. One extends 700 m along the floor of the eponymous arroyo (Fig. 7), and the other, separated by a 500-m-wide inlet of Laguna del Maule, extends 400 m north along the lakeshore (615/070). Overlain by deposits of lake sediment, here at least 30 m thick, the former is exposed only along the narrow arroyo floor and the latter only as a wave-stripped bluff along the lakeshore. Elsewhere unoxidized, the lava grades into oxidized flow breccia at the mouth of the arroyo. At the upper end of the arroyo exposure, the lava issues from a 10-m-high poorly exposed mound of stratified agglutinate and scoria (608/060), overlain by thick lake and aeolian deposits; clasts in the scoria-fall layers are of lapilli grade, suggesting that the buried vent is nearby. The lavas contain ~5% plagioclase phenocrysts, sparse olivine and cpx, and rare opx. The arroyo-flooring lava has 59.3% SiO_2 and the lakeshore exposure 57.0%, suggesting that they may be different flows; each is compositionally distinguishable from the nearby andesites of the west peninsula (unit **apj**) and Crater Negro (unit **acn**).

The **Dacite of Cordón Rodríguez** (unit **dcr**) is principally a single thick lava flow that erupted effusively from an inconspicuous vent on the narrow ridgecrest divide between the canyons of

the Saso and Rodríguez (Fig. 8). The main flow dropped 800 m in elevation down the steep north slope, ponding >20 m thick at the floor of Cajón de Saso ~2.5 km from vent and then flowing 2 km westward to an uneroded flow front where it is ~40 m thick. Its steep medial pitch has a striking pair of blocky levees ~10 m high; its ponded surface is less rugged but is nonetheless marked by blocky knobs and arcuate ridges with 2-6 m local relief. The steep terrain around the vent is strewn with a thin sheet of ejecta, but no vent cone was constructed. A small lobe of lava also advanced ~400 m from vent down the opposite (south) wall, and a short lateral lobe split off westward from the main flow near the bottom of its declivity. The lavas are mostly angular blocks of black vitrophyre, many 1-2 m across, generally bearing scoriaceous rinds. A sample from the piedmont lobe along the Río Saso has 65.1% SiO_2 and carries sparse plagioclase phenocrysts (0.5-1 mm), rare biotite, and abundant mafic blebs and enclaves (53.0% SiO_2), fine-grained, angular to amoeboid, and 0.5 to 7 cm across. The unit principally overlies deformed Tertiary andesitic lavas and tuffs but also, on the ridgecrest, a narrow stack of flat-lying intermediate lava flows of presumed Pliocene or early Quaternary age. The main flow overlies alluvial terrace deposits along the Saso, and its piedmont lobe is patchily spread with thin alluvium. Otherwise virtually free of soil and sediment, this may be one of the youngest eruptive units in the volcanic field.

The **Andesite of Río Saso** (unit **ars**) is a blocky intracanyon lava flow that erupted on the south wall of the Cajón de Saso, 14 km west of Laguna del Maule, and flowed 10 km westward along the canyon floor (Fig. 8). The effusive vent is flanked by a pair of 100-m-wide sidewall ramparts of scoria, which extend into a thin scoria-fall sheet that blankets the south wall of the canyon for ~1 km eastward. The lava flow is finely vesicular and almost everywhere coarsely blocky; the blocks are glassy with scoriaceous surfaces that weather red-brown or are dark gray on freshly broken internal surfaces. Levees are best developed 1-2 km from vent, where they are 10-20 m high on both sides of the flow (owing to central drainaway). Relief within the central trough is partly subdued by infill of stream alluvium and aeolian sediment, except that the Río Saso has incised a 6-m-deep gorge down the proximal axis of the flow; this gorge is 20 m deep where it cuts through the north levee. Distally, the flow remains blocky but is locally more rubbly and scoriaceous, and the surface of its terminal lobe is unusually rugged. Products are phenocryst-poor, containing <1% plagioclase phenocrysts but abundant plagioclase microphenocrysts and sparse cpx and opx microphenocrysts. A distal lava sample has 61.4% SiO_2; a near-vent lava has 59.6%; and a scoria bomb from the vent has 59.3%. The unit erupted through and flowed downvalley between walls of deformed Tertiary lavas and tuffs. Distally, where it dammed the Río Botacura, 7-10 m of alluvium are banked against the intracanyon andesite. The flow is overlain by scattered pumice-fall lapilli of tan biotite-hornblende-plagioclase dacite that erupted from Volcán San Pedro in the late Holocene, and its distal 1 km is overlapped by a debris-avalanche deposit, also from Volcán San Pedro.

TWO ISOLATED POSTGLACIAL LAVAS

Two nonglaciated lavas that crop out only as small isolated windows are so extensively covered by younger deposits that little can be inferred with confidence about their morphology or areal extent, although in both cases buried vents are necessarily nearby. One is at the present-day eastern shoreline of Laguna del Maule and the other 2 km west and 300 m higher than the western shoreline. Since both are exposed on the basin floor and lack any sign of glacial erosion, they clearly postdate the last recession of ice from the basin.

The **Andesite of Playa Oriental** (unit **apo**) is a blocky lava flow exposed for ~250 m along the head of the beach at 2,200 m elevation along the southeast shoreline of Laguna del Maule (UTM grid 675/063). Also exposed in patchy outcrops for ~200 m inland, its black blocky surface is vesicular to massive, retaining brown-weathering scoriaceous rinds, and is little eroded except for slight rounding of blocks at the beach-front rim, which appears to be the primary flow front of a single flow lobe. Extensively covered by lake and beach deposits and by pumice-rich alluvium,

the flow can be seen locally to be at least 15 m thick, but its base is nowhere exposed. The lava has 59.5% SiO_2 and contains 5-7% plagioclase phenocrysts, conspicuous opx and cpx, and rare olivine. The lava-flow surface is inclined slightly westward, but a similar slope to its east (~1 km to the base of the wall of Tertiary andesites and 2 km to the snout of Holocene rhyolite coulee of unit **rcd**) is thickly covered by lake and beach deposits and fans of pumiceous alluvium, providing no evidence for a vent location.

The **Dacite south of Arroyo Los Mellicos** (unit **dsm**) is a tiny window (UTM grid 577/091) of ruggedly block-jointed lava, only 20 x 30 m in area, largely covered by scoria-fall unit **asm**. On the north side of cerrillo 2484, 2 km west of Laguna del Maule and 1 km south of Arroyo Los Mellicos, much of the outcrop is rusty orange-brown or yellow-brown, as if lightly affected by transient fumarolic alteration. The overlying ejecta blanket of fissure-fed andesitic scoria of unit **asm** is rich in accidental fragments of the dacite, which account for 10-15% of the whole deposit. The dacite ejecta range in size from granules to 2 m and in lithology from micropumiceous to massive, glassy to felsitic, and dark gray to tan, rose, or pale gray. Their freshness and lithologic variety (relative to the altered outcrop) suggest the existence of a buried dacite dome of modest extent. Fresh dacite has 66.0% SiO_2 and carries ~10% plagioclase phenocrysts and 1-2% each of amphibole and biotite. The fragile outcrop is clearly unglaciated and, like the scoria fall overlying it, stood higher than the 2,350-m postglacial highstand of Laguna del Maule.

NINE POSTGLACIAL RHYODACITE LAVAS

An extraordinary flare-up of silicic eruptive activity virtually encircling Laguna del Maule (Fig. 7) took place in postglacial time, including nine separate rhyodacites (68-72% SiO_2) and eleven rhyolites. The multiplicity of silicic eruptions during so limited a time interval is unprecedented in the entire history of the volcanic field. Seven of the nine rhyodacites predate the highstand of Laguna del Maule, and all nine erupted within 5 km of the lake.

The **Rhyodacite of Arroyo de la Calle** (unit **rdac**) is a pancake-shaped coulee 2 x 3 km in area at the southeast shore of Laguna del Maule (Fig. 7). Its nearly featureless pumice-mantled surface slopes gently northwestward from a 2,330-m plateau to a 2,250-m distal rim that stands 100 m above the lakeshore. It apparently spread radially from a vent now covered by the slightly younger rhyolite coulee of unit **ras**, which may have shared the same vent area. All outcrops are of blocky phenocryst-rich vitrophyre, commonly crumbly, containing ~10% plagioclase (1-2 mm), ~1% biotite, and little or no amphibole. Samples from the north and south ends of the unit have 71.6% and 71.7% SiO_2, respectively. The southerly sample yields a $^{40}Ar/^{39}Ar$ plateau age of 21.1±0.9 ka and a total fusion age of 23.6±1.1 ka (Table 1). The base is nowhere exposed as the flow is surrounded by lake sediment and pumiceous alluvium. Its surface was planated during the highstand of the lake and subsequently mantled by post-highstand pumice deposits. The flow is directly overlain by unit **ras** and marginally by unit **rcb**.

Of six postglacial rhyodacite eruptive units just west of Laguna del Maule, the southernmost is the **Rhyodacite south of Estero Piojo** (unit **rdep**), a north-trending chain of three contiguous domes ~5 km southwest of the lake (Fig. 7). Each of the three has 50-75 m relief and is 300 to 400 m in diameter. All are similarly phenocryst-rich, containing 10-15% plagioclase (1-3 mm, rarely 7 mm) and abundant biotite and amphibole (both 1-3 mm). The middle dome (UTM grid 565/043) has 68.0% SiO_2 and the other two both have 68.7%. Their contiguity and their morphological, petrographic, and chemical similarity suggest that the three were dike-fed concurrently. The southern dome, its top at ~2,475 m elevation, is unglaciated, blocky, glassy, micropumiceous, pale gray, and weathers tan; its south (uphill) slope has a Neoglacial terminal moraine (from a cirque to its southwest) banked against it and mafic agglutinate of unit **mcp** draped over it. The middle dome is likewise blocky, finely pumiceous, and wholly glassy, but another Neoglacial moraine (from a cirque to its west) grazes its northern toe and extends 1 km farther east. The northernmost and lowest dome (down

at 2,300 to 2,350 m elevation) is partly glassy to felsitic, lightly strewn with erratics, and has had its pumiceous carapace largely stripped; its top is planated by the strandline bench cut during the highstand of Laguna del Maule, and it appears also to have been lightly eroded by Neoglacial ice that advanced a few kilometers from small cirques on the steep basin wall nearby. The domes overlie Pleistocene till; all three are partly overlain by Neoglacial till, the southern dome also by unit **mcp**, and the northern dome also by lake sediments.

The **Rhyodacite north of Estero Piojo** (unit **rdnp**) lies just 2 km north of the last unit described and 5 km west of Laguna del Maule (Fig. 7). It consists of two, apparently discrete, extrusions of rhyodacite lava inside the mafic scoria ring of postglacial unit **mnp**. Only 200 m apart and separated by a small cratered mound of mafic scoria, the northwesterly extrusion is a low dome 500 x 300 m across, whereas the southeastern one is a 550 x 200 m lava flow with only a few meters relief that floors a scoria-ringed bowl. Both consist entirely of micropumiceous pale-gray glass that weathers tan, and both carry 2-3% plagioclase and ~1% biotite phenocrysts, as well as abundant mafic blobs and streaks. There is no scoria atop the northwest dome, which appears to postdate eruption of the scoria ring; the southeastern lava, however, may be marginally overlapped by agglutinated scoria (but cinder scree makes the relationship ambiguous). The mafic andesite and rhyodacite clearly erupted in virtually the same place in postglacial time, but whether they alternated remains unproven. The northwestern rhyodacite has 68.3% SiO_2 and the other has 69.0%, though any difference might simply be attributable to the mafic contaminant. These rhyodacites are distinguishable compositionally from another postglacial rhyodacite dome nearby, unit **rdcd**, only 500 m north, which (at 69.4% SiO_2) is notably richer in K and poorer in Ti, Fe, Al, and Ca.

The **Rhyodacite of Colada Dendriforme** (unit **rdcd**) is a pair of contiguous lava domes 3-4 km west of Laguna del Maule and a diverging array of four coulees that extend 1-2 km, generally eastward toward the lake (Fig. 7). The western dome, ~700 m in diameter, appears to bank against the 1-km-wide eastern one, which marks the source of the coulees. Each dome has ~150 m relief, and the four flows are 30-50 m thick at distal termini, which have steep blocky flow fronts with coarse talus aprons. Flow surfaces are blocky, glassy, strongly flow-foliated (commonly convolutely), and have numerous rugged pressure ridges; delicately crenulated textures are conspicuous on block surfaces. Dense black vitrophyre layers predominate over pumiceous layers, which are pale-gray, tan, or oxidized; this contrasts with most other postglacial silicic lavas at Laguna del Maule, on which the carapace facies is widely or exclusively pumiceous. The lavas have 69.4-70.6% SiO_2 and contain varied amounts (5-10%) of plagioclase phenocrysts (0.5-2 mm), 1-2% each of amphibole and biotite, and abundant mafic enclaves (53.6-56.4% SiO_2), 1 to 30 cm across and crenulate, some stretched or complexly deformed. Angular xenoliths, 0.5 to 3 cm across, of hydrothermally altered felsite are also present locally. The western dome, though chemically quite similar, is somewhat poorer in phenocrysts, with only 2-3% plagioclase, ~1% biotite, and rare amphibole. The unit overlies Tertiary andesitic lavas and tuffs as well as units **acn**, **anc**, **apj**, and **asm**. The east-southeast coulee stopped at and overlies the 2,350 m highstand beach bar; neither it nor the southeast and north coulees were affected by wave erosion. The east-northeast coulee, however, advanced downslope as low as 2,300 m, and its steep blocky flow front is wrapped by a weak strandline (Fig. 21). Although most blocks there remain angular, some have suffered minor abrasion, and detached pumiceous ones were rounded by tumbling in the waves. It appears likely that this multipulse eruption took place during the highstand of Laguna del Maule.

The **Rhyodacite of Arroyo Los Mellicos** (unit **rdam**) is a 600-m-wide coulee ~50 m thick that extends 1.2 km northeastward along the south bank of the eponymous arroyo, from a vent near knob 2,352 to a flow front at 2,250 m elevation, only 500 m west of the Laguna del Maule shoreline (Fig. 7). The flow surface is everywhere blocky, glassy, micropumiceous, and pale gray. Although most of the flow was subjected to wave action during the lake highstand, it is little eroded. Its highest point, which stood barely a few meters above the highstand as a small peninsula, retains delicately crenulated crusts on its blocky surface, whereas similarly micropumiceous blocks just

downslope are slightly rounded and knobby. Three samples yield 69.7%, 71.9%, and 72.5% SiO_2. All contain ~5% plagioclase phenocrysts (1-2 mm) and ~1% each of biotite and amphibole. Rare mafic inclusions may contribute to the compositional variability. The coulee overlies deformed Tertiary andesitic and rhyolitic lavas and tuffs as well as units **aam** and **asd**.

The **Rhyodacite northeast of Loma de Los Espejos** (unit **rdne**) is a single small lava flow just below the northeast toe of the great coulee Loma de los Espejos and ~3.5 km northeast of the dam that impounds Laguna del Maule (Fig. 6). The flow, 700 m long and 250 m wide, slopes gently northward toward Cajón Chico de Bobadilla and has only ~20 m marginal relief, in part because heavily mantled by pumice deposits from the nearby Espejos vent (unit **rle**). The virtually uneroded flow is wholly glassy, blocky to locally craggy, flow-foliated, and pale gray, weathering tan to brown. It has 68.7% SiO_2 and carries 5-7% plagioclase phenocrysts and ~1% each of biotite and amphibole. The flow is rich in fine-grained mafic enclaves (53.7% SiO_2), 1 to 15 cm across, finely vesicular with chilled rinds.

The **Rhyodacite northwest of Loma de Los Espejos** (unit **rdno**) is a single 100-m-thick lava flow high on the east wall of the Río Maule outlet gorge, 2-3 km downstream from the dam that impounds Laguna del Maule (Figs. 6, 9). Much of the flow is concealed by the overlying Loma de los Espejos coulee, but the part exposed extends ~900 m northward and is as wide as 400 m at bench 2,357. Above the rim, the pale-gray flow surface is rugged, glassy, micropumiceous, and virtually uneroded, but the 50 m high steep wall below has spalled during postglacial gorge enlargement to expose the partly glassy to felsitic dense interior. Everywhere the lava is strongly flow-foliated, and a large flow fold is exposed on the gorge wall. It has 69.1-69.9% SiO_2 and contains 7-10% phenocrysts of plagioclase, 1-2% biotite, and sparse amphibole, as well as abundant fine-grained crenulate mafic enclaves (1-10 cm). The flow overlies a proximal stack of mafic lavas of unit **msm**, and it is directly capped by the thick coulee of unit **rle**. The unit should not be confused with the glaciated biotite-rhyolite lava (unit **rep**) that forms the east wall of the same outlet gorge just upstream (Fig. 16).

The **Rhyodacite of Northwest Coulee** (unit **rdcn**), one of the youngest eruptive units around Laguna del Maule, is a single major lava flow 1.5-2 km wide that extends 3.5 km northeast from a vent ~1 km northeast of Laguna Sin Puerto (Fig. 7). Craggy northeast-trending ridge 2,538 may overlie a fissure vent, from which the flow spread radially but predominantly northeastward. The flow surface is ruggedly corrugated (Fig. 22) with numerous blocky arcuate pressure ridges, convex downflow; its margins are everywhere steep and range in height from 20 to 70 m. The lava is medium-gray to black, flow-foliated, dense vitrophyre (locally microcrystalline), the blocks of which break unusually flaky or splintery. Blocks are mostly 20-200 cm across and, while few are vesicular, many retain thin rusty red-brown scoriaceous crusts. Three samples range from 68.2% to 69.1% SiO_2, and all contain 1-2% plagioclase and sparse biotite and amphibole phenocrysts, as well as abundant fine-grained relatively mafic enclaves. The north side of the flow blocked drainages (Fig. 22), impounding two small lakes that have not yet silted in and fully converted to vegas. A northeast-distal part of the flow descended to the shore of Laguna del Maule at 2,150 m elevation (Fig. 15), evidently some time after breaching of the highstand lake because the 2,350 m strandline cut on so many nearby units is not present on the Northwest Coulee. Numerous springs that emerge at its snout along the lakeshore may be fed in part by underflow from the small lakes impounded a few kilometers northwest.

The **Rhyodacite of Laguna Sin Puerto** (unit **rdsp**) is the last to be described and probably the youngest of the nine postglacial rhyodacite units. A 40-m-high lava dome, circular in plan view and 400 m in diameter, it lies on the northeast rim of Laguna Sin Puerto, only 200 m from its lakeshore (Fig. 7). The dome nearly fills the interior of the andesitic scoria ring of unit **asp**, leaving only a narrow moat, and its radially fissured summit is no higher than much of the ring and 40 m lower than its southeastern rim. The dome is craggy, blocky, entirely glassy, flow-foliated, and uneroded; layers are mostly 1-10 cm thick (within blocks) and consist of subordinate dense black vitrophyre alternating with predominant pale-gray micropumiceous layers that weather

pinkish tan to pale orange-brown. The phenocryst-poor lava carries <1% plagioclase laths (many partly resorbed) and a trace of biotite; it also has abundant fine-grained mafic blebs, generally only 2-5 mm across. A rhyodacite sample, hand-picked clean of such blebs, has 70.6% SiO_2. Although they evidently erupted at essentially the same place, extrusion of the rhyodacite dome postdates the andesitic scoria ring, which in turn drapes the Northwest Coulee (unit **rdcn**). Streaks and blobs of silicic magma occur within the scoriae, but no rhyodacite lithic ejecta are present in the scoria ring. Because the oldest of the three postglacial units here, the Northwest Coulee, postdates the highstand of Laguna del Maule and the seven previously described postglacial rhyodacite units do not, it appears well established that dome **rdsp** is the youngest rhyodacite in the volcanic field.

ELEVEN POSTGLACIAL RHYOLITE UNITS

In addition to the nine rhyodacite (68-72% SiO_2) units just described, the remarkable postglacial flare-up of silicic magmatism around Laguna del Maule produced 11 eruptive units of true rhyolite (72-77% SiO_2), some of which include several discrete lava flows. Of the 11, two predate the highstand of Laguna del Maule, one caused it by damming the outlet, and eight postdate it. The 11 postglacial rhyolites virtually encircle the lake (Fig. 7), with one unit each to the east, west, and northwest of the lake, three to the northeast, three to the southeast, and two to the southwest. The nine rhyodacites arrayed around the lake basin are comparably widely distributed, as previously described, but, taken overall, most of the rhyolites are younger.

The **Rhyolite of Arroyo de Sepúlveda** (unit **ras**) is a 1.5 x 2-km pancake-shaped coulee near the southeast corner of the lake (Fig. 22) that rests directly atop the broader rhyodacite coulee of unit **rdac** (21.1±0.9 ka). Apparently erupted from the same concealed vent as the flow below, the rhyolite is 50-100 m thick. It forms a nearly flat-topped mesa, which was planated during the 2,350 m highstand when only its top few meters stood above the waves of Laguna del Maule as a small island. The lava has 73.6% SiO_2 and carries ~7% plagioclase and 1-2% biotite; it is predominantly vitrophyric, only mildly eroded by the lake, but does expose spherulitic zones locally on its marginal scarps. The rhyolite, like most of the surrounding area, is heavily mantled with pumice-fall deposits from the Cerro Barrancas vents 5 km to the south.

The **Rhyolite of Colada Divisoria** (unit **rcd**) includes a pair of phenocryst-rich coulees and a 3-km-wide pumice ring that erupted from a common vent on the continental divide, 5.5 km east of and 900 m higher than the shoreline of Laguna del Maule. The first coulee, 1.5 km wide and 100 m thick, flowed 4 km southeast toward Laguna Negra and is thickly covered by the pumice ring and its eastward-thinning pumice-fall apron. The pumice ring is at least 50 m thick proximally and drapes downslope to the east and southeast such that, despite thinning eastward, it altogether has ~250 m of local relief; it wraps around the vent area for ~270°, being absent only in the northwest quarter where it was overrun by the younger coulee. This western coulee, likewise 1.5 km wide and 100 m thick, extends steeply down the east wall of the basin for 3 km to a steep flow front at 2,500 m elevation (Fig. 23). Unlike the other coulee, it is not overlain by its own pumice fall deposit, although aphyric rhyolite pumice lapilli from the younger Cari Launa center nearby are common on its rugged blocky surface. The western flow front did not extend as low as the 2,350-m-strandline, but the coarse pumice-fall sheet beneath it, thicker than 10 m, did so and was notched with a broad wave-cut bench, indicating that the Divisoria eruptions predated the highstand. In contrast, the snout of the southwestern coulee from the Cari Launa center, only 1 km away, did reach the strandline but remains uneroded and thus postdates the highstand (Fig. 23). Darker brown, slightly more weathered surfaces on Divisoria lavas are consistent with them being older than those of Cari Launa. The blocky flow-foliated lavas are everywhere glassy, with black vitrophyre predominating on steep flow margins and pale-gray brown-weathering pumiceous textures predominating on upper slopes and flow surfaces. The rhyolite has 74.1% SiO_2 and carries 1-2% plagioclase phenocrysts

(1-2 mm) and ≤1% biotite. No mafic enclaves were observed, but brittle and ductile inclusions of felsite are locally common along the flow foliation. Within the coarse proximal pumice-fall deposits, a few thin (1-m-thick) pumiceous pyroclastic flows are exposed along gullies. On the windswept rangecrest, the pumice-fall surface has been deflated and armored with a lag of andesitic lithics, mafic scoria (probably from subjacent unit **mvc**), and dense blocks of cognate rhyolite, some as big as 1 m. Plagioclase and biotite phenocrysts are conspicuous in the pumice, in contrast to the nearly aphyric pumice from the adjacent Cari Launa center.

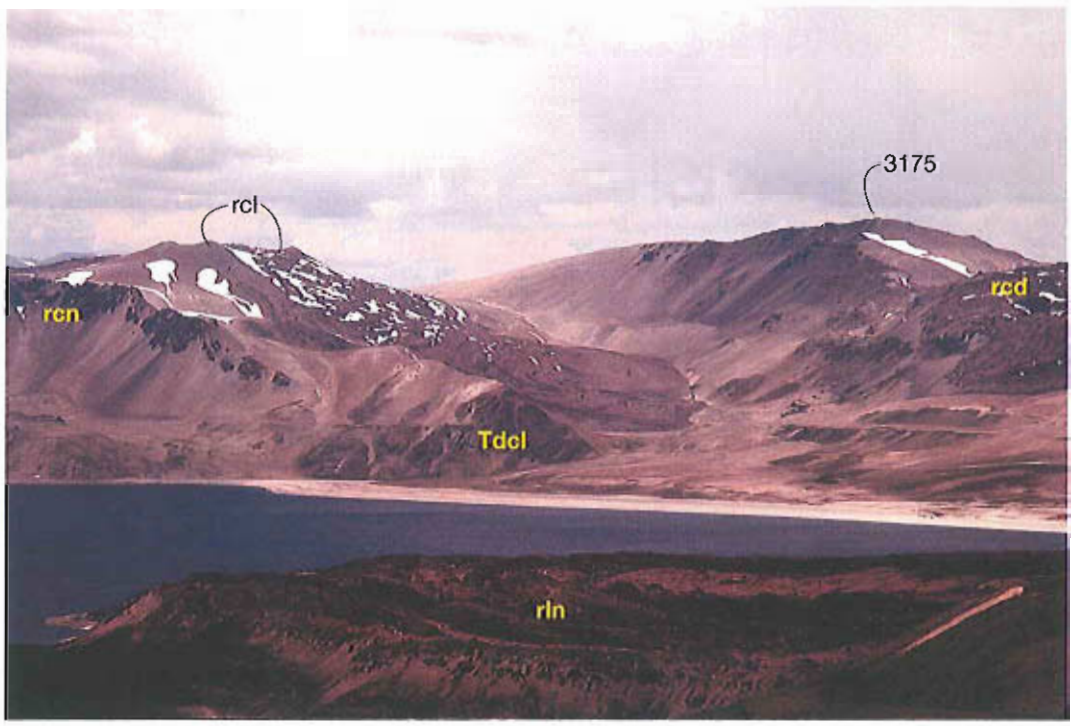

FIG. 23. East wall of Laguna del Maule basin, 2,350-m high strandline (200 m above lake), and three postglacial rhyolite coulees. View is east-northeastward across 100 m thick Colada Las Nieblas (unit **rln**, foreground), 15 km to crest of 3,175-m basin rim (1,000 m above lake), which is Argentine border and continental divide. Wall is stack of late Tertiary andesitic lavas (54-61% SiO_2), which yield ages of ~6.4 Ma at base of exposure and ~3.6 Ma at crest. On left skyline, Cari Launa coulee (unit **rcl**) breaches its own pumice cone and descends 700 m to strandline, which it postdates and slightly overruns. At far right, Divisoria coulee (unit **rcd**) descends from vent on high divide to a 2,500 m terminus, short of strandline, but coerupted pumice-fall deposit beneath coulee extends farther downslope and is cut by strandline. Black ridgeline at left center is glaciated rhyolite unit **rcn** (dated here at 468±6 ka); pumice-mantled lower end of ridge ends near lakeshore in steep gray exposure of 3.6-Ma diorite pluton (**Tdcl**).

The **Rhyolite of Loma de Los Espejos** (unit **rle**) is a sprawling bilobate coulee (Fig. 7) that erupted on the basin rim near the northwest end of present-day Laguna del Maule, damming the paleo-outlet and causing lake level to rise to 2,350 m, as recorded by the prominent high strandline that encircles the basin ~200 m above the modern lake (Figs. 21-23). The eruption first built a pumice cone, which is partly preserved as hill 2447 midway along the east margin of the coulee. The viscous blocky lava then overran part of the pumice cone, spread 2 km west, and descended 2.5 km northward to a terminus at 2,200 m elevation as well as 2.5 km southward to a

terminus at 2,150 m (near the modern lakeshore). Flow margins are steep and blocky with 100-150 m of relief, and the flow surface is craggy, blocky, and rugged, except for its southernmost 1.5 km where highstand inundation subdued its roughness (Fig. 17). The lava is flow-foliated, exhibiting abundant layers of obsidian as well as brown-weathering pumiceous layers and surfaces, which range from finely to coarsely vesicular. The only place marked by substantial erosion is a short reach of the outlet gorge where the steep west wall of the coulee spalled off (perhaps during the outbreak flood), exposing a cliff of interior felsite. The southern surface of the coulee is gently sloping up to an elevation of 2,350 m, where it is marked by a set of several beach lines defined by berms of rounded blocks (mostly 10-50 cm in diameter) torn from its pumiceous carapace and tumbled by wave action; below that elevation, the surface is only lightly eroded but subdued by ashy lake sediment and aeolian reworked pumice-rich sand. Pumice clasts in the cone and a subplinian pumice-fall sheet that extends eastward are mostly lapilli but are as big as 30 cm proximally. Extending 500 to 1,500 m northward from beneath the north snout of the coulee is a pale-gray nonwelded pyroclastic-flow sheet, 10-20 m thick, massive, and poorly sorted, in which highly frothy cellular pumice as big as 30 cm is conspicuous; an eroded remnant is also preserved along the road near Arroyo Arenas Blancas, 5 km downvalley. A bulk proximal sample (excluding pumice blocks) has a median grainsize of 0.45 mm and is fines-poor [only 4 wt% finer than 0.0625 mm (4ø)]. Pumice blocks in the pyroclastic-flow deposit contain 76.4-76.7% and obsidian samples from the lava flow contain 75.6-75.8% SiO_2, all high-silica rhyolite. The lava has ≤1% plagioclase phenocrysts (≤1 mm) and very sparse thin flakes of biotite. An obsidian sample from the west margin of the southerly lobe gave a $^{40}Ar/^{39}Ar$ plateau age of 23.3±0.4 ka (Singer *et al.*, 2000; Table 1). The unit overlies till at the lakeshore and glaciated eruptive units **mpl**, **rep**, and **igcb**, as well as postglacial units **rdne** and **rdno**.

The **Rhyolite of Arroyo de Palacios** (unit **rap**) is a pumice-mantled coulee in the headwaters of the eponymous arroyo near the south margin of the Laguna del Maule basin, only 500 m north of the rim above Laguna Fea (Fig. 7). From a pumice-ringed vent at 2,750 m elevation, the 1-km-wide coulee descended 2.5 km northward to a terminus at 2,350 m. It is everywhere glassy and uneroded; its steep margins have up to 50 m relief and are pale-to-medium gray and finely to micropumiceous; dense obsidian is nowhere exposed. The flow surface is thickly covered by its own pumice-fall deposit and by that from the nearby vent of Colada Las Nieblas (unit **rln**). The narrow horseshoe-shaped pumice ring that semi-encircles the vent is sharp-crested and uneroded, suggesting a mid to late Holocene age. The lava has 75.7% SiO_2 and is strictly aphyric. Although their vents are separated by only 2.5 km, the slightly younger Colada Las Nieblas contains plagioclase and biotite phenocrysts and has ~2% less SiO_2. The rhyolite overlies deformed Tertiary intermediate lavas, tuffs, and breccias.

The **Rhyolite of Colada Las Nieblas** (unit **rln**) is one of the largest postglacial coulees around Laguna del Maule, forming 5 km of its southwest shoreline (Figs. 7, 22, 23). From a pumice-ringed vent complex, ruggedly viscous flows advanced 5 km northward to the lakeshore. Distal flow fronts there are as high as 150 m, but generally 50-75 m along the medial margins. The eruptive sequence began with construction of a pumice ring as high as 50 m that semi-encircles the south end of the complex. Extrusion of lesser lava flows (now exposed only locally beneath the southeast and northwest margins of the complex) was followed by concurrent emplacement of two contiguous voluminous flow lobes, together as wide as 4 km, each extremely rugged and marked by dozens of concentric pressure ridges, convex downflow. At a late stage, a second pumice ring, slightly inboard and parallel to the first, was built atop the proximal lavas. This inner ring is pitted by two 150-m-wide craters, forms the highest point on the complex at 2,565 m, and wraps ~220° around the sequence-closing vent dome, which is 400 m wide and pumice-free. Pumice-fall deposits mantle much of the nearby terrain and are as thick as 20 m on the basement ridge 1 km east of the vent. Giant pumice blocks as big as 2.5 m are distributed along the head of the beach in the cove 1 km north of the coulee's flow front at Laguna del Maule; only a few meters

above present-day lake level, they probably spalled from the carapace of the coulee and floated into place. Eruption postdated the 2,350-m highstand of the lake, as no strandline is notched into the flow front, which extends at least as low as 2,150 m. The lavas are blocky and flow-foliated, widely exposing layers of dense vitrophyre but dominated by pale-gray micropumiceous surfaces that weather tan to brown. Four analyzed samples range in SiO_2 from 73.4% to 74.0%. The lavas carry 2-4% plagioclase phenocrysts (0.5-1.5 mm) and ~1% biotite. They overlie Tertiary andesitic lavas and breccias and bank against postglacial unit **rap**. An attempt to date a dense proximal lava sample yielded no detectable radiogenic Ar.

The **Rhyolite of Arroyo Los Mellicos** (unit **ram**) is a postglacial minidome <150 m in diameter that intrudes glaciated unit **aam** just south of the eponymous arroyo and 500 m west of the northwest arm of Laguna del Maule (Fig. 7). The dome stands only a few meters higher than the west end (UTM grid 588/110) of the degraded spatter ring that defines the vent of the glacially striated andesite plateau of unit **aam** (Fig. 17). Circular in plan view, the weakly flow-foliated dome consists of angular blocks, everywhere glassy, micropumiceous to massive, and cream to very pale gray, weathering tan. It contains 3-4% plagioclase phenocrysts (≤1 mm), 1-2% biotite (mostly ~1 mm, rarely to 5 mm), and rare amphibole, as well as sparse fine-grained mafic enclaves, 1-8 cm, finely vesicular, and crystal-poor. Angular blocks of the dome lava are uneroded, although its top at ~2,260 m is nearly 100 m lower than the highstand of the lake. It lacks the gravel and lake-sediment deposits present on the adjacent andesite plateau, and the pumice and sand that infill some of the microrelief on the dome may simply be aeolian. Two dome samples have 73.2% and 73.3% SiO_2 and are a fairly good match for pumice lapilli in a 58-cm-thick fall unit (72.9% SiO_2) exposed in a roadcut (623/126) at 2,280 m elevation atop the postglacial Loma de Los Espejos coulee (unit **rle**) ~4 km east-northeast of the dome. The rhyolitic fall unit consists of coarse ash and subangular buff pumice lapilli (mostly <5 mm but as big as 10 mm) along with sparse obsidian granules but no crystals >0.25 mm.

The **Rhyolite south of Laguna Cari Launa** (unit **rsl**) is a 1-km-wide pumice-mantled coulee that provides the natural barrier that impounds Laguna Cari Launa (Fig. 7). Although erupted from a common vent complex (at peak 3,031), 3 km east of Laguna del Maule, this initial coulee preceded the subplinian pumice fall and lava flows of more extensive unit **rcl**. Two stubby lava flows just west of the vent are likewise heavily pumice-covered and probably also part of unit **rsl**. Emerging from beneath the younger **rcl** lavas only 500 m east of the vent, the 2.5-km-long coulee spread 1 km northeastward to dam the lake and 1.5 km southwestward down the former valley that had drained the basin now occupied by the lake. The lavas (75.1% SiO_2) are strictly aphyric, flow-foliated, and mostly micropumiceous and pale-gray, weathering tan, but some layers are either massive obsidian or coarsely vesicular and dark gray or oxidized brown. They also contain sparse (but not rare) angular to rounded inclusions (1-3 cm) of dark-gray rhyolite rich in tiny amphibole needles and flakes of oxidized biotite, perhaps cognate material entrained from a margin of the magma conduit. The only good exposure of the unit through the 5 m thick pumice cover is the flow front along the southwest shore of the lake. It banks against a stack of Tertiary andesite lavas (6.7 to 3.6 Ma; Table 1) that make up the east wall of the Laguna del Maule basin. The SiO_2 content of this opening extrusion (unit **rsl**) of the Cari Launa sequence is ~1.5% greater than that of the subsequent lavas assigned to unit **rcl**. Although impounded by this 150 m thick lava flow, not by the permeable pumice deposits, Laguna Cari Launa has fluctuated in level by at least 10 m, as shown by multiple strandlines higher than the lake level exposed during our summer visits. Such fluctuations seem likely to reflect seasonal variations in precipitation and snowmelt.

The Rhyolite of Cari Launa (unit **rcl**) includes two rugged coulees and remnants of a pumice cone centered high on the northeast wall of the Laguna del Maule basin, 3 km east of the lakeshore (Fig. 7). The pumice cone was ~1 km wide with ~130 m relief, and remnants still form a partial ring around the highest point of the complex at 3,031 m elevation. A small vent dome now separates pumice-cone remnants at the effusive site where two large (post-pumice) coulees distended and

disrupted the cone. One coulee forms a broad northeasterly apron, 2.5 km wide and long, that extends into pre-existing Laguna Cari Launa and also impounded the small lake 2605 at its north margin. The other coulee is 1.5 km wide and descends 3.5 km southwestward to a steep 50-m-high flow front at 2,350 m, ~2 km from the modern shore of Laguna del Maule (Fig. 23). Both coulees are ruggedly blocky and pervasively flow-foliated, and their surfaces have abundant pressure ridges, longitudinal near flow margins and concentrically convex-downflow distally. Lavas are predominantly micropumiceous and pale gray, although obsidian layering widely makes up as much as a third of outcrops and sparse spherulitic and felsitic layers and lenses locally accompany the obsidian. Lavas and ejecta are aphyric or nearly so, but, perhaps inhomogeneously, some carry as much as 1% plagioclase (≤1 mm) and traces of biotite (<1 mm). Five samples analyzed have 73.5-73.8% SiO_2.

The snout of the southwestern coulee descended slightly below the level of the highstand strandline, which is well-defined nearby on both bedrock and surficial deposits (Fig. 23); because the snout shows no evidence of erosion by wave action or beach processes, the flow appears to be younger. The widespread pumice-fall deposit that accompanied construction of the pumice cone is as thick as 5 m atop the early flows from the Cari Launa vent (unit **rsl**) and was apparently subplinian (or weakly plinian). It was evidently dispersed narrowly eastward because it thickly mantles the slope and continental divide (ridge 3033) as far as 5 km due east of the vent but is thinner and widely wind-stripped from ridges to the northeast and southeast. An isolated lapilli-fall layer of white pumice, ~70 cm thick, preserved in a roadcut (UTM grid 687/147) ~5 km northwest of the Cari Launa vent is compositionally identical to unit **rcl**, not to pumice of nearby unit **rle**.

The **Rhyolite of Paso Pehuenche** (unit **rpp**) is a postglacial minidome 2620, ~1 km south of the road, 1.5 km west of the north edge of Laguna Cari Launa (Fig. 7; UTM grid 721/141), and 4 km southwest of Paso Pehuenche (Fig. 6). The dome is only ~100 m in diameter and 30 m high with a jaggedly fissured top; it is enclosed within a shallow explosion crater ~400 m wide, blasted through the steep sidewall of Pleistocene rhyolite unit **rcn**. It consists of angular blocks that are faintly flow-foliated and pale gray, weathering tan, and mostly micropumiceous although sparse obsidian and felsite interlayers are also present. The lava has 74.4% SiO_2 and is virtually aphyric, only very rare biotite having been observed. The ejecta ring around the crater consists mostly of accidental lithic debris explosively excavated from the Pleistocene rhyolite and from underlying andesitic lavas and stratified palagonitized scoria lapilli, all of which are exposed in the moat around the dome. The dome has its own talus apron but fragments of juvenile rhyolite are uncommon in the ejecta ring, which is rich in blocks (as big as 50 cm) of slabby felsite and obsidian of unit **rcn**. Sparse breadcrusted blocks of juvenile rhyolite are present, but juvenile pumice blocks are virtually absent. Coarse accidental ejecta are scattered as far as 500 m from the crater. The stratified andesitic scoria lapilli exposed in the crater suggest the presence of a nearby vent, presumably covered by unit **rcn** and probably of early Pleistocene age. Caution should be exercised in approaching the crater, because the area surrounding it was a mine field around 1978-1982.

The **Rhyolite of Laguna Negra** (unit **rng**), earliest-erupted component of the Cerro Barrancas complex (unit **rcb**), consists of a pumice cone (UTM grid 737/955) and two pumice-mantled lava lobes, all located 3-5 km southeast of the international border (Fig. 7). Its top at an elevation of ~2,500 m, the pumice cone is ~1 km wide with 250 m relief and overlies its lavas, one lobe of which descends 1 km southeast to a terminus at 2,000-m in the headwaters of the Río Barrancas. The other lobe extends 1 km northeast and impounds Laguna Negra at 2,162 m (Fig. 24). Where exposed through the heavy pumice-fall cover, the lavas reveal only a pale gray finely pumiceous carapace. They are virtually uneroded except for minor wave action at the lakeshore flow front. Almost aphyric, the lavas carry trace amounts of plagioclase and biotite. At 73.5% SiO_2 and 14.41 Al_2O_3, they are slightly less evolved than overlying lavas of the Cerro Barrancas complex (73.8-74.1% SiO_2 and 14.08-14.18% Al_2O_3; n=6).

The **Rhyolite of Cerro Barrancas** (unit **rcb**) is a 10-km-wide postglacial complex of three main vents and eight coulees, some of them multi-lobate, centered on the continental divide ~7 km south

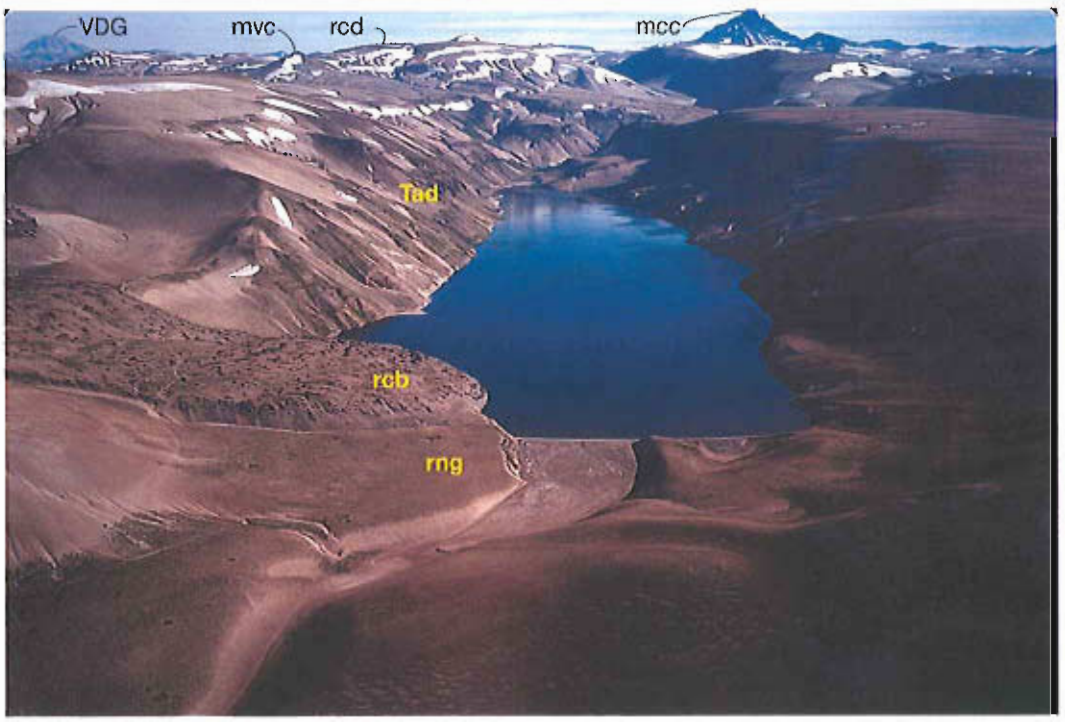

FIG. 24. Laguna Negra, 5-km-long and 1-km-wide, viewed northward toward Cerro Campanario (**mcc**; upper right, 23 km beyond far end of lake) and Volcán Descabezado Grande (VDG; upper left, 70 km northwest). Lake is impounded by two postglacial coulees from Cerro Barrancas complex-unit **rng** (which crops out only at lakeshore and is heavily mantled by nonwelded Barrancas ignimbrite and pumice-falls) and blocky unit **rcb** (with thinner pumice cover). Terrain is covered by pumice-fall deposits from Barrancas vents and, north of lake, from Divisoria vent (unit **rcd**). Glacial valley occupied by lake is cut through a stack of as many as six andesitic lava flows (**Tad**) that dip 5-15° southeast (to right); they appear to be continuous across the lake and with a subhorizontal stack that forms 750 m high southeast wall of Laguna del Maule basin, 5 km northwest. It is likely but not proven that these lavas are same ages as stack of similar andesitic lavas dated at 6.4 to 3.6 Ma on east wall of Laguna del Maule basin (Fig. 23), 7 km north of Laguna Negra. Near-vent remnant of 153 ka mafic shield (unit **mvc**) overlies

of the southeast arm of Laguna del Maule (Fig. 7, 22). Not included here is a fourth postglacial vent and its lavas, assigned to slightly older unit **rng** (just described), which appears to be the earliest part of the local eruptive sequence. The summit of Cerro Barrancas at 3,092 m is a 1-km-wide pumice cone with ~200 m relief. Two multilobate coulees to its west and northwest appear to have filled a glaciated paleovalley that had drained Laguna Fea into Laguna del Maule at some point during the Pleistocene (Fig. 25). The present-day outlet of Laguna Fea is subterranean, through surficial deposits and nonwelded ignimbrite to the southeast. Although the threshold for southeastward overflow is only 20-30 m above lake level (2,486 m), there is no evidence that this surface outlet has been used since the Cerro Barrancas eruptions (Fig. 25). The alternative northward outlet from Laguna Fea to Laguna del Maule via Arroyo de Sepúlveda, now buried by postglacial rhyolites, was nowhere higher than 2,500 m and was apparently used at times during the Pleistocene. The southeasterly outlet to the Río Barrancas was certainly also used during the Pleistocene, but at some point Laguna Fea was captured by a tributary of Laguna del Maule, the surface of which lies 300 m lower in elevation than Laguna Fea.

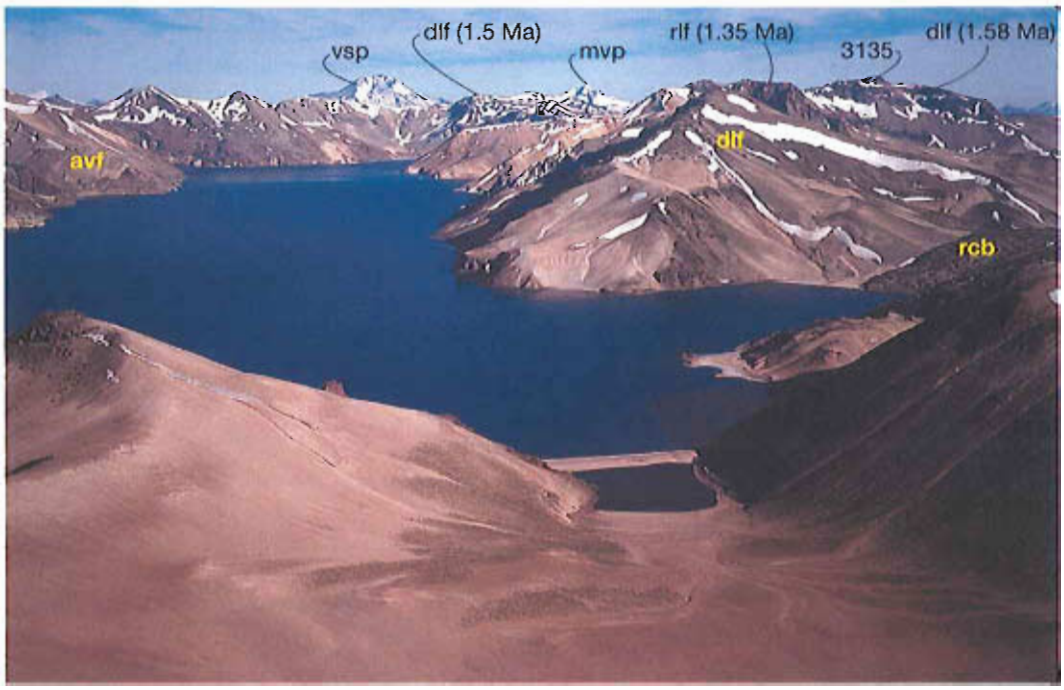

FIG. 25. Laguna Fea, 11 km long and up to 2 km wide, viewed northwestward toward Volcán Pellado (**mvp**) and Volcán San Pedro (**vsp**), on volcanic front 30 km beyond far end of lake. Glacial valley cuts through stacks of andesite-dacite lavas and breccias that dip gently toward right on both sides of lake, having erupted from ice-ravaged early Pleistocene stratovolcano, Volcán Laguna Fea (unit **avf**), which is centered ~3 km left of image. Smooth tan slopes in foreground are mantled by postglacial rhyolitic ignimbrite and pumice-fall deposits from nearby Cerro Barrancas. At far right, a postglacial (and post-pumice) rhyolite coulee from Cerro Barrancas (unit **rcb**) blocks former outlet of Laguna Fea northward toward Laguna del Maule. Present-day threshold for overflow would be southeastward (beneath the camera) where sill is only 20-30 m higher than lake, but gullying pattern on pumice deposits indicates that such overflow has not taken place since Barrancas eruptions blocked former alternative outlet. On ridgecrest at right skyline (peak 3,135), lowest of three gently north-dipping lava flows (unit **dlf**) that unconformably overlie deformed Tertiary breccias yields an $^{40}Ar/^{39}Ar$ plateau age of 1582±9 ka. To its left on rim above lake, dark cliffy buttress is rhyolite lava dome as thick as 400 m (unit **rlf**; 1,353±17 ka).

The Barrancas rhyolite complex altogether has 1,100 m of relief, but much of that owes to draping the ruggedly glaciated divide. Basement rocks crop out within the complex to elevations as high as 2,850 m and up to 2,983 m on a ridge 2 km south of the pumice-cone summit. Most of the lava flows are blocky, glassy, flow-foliated, and either aphyric or carry trace amounts of plagioclase and biotite. Exceptionally, the southwestern coulee, which reaches Laguna Fea, contains 1-2% plagioclase and sparse biotite. Pumice blocks and lapilli in pumice cones and subplinian fall deposits are pale gray to white and likewise aphyric. Six widely spaced samples range in SiO_2 only from 73.8 to 74.1%. Flow fronts are steep, and upper surfaces rugged and marked by numerous pressure ridges, which are typically longitudinal medially and convex-downflow distally. Because none of the flows are significantly eroded, exposures are principally of pale-gray pumiceous carapace that weathers tan, although steep spalling flow fronts also expose obsidian layers.

Three vents appear to account for eight coulees. **(1)** The easterly vent now marked by dome 2,888 produced three rugged coulees and a pumice ring preserved only on its northwest side. A southeastern flow is 1.5 km wide, 50-75 m thick, extends 2.5 km downhill to a terminus at 2,000 m, and is mantled by pumice from its own vent. A second flow lacks the pumice-fall cover, is 1 km wide,

and extends 3 km eastward to the shore of Laguna Negra where its steep terminus is ~50 m high (Fig. 24). The third flow is continuous with the vent dome, which is ~1 km wide and as high as 300 m; the flow is also largely pumice-free, 1 km wide, extends 1.5 km east-northeast from the dome, and is >50 m thick distally. The first two flows wrap around the pumice cone of unit **rng** and overlie its lavas. **(2)** The summit pumice cone of Cerro Barrancas (3,092 m) marks the vent for four coulees, three that flowed generally northward and one to the south. The northeast flow is oldest, widely pumice-mantled, 1 km wide, and 2.5 km long. The northwest flow erupted next, is pumice-covered only proximally, widens downslope from <1 km to 3 km wide, descends 5 km from vent, and divides distally into two terminal lobes, the steep flow fronts of which are 30-50 m high. Youngest of the northerly three is the central flow, also 5 km long, which is likewise pumice-covered only proximally, overrides the previous two flows, doubles in width downslope to 2 km, and diverges into two terminal lobes with flow fronts 30-50 m high. The southerly fourth flow lacks any pumice cover, even where it emerges from the east side of the pumice cone; the steep rugged flow, 5 km long, widens from 500 m to 2 km as it drops >800 m to a flow front 50-70 m high at an elevation of 2,080 m. **(3)** Finally, the westernmost vent produced a small dome (knob 3,010) at the western toe of the pumice cone. The vent dome marks the source of a 2.5-km-wide pumice-free westerly apron of rugged rhyolite lava that overlies all earlier pumice deposits and divides distally into three stubby lobes, two of which drape steeply down for 2.5 km to the shore of Laguna Fea (Fig. 25). The total distance is only 4.5 km from the eastern pumice cone (of unit **rng**) to the western dome 3,010. It seems well constrained on the basis of overlapping relationships that the four main vents were sequentially active from east to west.

Lavas of the Barrancas complex principally overlie late Tertiary and early Pleistocene intermediate lavas and tuffs, but the northernmost coulee also overlaps unit **rdac** (21.1±0.9 ka). Three northerly lobes descend below the 2,350-m highstand strandline of Laguna del Maule, yet they show no evidence of the wave-cut bench so prominent on basement rocks nearby. An attempt to date obsidian (4.06% K_2O) of the westerly (youngest) coulee of the Barrancas complex near Laguna Fea produced low radiogenic Ar, an unusable plateau, and a suspect $^{40}Ar/^{39}Ar$ isochron age of 19±12 ka. The complex is so pristine and uneroded, despite its high elevation, that we infer its eruption to have been in the mid to late Holocene.

Further evidence of so young an age for the Barrancas complex is preservation on adjacent canyon floors of a sheet of nonwelded rhyolitic ignimbrite that extends southeastward from beneath its two southeastern coulees. Because the sheet is wholly in Argentina, we were not authorized at the time to investigate it, but distant observations and aerial photographs make the main outlines clear. From beneath the Barrancas lavas, the ignimbrite extends >8 km southeast as an uneroded plateau as wide as 3.5 km and as thick as 50 m in stream gorges incised along its margins. West of the plateau, the nonwelded deposit also occupies the floors of two valleys (Arroyo Puente de Tierra and Arroyo de Curamilio) that head on steep basement rocks south of the Barrancas complex. This distribution requires that pyroclastic flows had surmounted a 150-m-high divide and had dispersed across a 90° sector to fill transverse valleys at least 6 km southwest and south of Cerro Barrancas. The three ignimbrite-floored valleys all converge downstream into the canyon of the Río Barrancas, along which sidewall remnants are preserved for an unknown distance southward.

IMPLICATIONS OF 24 POSTGLACIAL SILICIC VENTS ENCIRCLING LAGUNA DEL MAULE

The 20 postglacial silicic map units just described (Table 4) erupted from 24 discrete vents, and they include 36 separate silicic coulees and domes (15 rhyodacites and 21 rhyolites). Most

of these lavas were preceded or followed by explosive eruptions of pumice and ash, which an observer might have counted as discrete eruptive events if separated by hours to weeks from the comagmatic effusions. None of the tephra eruptions are known to have had plinian dispersal, but downwind investigations in Argentina have not yet been undertaken to assess this. Some near-vent pumice deposits are 5-20 m thick and a few pumice rings and cones are thicker still, but all the fallout sheets we observed thin to a few centimeters within several kilometers from vent. None are known to be on the scale of the 1932 plinian eruption of Quizapu, 50-km-north of Laguna del Maule, where the pumice-fall deposit is still thicker than 1 m at the Argentine border 35 km east of its vent (Hildreth and Drake, 1992). Most or all of the postglacial pumice-fall deposits around Laguna del Maule are probably subplinian.

TABLE 4. SILICIC ERUPTIVE UNITS.

Unit	Name	Age*	Area km²	Volume km³	Notes
postglacial rhyolites					
ram	Arroyo Los Mellicos	pre	0.02	0.0002	Minidome intrudes unit **aam**
rap	Arroyo de Palacios	post?	2.2	0.11	Mantled by **rln** pumice fall
ras	Arroyo de Sepúlveda	pre	2.28	0.11	Upper coulee; rests on **rdac**
rcb	Cerro Barrancas	post	37.45	1.87	3 vents, 8 coulees, pumice cone
	Barrancas ignimbrite	post	>20	>1	Nonwelded sheet SE of complex
rcd	Colada Divisoria	pre	9.3	0.65	2 coulees, pumice cone
rcl	Cari Launa	post	7.62	0.38	2 coulees. pumice ring
rle	Loma de Los Espejos	23.3	9.84	1.0	Coulee dams LdM; pumice cone
rln	Colada Las Nieblas	post	12.14	1.2	2-part coulee, pumice rings
rng	Laguna Negra	post	1.47	0.074	Coulee dams L. Negra; pumice cone
rpp	Paso Pehuenche	post?	0.024	0.0003	Minidome intrudes unit **rcn**
rsl	South of Laguna Cari Launa	post	3.28	0.164	Coulee dams L. Cari Launa
postglacial rhyodacites					
rdac	Arroyo de la Calle	pre	4.66	0.33	Lower coulee; underlies unit **ras**
rdam	Arroyo Los Mellicos	pre	0.56	0.03	Top 10 m above highstand as islet
rdcd	Colada Dendriforme	pre	2.95	0.15	2 vent domes, 4 coulees
rdcn	Northwest Coulee	post	4.56	0.32	Coulee touches NW arm of LdM
rdep	South of Estero Piojo	pre	0.29	0.01	Chain of 3 contiguous domes
rdne	Northeast of Loma de Los Espejos	pre	>0.20	>0.006	Mantled by unit **rle** pumice fall
rdno	Northwest of Loma de Los Espejos	pre	>0.23	>0.11	Beneath **rle**; cut by LdM outlet gorge
rdnp	North of Estero Piojo	pre?	0.16	0.002	2 domelets intrude scoria ring mnp
rdsp	Laguna Sin Puerto	post	0.08	0.002	Dome intrudes scoria ring **asp**
late Pleistocene					
reb	Estero de Bobadilla (dome 2667)	--	0.25	0.014	Till-mantled minidome
rep	East of Presa Laguna del Maule	~38	0.33	--	Beneath **rle**; cut by LdM outlet gorge
ret	Estero Terneros	97	2.0	--	Coulee south of Cerro San Pedro
rez	Estero El Zorro	83	3.0	--	Obsidian flow east of Valle Chico
rddm	Domo del Maule	115	1.5	>0.2	Uneroded dome and glaciated lava flow
rdop	West of Presa Laguna del Maule	--	0.71	>0.05	Pair of domes just west of LdM outlet

Table 4 continued: Older units.

Unit	Name	Age*	Area km²	Notes
middle Pleistocene				
rca	Cajón Atravesado	712	1.2	Ridgecrest remnant; biotite rhyolite lava
rcn	Cerro Negro	460	12.5	Northeast wall of basin >900 m high
rlm	Los Murciélagos	335	12.7	11-km-long chain of lava remnants
rdcb	West of Cajón Bahamondes	--	0.63	Pyroxene-bearing lower coulee
rdcp	Cabeceras de la Plata	--	0.06	Small hornblende-biotite lava dome
rdct	Arroyo Cabeceras de Troncoso	203	1.38	Modest hornblende-biotite coulee
rdes	East of Cerro San Pedro	--	0.88	Biotite-bearing upper coulee
rdet	Estero Terneros	--	>0.75	Two coulees rich in hornblende, plag, and opx
rdez	Estero El Zorro	--	>0.5	Phenocryst-rich coulee of pyroxene rhyodacite
rdpñ	Puntilla Los Ñirales	680	0.71	300-m-thick dome; ~0.14 km³ remain
rdvc	Valle Chico	695	0.47	300-m-high dome; ~0.1 km³ remain
early Pleistocene and older				
rlf	Laguna Fea	1,353	0.58	Severely eroded lava dome >300 m thick
rls	Las Salinas	--	0.20	Cryptodome of biotite rhyolite
rnf	North of Laguna Fea	--	0.07	Small lava dome remnant on Laguna Fea divide
rdap	Plug of Arroyo de Palacios	--	0.22	Rhyodacite intrusion N of Laguna Fea divide
rdcr	Cordón Las Romazas	--	>3.3	Chain of ridgecrest lava remnants
rddp	Dike south of Laguna del Piojo	--	>0	Dike 5 m thick
rdla	Lo Aguirre	880	1.52	Lava dome cut by road tunnel; >0.2 km³ remain
Trcf	Cajón Filume	2,572	2.9	3-km-long coulee; >0.5 km³ remain
Trea	Estero Aguirre	2,280	0.18	Roadside dome, Río Maule; remnant
		3,740	2.65	2 domes in Cajones Lo Aguirre; remnants

* For postglacial units, pre and post refer to ages relative to highstand of Laguna del Maule, during which a strandline was cut into many units. Numbers are radiometric ages in ka; for details and uncertainties, see Tables 1 and 2. Volumes are estimated only for postglacial or little-eroded units. Areas of glaciated units are reconstructed conservatively where feasible; some may be far short of original area covered.

The 24 postglacial silicic vents are inside or on the rim of the Laguna del Maule topographic basin (except that two vents of the Barrancas complex lie just beyond the divide). Dimensions of the vent field are 16.5 km east-west (**rcd** to **rdcd**), 18 km southwest-northeast (**rdep** to **rpp**), and 23 km southeast-northwest (**rng** to **rdne**). With respect to the center of the lake, vents for the major coulees lie at the following distances: **rle** 5.5 km northwest, **rdcn** 9 km west-northwest, **rdcd** 8-9 km west, **rln** 8 km south-southwest, **rcb** 14 km south-southeast, **rcd** 8.5 km east-southeast, and **rcl** 7 km east-northeast. The lake is thus virtually encircled by postglacial rhyolites and rhyodacites (Fig. 7), and, during that postglacial time interval, little else is known to have erupted far inside the circle. Of 11 postglacial mafic and intermediate eruptive units, all but orphan lava flow **apo** lie west of the lake, and of the westerly 10, six erupted essentially along the silicic-vent circle. Four others [units **aan**, **acn**, **anc**, and **apj** (24.6±2.2 ka)] erupted only 1-2 km inboard of such a projected circle, between and close to coulees **rln** and **rdcd** (or in the case of unit **apj** somewhere beneath coulee **rdcd**); all four predate the adjacent silicic coulees. A bathymetric map of the lake by the Dirección de Riego suggests, however, that there could also be a few more small eruptive units beneath the northwest part of the lake; even if this be so, it is not known whether they are postglacial or glaciated units like the nearby outcrops of units **mpl** and **aam** (Figs. 7, 17).

In contrast to postglacial time (<25 ka), only six silicic lavas (Table 4) are known to have erupted within or close to the basin during the late Pleistocene (<126 ka), a remarkable difference consider-

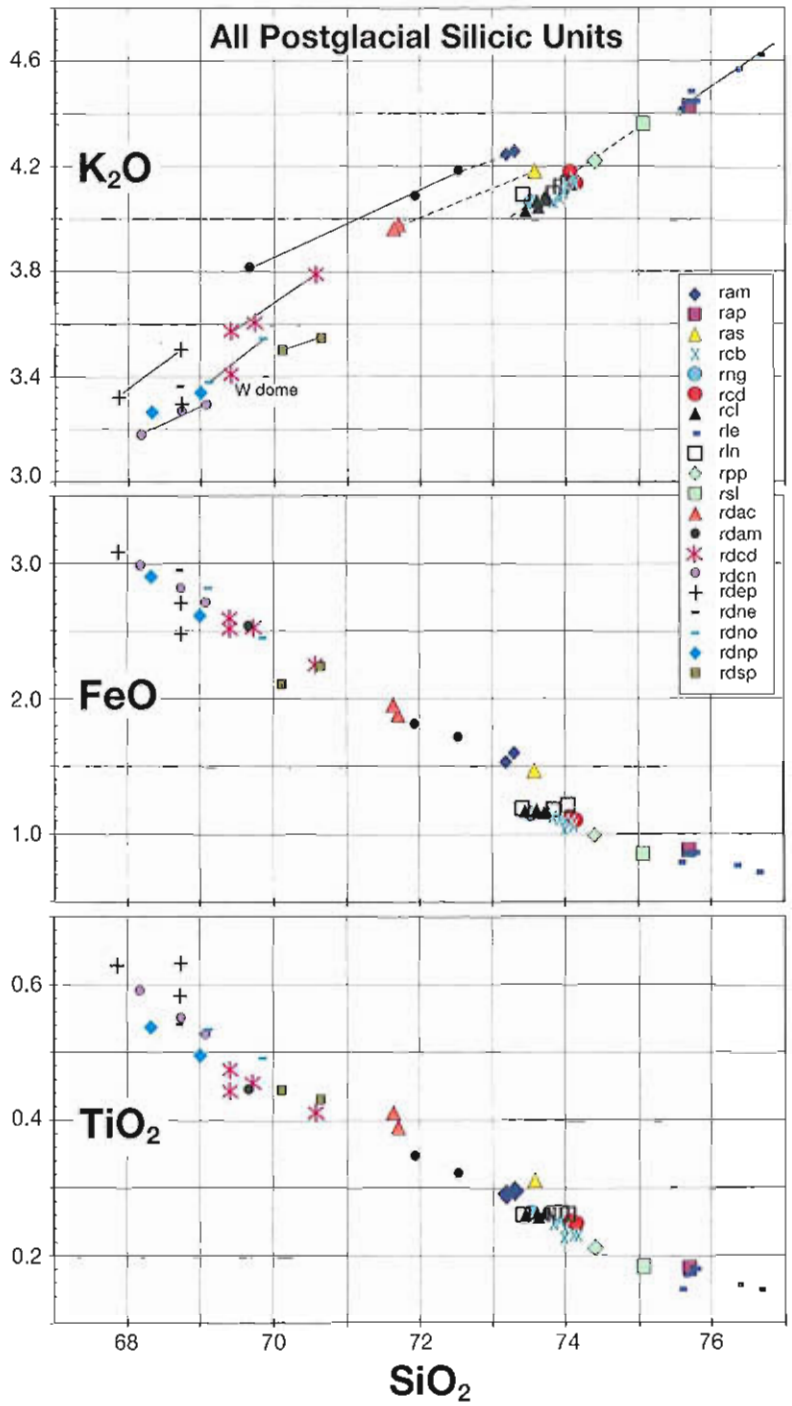

FIG. 26. Compositions of all 20 postglacial rhyolitic and rhyodacitic units: K_2O, FeO*, and TiO_2 *versus* SiO_2, all in weight percent. Unit labels in inset are identified in Appendix 1 and given for each unit discussed in text. Solid tielines in K_2O panel connect samples of same unit. Dashed tielines connect different units, perhaps magmatically closely related.

ing that the time interval is four times longer. These include the small dome of hornblende-biotite rhyolite (unit **reb**) 5 km north of the northeast arm of the lake; the hornblende dacite lava flow at Laguna del Piojo (unit **dlp**) in the southwest corner of the basin; and four lavas within 2 km of the outlet: the Domo del Maule (unit **rddm**), the twin domes west of the dam (unit **rdop**), and the rhyolite lava flows at the east end of the dam (unit **rep**).

Late Pleistocene (glacially scoured) mafic and intermediate eruptions were likewise concentrated in the western part of the basin. Of nine such units identified, eight lie in the west to northwest corner of the basin and the Laguna Turbia crater group (unit **mlt**) in the southwest corner. Of the eight, five vents lie within 3 km of the outlet dam (units **bec**, **mpl**, **msm**, **aam**, and **asd**), and the other three are 5-8 km from it (**mpn**, **alp**, and **apv**). Together with the four late Pleistocene silicic lavas that vented within 2 km of the outlet (see preceding paragraph), these eight vents mark an area only 5 x 9 km wide that was during its time the most intense focus of volcanism in the entire distributed volcanic field. In postglacial time, eruptive activity persisted within this westerly focus but also spread to the entire periphery of Laguna del Maule.

The 36 postglacial silicic coulees and domes cover a combined area of 100 km^2 and have a total lava volume of ~6.4 km^3 (Table 4). The 15 rhyodacites account for 14% of the total volume and the 21 rhyolites for 86%. Most voluminous of the rhyodacites are the Northwest Coulee (unit **rdcn**) and the lower coulee at Arroyo de la Calle (unit **rdac**), each amounting to ~0.33 km^3. The multivent Barrancas complex (units **rng** and **rcb**) is by far the most voluminous of the rhyolites at ~1.9 km^3, followed by Colada Las Nieblas at 1.2 km^3 (unit **rln**, the most voluminous lava from a single vent), and then by the Loma de Los Espejos coulee (unit **rle**; ~1 km^3) and the bilobate Divisoria complex (unit **rcd**; 0.65 km^3). The minidomes, units **ram** and **rpp**, each have volumes smaller than 0.0003 km^3. The poorly known volume of the nonwelded Barrancas rhyolitic ignimbrite sheet (part of unit **rcb**) certainly exceeds 0.5 km^3 and, considering downstream erosion, might have been as great as 1 km^3, equivalent to about half as much lava. Much smaller is the thin nonwelded rhyolitic Espejos ignimbrite (part of unit **rle**), which is preserved as a 1.5-km^2 remnant at the north toe of the Espejos coulee. Another remnant 5 km downvalley suggests that the deposit could once have covered an area at least five times greater, but, even if so, the total nonwelded volume is unlikely to have exceeded 0.05 km^3.

More impressive than the postglacial volume of silicic magma released is the ubiquity of the 24 postglacial silicic vents on all sides of the lake. The basin containing the 54-km^2 lake has a total area of 300 km^2, of which 100 km^2 are covered by postglacial rhyolite and rhyodacite lavas. There is no other place in the entire 1,400-km-long Southern Volcanic Zone of the Andes with such a concentration of distributed silicic vents, let alone of postglacial silicic vents. This suggests either **(a)** that an upper-crustal silicic magma chamber of potentially caldera-forming dimensions has been evolving beneath the lake basin throughout postglacial time, or **(b)** that a deep-crustal melting zone roughly 20 km wide has been releasing distributed batches of ascending silicic magma, recurrently for last 25 kyr. Several circumstantial observations favor the hypothesis of an evolving upper-crustal magma chamber. **(1)** The overall postglacial progression from predominance of modest-volume rhyodacites toward predominance of larger batches of rhyolite. **(2)** Narrow collinear arrays of chemical data, similar for most postglacial silicic units (Fig. 26) but distinct from most older rhyolites (Table 4) of the LdM volcanic field. **(3)** Near absence of postglacial mafic and intermediate eruptions within the focal area close to the lake. **(4)** Rarity of mafic magmatic enclaves (common in rhyodacites) in the postglacial rhyolites, suggesting the shadow effect of a voluminous and growing silicic reservoir. **(5)** Distribution of the 24 postglacial silicic vents in a ring around the basin (and not centrally), suggesting that conduit locations are influenced by the stress field peripheral to the roof of a basin-scale magma reservoir.

Scrutiny of figure 26 brings out the following relationships among the postglacial silicic lavas. **(1)** Units **rle** and **rap** are compositionally indistinguishable, even though their vents are 13 km apart, north and southwest of the lake. **(2)** Units **rpp**, **rcl**, **rsl**, **rcd**, **rcb**, and **rng**, all east and south

of the lake, provide a tight collinear compositional array, although their vents are separated by as much as 18 km. **(3)** Unit **rln**, which erupted southwest of the lake, is compositionally almost identical to those six units, which vented as far as 15 km away. **(4)** Unit **rsl**, the first lava erupted at the Cari Launa vent, is collinear but notably more evolved than the subsequent lavas of unit **rcl**. **(5)** Superimposed coulees **rdac** and **ras** are compositionally collinear, but the younger unit is 2% richer in SiO_2. **(6)** Similarly, units **rdam** and **ram** plot collinearly, despite erupting at different times from vents ~1 km apart. Such relationships are consistent with existence of a physically continuous silicic magma reservoir, possibly enlarging with time and progressively integrating previously separate pods and chambers.

It warrants re-emphasis that the postglacial silicic flare-up, concentrated around Laguna del Maule, has no precedent in this volcanic field, at least since collapse of the Bobadilla caldera ~950 ka (when voluminous ignimbrite but no known rhyolite lavas erupted). Although rhyolite lavas have erupted sporadically throughout the long history of the volcanic field, they had previously been widely scattered, infrequent, and generally solitary (Table 4). If the late Pleistocene rhyolites and rhyodacites concentrated near the northwest end of the lake were predecessors related to the subsequent postglacial flare-up, the crustal melting anomaly would have been underway by 100 kyr ago.

It also needs to be emphasized that true rhyolites (72-78% SiO_2) are very uncommon in the SVZ and, indeed, in the Quaternary Andes as a whole. Several Quaternary SVZ systems have produced minor fractions of rhyodacite (68-72% SiO_2), while in the Descabezado-Quizapu-Calabozos region (Figs. 1, 2) and in the Puyehue-Cordón Caulle system (40.5ºS; Gerlach *et al.,* 1988; Lara *et al.,* 2006; Jicha *et al.,* 2007; Singer *et al.,* 2008) rhyodacites are abundant. They are typically the most evolved eruptive products at arc volcanoes globally. Some notable exceptions occur where intracrustal melting helps generate true rhyolites in areas of intra-arc extension (such as the Taupo Volcanic Zone or the Lassen and Three Sisters segments of the Cascade arc; Hildreth, 2007). Among the rare Quaternary rhyolites in the SVZ are the Cerro Amarillo dome complex (Fig. 1; 33.9ºS; Godoy and Hildreth, 2001); the extensive ignimbrite associated with the Diamante caldera (34.2ºS; Stern *et al.,* 1984; Harrington, 1989); numerous lavas of the Puelche volcanic field (35.8ºS; Figs. 1, 2); and the 2008 and early Holocene products of Volcán Chaitén (42.85º S; Naranjo and Stern, 2004; Muñoz *et al.,* 2008; Lara, 2009; Watt *et al.,* 2009). Such rarity elsewhere, in both space and time, underscores the extraordinary anomaly posed by the many postglacial rhyolites that surround Laguna del Maule, and the exceptionally great potential hazard they portend.

BIMODAL TWO-MAGMA ERUPTIVE VENTS

Although our scrutiny was seldom intensive or thorough, field observations are adequate to assert that mafic magmatic enclaves are rare or absent in the postglacial rhyolites. In many of the postglacial rhyodacites, on the other hand, chilled enclaves are conspicuous, commonly crenulate, finely granular with few phenocrysts, and typically 1-10 cm across but as big as 30 cm. In addition, there are five places near Laguna del Maule where substantial batches of mafic and silicic magma erupted from a common vent and close in time. **(1)** The spatter ring of the Andesite of Arroyo Los Mellicos (unit **aam**; 26.6±0.8 ka) was intruded (Fig. 17) by a postglacial rhyolite minidome (unit **ram**). **(2)** The postglacial Dacite south of Arroyo Los Mellicos (unit **dsm**), probably a small dome, was disrupted and extensively blanketed by a fissure eruption of andesite scoria (unit **asm**), leading to an abundance of dacite blocks in the scoria-fall deposit. **(3)** The postglacial fissure vent of the scoria eruption of unit **mnp** was intruded by two discrete masses of rhyodacite unit **rdnp**. **(4)** The 40-m-high rhyodacite dome of unit **rdsp** intrudes and nearly fills the postglacial scoria ring of unit **asp**, adjacent to Laguna Sin Puerto. Their joint vent is contiguous with that of the slightly older Northwest Coulee (unit **rdcn**), which is itself quite young, postdating the highstand of Laguna del

Maule. **(5)** The south end of the dike-fed chain of three contiguous rhyodacite domes of unit **rdep** was draped by mafic agglutinate of unit **mcp**, the fissure vent of which extends right to the toe of the south dome. Additionally, it can be noted that units **acn** and **rdcd** erupted only 2 km apart, both in the brief postglacial pre-highstand time interval.

In figure 27, chemical data are plotted for the mafic and silicic members of the five two-magma complexes, along with enclave-host pairs for three more units. Tie-lines to connect mafic with silicic members of pairs would be essentially parallel to the remarkably collinear arrays for the whole data set. The linearity of the arrays, embracing the patent examples of enclave mingling as well as successively erupted silicic-mafic pairs, suggests the influence of pre-eruptive mixing on producing the compositional ranges of both the rhyodacitic-dacitic and andesitic segments of the arrays. The five two-magma eruptive sites are all on the western fringe of the LdM basin; no two are closer than 2 km, but all five are distributed along a north-south belt only 8 km long (Fig. 7). All five are younger than ~27 ka and, though most are undated, their eruptions were spread out over latest glacial, pre-highstand, and post-highstand time, with the sequence of units **rdcn-asp-rdsp** possibly as young as mid-Holocene. All five mafic members represent eruptions of small volume (each 0.01 to 0.05 km^3), and the five silicic members are smaller still (0.0002 to 0.01 km^3; Table 4).

From these observations, we speculate on the influence of magma reservoir configuration as follows. If dikes and pods of ascending magma are well distributed as they reach the upper crust, encounters between previously separate batches variously lead to composite dikes, mingling and mixing, or bimodal mafic-silicic eruptive sequences. When pods or sills of silicic magma grow to moderate dimensions, their enhanced capacity to intercept mafic batches favors mixing or (if eruption ensues soon enough) enclave-rich lavas. When reservoir components grow large and a thick rhyolitic zone accumulates at the roof (Hildreth, 2004), recharge batches are trapped at deeper levels and the resulting dispersed enclaves are seldom circulated into the uppermost low-density part of the chamber.

COMPOSITIONS OF ERUPTIVE PRODUCTS

About 425 major-element XRF analyses, >400 trace-element analyses by XRF, and 43 trace-element analyses by INAA are given in Appendices 2-4, and 30 Sr-isotope determinations in Table 5. On the canonical TAS diagram (Fig. 28a), rocks of the LdM volcanic field straddle the arbitrary dividing line between subalkaline and mildly alkaline suites. They range continuously from 49.3% to 77.6% SiO_2, though only a few samples plot near 67% SiO_2. The data yield an alkali-lime index of 58 (Fig. 28b), indicating a calc-alkalic suite, as originally defined (Peacock, 1931; Arculus, 2003). By the rather different criteria of Miyashiro (1974), LdM samples scatter widely at all SiO_2 contents on both sides of the arbitrary tholeiitic/calcalkaline dividing line (Fig. 28c).

The LdM suite is medium-K at 50-60% SiO_2 but high-K in its silicic portion (Fig. 29a). Contents of K_2O are ~0.8% at 50% SiO_2 but, far more variably, 1-2% at 54% SiO_2, 2-3% at 62%, and 4-5% at 75%. The SiO_2 arrays of FeO*, MgO, Al_2O_3 (Fig. 29) and to a lesser extent of CaO (Fig. 28b) are broad at their mafic ends and much narrower at their silicic ends. For example, at 53% SiO_2, FeO* ranges from 7% to 10%, but at 70% SiO_2 only from 2% to 2.5%. At 53% SiO_2, Al_2O_3 ranges between 17% and 20%, but it narrows drastically along the silicic part of the array. Na_2O contents range widely at all SiO_2 values but reach a maximum near 70% SiO_2 and decline slightly in rhyolites (even nonhydrated ones). TiO_2 contents are ~1% at 50% SiO_2, diversify greatly to 0.8-1.5% at 54% SiO_2, then exhibit a progressively narrowing evolutionary array toward rhyolites. P_2O_5 contents are 0.15-0.33% in basalts and only 0.04-0.12% in rhyolites but are extremely varied among intermediate members of the suite (0.15-0.50%), reflecting the vagaries of apatite saturation, transport, accumulation, and entrapment in other crystals.

None of the 425 analyzed rocks from the LdM volcanic field are primitive. Excluding a few olivine-accumulative samples, basalts range in MgO content from 4% to 7% and mafic andesites from 2.5% to 5.5%. The few basalts (49-52% SiO_2) have mg-numbers [mg # = 100 $Mg/(Mg+Fe)_{mol}$] of only 49-58, Cr<170 ppm, and Ni<70 ppm. For the entire LdM suite, Cr and Ni concentrations are less than 20 ppm for all samples with ≥59% SiO_2. Mafic andesites, taken narrowly at 54% SiO_2, range in mg-number from 38 to 59 and in K_2O content from 1% to 2%, showing that the compositional diversity originates early in the differentiation sequences. For 17 of the least evolved ('most primitive') samples, some illustrative data are tabulated in Table 6.

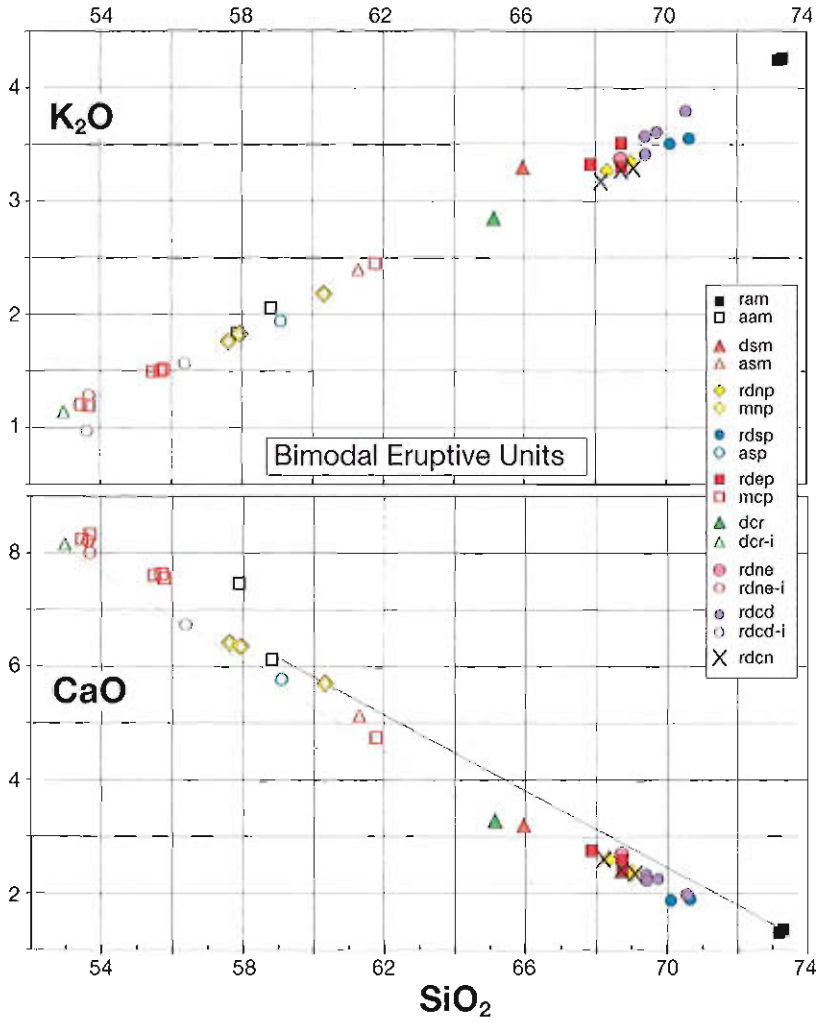

FIG. 27. Bimodal eruptive units. Plots of wt% K_2O and CaO *versus* SiO_2 for eight pairs of mafic and silicic magmas, each pair erupted jointly or at virtually same location, all within last 27 kyr. See text for details. Unit labels are identified in Appendix 1, and all units are discussed in text. Key at right uses open symbols for mafic members, in same color as filled symbols for silicic counterparts. Three labels with suffix -i represent samples of chilled crenulate magmatic enclaves in host lava of unit preceding on list. Unit **rdcn** is unpaired (though rich in unanalysed mafic enclaves), but its vent is almost contiguous with that for paired units **rdsp** and **asp**, which are very slightly younger than **rdcn**.

TABLE 5. Sr-ISOTOPE DATA FOR 30 LAGUNA DEL MAULE SAMPLES.

Sample	% SiO_2	Unit	UTM Grid	$^{87}Sr/^{86}Sr$†	Rb	Sr	Rb/Sr	Lab*
LdM-2	70.6	rddm	588/123	0.70412±5	143	250	0.572	1
LdM-3	69.1	rdcn	585/127	0.70406±4	122	273	0.447	1
LdM-6	75.6	rle	603/126	0.70412±5	179	70	2.557	1
LdM-15	70.2	igsp	583/147	0.70431±1	143	164	0.872	2
LdM-16	51.4	bec	586/148	0.70406±3	18	549	0.033	1
LdM-25	53.1	mlp	585/166	0.70404±4	30	554	0.054	1
LdM-32	71.4	igcb	631/175	0.70428±1	164	127	1.291	2
LdM-33	52.0	bbc	643/167	0.70409±6	30	599	0.050	1
LdM-33A	52.0	bbc	643/167	0.70408±1	24.1	606	0.040	2
LdM-38	59.3	aab	580/188	0.70404±4	59	501	0.118	1
LdM-52	77.6	rcn	695/110	0.70483±1	315	25	12.60	2
LdM-114	53.2	mvñ	425/111	0.70406±1	27	674	0.040	2
LdM-146	49.3	mcs	499/246	0.70404±1	13.7	713	0.019	2
LdM-239	54.2	mcc	762/218	0.70424±1	35	570	0.061	2
LdM-243	50.3	mvm	743/194	0.70396±1	10.3	521	0.020	2
LdM-248	75.1	rsl	736/112	0.70414±1	182	60	3.03	2
LdM-249A	74.1	rcd	726/072	0.70415±1	163	93	1.753	2
LdM-278	54.7	mvm	708/187	0.70435±1	42	490	0.086	2
C84-2	70.6	igcb	636/133	0.70430±5	156	177	0.881	1
C84-3	60.5	ava	633/136	0.70422±5	77	378	0.204	1
C84-4	73.6	rep	600/136	0.70423±4	169	157	1.076	1
C84-6	57.9	apv	599/094	0.70409±4	53	556	0.095	1
LM-1	63.4	mlc	560/2085	0.70396±3	69.1	425	0.163	3
LM-4	53.2	msm	~567/204	0.70414±3	25.4	632	0.040	3
LM-3	65.1	dcc	561/208	0.70388±3	97.9	380	0.258	3
FM-37	56.5	acn	591/074	0.70424±3	52.5	584	0.090	3
FM-78	73.4	rcb	680/007	0.70418±5	150	93.8	1.599	3
FM-94	50.3	bec	~590/145	0.70419±3	17.9	592	0.030	3
FM-123	62.8	dcc	560/2085	0.70400±3	90.8	408	0.223	3
FM-205	69.5	rdno	603/157	0.70418± 5	154	231	0.667	3

* Isotope ratios measured at **(1)** University of Oxford (methods reported by Hildreth and Moorbath, 1988); **(2)** UCLA by F. Ramos (methods reported by Feeley and Davidson, 1994); **(3)** MIT as reported by Frey *et al.* (1984). Rb and Sr (ppm) determined by isotope dilution in Labs 1 and 3. Wt% SiO_2 for all samples by XRF at USGS lab, Lakewood, Colorado. Rb and Sr for Lab 2 samples determined by XRF at USGS or University of Massachusetts.

† Isotope ratios listed are as measured. Age corrections gives initial ratios of 0.70427 for sample LdM-15; 0.70424 for LdM-32; 0.70460 for LdM-52; 0.70426 for C84-2.

PHENOCRYST CONTENTS

Most of the 21 rhyolite units (72-77% SiO_2; Table 4) carry phenocrysts of plagioclase and biotite, although units **rap**, **rez**, **rng**, **rpp**, **rsl**, and some flows of units **rcb** and **rcl** are strictly aphyric. Units **ram**, **reb**, **rep**, **rls**, and **rnf** also contain sparse amphibole subordinate to biotite, and unit **rlm** contains subequal amounts of opx and biotite. Among the phenocryst-bearing rhyolites, plagioclase predominates over the mafic phases in all units but **rnf**. Most of the rhyolites contain 0-3% phenocrysts; units **ram**, **ras**, **rca**, **ret**, **rlf**, and **rln** have 3-7%; and units **reb** and **rls** have 7-12%.

Most of the 23 rhyodacite units (68-72% SiO_2) carry phenocrysts of coexisting amphibole and biotite, and plagioclase predominates in all 23. Contrary to the rhyolites, no rhyodacite is aphyric, few are phenocryst-poor, and most have 5-25% phenocrysts. Only units **rdcb**, **rdez**, and **rdvc** lack

TABLE 6. LEAST EVOLVED SAMPLES.

LdM #	Unit	SiO_2	MgO	mg#	Cr	Rb	Ba	Nb	La	Y	Sr/Y	Zr/Y	K/Rb
16	bec	51.4	5.7	53	82	19	269	4.3	13.5	16	35	7.6	396
33	bbc	52.0	5.1	51	92	24	346	5.8	16	18	33	7.9	370
42	mva	51.4	10.9	71	654	13	214	2.1	9	13	48	5.9	531
76	mcf	52.8	5.0	53	45	26	264	2.7	10	16	39	5.3	343
83	avz	53.9	5.4	57	73	33	259	3.1	9	15	39	6.0	330
85	mcs	50.8	6.2	57	73	22	263	2.5	22	16	51	5.5	424
109	mvñ	51.4	6.3	56	168	23	356	5.5	15	18	35	6.1	431
137	mvp	53.0	5.6	55	102	25	361	6.9	19	16	40	8.1	387
140	mvp	53.1	5.7	55	89	33	395	5.7	15	16	36	7.7	281
146	mcs	49.3	7.2	58	81	14	198	2.6	15	15	49	4.0	483
150	mcb	53.5	5.6	54	128	30	359	6.4	16.5	15.5	38	9.1	336
230	mct	53.6	5.0	53	65	30	391	6.7	20	18	33	7.8	331
243	mvm	50.3	6.8	56	37	10	231	3.3	10.5	17	30	5.4	575
324	bcf	51.1	5.6	54	32	9.4	274	3.1	9	17	35	5.5	703
371	bhc	50.0	10.3	66	332	18	288	5.1	13	13	44	9.1	376
498	mcr	52.6	5.9	56	133	26	391	6.6	17	15	42	9.5	339
508	mpc	54.0	6.6	59	271	74	316	7.5	16	24	18	7.3	220
Volcanic Front													
QCNE-1	TSP	49.0	9.9	66	522	7.4	190	2.3		15	29	5.2	657
EML-7	TSP	51.0	7.2	60.5	167	20	260	3.2		18	35	6.2	409
QTW12-18	TSP	52.7	7.3	64	151	20	262	1.9		14	38	5.4	379
ESPE1-4	TSP	51.7	7.3	61	203	22	281	2.0		16	35	6.7	357

LdM data are from Appendices 2-4; Unit labels in Appendix 1 and text; Volcanic front data for comparison are four of most primitive samples of Volcán Tatara-San Pedro (TSP) from Dungan *et al.* (2001).

both biotite and amphibole, each carrying opx instead. Biotite occurs alone with plagioclase in units **rdac**, **rdnp**, and **rdsp**. Opx coexists with biotite in unit **rdap**, and opx accompanies both amphibole and biotite in units **rdcp**, **rdct**, **rddm**, **rdes**, **rdla**, and **rdpñ**. Cpx occurs in trace amounts in some thin sections, usually in crystal clots with plagioclase, opx, or rare olivine; it may be antecrystic, entrained from conduit rinds, or alternatively disaggregated from mafic enclaves.

All eleven dacite units (63-68% SiO_2) are plagioclase-dominant, eight of them have amphibole, six have biotite, and nine have opx. Unit **dsm** has biotite and amphibole without pyroxenes, and unit **dcr** carries biotite without either pyroxene or amphibole and is the only extremely crystal-poor (<1% phenocrysts) dacite unit here. Units **dct** has opx and **dlf** carries both opx and cpx, and both lack hydrous phenocrysts. In units **dab**, **dcc**, and **dpr**, amphibole coexists with opx (± trace amounts of cpx), whereas in units **det**, **dlp**, **dsp**, and **dvñ**, biotite and amphibole coexist with opx (± minor cpx).

Of the 33 andesite units (57-63% SiO_2), 13 contain olivine as well as cpx (± opx). Most products carrying olivine have ≤59% SiO_2, but olivine survives in some lavas having as much as 61% SiO_2 in units **ars**, **ava**, and **avz**. In products of 13 andesite units (58-62% SiO_2), pyroxenes are the only mafic silicate minerals in units **aam**, **acc**, **aeb**, **ams**, **ans**, **apg**, **arp**, **asb**, **avc**, and in some of the lavas of comprehensive units **acs**, **alz**, **ava**, and **avz**. Amphibole coexists with pyroxenes in units **acr**, **alm**, **alp**, **asd**, **avr**, and in some flows of units **acs** and **alz** (all with 59-62% SiO_2). Thoroughly opacitized amphibole accompanies cpx in units **acn**, **acp**, and **als**. Amphibole coexists with biotite but without pyroxenes in unit **asm** (61.3% SiO_2). Plagioclase is the predominant phenocryst in all the andesites except unit **apñ**, in which it occurs only as microphenocrysts and microlites. As in most arc andesites globally, coexisting generations of plagioclase in varied conditions of resorption

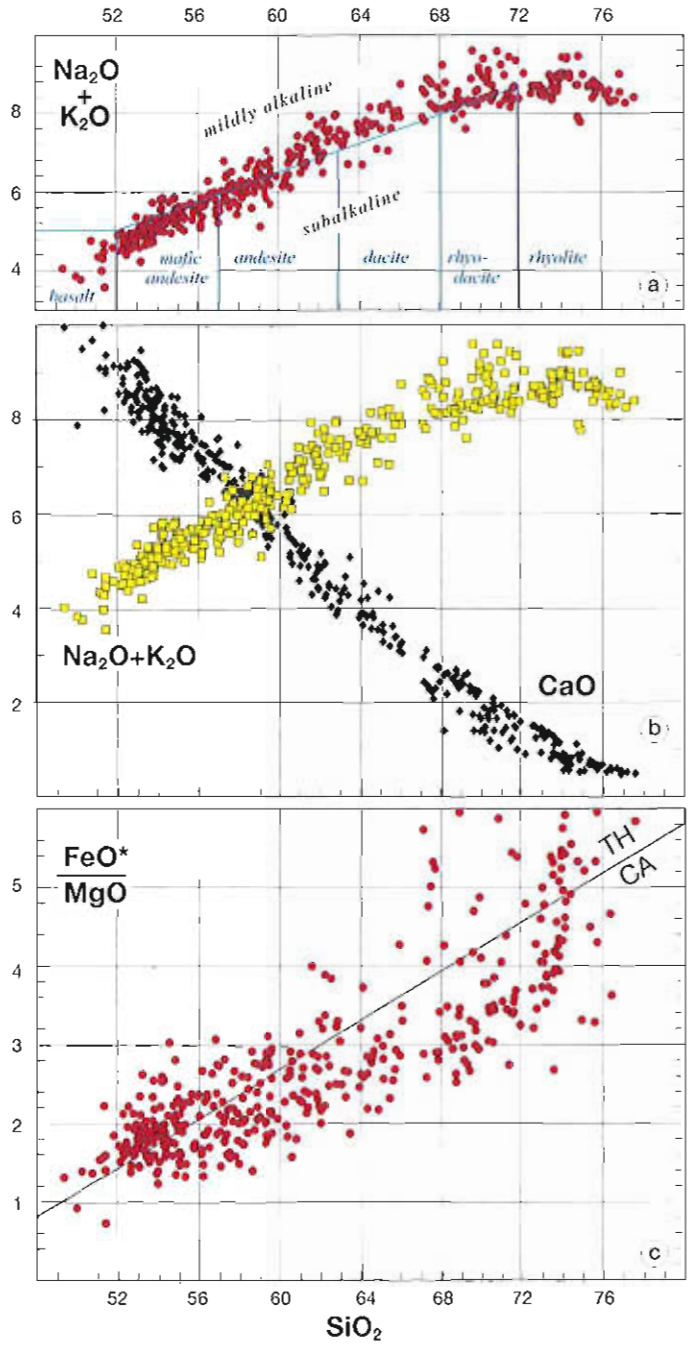

FIG. 28. Whole-rock chemical data for entire Laguna del Maule volcanic field suite of 425 Quaternary samples. **(a)** Total alkalies *versus* SiO_2, in weight percent, modified from LeBas *et al.* (1986). **(b)** CaO and total alkalies *versus* SiO_2, in weight percent; alkali-lime index (intersection) is ~58, the suite thus calc-alkalic, following Peacock (1931). **(c)** FeO*/MgO *versus* SiO_2, in weight percent; FeO* is total iron recalculated as FeO. TH/CA line is tholeiitic/calcalkaline suite boundary according to Miyashiro (1974); LdM suite would straddle entire low-Fe and medium-Fe fields of Arculus (2003).

and overgrowth are the most visible evidence of complex parentage and crustal histories. Most of the andesites contain 7-25% total phenocrysts, and only units **acn**, **als**, **apñ**, **ars**, **asm**, **asp**, **avc**, and most lavas in **acs** can be described as phenocryst-poor, in having only 1-3%.

Of 28 mafic andesite units (52-57% SiO_2) and four true basalts, nearly all contain coexisting olivine and cpx, and some (generally the more silicic) lavas also have subordinate opx. Only in units **mas**, **mlt**, **bbc**, **bcf**, parts of **bec**, and basaltic lavas of **mcs** is olivine the lone mafic silicate. Such products lacking pyroxene are limited to the range 49-54% SiO_2, but in other units cpx coexists with olivine in lavas as poor in SiO_2 as 51.3%. Plagioclase predominates over mafic phenocrysts in all units except some lavas of unit **mvñ**, in which it occurs only as microphenocrysts. Among mafic units, only **mcp**, **mct**, **mlt**, **mnp**, and **mor**, and some lavas of comprehensive units **mcb**, **msp**, **mva**, **mvñ**, and **mvp** are phenocryst-poor (<3%).

Among the six Quaternary ignimbrites, all are plagioclase-dominant and, in three (**igcb**, **igcc**, and **igcg**), biotite is the only mafic silicate phenocryst. The other three lack hydrous phenocrysts; unit **igbc** contains opx, **igeb** carries sparse cpx and opx, and **igsp** has abundant opx and sparse cpx. All the ignimbrites contain Fe-Ti-oxide microphenocrysts, as do the great majority of eruptive units of all compositions.

Quartz has been observed here only in Miocene ignimbrite unit **Tigh**, in Pliocene rhyolite lavas and tuffs of unit **Trea**, and very sparsely in unit **igcb**. In no thin section have we observed sanidine.

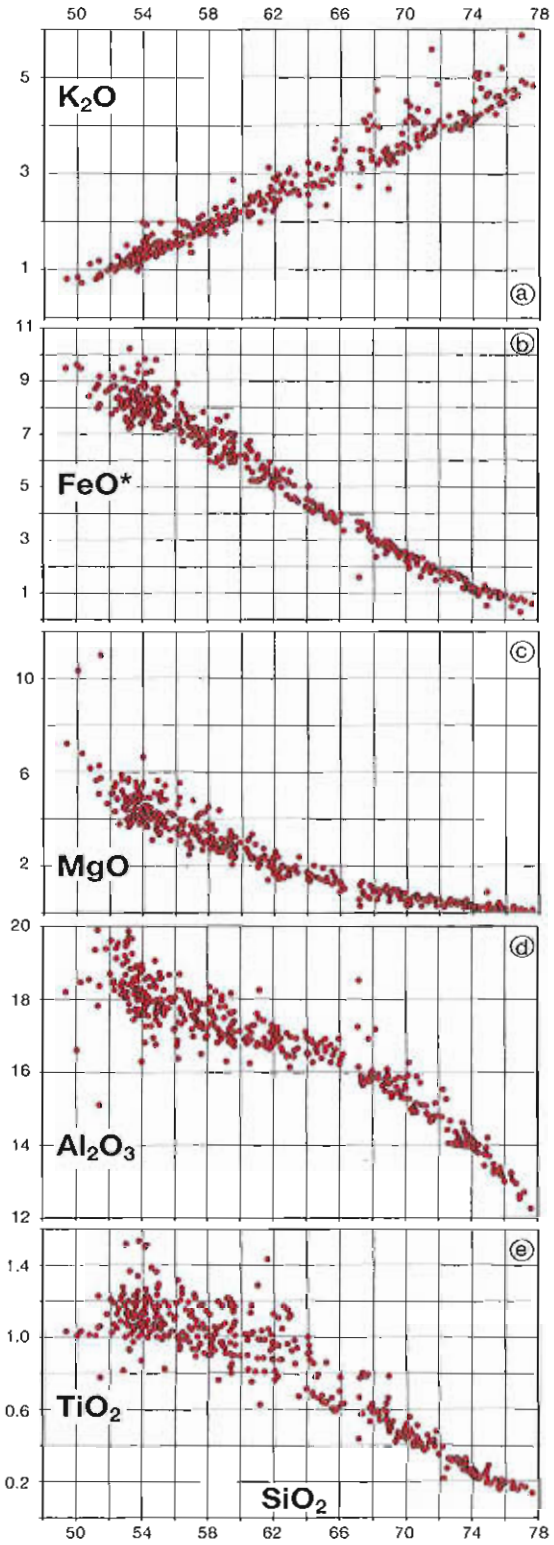

FIG. 29. Compositional variation with SiO_2, in weight percent, of selected major-element oxides for 425 Quaternary samples from Laguna del Maule volcanic field. **(a)** K_2O. **(b)** FeO* (total iron calculated as FeO). **(c)** MgO (two high-MgO samples are olivine-accumulative). **(d)** Al_2O_3 (two low-Al_2O_3 basaltic samples are olivine-accumulative). **(e)** TiO_2. All data in Appendix 2.

MAGMATIC DIVERSITY WITHIN THE LdM ARC FAMILY

The consummate flow-by-flow investigation of nearby Volcán Tatara-San Pedro (Dungan *et al.,* 2001) demonstrated that attempts to treat as simple comagmatic evolutionary arrays any collection of 10 or 100 samples from a long-lived arc edifice is wishfully naive. Stratovolcanoes grow in spurts (Hildreth and Lanphere, 1994; Singer *et al.,* 1997; Bacon and Lanphere, 2006), and each successive magma batch is a potentially unique product of distinctive mantle parentage and an irreproducible sequence of encounters in passing fitfully through the magma-percolation labyrinth in heterogeneous arc crust (Hildreth, 1981; Hildreth and Moorbath, 1988; Dungan *et al.,* 2001). Each short-lived magma batch that erupts a definable package of lava flows is itself typically heterogeneous owing to ongoing crystal fractionation, entrainment of cumulates and rind crystals, assimilation of wall-rock melts and stoped fragments, mixing with contending batches, and mingling of recharge batches into transiently crystallizing sills, pods, and chambers. Dungan and Davidson (2004) further demonstrated that assimilative recycling of the voluminous intracrustal cumulates left behind beneath any long-lived arc volcano, by blending grain-boundary melts and varied fractions of the disaggregated spinel-olivine-pyroxene-plagioclase antecrysts (or xenocrysts) into each new magma batch, can elevate both incompatible and compatible elements, thus violating their (usually assumed) inverse relationship during magma evolution.

The degree of diversity demonstrated by Dungan *et al.* (2001) for the large volcanic-front center is approached by products of the distributed LdM volcanic field just inboard of it. Behind the front there are fewer basalts, far more rhyolites, and rather broadly diverse compositional arrays in the mafic-to-intermediate compositional range (Figs. 28-34). Chemical data for products of the 130-odd scattered Quaternary vents identified (Fig. 4) do display a general family resemblance, reflecting passage of all batches through arc mantle and arc crust of broadly similar thermal and physical structure. Each batch erupting at each of the many independent distributed volcanoes, however, had a unique ascent path and sequence of intracrustal encounters. A partial exception may be represented by some of the postglacial rhyolites, several of which (as discussed earlier; Fig. 26) might have been successive leaks from an evolving chamber.

Variation of K/Rb with SiO_2 (Fig. 30a) epitomizes several points just made: **(1)** scarcity of primitive eruptive products, **(2)** highly varied intracrustal differentiation trajectories, **(3)** ubiquitous crustal contributions, and **(4)** strong diversification of the evolutionary arrays within the mafic interval (up to ~56% SiO_2). K/Rb in mafic magmas would be little affected by closed-system fractionation of anhydrous phenocrysts but is severely modified by only modest assimilation of Rb-rich crustal melts (Davidson *et al.,* 1987, 1988; Hildreth and Moorbath, 1988). Indicative of the wide range of magmatically integrated crustal assimilants available is the K/Rb field of Tertiary granitoids (Fig. 30a) exposed in this part of the Andean arc (Dungan *et al.,* 2001). In the LdM volcanic field, while K_2O increases from 0.8% in basalts to 4-5% in rhyolites (Fig. 29), Rb rises from 10-25 ppm in basalts to 130-210 ppm in rhyolites, roughly twice as steeply as K_2O. As rhyolites have been produced widely and persistently during development of the volcanic field, admixture of silicic melts to mafic magma batches is probably routine. Figure 30b illustrates the divergent fan of differentiation trajectories represented within the LdM volcanic field, entailing wide ranges of both excess Rb enrichment and relative Fe enrichment (cf. Fig. 28c). Figure 30c shows, however, that the degree of intracrustal Rb enrichment reflected in K/Rb values does not change systematically across the arc.

COMPOSITIONAL VARIATIONS ACROSS THE ARC

What can be learned from the compositions of a heterogeneous suite of variably fractionated, contaminated, and hybridized volcanic rocks that erupted from 130-odd vents during an interval of 1.5 Myr? By concentrating on incompatible trace elements in mafic members of the assemblage, one might hope to find some evidence not wholly obscured by crustal processes for compositional

trends that reflect cross-arc changes in slab contributions, intraplate mantle contributions, mantle fertility, or degree of mantle melting (as discussed by Hildreth *et al.*, 2004).

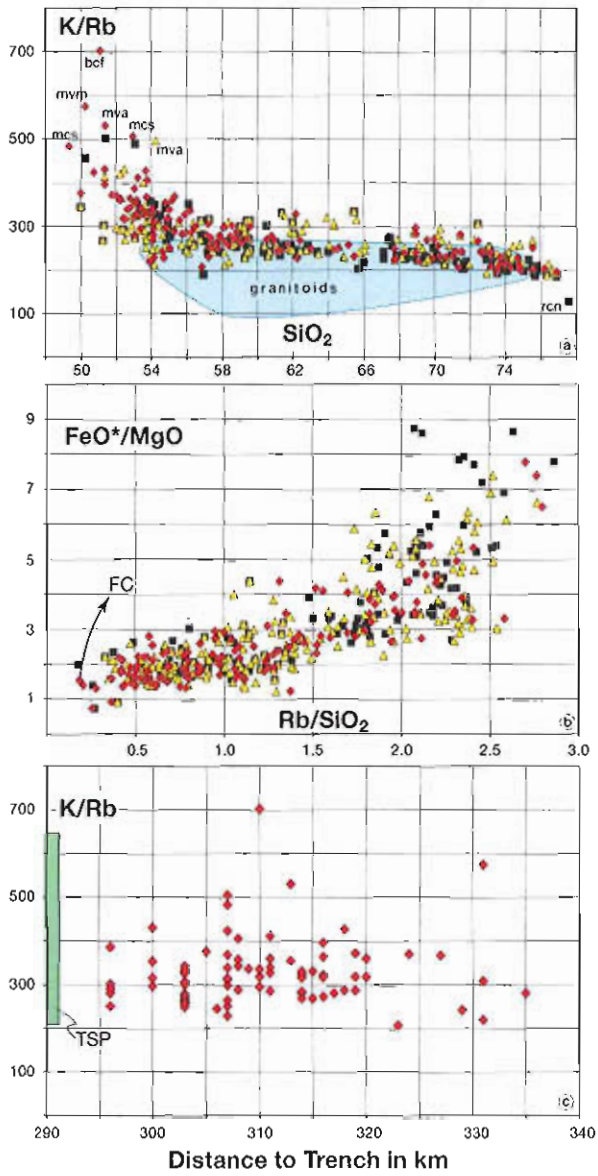

FIG. 30. Rb contents as indicator of LILE enrichment in excess of closed-system fractionation. **(a)** K/Rb *versus* weight % SiO_2, illustrating wide array of K/Rb values, especially over 49-57% SiO_2 range. **(b)** FeO*/MgO *versus* Rb-enrichment rate (ppm Rb/wt% SiO_2), showing wide range of trajectories. Compare with FeO*/MgO *versus* SiO_2 in figure 28C. Rb/SiO_2 is >2 for rhyolites and some rhyodacites; for basalts and mafic andesites, it is <1. **(c)** K/Rb for mafic rocks only, plotted against distance in kilometers from inboard margin of trench floor to vent for each eruptive unit. Field of nearby SVZ granitoids (mostly Miocene), K/Rb range for Volcán Tatara-San Pedro (**TSP**) on volcanic front, and low-pressure trajectory for fairly dry, closed-system, olivine-plagioclase crystal fractionation (**FC**)-all after Dungan *et al.* (2001). [Data in Appendices 2 and 3. In panels A and B, Rb data are from four sources: Diamonds, WDXRF by UMass or Lausanne labs; squares, WDXRF by USGS lab; triangles, EDXRF by USGS lab].

In a seminal study of mafic products of several SVZ volcanoes, Hickey *et al.* (1986) pointed out that several rear-arc centers, although richer in LILE, REE, and HFSE than nearby volcanic-front centers, have lower ratios of Ba/La, Ba/Th, Ba/Nb, La/Nb, Zr/Nb, and Cs/Rb. They explored complementary models in which greater contributions of LILE-rich slab-derived fluid enhance the degree of melting beneath the front (thereby lowering incompatible–element abundances generally) or in which all or part of the rear-arc mantle might be more fertile than that beneath the front. Likewise, in comparing two Mexican volcanoes, Luhr (1992) identified a similarly inverse relationship between key abundances and ratios that he linked to a greater flux of slab-derived fluid resulting in a more hydrated mantle source and consequently in larger melt fractions beneath the more trenchward center. A similar inverse pattern has by now been documented in transects across several arcs (see Hildreth *et al.*, 2004, for a review).

Products of the Laguna del Maule volcanic field have incompatible-element patterns typical of continental arcs. In mafic samples (49-56% SiO_2), LILE are enriched relative to LREE (Ba/La=12-33), though not as strongly as in intraoceanic arcs, and both groups are enriched relative to HFSE (Ba/Nb=40-130 and Ba/Ta=530-1060; La/Nb=2-5 and La/Ta=37-63).

REE data for 43 samples are given in Appendix 4. For 22 mafic samples (49-54% SiO_2) La contents are 9-22 ppm and Yb 1.2-2.0 ppm. For 13 silicic samples (69-77% SiO_2) La is 28-38 ppm and Yb is 1.7-2.0 ppm (plus four ignimbrite fiamme at 2.5-3.7 ppm Yb). La/Yb (steepness of the REE pattern) is 6-14 among the mafic rocks and 9-17 among the silicic, with significant scatter at all values of SiO_2 (Fig. 31). There is no systematic trend in La/Yb across the volcanic field, neither among mafic rocks nor in the whole data set (Fig. 31). La/Sm (steepness of the LREE pattern) generally increases with SiO_2 (from 3 to 9) but not across-arc, while Sm/Yb (slope of the HREE pattern) scatters from 1.8 to 3.4 but shows no correlation with either SiO_2 or longitude (Fig. 32). Quaternary volcanoes at the northern end of the SVZ (250-300 km north of LdM), where the crust may be as thick as 60 km, have La/Yb values as high as 20-28 and Sm/Yb values as high as 4 to 5, indicating retention of HREE by residual garnet in the deep source of crustal melts contributed to the magmas (Hildreth and Moorbath, 1988). Beneath the LdM field, where the crust is 40-50 km thick, crustal garnet is less likely to be important, although the few basalts with Sm/Yb >3 might reflect slight garnet influence. The same ambiguity can be inferred from contents of Y (which behaves much like the HREE), 13 to 18 ppm in basalts, 12-30 ppm in mafic andesites, and 12-44 ppm in rhyolites. There is no systematic trend in Y contents across the arc, but the handful of mafic lavas that have only 12-15 ppm Y may retain the effects of residual garnet from early in their crustal ascent, despite blurring of the garnet signature during subsequent passage through the Y-richer, garnet-free, middle and upper crust.

If an intraplate or enriched mantle component contributes subordinately to some of the arc magmas here, its distribution is scattered, and its contribution does not increase across the arc. Among mafic rocks, TiO_2 content ranges widely from 0.8% to 1.2% in basalts and from 0.8 to 1.5% in mafic andesites (52-56% SiO_2), but there is no suggestion of a cross-arc increase. Likewise, Zr abundance varies greatly, 60-120 ppm in basalts and 80-220 ppm in mafic andesites, and Nb abundance displays proportionately wide ranges of 2-6 ppm in basalts and 2-9 ppm in mafic andesites, but neither element exhibits any systematic trend across the arc. Similarly, among the mafic rocks, values of Zr/Y (4-12) and Nb/Y (0.13 to 0.5) are widely scattered, show no correlation with TiO_2 or SiO_2, and exhibit no tendency to increase inboard (Fig. 33). It was observed by Dungan *et al.* (2001) that Nb/Y is a key ratio for discriminating among parental basalts because the ratio changes little with crystal fractionation and is modified only modestly by crustal contributions. Because the rhyolites of the LdM volcanic field range in Nb/Y from 0.5 to 0.8, assimilation of crustal melts may contribute to some of the Nb/Y variation in the LdM mafic magmas, but we agree that the 3-fold range of Nb/Y (0.15 to 0.4) in LdM basalts (virtually the same range found by Dungan *et al.* (2001) at Volcán Tatara-San Pedro) also reflects variability among deep-seated parental magmas.

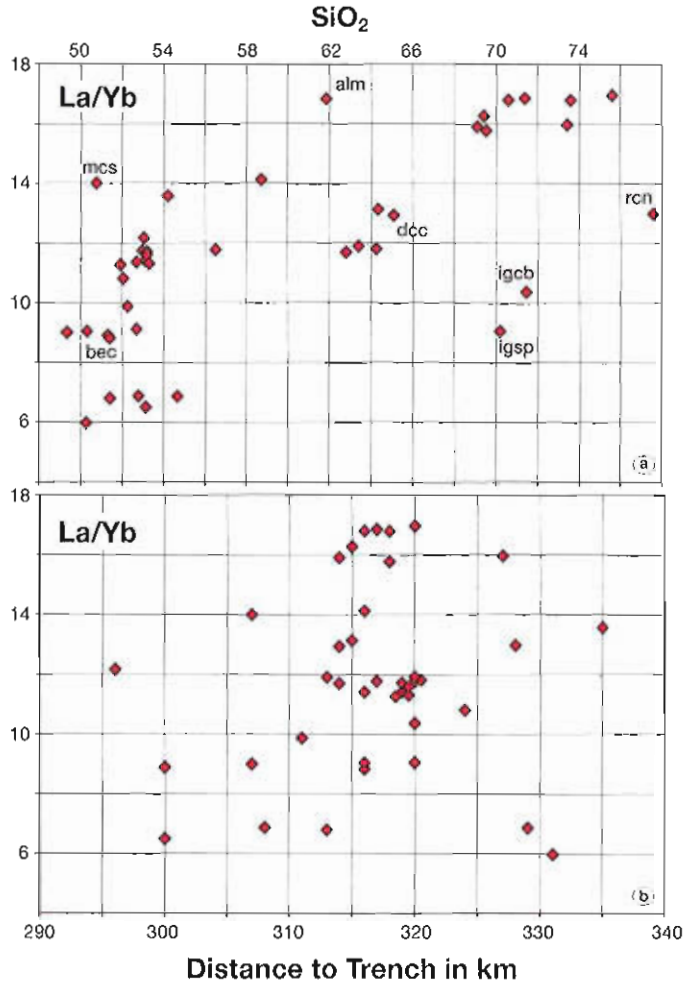

FIG. 31. La/Yb (steepness of REE pattern) plotted against weight % SiO_2 and across-arc distance from inboard margin of trench floor to vent location. Tie-lines connect sample pairs from particular eruptive units. There is no systematic trend across arc, among all data or among mafic samples alone. Two ignimbrites (**igsp** and **igcb**) and high-silica rhyolite lava unit **rcn** have lower ratios than other rhyolites. REE data in Appendix 4.

Despite the apparent range of parental basalts, there is little evidence here for an enriched intraplate mantle contribution. For mafic samples, ratios of Sr/Nd (20-45), Sr/P (0.3-1.1), Sr/Y (30-50), La/Ta (40-80), Th/Ta (7-27), and Zr/Nb (19-42) are far greater than the low values typical of average OIB (Sun and McDonough, 1989). Likewise, the ratios of Ta/Yb (0.1-0.3), Ti/Yb (3,000-5,500), and La/Yb (6-14) for mafic samples are well below the elevated values typical of OIB-type intraplate basalts. Such relations are epitomized by the Th/Yb *versus* Ta/Yb plot (Fig. 34) which illustrates the subduction-related Th-enrichment trend (Pearce, 1982), a normal arc signature for all LdM samples. By comparison, Quaternary products of the Llancanelo volcanic field, mostly mafic monogenetic scoria cones and lavas 70-220 km due east of Laguna del Maule (Fig. 1), are alkali basalts with such intraplate values as 1.5-2.5% TiO_2 at 47-49% SiO_2, Ba/Nb=10-25, Nb/Y=0.7-1.9, La/Ta=11-30, and Th/Ta=1-6 (Muñoz *et al.*, 1989). The Th/Ta data for that back-arc extensional volcanic field would plot along the mantle-enrichment trend in figure 34.

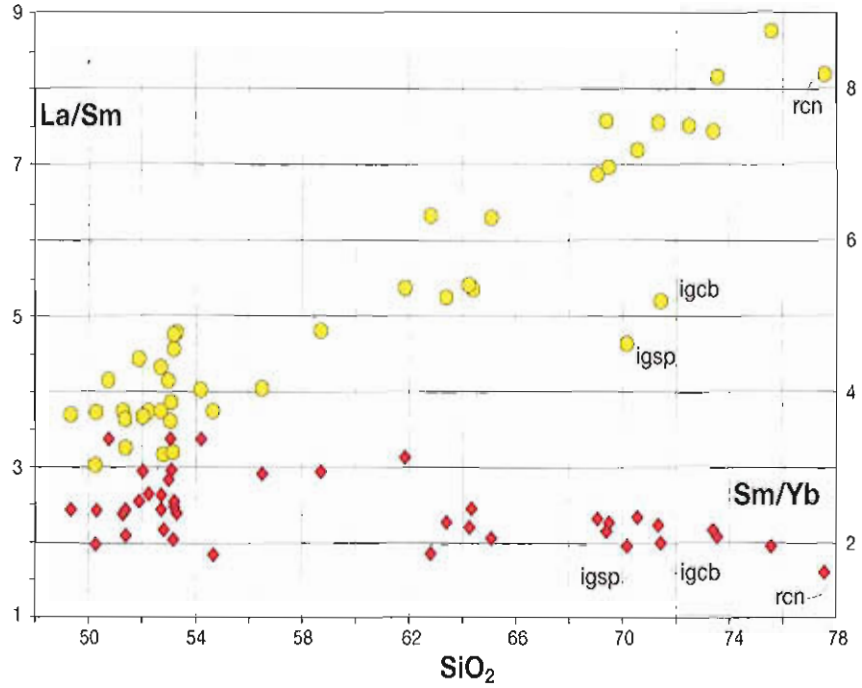

FIG. 32. La/Sm (LREE pattern) and Sm/Yb (HREE pattern) *versus* weight % SiO_2. LREE become more fractionated (steeper) with increasing SiO_2, whereas HREE patterns become flatter and less varied. Both ratios exhibit significant ranges among mafic samples but narrower arrays among silicic ones. Rhyodacite ignimbrite units **Igsp** and **Igcb** (fiamme) are enriched in all REE (La, Sm, Yb, and the rest) relative to the silicic lavas. REE data in Appendix 4.

Ba/Nb is the signature LILE/HFSE ratio that distinguishes arc suites from intraplate suites, and it epitomizes the Nb-Ta trough characteristic of arc magmas on mantle-normalized extended incompatible-element diagrams ('spidergrams'). Among LdM basalts, Ba/Nb ranges widely from 50 to 110 and among mafic andesites from 40 to 130. Because LdM rhyolites also range in Ba/Nb from 40 to 105, crustal contamination does not greatly modify the ratio in the mafic magmas. These high continental-arc values can be compared to Ba/Nb=7.3 for average OIB (Sun and McDonough, 1989) and typical ranges of 5-20 for relatively uncontaminated intracontinental alkali basalts. (The range of Ba/Nb for some extensional intraplate alkali basalt fields extends as high as 50-60, overlapping with arc values; rather than representing a proximate slab contribution, such high ratios probably reflect a fossilized subduction contribution remobilized by partial remelting of older subcontinental lithosphere). In figure 33, Ba/Nb values for mafic rocks (49-55% SiO_2) of the LdM field are plotted against the cross-arc distance from the Chile Trench to each vent location. This ratio provides the only evidence detected here for eastward weakening of the slab signature across the arc, and it needs to be noted that the Ba/Nb pattern displayed in figure 33 entails only eastward diminution of higher ratios, with little change in the baseline ratios of 40-60. Several other ratios that could potentially reflect an eastward decline in the slab contribution were similarly plotted against trench-vent distance. All of the following ratios have wide ranges among the mafic rocks, but none show systematically significant change across the arc: Ba/Th (40-150), Ba/Zr (2-3.5), Zr/Y (4-12), La/Yb (6-17), K_2O/TiO_2 (0.7-1.5), and Rb/Cs (10-70). Concentrations of Y in the mafic rocks scatters widely from 13 to 30 ppm, with no cross-arc pattern, and baseline Y values remain 15±2 ppm across the volcanic field. Likewise, Nb concentration in mafic rocks

ranges from 2 to 9 ppm and maintains a cross-arc baseline of 3±1 ppm. The Nb/Y range of mafic products narrows a bit across arc (Fig. 33) but, like so many other ratios, reveals no systematic trend. Notably, there is no trend toward the high Nb/Y values (Fig. 33) of the intraplate basalt field 70-220 km east of Laguna del Maule (Fig. 1).

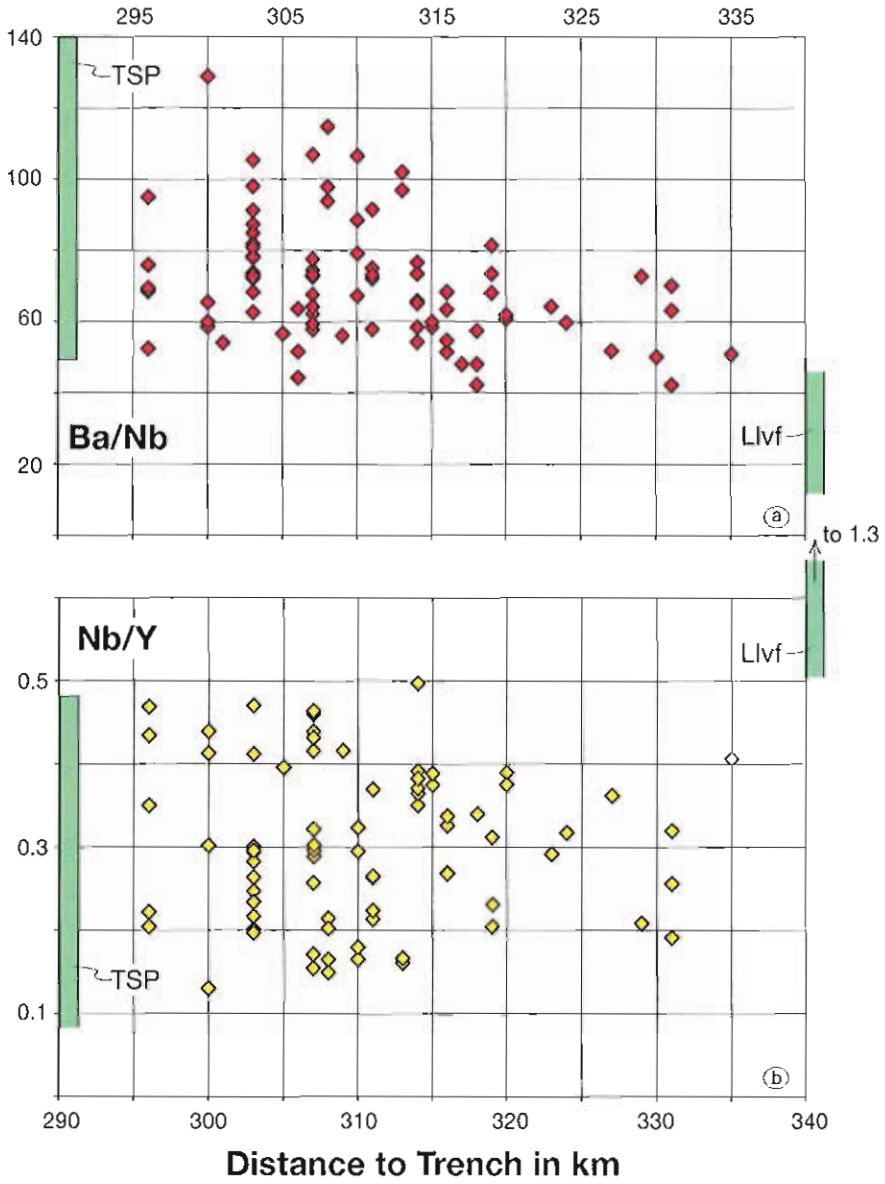

FIG. 33. Ba/Nb and Nb/Y for mafic samples (49-55% SiO_2) plotted against across-arc distance from inboard margin of trench floor to vent location. **TSP** fields show ranges of ratios reported by Dungan *et al.* (2001) for Volcán Tatara-San Pedro on volcanic front. **Llvf** fields show ranges of ratios reported by Muñoz *et al.* (1989) and Bermúdez and Delpino (1989) for Quaternary intraplate alkali-basaltic Llancanelo volcanic field (70-220 km east of Laguna del Maule). [WDXRF data only, from Appendix 3; EDXRF data are less precise for Nb, not plotted here].

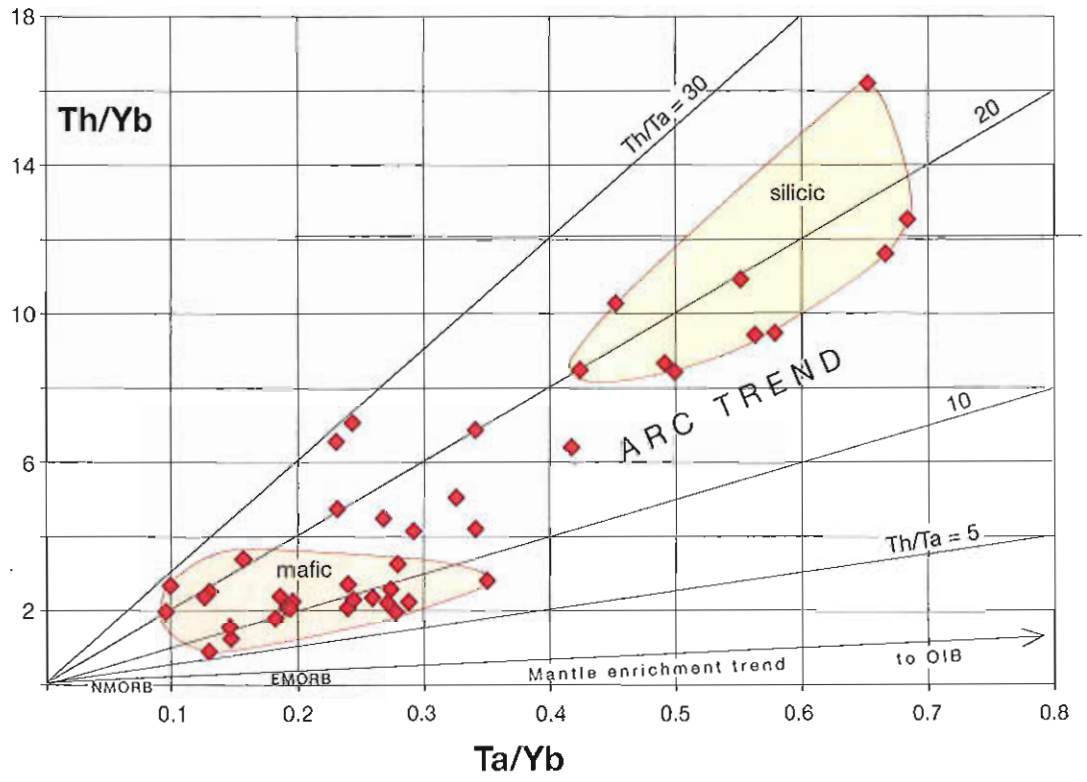

FIG. 34. Th/Yb *versus* Ta/Yb for 42 samples, illustrating that LdM magmas share variably in the Th/Ta-enrichment trend globally characteristic of arc magmas (Pearce, 1982). None are close to the mantle-enrichment trend from MORB toward average intraplate OIB, which would plot at (1.25, 1.85), well outside the diagram (Sun and McDonough, 1989). Intraplate alkali basalts of the Llancanelo volcanic field (70-220 km east of Laguna del Maule) would plot close to the mantle-enrichment trend. Data in Appendix 4.

If mantle melt fraction producing primitive parent magmas diminishes eastward across the arc (potentially reflecting weaker slab fluid flux), then such ratios as La/Yb, Nb/Zr, Nb/Y, and Na/Ca and concentrations of such (poorly fluid-mobile) elements as Nb, Ta, Zr, Hf, and Y might be expected to increase eastward in the mafic magmas. Despite wide ranges in all such quantities, none exhibit systematic increases inboard, so it can be concluded that either **(1)** degree of mantle melting ranges unsystematically across the arc, or **(2)** any mantle-derived cross-arc differences have been overprinted by crustal processes.

In summary, compositional data show diversity inconsistent with closed-system fractionation within almost every eruptive unit, even in most rhyolites. The diversity is greatest, with few exceptions, among the mafic products of many individual volcanoes. The slab-derived contribution remains so dominant across the 50-km-wide Quaternary arc that any cross-arc trends in degree of mantle melting or in mantle source fertility are difficult to discern, even in the least crustally modified rocks. Arc magmatism virtually continuous here since ~25 Ma, spanning intervals of arc extension and contraction, has so permeated the sub-arc mantle and crust with an enduring repository of slab-derived contributions that a strong arc signature is imposed on Quaternary magmas, whether or not the proximate (modern) slab contribution actually diminishes inboard.

Sr ISOTOPES

Table 5 gives Sr-isotope ratios for 30 samples from 25 eruptive units that range in SiO_2 content from 49 to 77%. Eleven mafic samples (49-55% SiO_2) range from 0.70396 to 0.70435, and seven intermediate samples (56-65% SiO_2) from 0.70388 to 0.70422. Eleven silicic samples (69-76% SiO_2) have (age-corrected) initial ratios that range from 0.70406 to 0.70426, plus high-silica rhyolite unit **rcn** (77.6% SiO_2 with Rb/Sr=12.6) that has an outlying initial ratio of 0.70460. The data set shows no correlation of $^{87}Sr/^{86}Sr$ with either SiO_2 or Rb/Sr (Table 5), implying for the volcanic field a general absence of repeatedly systematic paths of magma generation and assimilation. Neither is there any systematic change in $^{87}Sr/^{86}Sr$ from east to west across the volcanic field (Fig. 35). The relatively narrow range of Sr-isotope ratios for Quaternary magmas of all compositions reflects, of course, their low to modest degrees of isotopic contrast with the Mesozoic and Tertiary crustal rocks through which they ascended (Hildreth and Moorbath, 1988). Limited isotopic contrast between basement and volcanics is likewise responsible for the restricted range at Volcán Tatara-San Pedro on the nearby volcanic-front (0.7038-0.7040 for the least crustally modified and up to 0.70425 for nearly all the rest), as reported by Davidson *et al.* (1987, 1988), Nelson *et al.* (1999), and Dungan *et al.* (2001).

Pairs of Sr-isotope determinations for different samples from five eruptive units appear in Table 5. For two units, values for the pairs are nearly identical, but for three units the ratio pairs are quite different (Fig. 35a): Unit **bec** gives 0.70406 and 0.70419; unit **mvm** gives 0.70396 and 0.70435; and unit **dcc** gives 0.70388 and 0.70400. Such data suggest significant amounts of crustal assimilation across the whole compositional range, as too does the range of initial ratios among rhyolites alone (0.70412 to 0.70460; Table 5). It is now well-established that most of the Sr-isotopic variability of arc magmas develops by intracrustal mixing and assimilation and, moreover, that much (not all) of it takes place in the deep crust while magmas are still in the mafic stages of their evolutionary arrays (Hildreth and Moorbath, 1988; Dungan *et al.*, 2001; see also Fig. 29 of Hildreth, 2007, for the compositionally unsystematic $^{87}Sr/^{86}Sr$ diversity of the Cascade arc).

GEOCHEMISTRY OF THE RHYOLITES

The Quaternary rhyolites range in SiO_2 from 72% to 77.6% and plot collinearly with the comparably abundant rhyodacites (68-72% SiO_2). Of 58 unaltered rhyolite samples analyzed, 15 are high-silica rhyolites with ≥75% SiO_2 (units **rap**, **rcn**, **rle**, and **rsl**). Pliocene units **Trea** and **Trcf** are also high-silica rhyolites, as is ignimbrite unit **igcg** (but most ignimbrites here are not).

Rhyolite lavas of the Laguna del Maule volcanic field are ordinary continental-margin arc rhyolites with low TiO_2 (0.33-0.15%), low FeO* (1.8-0.5%), and moderate Al_2O_3 contents (15.2-12.5%), each of which varies inversely with SiO_2 (Fig. 29). All are high-K (K_2O=4-5%) and subalkaline to weakly alkaline (Figs. 28A, 29). From 72% to 77% SiO_2, the Na_2O/K_2O ratio decreases from ~1.25 to ~0.6. The rhyolites have low concentrations but wide ranges of P_2O_5 (0.12-0.03%), MgO (0.56-0.08%), and CaO (1.5-0.5%).

Like most arc rhyolites, those of Laguna del Maule are not as highly evolved in trace-element signature as intracontinental rhyolites of various distinctive types: Cl-rich peralkaline, F-rich topaz-bearing, high-temperature Fe-rich 'anorogenic', or allanite-monazite-bearing LREE-depleted subalkaline rhyolites. Among true rhyolites, those of Laguna del Maule have moderate abundances (*i.e.*, compared globally, neither high nor low) of Rb (150-220 ppm), Sr (44-170 ppm), Ba (550-820 ppm), Y (11-34 ppm), Zr (87-220 ppm), Nb (7-19 ppm), Zn (18-50 ppm), and Th (16-24 ppm). The average concentrations for continental-margin arc rhyolites worldwide compiled by Macdonald *et al.* (1992) fall within the stated ranges for all elements reported here, except Th (12:9 ppm). Such ratios as K/Rb (260-185), Rb/Sr (1-3), Ba/La (17-37), Ba/Nb (40-90), and La/Yb (13-17) are in the normal ranges for rhyolites of continental-margin arc suites.

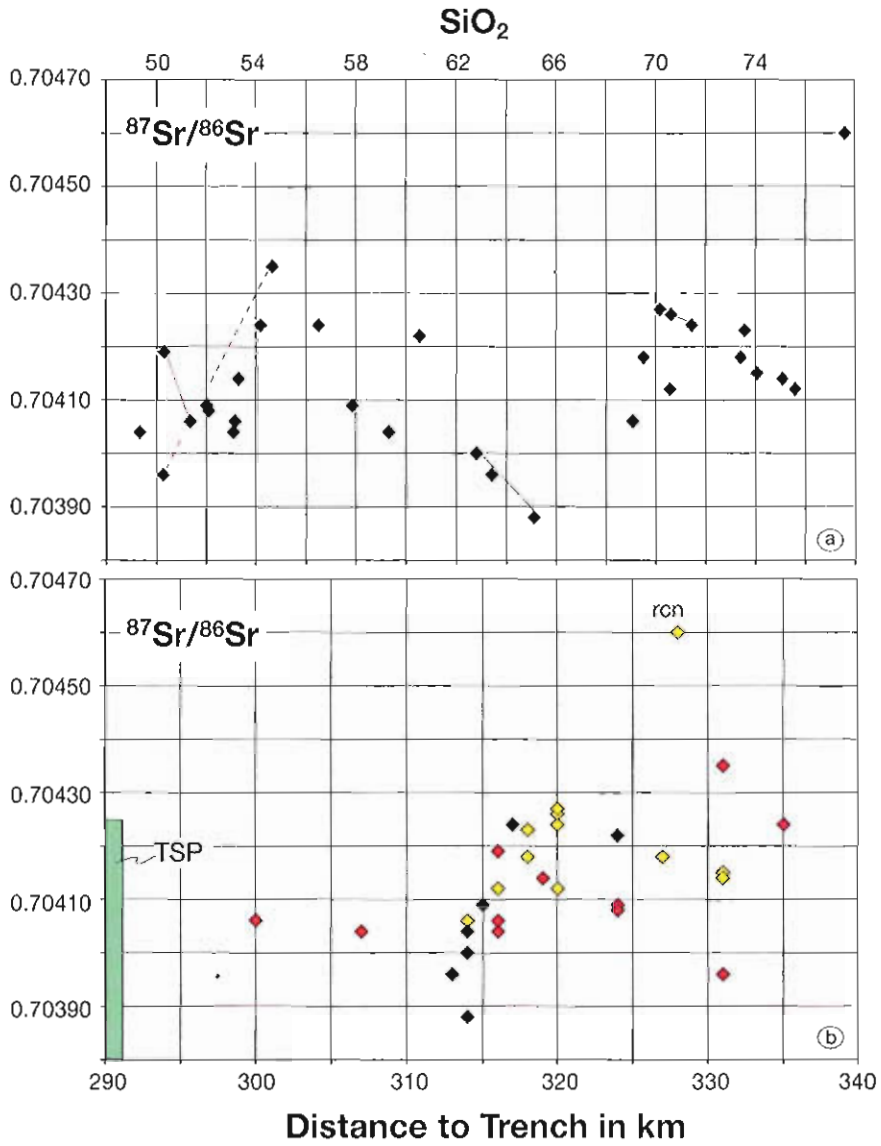

FIG. 35. Initial $^{87}Sr/^{86}Sr$ ratios for 30 samples; data in Table 5. **(a)** $^{87}Sr/^{86}Sr$ *versus* weight % SiO_2. Tielines connect pairs of separate samples from same eruptive unit. **(b)** $^{87}Sr/^{86}Sr$ plotted against distance in kilometers from inboard margin of trench floor to vent for each eruptive unit. Red symbols for 11 mafic units; black for 7 intermediate units; yellow for 12 silicic units. **TSP** represents field for Volcán Tatara-San Pedro on volcanic front (Dungan *et al.*, 2001).

The concentration of Zr in the rhyolites is evidently controlled by zircon fractionation; its abundance is scattered at 200-270 ppm in rhyodacites, but from 72% to 77% SiO_2, it declines from 220 to 87 ppm. On the other hand, Ba concentration and Ba/K drop only weakly in a few of the rhyolites, most values scattering widely in the same ranges as the rhyodacites, consistent with the absence of sanidine phenocrysts. Decline in both Ba and Zr at high SiO_2 might alternatively reflect retention of alkali feldspar and zircon in residues of high-silica partial melts of basement granitoids

that contributed to the rhyolites, but cryptic fractionation of zircon and sanidine or Ba-rich biotite in the pre-eruptive magma reservoir is also plausible.

Rhyolite compositions here are remarkably similar to those of the numerous Pleistocene rhyolites of the Puelche volcanic field (Hildreth *et al.*, 1999), 20-35 km north of Laguna del Maule (Fig. 1). On the other hand, rhyodacites and rare rhyolites reported farther south along the SVZ have less than half the Rb and Th but more than twice the Y and Yb of equivalents reported here, suggesting that the Laguna del Maule and Puelche silicic suites contain much larger crustal contributions.

A unique sample (LdM-52) from 450-ka unit **rcn** on the east wall of the lake basin is the most evolved sample analyzed, in many respects more extreme than our five other samples of the same complex. At 77.6% SiO_2, it has lower Al_2O_3 (12.2%), TiO_2 (0.13%), CaO (0.48%), Sr (25 ppm), Ba (66 ppm), and K/Rb (127) than any other sample in our data set; and it has higher Rb (315 ppm), Nb (21 ppm), Th (39 ppm), Rb/Sr (12.6), and initial $^{87}Sr/^{86}Sr$ (0.70460) than any other. Although tempting to regard it a minimally contaminated partial melt of granitic crust, its association with a voluminous dome complex of only slightly less evolved rhyolite (75.3-76.9% SiO_2) suggests that it instead represents simply the most fractionated part of its silicic magma batch.

GEOCHRONOLOGY

Radioisotopic ages are given for 73 samples in Tables 1 and 2. Table 1 lists analytical data and $^{40}Ar/^{39}Ar$ ages for 47 samples analyzed by Singer at the Laboratoire de Géochronologie, Université de Genève, following methods described by Singer *et al.* (2000), Singer *et al.* (2004a), and Singer *et al.* (2004b). Table 2 lists analytical data and K-Ar ages for 26 samples, of which six were run in 1993 by Singer in the USGS Menlo Park laboratory then supervised by M.A. Lanphere, and 20 were run between 1970 and 1988 by R.E. Drake in the University of California Berkeley laboratory then supervised by G.H. Curtis. Analytical and sampling methods for the K-Ar determinations are described in Hildreth and Lanphere (1994), Lanphere (2000), and Dalrymple and Lanphere (1969).

Figure 36 summarizes the radioisotopic-age data, each of which was cited contextually for individual eruptive units in the text. The diagram illustrates several generalities: **(1)** Predominance of polygenetic edifices (stratocones and shields) and extensive ignimbrites during the early Pleistocene; **(2)** predominance of monogenetic pyroclastic cones and lava flows during the last 100 kyr; **(3)** scarcity of dacites relative to more mafic and more silicic eruptive units; **(4)** scarcity of true basalts (≤52% SiO_2); and **(5)** few eruptions between 700 ka and 450 ka.

OLDER ROCKS OF BASIN WALLS

Because so much of the lake basin is surrounded by late Pleistocene and postglacial eruptive units (and related surficial deposits), the older bedrock walls are too easily ignored. The northern part of the basin was probably the source of the 1.5-Ma pyroxene-dacite ignimbrite (unit **igsp**), subsequently modified by collapse of the Bobadilla caldera on eruption of the 950 ka biotite-rhyodacite ignimbrite (unit **igcb**), which now forms most of the basin's north wall. The southern slopes of the basin and its east and west walls, however, consist of subhorizontal or modestly dipping Tertiary volcanic strata, mostly andesite-dacite lavas, breccias, and tuffs that are entirely precaldera, extracaldera, and unaffected by the early Pleistocene subsidence nearby. Integration of the basin and evolution of its morphology has resulted from excavation and enlargement by glacial and fluvial erosion during the last 950 kyr. Tertiary rocks of the basin walls were not studied in detail, but a summary of our many passing observations follows here.

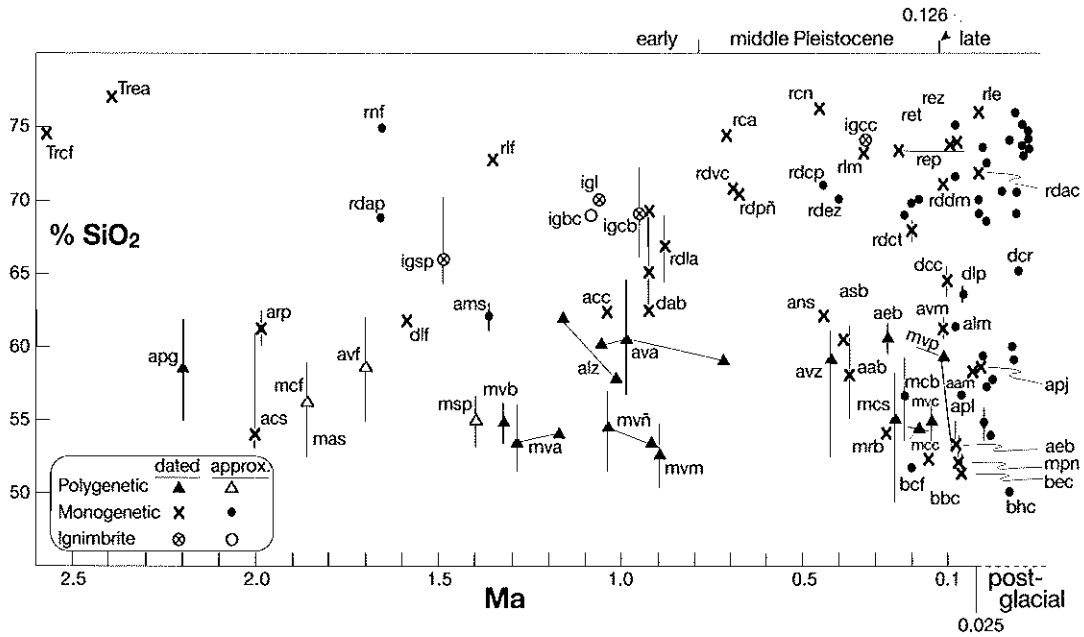

FIG. 36. Eruptive ages *versus* wt% SiO_2 for products of Laguna del Maule volcanic field. Polygenetic, monogenetic, and ignimbrite units are distinguished by symbols in inset. Ages are approximated for undated units with fairly well constrained stratigraphic relationships; other undated units are omitted. Ages and uncertainties for all dated units are listed in Tables 1 and 2. All unit labels are given in Appendix 1, and each unit is discussed in the text. Vertical lines indicate known compositional ranges of polygenetic and other inhomogeneous units. Nonvertical lines indicate age ranges for long-lived edifices with more than one radiometric date. Postglacial interval (here younger than ~25 ka) is shaded and its timescale expanded for clarity.

The **East Wall**, 600 m high as exposed (Fig. 23) between Laguna Cari Launa and the Divisoria coulee (unit **rcd**), consists of a gently east-dipping (3°-8°E or SE) stack of more than 20 Miocene and Pliocene andesite-dacite lava flows and breccia sheets. The lowest unit exposed on the wall is a coarse glassy andesite breccia (57% SiO_2) at least 50 m thick that yielded a $^{40}Ar/^{39}Ar$ plateau age of 6.4±1.3 Ma. This is overlain by 15-20 intermediate lava flows and breccia sheets, each one 5-20 m thick, with which several fall layers (1 to 10 m thick) of coarse scoria are intercalated. The stack is capped on the ridgecrest by a few thicker flows that range from olivine andesite (54.7% SiO_2) to flow-foliated pyroxene dacite; the topmost lava flow at Hito Maule (Peak 3,175; mafic andesite of unit **QTad**) gave a total fusion age of 3.6 Ma. Numerous east- and southeast-striking vertical dikes cut the wall stack, some coarsely porphyritic and some as thick as 7 m. Much of the vent complex inferred for this dike-ridden stack has been eroded to form the 1-km-wide valley now occupied by the postglacial Cari Launa coulee (unit **rcl**), but just west of the coulee is a diorite pluton that was probably a late-crystallizing component of the andesite-dacite edifice. The porphyritic diorite (unit **Tdcl**; 52.4% SiO_2) is ~1 km in diameter, forms a 300-m-high nose near the lakeshore (Fig. 23), intrudes wall rocks of green-altered intermediate lavas and breccias, and yields a $^{40}Ar/^{39}Ar$ total-fusion age of 3.6 Ma. Quaternary excavation of the LdM lake basin has thus removed all but the east flank and deep interior of a substantial late Tertiary stratovolcano.

The **Southeast Wall** (Fig. 22) is exposed between the Divisoria coulee and the postglacial Barrancas complex, cropping out in two segments separated by an erosional recess, which is draped by mafic lava flows of unit **mvc** (143±7 ka). Both segments rise ~700 m above the lake and appear

to be elements of a single andesite-dacite eruptive complex. The southerly wall segment, heavily mantled by Barrancas pumice-fall deposits, consists of a stack of at least 6 or 8 intermediate lava flows (along with intercalated fragmental layers) dipping 10°-20°SE toward Laguna Negra (Fig. 24); flows examined are all plagioclase-rich pyroxene andesites, thick or thin but generally thickest on the ridgecrest. The stack making up the northerly segment consists of about 15 similar layers of intermediate lava and breccia, which are subhorizontal on the ridgecrest but dip 10°-15°W toward Laguna del Maule near the south end of the exposure. It appears that the vent complex for products of both segments is partly exposed on the north wall of Arroyo de la Calle and along its southwest-draining tributaries (UTM grid 700/035), where stratified breccia, white tuff, and several dikes crop out on both sides of the swale-filling drapery of mafic lavas of unit **mvc**. None of the wall-forming strata have been dated here, but physiographic similarity to the east-wall stack (~1 km away, separated only by the gap filled by the Divisoria coulee) suggests that they too may be of Pliocene and late Miocene age. Because the southeast-dipping stack of lava flows merges into a gently dipping lava plateau that extends right across the linear valley now occupied by Laguna Negra (Fig. 24), it is clear that the north-south trough does not reflect a caldera fault.

The **South Wall** includes the sharp 10-km-long divide between Laguna del Maule and Laguna Fea, its 500 m high wall above Laguna Fea (Fig. 25), and the 6-km-long slope from the divide to the shoreline of Laguna del Maule (Figs. 7, 22). Except for remnants of early Pleistocene lavas along its crest, the divide and both its slopes are eroded from a pile of Tertiary andesitic lavas and breccias apparently related to a deeply ravaged vent complex that may have been centered between present day Arroyo de Palacios and Arroyo de Sepúlveda. Total relief on the stratified package exceeds 800 m, yet it everywhere appears to belong to the same lithologic assemblage, whether north or south of the divide or east or west of Colada Las Nieblas. This assemblage includes andesitic lava flows but is dominated by stratified breccias, including lava-flow breccias, fragmental flow deposits, and lithic-rich or scoria-rich fall deposits. In the inferred near-vent area south of Arroyo de Palacios, some such fallout layers are 3-4 m thick, and sections of tuff-breccia as thick as 25 m contain meter-sized angular blocks of glassy andesite in a white matrix dominated by coarse ash. Here and southward toward the high divide, the strata dip 15°-25°S, but 1-2 km farther east (near Arroyo de Sepúlveda) they dip 10°NE. Clasts in the breccias are principally plagioclase-rich pyroxene andesite and phenocryst-poor olivine andesite. Much of the assemblage remains partly glassy and, although zeolites are present locally, no propylitic alteration was observed; deformation is not obvious and, if present, is modest. The assemblage is undated but inferred to be Pliocene or late Miocene. It is overlain unconformably along the crest by gently northeast- or east-dipping (5°-15°) andesite-dacite lava flows (unit **dlf**) that erupted at Volcán Laguna Fea, south of the lake. One of these thick flows on Peak 3,135 just northeast of the divide yields a $^{40}Ar/^{39}Ar$ plateau age of 1,582±9 ka; another that caps Peak 3,056 on the triple divide above the northwest end of Laguna Fea gives a total-fusion age of ~1.5 Ma. Also on the divide, a large rhyolite dome (unit **rlf**) that intrudes the Tertiary andesitic assemblage yields a $^{40}Ar/^{39}Ar$ plateau age of 1,353±17 ka. Incision of the glacial valley now occupied by Laguna Fea evidently began well after 1.5 Ma, and because northeast-dipping lavas of that age extend right across the valley from their source edifice south of the lake, it is also clear that the linear trough does not reflect a caldera fault (Fig. 25).

The **Southwest Wall** (Fig. 21) curves around from saddle 2,558 on the Troncoso-Maule divide through Peak 2,942 on the Rodríguez-Maule divide to a triple divide above the upper Cajón de Saso. Three main suites of rocks crop out around this rugged divide: **(1)** Miocene ignimbrite; **(2)** late Tertiary stratified andesite-dacite lavas, breccias, and tuffs (continuous with those on the south wall), overlain by **(3)** ridgecrest remnants of thick, gently dipping or subhorizontal, intermediate lava flows of early Quaternary age. The buff to ochre-weathering ignimbrite forms both walls of the upper Cajón de Troncoso for at least 6 km downstream from its headwaters (saddle 2,558), including its high divides with Laguna del Maule and with Laguna Fea, where it is at least 800 m thick.

If the lithic-rich silicic ignimbrite represents a single eruption (as we think), such a great thickness would be expected to represent a caldera fill. On the west wall of the Troncoso, the ignimbrite is cut by numerous dikes and by the plug and ravaged flanks of a small intermediate center (UTM grid 565/010). Four km west of the upper Troncoso, what is probably the same ignimbrite was K-Ar dated at 6.1±0.5 Ma by Muñoz and Niemeyer (1984). At the head of the Troncoso, the ignimbrite is overlain by the widespread stratified package of Tertiary intermediate lavas, breccias, and tuffs and, at the triple divide above Laguna Fea, both are capped by a 100-m-thick dacite lava (unit **dlf**) dated at ~1.5 Ma on Peak 3,056. Farther west, ignimbrite exposure is lost and the Rodríguez-Maule divide consists of the Tertiary intermediate suite, which dips ~20ºE and is capped along the crest (on Peaks 2,918, 2,856, and 2,942; Figs. 8, 21) by craggy remnants of thick pyroxene-andesite lavas (unit **arp**) that dip gently southeast and yield a $^{40}Ar/^{39}Ar$ plateau age of 2,010±23 ka. Along the divide ~1 km northwest of these crags, Peak 2,910 (Fig. 8) is a deeply eroded vent complex, with variably dipping altered lavas and tuffs cut by numerous dikes, that may be the source of the stacks of 2 Ma lavas. Beyond the divide, the stratified Tertiary intermediate assemblage continues west along both walls of upper Cajón Rodríguez, where it is openly folded, as thick as 600 m, and includes a large proportion of pale-gray fragmental deposits: minor ignimbrites, block and ash flows, and explosive vent fills. The varied dips of the Tertiary strata (0º-30º) contrast with the subhorizontal early Quaternary, thicker and fresher, ridge-capping lavas that overlie them.

The **West Wall** runs from the southwest corner of the basin through Peak 2,849, extending 8 km northward as a narrow ridgecrest arête (Fig. 15) that forms the Saso-Maule divide as far as Laguna Sin Puerto. Cirques on both sides cut down into late Miocene rocks beneath a strip of early Quaternary lavas and welded ignimbrite preserved along the crest. The older suite consists of brown-weathering stratified intermediate lavas, breccias, and tuffs much like those in Cajón Rodríguez and on the slopes south of Laguna del Maule. On the basin wall where as thick as 500 m, the strata dip 10º-20ºSE, but they are also exposed discontinuously as far east as the northwest shoreline of Laguna del Maule, where they dip 20ºW. Along upper Cajón de Saso they are openly folded (generally dipping 15º-20º either northeast or southwest) and include a greater proportion of stratified breccias than in other sectors. On the east wall of Cajón de Saso, 1.5 to 3.5 km downstream from Laguna Sin Puerto, this suite overlies a massive white nonwelded biotite-rhyolite ignimbrite (presumed to be Miocene), which is crystal-poor, at least 200 m thick, and lithic-poor except in its uppermost 30 m, which is yellow-brown and weakly sintered. The younger suite capping the high divide includes the 1.5-Ma welded pyroxene-dacite ignimbrite (unit **igsp**), here 50-100 m thick, and several andesitic lava flows beneath and above it. Those beneath (lumped as unit **acs**) are a varied assemblage of lavas, ranging from 20 to 70 m thick, from phenocryst-poor and olivine-bearing to plagioclase-rich and hornblende- or pyroxene-bearing, and from 53% to 62.5% SiO_2 (n=6); two samples, one from each side of the divide, failed to yield interpretable $^{40}Ar/^{39}Ar$ plateau ages but gave total-fusion ages of 2.0 and 2.1 Ma. Lava flows atop the ignimbrite (unit **ams**) are chemically more uniform pyroxene andesites (61% to 63% SiO_2) but include flows both rich and poor in plagioclase. Composite slabs of these lavas and the welded ignimbrite, thin but as long as 1.2 km, have detached from the ridge-crest arête in postglacial time and slumped downslope as far as 1 km (up to 200 m vertically) into the upper bowl of Arroyo Los Mellicos (Fig. 15).

The **North Wall** consists of three segments separated by the (largely concealed) margins of the 950 ka Bobadilla caldera. West of the outlet gorge, the north wall is a narrow east-west arête that separates the lake basin from Estero Aguirre. It is composed principally of the 1.5-Ma pyroxene-dacite ignimbrite (unit **igsp**), 300 m thick and in large part densely welded. Discontinuously exposed beneath the ignimbrite on the south side of the divide are a tiny window of aphyric rhyolite, a 50 m thick ledge of platy hornblende dacite, and (along an arcuate lake-filled depression; Fig. 22; UTM grid 575/145) a sheet of plagioclase-rich pyroxene-andesite breccia and an underlying crystal-poor flow of mafic lava, each 50 m thick. These units extend no higher than 2,500 m elevation, lower than rimrocks elsewhere around the basin, suggesting that what-

ever kind of paleodrainage system may have existed prior to eruption of the 1.5 Ma ignimbrite, its outlet to the Río Maule was, as today, generally northwestward. The 1.5 Ma ignimbrite arête also covers a significant boundary between **(1)** the weakly deformed stratified assemblages of andesitic lavas, breccias, and tuffs (Pliocene and/or late Miocene) that ring so much of the basin to the south and **(2)** a terrain to the north dominated by synclinally deformed Miocene ignimbrite (unit **Tigh**; Fig. 18), which extends more than 20 km northward, has 1,200 m vertical exposure, and yields a K-Ar age of 12.9±0.7 Ma (Table 2).

East of the outlet gorge, the 1.5-Ma ignimbrite is missing, having foundered with the 950-ka Bobadilla caldera, which during subsidence filled with the biotite-rhyodacite ignimbrite (unit **igcb**) that now dominates the east-west ridges that form the main north wall of the lake basin. Although its base is nowhere exposed, the biotite ignimbrite today exhibits as much as 550 m of relief on the divide between Laguna del Maule and Cajón Chico de Bobadilla. On that divide, it is overlain by remnant stacks of andesite-dacite lavas (unit **ava**; 0.9 to 0.7 Ma) that dip generally northward and appear to have erupted from intracaldera vents now glacially eroded and reduced to dikes within the lake basin. Several arcuate south-side-down faults that cut the biotite ignimbrite on and near the promontories at the north shore of the lake are likely to reflect gravitational instability of the weak tuffs in response to glacial deepening of the lake basin. On the rim just north of there (UTM grid 675/157), a northeast-striking fault with ~50 m vertical displacement, east-side-down, that cuts the 712 ka rhyolite (unit **rca**) and subjacent andesitic strata (unit **ava**) is enigmatic and unique in the area.

Little is known of the nature of the north-central wall of the basin prior to the 950-ka caldera collapse, the ring-faulted western margin of which is now covered by the Espejos coulee (unit **rle**) and the lake. Along the outlet gorge, Miocene welded ignimbrite crops out only close to river level, where it is overlain by late Pleistocene and younger units. About 6 km north of the lake where the structural caldera margin is exposed (Fig. 6), stacks of altered Tertiary andesitic lavas and tuffs dip 10°-20° north or northwest, but all these older rocks have foundered or been buried by Pleistocene volcanics on the north-wall divide between the lake basin and the Cajones de Bobadilla.

The eastern segment of the north wall lies east of the buried margin of the 950 ka caldera and consists of varied andesite-dacite lavas, severely eroded and assigned to unit **alz**, large parts of which are hydrothermally altered. Two andesite samples were dated, yielding a K-Ar age of 1.16±0.04 Ma (Drake, 1976; Table 2) and a $^{40}Ar/^{39}Ar$ plateau age of 1,013±28 ka (Table 1). This poorly known pile of lavas crops out on both sides of the northeast arm of Laguna del Maule, stands as high as 750 m above the modern lake, and may have formed the highest part of the basin's north rim prior to caldera collapse.

In summary, because Tertiary strata extend to the northwestern, southern, and east-central shorelines of Laguna del Maule, it is clear that the basin as a whole is not a caldera. Nor were the linear glacial troughs of Laguna Fea and Laguna Negra excavated along caldera faults, because gently dipping stacks of (early Quaternary or latest Tertiary) andesitic lavas are continuous across both of them. The southern third of the 950-ka Bobadilla caldera fill underlies only the northern half of Laguna del Maule; the southern half of the basin was excavated by glacial and fluvial erosion of the weakly deformed or undeformed Tertiary andesitic strata that surround it. Because pre 1.5 Ma rocks maintained their lowest elevation around the northwest rim of the basin, it seems likely that the precaldera outlet toward the Río Maule drainage system lay in that direction, then as now. Nonetheless, because eroded north-rim ridges of both the 950-ka ignimbrite and the 1.5-Ma ignimbrite now stand as high as 450-500 m above the level of the lake (which is as deep as 50 m), it seems clear that most of the erosive deepening of the basin took place subsequent to formation of the 950 ka caldera. Atop the north-wall biotite-rhyodacite ignimbrite, postcaldera lavas of unit **ava** (0.9-0.7 Ma) are preserved as high as 730 m above the modern lake floor, implying a secular average rate of basin deepening close to 1 m/kyr. In contrast to the many long narrow glacial valleys in the surrounding region (those of Laguna Fea and Laguna Negra, those of the Troncoso,

Rodríguez, Saso, Botacura, Bahamondes, and La Plata, and those of the Cajones Bobadillas and Río Campanario), the broad and equant basin of Laguna del Maule (16 to 19 km in diameter) developed a radial drainage pattern that may have been nucleated or reorganized by the caldera subsidence at its north end.

Not a single outflow-sheet remnant of either Pleistocene ignimbrite survives along the east, south, and southwest walls of the basin. The nearly flat-lying remnants of ridge-capping Quaternary lavas (generally thick resistant flows) that overlie the Tertiary strata around the basin rim are largely in the age range 1.5 to 2 Ma (though 3.6 Ma on the eastern divide). More detailed work on the stratified Tertiary packages that surround the basin would help separate and describe Miocene eruptive centers, and it might help outline paleodrainage evolution better than our reconnaissance has done, but it is nonetheless now well established that the broad Laguna del Maule basin is fundamentally an erosional feature of Quaternary age.

GRANITOID ERRATICS

In several places around Laguna del Maule, we found rounded boulders and cobbles of hornblende-biotite granodiorite, although no such rock is known to outcrop within the basin. Rounded granitoids as big as 15 cm are sparsely strewn around Laguna Cari Launa, and a 25-cm boulder was found atop the Cerro Negro scoria cone; in each case entrainment of till from beneath the postglacial explosive vent seems a probable explanation. Along the lakeshore 1-2 km east of the Espejos coulee and on the promontory below its southwest terminus, till and beach gravels reworked from till contain abundant granitoids, including some with pink feldspars. Several ridges north of the lake and east of the Espejos coulee are strewn with granodiorite boulders, mostly fine to medium grained and fewer coarse grained, that range in size from 10 to 100 cm. They accompany stones of a variety of volcanic lithologies, and all are thought to be lag veneers from glacial deposits now being eroded from slopes as high as 400 m above the lake. One such boulder loose on the north slope above the lake (UTM grid 649/135) failed to yield an acceptable $^{40}Ar/^{39}Ar$ plateau age but gave a total fusion age of ~1.1 Ma. Because no source is recognized within the basin, three explanations seem feasible: **(1)** A granitoid outcrop was overlooked or was buried by postglacial lavas; **(2)** glacial ice entered the basin from beyond its surrounding high divides; or, our favored interpretation, **(3)** a granodiorite pluton is concealed somewhere beneath the lake, contributed material to downlake till during glacial advances, and may have been magmatically related to one of the early Pleistocene ignimbrites (units **igsp** and **igcb**) we infer to have erupted from the northern part of the present lake basin. Explosive ejection of granitoid blocks from the roof or margins of a composite multi-stage magma chamber during a great caldera-forming eruption, as documented for Mount Mazama, Oregon (Bacon *et al.*, 2000; Bacon and Lowenstern, 2005), is a mechanism worthy of investigation.

EROSION RATES

Radiometric ages determined for volcanic units on the floors, walls, and rims of the several drainages place some loose constraints on rates of erosive deepening of canyons in the map area.

Estero Rodríguez, 18 km long, is floored by glacial and slump deposits, thick and little incised, between elevations of 2,700 m and 2,150 m along its uppermost 5 km reach and in the cirques of its headwaters. For 2 km downstream from 2,150 m, the stream runs shallowly on a late Pleistocene intracanyon andesite lava flow (unit **acr**), but below 2,000 m, a steeper 1.5-km-long reach has eroded headward into the lava flow, incising a 50-m-deep gorge through the flow and into Tertiary bedrock. Downstream from the gorge mouth at ~1,900 m, the stream runs shallowly on a

broad alluvial plain, which is contiguous with the uneroded toe of the postglacial Hoyo Colorado scoria cone (unit **bhc**).

The **Río Saso**, 17 km long, is floored by thick alluvium (which locally mantles till) in its uppermost 4-km reach, between elevations of 2,500 m and 2,100 m. For the rest of its downstream course, the valley is floored by postglacial intracanyon lava flows (units **dcr** and **ars**). The stream has cut a narrow slot 5-20 m deep around the snout of the dacite from 2,100 m to 2,000 m, and through the downstream andesite a 9-km-long trench, which is typically ~6 m deep but as deep as 20 m where it cuts across the north levee of the flow.

Arroyo de Botacura, 20 km long, runs shallowly across thick glacial and alluvial fill in its uppermost 6 km reach, from 2,450 m downstream to 2,050 m, where the valley floor is abruptly swamped by a hummocky postglacial debris-avalanche deposit rich in blocks of rhyolite, rhyodacite, and andesite derived from the walls of Estero Terneros (Fig. 12). The deposit is 30 to 50 m thick and fills the canyon floor for 3.5 km downstream to an elevation of 1,850 m. Farther downstream, the stream runs shallowly through a composite valley fill of slumps, talus, alluvium, and minor till, as far as the confluence with Estero Valle Chico near ~1,580 m elevation, beyond which it cuts deeply into a large hummocky postglacial debris-avalanche deposit from Volcán San Pedro (Singer *et al.*, 1997). Both avalanche deposits as well as the snout of the postglacial intracanyon andesite lava flow from the Río Saso (unit **ars**) induced thick alluvial aggradation along the valley of the Botacura. During the late Pleistocene, two rhyolite coulees had flowed southward to the Botacura, which has subsequently cut deeper adjacent to their termini (Figs. 12, 14). The base of rhyolite unit **rez** (83±3 ka) is now at an elevation of 1,950 m, 200 m above the valley-floor fill (or as much as 250 m above underlying bedrock), implying an incision rate of 2.3 to 3.1 meters per thousand years (m/kyr). Farther upstream, the base of rhyolite unit **ret** (97±15 ka) is now at 2,100 m, ~100 m above the valley floor (where fill is also ~50 m thick), implying incision of 0.9 to 1.8 m/kyr. In the low-relief vegas at the head of the Botacura, however, lava flows from Cerro San Pedro (unit **mcs**; ~243 ka) are flush with the banks of the non-incised meandering stream at 2,200 m elevation, probably the result of thick aggradation and glacial deposition in the headwaters during waning stages of the Last Glacial Maximum.

Estero Bahamondes, 11 km long, runs shallowly across thickly alluviated, low-relief vegas in its uppermost 4 km, then pitches over a 100-m-high fall cut into lavas of unit **mcs**, below which it follows a smooth gradient along the floor of a 350-m-deep bedrock canyon from elevation 2,050 m down to 1450 m, where it joins the Río de La Plata. Above the north end of the Bahamondes (Fig. 13), where the rhyolite lava flow of unit **rlm** (341±8 ka, 335±2 ka) crosses its canyon, the base of the rhyolite lies 275-300 m above the floor, implying a downcutting rate of 0.8 to 0.9 m/kyr. Where the 100 m stack of (more easily erodible) rubbly mafic shield lavas from Cerro San Pedro (unit **mcs**; 243±43 ka) crosses the Bahamondes (Fig. 13), its base lies 250 m above the bedrock floor, implying a faster average incision rate of ~1.4 m/kyr.

The **Río de La Plata**, 14 km long, drains from ~2,500 m elevation on the east side of Volcán Pellado and the north side of Volcán El Zorro to join the Río Maule at ~1,230 m. Its floor has a relatively smooth gradient (Fig. 13) despite its upper third being cut into Tertiary andesite lavas and tuffs and its lower two-thirds through Cretaceous granodiorite. The floor of its middle reach from elevation 1,750 m to 1,500 m is covered by a 3-km-long debris-avalanche deposit from the west wall with numerous hummocks as high as 20 m. Farther downstream, separated by a 1-km-long gap, another debris-avalanche deposit, this one from the east wall, overlies lateral moraines and extends 4 km from the Bahamondes junction to the Río Maule. In the upper bowl of the Río de La Plata, the base of the stack of lava flows from Volcán Pellado (unit **mvp**, which here may be as old as 188±21 ka) lies 300 to 350 m above the Tertiary andesite floor of the valley, implying an incision rate in the range 1.5 to 2 m/kyr. Farther downstream where the canyon walls are of granodiorite, a rhyolite lava flow of unit **rlm** (341±8 ka; 335±2 ka) crops out on both rims, 250 to 300 m above the floor, implying a lesser rate of 0.75 to 0.90 m/kyr.

The **Río Maule** begins at the 2,160-m outlet of Laguna del Maule, drops to 1,600 m elevation in its first 8 km, a gradient of 70 m/km for a reach that includes the outlet gorge and the Salto del Maule. The river next flows shallowly on a bouldery alluvial plain (Fig. 18) for 21 km to the confluence of the Río Puelche at 1,040 m, a gradient of 27 m/km. As one of Chile's major rivers, the Maule then extends 175 km farther westward (via several hydroelectric installations) to the Central Valley and across the Coast Range to Constitución at the sea, a gradient of 6 m/km.

Along Cordón de Constanza, the narrow Maule-Campanario divide, remnants of several Pleistocene volcanic units are preserved atop deeply incised Tertiary rocks (Fig. 37). The flat-lying base of the widespread pyroxene-dacite ignimbrite (unit **igsp**; 1.5 Ma) is now 470 m above the bedrock floor of the adjacent Río Campanario, which is smoothly graded to its confluence with the Río Maule, implying a long-term Quaternary average incision rate of 0.3 m/kyr. The next remnant west along the divide is a 1.04 Ma andesite lava flow (unit **acc**; Figs. 37, 38), the base of which lies 400 m above the Río Campanario, implying an average downcutting rate of 0.4 m/kyr. Incision rates are inferred to have been greatest during the latter part of the middle Pleistocene (which includes the MIS-6 glaciation), because the next two units along the crest (Fig. 37), units **ans** (429 ka; 350 m above the canyon floor) and **asb** (374 ka; 300 m above the Maule, 325-350 m above the Campanario) both yield average rates in the range 0.8 to 0.9 m/kyr. All these rates for Cordón de Constanza should be considered maxima because the remnants survive only on the ridgecrest, and it has not been demonstrated that the flows were emplaced strictly along valley floors or whether, alternatively, they were laterally confined by glaciers that floored adjacent paleovalleys (cf. Lescinsky and Sisson, 1998).

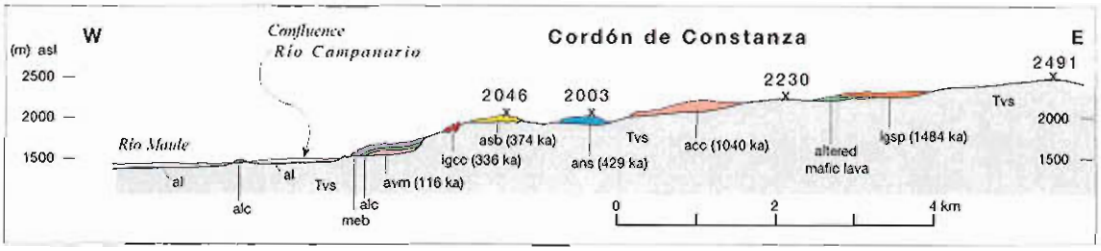

FIG. 37. Profile along Cordón de Constanza, the narrow divide between the Ríos Maule and Campanario. Ages of Quaternary volcanic units (Tables 1, 2) record 750 m of progressive canyon deepening over the course of 1.5 Myr. At nose just before the confluence (cf. Fig. 19), the middle of three lava flows (unit **alc**) is compositionally identical to a remnant 1.7 km downstream; the top flow (unit **meb**) has correlatives as far as 7 km upstream; and the bottom flow (unit **avm**) is dated at 116±27 ka and is compositionally identical to a large remnant at Vacas Muertas (Figs. 18, 20) on the opposite (south) wall of the Maule canyon. Elevations in meters. No vertical exaggeration.

The late Pleistocene and Holocene appear, in contrast, to have been largely a time of aggradation along the Río Maule, presumably involving deglaciation following MIS-6, accumulation and erosion of a 150 m thick valley-filling stack of lavas, and fluvial gravels related to late Pleistocene glaciers and to the outburst flood from Laguna del Maule. The base of the lowest lava flow on the Maule-Campanario nose (unit **avm**; 116±27 ka; Figs. 19, 37) lies virtually at the valley floor, which here consists of terraced alluvial gravels of unknown thickness. On the west bank 5 km downstream from that nose, the base of a set of mafic lavas from Cerro San Pedro (unit **mcs**; 243 ka) that crossed the Bahamondes and flowed into the Río Maule now lies ~75 m above its alluvial floor; this suggests a downcutting rate of 0.3 m/kyr or double that if the gravels are 75 m thick. Just 1-2 km upstream from the Campanario confluence, however, the plateau-forming stack of intracanyon mafic and intermediate lavas has been eroded headward by the Río Maule

to produce a 150-m-high scarp at and near the Salto del Maule (Figs. 18, 20). The scarp lavas have not been accurately dated but are likely to be ~100 ka or younger; if so, this implies a down-cutting rate by headward retreat of ~1.5 m/kyr.

It should be no surprise that incision rates vary greatly with glaciation and deglaciation, with secular maturity and size of the stream and its drainage basin, with disturbances caused by abrupt valley-filling debris avalanches and intracanyon lavas, and with lithologic differences in erodibility among the lavas, pyroclastic units, and plutonic rocks that wall the canyons.

HIGH STRANDLINE: OUTLET BLOCKAGE AND OUTBREAK FLOOD

A single wave-cut strandline rings the Laguna del Maule basin at 2,350±20 m elevation, approximately 200 m above the (fluctuating) level of the present-day lake (which was elevated only ~15 m by construction of the outlet dam). Notches, benches, and beach deposits mark the highstand paleoshoreline, which is cut on numerous postglacial eruptive units as well as on many older units. Beach deposits of sand and gravel are commonly marked by one or several parallel berms rich in rounded clasts of pumice and scoria. Deposits of lake mud rich in ash and diatoms, typically 1 to 5 m thick, are widely preserved between the high strandline and the modern lakeshore. During late summer intervals of exceptionally low (managed) drawdown of lake level, thicknesses as great as 30 m of such postglacial lake mud are exposed nearshore in sheltered inlets. Six lava flows, all silicic, overrun and thus postdate the high strandline-Colada Las Nieblas, the Northwest Coulee, one coulee from the Cari Launa edifice, and three from Cerro Barrancas.

The basin outlet was blocked at 23.3±0.4 ka by emplacement of the nonglaciated high-silica-rhyolite coulee, Loma de Los Espejos, which banked against the fragmental basaltic cone, El Candado (62±4 ka). The 2,350-m strandline was cut on both, and as much as 2.6 m of laminated diatomite was deposited between those units near the floor of the present outlet gorge, from near the base of the modern dam to a point as far as 1.2 km northward, indicating that the natural blockage lay a bit farther downstream (near UTM grid 600/150), some 800 m north of the present-day traffic control gate. At this site, a small lateral lobe of the Espejos coulee had draped down the gorge wall (Fig. 39) through a gap between cliff-forming units **rep** and **rdno**, and banked against the then-larger basaltic edifice of El Candado, raising the overflow to ~2,350 m (>200 m higher than the gorge floor at the site of blockage).

Encirclement of the entire basin by the 2,350-m strandline indicates that glacial ice was not involved in damming the outlet, as does the singularity of the high strandline (because glacial dams typically release repetitive outburst floods, thereby leaving multiple strandlines). The gently sloping wave-cut bench on an easily erodible substrate can be 75-100 m wide with several parallel (probably seasonal) beach berms and a vertical extent of 5-10 m. Rapid filling and abrupt draining is inferred, but duration of the highstand is unknown. Because the strandline notches dense bedrock units as well as vesicular lavas and surficial deposits, a duration of centuries seems likely. The white, nearly pure, laminated (varved) diatomite that accumulated to a thickness as great as 2.6 m just upstream of the blockage (where the lake has never extended except during the highstand) would represent 520 years or 2,600 years at sedimentation rates of 5 mm/yr or 1 mm/yr, respectively.

Ultimately, sapping or overtopping of the fragmental edifice of Candado basalt led to runaway incision, landsliding from both walls of the gorge, and flooding downstream. If the highstand level of a 75-km^2 lake dropped by 200 m all at once, ~15 km^3 of water poured out through the gorge, probably in a single event. Along with a much larger mass of Candado basalt, the blockage-inducing lobe of Espejos rhyolite was swept away by the outburst, leaving a 250-m-long near-vertical wall, ~150 m high, of flow-foliated felsite, the only place in the entire Espejos coulee where its

devitrified interior is exposed (Fig. 39). The plateau of late Pleistocene mafic lavas (unit **msm**), 2 to 5 km downstream from the blockage, was denuded and pitted by plunge pools, leaving recessional cataracts and a shallowly channeled scabland (Figs. 5, 20, 38; Bretz, 1925, 1969). Where the confined outlet gorge debouches onto the broad plateau, the flood deposited a splaying set of radiating boulder bars (Scott and Gravlee, 1968), 3-8 m high and rich in clasts as big as 1 to 4 m (Fig. 38). Among the boulders are abundant clasts of Candado basalt and phenocryst-rich rhyodacite (unit **rdno**), fewer of pyroxene ignimbrite (unit **igsp**) and various andesite lavas, and sparse representatives of biotite ignimbrite, green-altered Tertiary andesite, and phenocryst-poor Espejos rhyolite. While boulders armor the bars, their internal material is predominantly cobble-sized and finer gravel that appears to be relatively richer than the boulder population in rhyolite and Tertiary intermediate clasts.

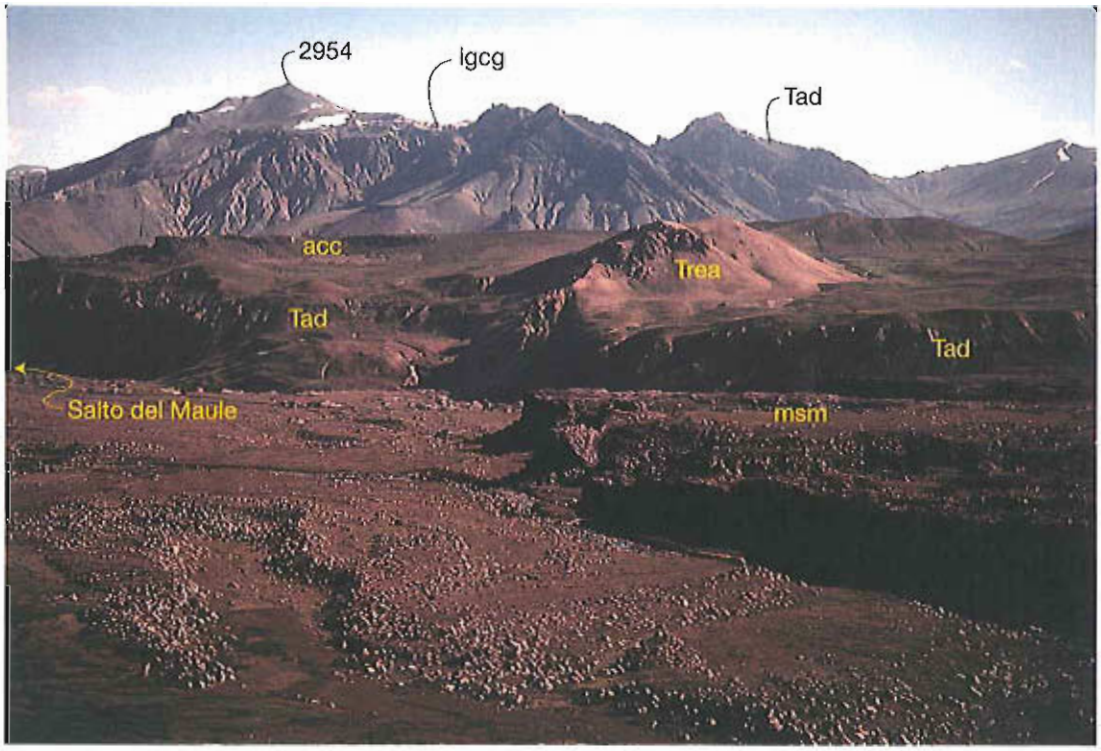

FIG. 38. Flood-scoured scabland plateau 3 km north of outlet of Laguna del Maule and 300 m downstream from mouth of narrow outlet gorge where Río Maule debouches onto previously glaciated stairstep plateau of late Pleistocene mafic lava flows (unit **msm**). Foreground scarp is 15-25 m high. Following temporary highstand caused by outlet blockage by rhyolite coulee (unit **rle**), outbreak flood abruptly lowered lake by 200 m, stripped scabland plateau, cut plunge pools, and deposited splaying gravel bars that contain abundant boulders as big as 1 to 4 m. Río Maule crossing center foreground was at unusually low discharge, owing to control at dam. Beyond lava plateau, scarp in middle distance consists of deformed Tertiary lavas and tuffs (**Tad**), which are intruded and overlain by pale orange-brown feeder dike and dome of Pliocene high-silica rhyolite (unit **Trea**). To left of dome, single 50-m-thick andesite lava flow on crest (unit **acc**; 1.04 Ma) rests unconformably atop Tertiary pile on Maule-Campanario divide (see Fig. 37). Distant view is northward beyond canyon of Río Campanario to skyline edifice of Cerro Galaz (peak 2,954), a deformed Miocene mafic-to-andesitic center (its peak 10 km from camera); banked high against its right side, white-rimmed skyline bench is undated Pleistocene ignimbrite unit **igcg**, nonwelded biotite-bearing high-silica rhyolite.

FIG. 39. East wall of outlet gorge of Río Maule, 1.5 km downstream from dam. Relief from river at 2,150 m to rim at 2,400 m is ~250 m. Three silicic coulees are visible as eroded scarps: Rhyodacite unit **rdno** forms shoulder at left; rhyolite unit **rep** forms scarp at right; and both are overlain centrally by postglacial coulee, Loma de Los Espejos (unit **rle**) on skyline. View is eastward from rim of 62-ka basaltic scoria cone, El Candado (**bec**), which filled much of present gorge in late Pleistocene. At about 23 ka, emplacement of a lateral lobe (seen at center) of Espejos coulee against Candado edifice blocked outlet here and raised level of Laguna del Maule by 200 m, resulting in 2,350-m strandline being cut on Candado, Espejos, and many other units all around the lake basin. As much as 1.6 m of laminated diatomite was deposited on the gorge floor near right side of image during the highstand. Eventual outbreak flood cleared blockage, reamed gorge, promoted repeated failure of Candado edifice, and removed lateral Espejos tongue that had invaded the gorge. Sheared-off scarp of that tongue is the only exposure of devitrified interior facies on entire, elsewhere glassy and pumiceous, Espejos coulee.

The three glacially eroded silicic lava domes (units **rep** and **rdop**) marginal to the modern outlet are cut by a pair of glacially scoured channels (Fig. 16), showing that paleo-outlets to the Río Maule had also been located there prior to the blockage. Alternative paleo-outlets around the basin rim to the southwest, southeast, and northeast are all higher than 2,500 m, more than 150 m above the high strandline. Westerly overflow into the Arroyo de Botacura could take place at a 2,482-m saddle, but it clearly did not happen because the upper Botacura is thickly filled with non-incised glacial and alluvial deposits. Minor north-trending arroyos on the plateau just north of the snout of the Espejos coulee lack gravels from the lake basin and are far too small to represent a pre-Espejos paleo-outlet for Laguna del Maule. It can be securely concluded that the late Pleistocene and younger location of the basin outlet is right where it is today and that the outbreak flood restored the original channel without significantly deepening it (except for removing the blockage).

The gorge floor adjacent to and downstream from the outlet domes but upstream from the blockage site is mantled by drumlinoid hillocks of till that is rich in clasts of Tertiary andesite from the lake basin but poor in clasts of rhyolite and basalt; the till is overlain by thin diamicts rich in Candado basalt (probably local debris-flow deposits) and by the diatomite deposit mentioned above. At and downstream of the inferred site of blockage, however, the gorge floor was widely scoured down to Tertiary ignimbrite bedrock, leaving only discontinuous veneers of till and alluvium. Deposition of flood-borne boulder-gravel began just below the mouth of the (ignimbrite-walled) gorge, where the Río Maule spreads out onto the scabland plateau. The chaotic jumble making up the lower slopes of El Candado (below ~2,280 m) is the product of several discrete avalanche masses that were emplaced after the outbreak flood had laterally undercut the toe of the fragmental basaltic edifice.

ACKNOWLEDGMENTS

We recall with pleasure the companionship, assistance, and advice of several colleagues who in various years accompanied us to the Laguna del Maule volcanic field: B. Drake, D. Tormey, F. Munizaga, F. Celhay, L. Lara, A. Carpinelli, K. Scott, R. Ackert, S. Lanés, S. Lohmar, and J. Fulton. In the course of his monumental investigation of the Tatara-San Pedro complex on the adjacent volcanic front, M. Dungan encouraged and supported this project materially, analytically, and logistically, including twice sending us off into remote territory on horseback. During the enlightened programme leadership of M. Gardeweg, SERNAGEOMIN also supported this project logistically and materially, encouraging participation of E. Godoy and providing thin sections and field vehicles, which were skillfully and helpfully operated by J. Espinoza and the late R. Morales. Hildreth's first two visits to Laguna del Maule were supported by a G.K. Gilbert Fellowship awarded by the U.S. Geological Survey, which also authorized his subsequent collaborative work there. We will always be grateful to B. Drake, who pioneered volcanological-geochronological investigations in the Maule region, exploring on foot most of its remote upper tributaries by 1970, enticing W. Hildreth to the region in 1980, and first introducing him to Laguna del Maule in 1984. Helpful reviews of the manuscript were provided by M. Dungan, L. Lara, F. Munizaga, and C. Hickson.

REFERENCES

Arculus, R.J. 2003. Use and abuse of the terms calcalkaline and calcalkalic. Journal of Petrology 44: 929-935.

Bacon, C.R.; Druitt, T.H. 1988. Compositional evolution of the zoned calcalkaline magma chamber of Mount Mazama, Crater Lake, Oregon. Contributions to Mineralogy and Petrology 98: 224-256.

Bacon, C.R.; Lowenstern, J.B. 2005. Late Pleistocene granodiorite source for recycled zircon and phenocrysts in rhyodacite lava at Crater Lake, Oregon. Earth and Planetary Science Letters 233: 277-293.

Bacon, C.R.; Lanphere, M.A. 2006. Eruptive history and geochronology of Mount Mazama and the Crater Lake region, Oregon. Geological Society of America Bulletin 118: 1331-1359.

Bacon, C.R.; Persing, H.M.; Wooden, J.L.; Ireland, T.R. 2000. Late Pleistocene granodiorite beneath Crater Lake caldera, Oregon, dated by ion microprobe. Geology 28 (5): 467-470.

Baedecker, P.A.; McKown, D.M. 1987. Instrumental neutron activation analysis of geochemical samples. *In* Methods for geochemical analysis (Baedecker, P.A.; editor). U.S. Geological Survey Bulletin 1770: H1-H14.

Bermúdez, A.; Delpino, D. 1989. La provincia basáltica andino cuyana (35°-37°S). Revista de la Asociación Geológica Argentina 44: 35-55.

Bermúdez, A.; Delpino, D.; Frey, F.; Saal, A. 1993. Los basaltos de retroarco extraandinos. *In* Congreso Geológico Argentino, No. 12 y Congreso de Exploración de Hidrocarburos, No. 2, Geología y Recursos Naturales de Mendoza (Ramos, V.A.; editor), Relatorio: 161-172.

Bretz, J.H. 1925. The Spokane flood beyond the Channeled Scabland. Journal of Geology 33: 97-115.

Bretz, J.H. 1969. The Lake Missoula floods and the Channeled Scabland. Journal of Geology 77: 505-543.

Burns, W.M.; Jordan, T.E.; Copeland, P.; Kelley, S.A. 2006. The case for extensional tectonics in the Oligocene-Miocene Southern Andes as recorded in the Cura Mallín basin (36°-38°S). *In* Evolution of an Andean margin: A tectonic and magmatic view from the Andes to the Neuquén basin (35°-39°S lat) (Kay, S.M.; Ramos, V.A.; editors). Geological Society of America Special Paper 407: 163-184.

Campos, J.; Hatzfeld, D.; Madariaga, R.; López, G.; Kausel, E.; Zollo, A.; Iannacone, G.; Fromm, R.; Barrientos, S.; Lyon-Caen, H. 2002. A seismological study of the 1835 seismic gap in south-central Chile. Physics of the Earth and Planetary Interiors 132: 177-195.

Dalrymple, G.B.; Lanphere, M.A. 1969. Potassium-Argon Dating. W.H. Freeman and Co.: 258 p. San Francisco.

Davidson, J.P.; Dungan, M.A.; Ferguson, K.M.; Colucci. M.T. 1987. Crust-magma interactions and the evolution of arc magmas: The San Pedro-Pellado volcanic complex, southern Chilean Andes. Geology 15: 443-446.

Davidson, J.P.; Ferguson, K.M.; Colucci. M.T.; Dungan, M.A. 1988. The origin and evolution of magmas from the San Pedro-Pellado volcanic complex, S. Chile: Multicomponent sources and open-system evolution. Contributions to Mineralogy and Petrology 100: 429-445.

Drake, R.E. 1976. Chronology of Cenozoic igneous and tectonic events in the central Chilean Andes-latitudes 36°30' to 36°S. Journal of Volcanology and Geothermal Research 1: 265-284.

Dungan, M.A.; Davidson, J. 2004. Partial assimilative recycling of the mafic plutonic roots of arc volcanoes: An example from the Chilean Andes. Geology 32: 773-776.

Dungan, M.A.; Wulff, A.; Thompson, R. 2001. Eruptive stratigraphy of the Tatara-San Pedro complex, 36°S, Southern Volcanic Zone, Chilean Andes: Reconstruction method and implications for magma evolution at long-lived arc volcanic centers. Journal of Petrology 42: 555-626.

Feeley, T.C.; Davidson, J.P. 1994. Petrology of calc-alkaline lavas at Volcán Ollagüe and the origin of compositional diversity at Central Andean stratovolcanoes. Journal of Petrology 35: 1295-1340.

Feeley, T.C.; Dungan, M.A. 1996. Compositional and dynamic controls of mafic-silicic magma interactions at continental arc volcanoes: Evidence from Cordón El Guadal, Tatara-San Pedro Complex, Chile. Journal of Petrology 37: 1547-1577.

Feeley, T.C.; Dungan, M.A.; Frey, F.A. 1998, Geochemical constraints on the origin of mafic and silicic magmas at Cordón El Guadal, Tatara-San Pedro Complex, central Chile. Contributions to Mineralogy and Petrology 131: 393-411.

Frey, F.A.; Gerlach, D.C.; Hickey, R.L.; López, L. 1984. Petrogenesis of the Laguna del Maule volcanic complex, Chile (36°S). Contributions to Mineralogy and Petrology 88: 133-149.

Gerlach, D.C.; Frey, F.A.; Moreno-Roa, H.; López-Escobar, L. 1988. Recent volcanism in the Puyehue-Cordón Caulle region, southern Andes, Chile (40.5°S): Petrogenesis of evolved lavas. Journal of Petrology 29: 333-382.

Gibbard, P.L.; Head, M.J.; Walker, M.J.C. and the Subcommission on Quaternary Stratigraphy. 2009. Formal ratification of the Quaternary System/Period and the Pleistocene Series/Epoch with a base at 2.58 Ma: Journal of Quaternary Science. doi: 10.1002/jqs.1338.

Gilbert, H.; Beck, S.; Zandt, G. 2006. Lithospheric and upper mantle structure of central Chile and Argentina: Geophysical Journal International 165: 383-398.

Godoy, E.; Hildreth, W. 2001. Cerro Amarillo rhyolites, advanced AFC in the northern SVZ, Chile: Comunicaciones 52: 81 (abstract). Extended to 4 pages in CD of III Simposio Sudamericano de Geología Isotópica, Pucón 21-24 Octubre, Sernageomin. Available through Sernageomin digital library at http://www.sigeo.cl/

González-F., O.; Vergara, M. 1962. Reconocimiento geológico de la Cordillera de los Andes entre los paralelos 35° y 38° latitud sur. Universidad de Chile, Instituto de Geología, Publicaciones 24: 121 p.

Gradstein, F.M.; Ogg, J.G.; Smith, A.G.; Bleeker, W.; Lourens, L.J. 2004. A new geologic time scale, with special reference to Precambrian and Neogene: Episodes 27: 83-100.

Grunder, A.L.; Mahood, G.A. 1988. Physical and chemical models of zoned silicic magmas: The Loma Seca Tuff and the Calabozos caldera. Journal of Petrology 29: 831-867.

Harrington, R. 1989. The Diamante caldera and Maipo caldera complex in the southern Andes of Argentina and Chile (34°10'S). Revista de la Asociación Geológica Argentina 44: 186-193.

Heit, B.; Yuan, X.; Bianchi, M.; Sodoudi, F.; Kind, R. 2008. Crustal thickness estimation beneath the southern central Andes at 30°S and 36°S from S wave receiver function analysis. Geophysical Journal International 174: 249-254.

Hickey, R.L.; Frey, F.A.; Gerlach, D.C. 1986. Multiple sources for basaltic arc rocks from the Southern Volcanic Zone of the Andes (34°-41°S): Trace-element and isotopic evidence for contributions from subducted oceanic crust, mantle, and continental crust. Journal of Geophysical Research 91: 5963-5983.

Hildreth, W. 1981. Gradients in silicic magma chambers: Implications for lithospheric magmatism: Journal of Geophysical Research 86: 10153-10192.

Hildreth, W. 2004. Volcanological perspectives on Long Valley, Mammoth Mountain, and Mono Craters: Several contiguous but discrete systems. Journal of Volcanology and Geothermal Research 136: 169-198.

Hildreth, W. 2007. Quaternary magmatism in the Cascades-Geologic Perspectives. United States Geological Survey, Professional Paper 1744: 125 p.

Hildreth, W.; Drake, R.E. 1992. Volcán Quizapu, Chilean Andes. Bulletin of Volcanology 54: 93-125.

Hildreth, W.; Lanphere, M.A. 1994. Potassium-argon geochronology of a basalt-andesite-dacite arc system: The Mount Adams volcanic field, Cascade Range of southern Washington. Geological Society of America Bulletin 106: 1413-1429.

Hildreth, W.; Grunder, A.L.; Drake, R.E. 1984. The Loma Seca Tuff and the Calabozos caldera: A major ash-flow and caldera complex in the southern Andes of central Chile. Geological Society of America Bulletin 95: 45-54.

Hildreth, W.; Drake, R.E.; Godoy, E.; Munizaga, F. 1991. Bobadilla caldera and 1.1 Ma ignimbrite at Laguna del Maule, central Chile. *In* Congreso Geológico Chileno, No. 6, Actas 1: 62-63. Viña del Mar.

Hildreth, W.; Singer, B.; Godoy, E.; Munizaga, F. 1998. The age and constitution of Cerro Campanario, a mafic stratovolcano in the Andes of Central Chile. Revista Geológica de Chile 25 (1): 17-28.

Hildreth, W.; Fierstein, J.; Godoy, E.; Drake, R.E.; Singer, B. 1999. The Puelche volcanic field: Extensive rhyolite lava flows in the Andes of central Chile. Revista Geológica de Chile 26: 275-309.

Hildreth, W.; Fierstein, J.; Siems, D.F.; Budahn, J.R.; Ruiz, J. 2004. Rear-arc *versus*. arc-front volcanoes in the Katmai reach of the Alaska Peninsula: A critical appraisal of across-arc compositional variation. Contributions to Mineralogy and Petrology 147: 243-275.

Jicha, B.R.; Singer, B.S. 2006. Volcanic history and magmatic evolution of Seguam Island, Aleutian Island arc, Alaska. Geological Society of America Bulletin 118: 805-822.

Jicha, B.R.; Singer, B.S.; Beard, B.L.; Johnson, C.M.; Moreno-Roa, H.; Naranjo, J.A. 2007. Rapid magma ascent and generation of 230Th excesses in the lower crust at Puyehue-Cordón Caulle, Southern Volcanic Zone, Chile. Earth and Planetary Science Letters 255: 229-242.

Johnson, R.G.; King, B.-S.L. 1987. Energy-dispersive x-ray fluorescence spectrometry. *In* Methods for geochemical analysis (Baedecker, P.A.; editor). United States Geological Survey Bulletin 1770: F1-F5.

Jordan, T.E.; Burns, W.M.; Veiga, R.; Pangaro, F.; Copeland, P.; Kelley, S.; Mpodozis, C. 2001. Extension and basin formation in the Southern Andes caused by increased convergence rate: A mid-Cenozoic trigger for the Andes. Tectonics 20: 308-324.

Kay, S.M.; Burns, W.M.; Copeland, P.; Mancilla, O. 2006. Upper Cretaceous to Holocene magmatism and evidence for transient Miocene shallowing of the Andean subduction zone under the northern Neuquén Basin. *In* Evolution of an Andean margin: A tectonic and magmatic view from the Andes to the Neuquén basin (35°-39°S lat) (Kay, S.M.; Ramos, V.A.; editors). Geological Society of America Special Paper 407: 19-60.

Lanphere, M.A. 2000. Comparison of conventional K-Ar and $^{40}Ar/^{39}Ar$ dating of young mafic volcanic rocks. Quaternary Research 53: 294-301.

Lara, L.E. 2009. The 2008 eruption of Chaitén volcano, Chile: A preliminary report. Andean Geology 36: 125-129.

Lara, L.E.; Moreno, H.; Naranjo, J.A.; Mathews, S.; Pérez de Arce, C. 2006. Magmatic evolution of the Puyehue-Cordón Caulle Volcanic Complex (40°S), Southern Andean Volcanic Zone: From shield to unusual rhyolitic fissure volcanism. Journal of Volcanology and Geothermal Research 157: 343-366.

LeBas, M.J.; LeMaitre, R.W.; Streckeisen, A.; Zanettin, B.; 1986. A chemical classification of volcanic rocks based on the total alkali-silica diagram. Journal of Petrology 27: 745-750.

Lescinsky, D.T.; Sisson, T.W. 1998. Ridge-forming, ice-bounded lava flows at Mount Rainier, Washington. Geology 26: 351-354.

López-Escobar, L.; Vergara, M.; Frey, F.A. 1981. Petrology and geochemistry of lavas from Antuco volcano, a basaltic volcano of the Southern Andes (37°25'S). Journal of Volcanology and Geothermal Research 11: 329-352.

Macdonald, R.; Smith, R.L.; Thomas, J.E. 1992. Chemistry of the subalkalic silicic obsidians. United States Geological Survey, Professional Paper 1523: 214 p.

Manceda, R.; Figueroa, D. 1995. Inversion of the Mesozoic Neuquén rift in the Malargüe fold and thrust belt, Mendoza, Argentina. *In* Petroleum Basins of South America (Tankard, A.J.; Suárez, S., R.; Welsink, H.J. editors). American Association of Petroleum Geologists, Memoir 62: 369-382.

Melnick, D.; Rosenau, A.; Folguera, A.; Echtler, H. 2006. Neogene tectonic evolution of the Neuquén Andes western flank (37-39°S), *In* Evolution of an Andean margin: A tectonic and magmatic view from the Andes to the Neuquén basin (35°-39°S lat) (Kay, S.M.; Ramos, V.A.; editors). Geological Society of America, Special Paper 407: 73-95.

Miyashiro, A. 1974. Volcanic rock series in island arcs and active continental margins. American Journal of Science 274: 321-355.

Morrison, R.; Kukla, G. 1998. The Pliocene-Pleistocene (Tertiary-Quaternary) boundary should be placed at about 2.6 Ma, not at 1.8 Ma. GSA Today, August 1998: 9.

Munizaga, F. 1978. Geología del complejo volcánico Laguna del Maule. Memoria de Titulo (Inédito), Universidad de Chile, Departamento de Geología: 157 p.

Muñoz, B., J.; Niemeyer R., H. 1984. Hoja Laguna del Maule. Servicio Nacional de Geología y Minería, Carta Geológica de Chile 64: 98 p., 1 mapa escala 1:250.000.

Muñoz, J.; Stern, C.R.; Bermúdez, A.; Delpino, D.; Dobbs, M.F.; Frey, F.A.; 1989. El volcanismo Plio-Cuaternario a través de los 34-39°S de los Andes. Revista de la Asociación Geológica Argentina 44: 270-286.

Muñoz, J.O.; Basualto, D.; Moreno, H.; Peña, P.; Mella, M. 2008. Geochemistry and magma genesis of the early May 2008 rhyolitic magma erupted by Chaiten volcano, Southern Andes Volcanic Zone. EOS Transactions, American Geophysical Union 89 (53), Fall Meeting Supplement, Abstract V43D-2181.

Naranjo, J.A.; Stern, C.R. 2004. Holocene tephrochronology of southernmost part (42°30'-45°S) of the Andean Southern Volcanic Zone. Revista Geológica de Chile 31 (2): 225-240.

Nelson, S.T.; Davidson, J.P.; Heizler, M.T.; Kowallis, B.J. 1999. Tertiary tectonic history of the southern Andes: The subvolcanic sequence to the Tatara-San Pedro volcanic complex, lat 36°S. Geological Society of America Bulletin 111: 1387-1404.

Ogg, J. 2004. Introduction to concepts and proposed standardization of the term 'Quaternary'. Episodes 27: 125-126.

Peacock, M.A. 1931. Classification of igneous rock series. Journal of Geology 39: 54-67.

Pearce, J.A. 1982. Trace element characteristics of lavas from destructive plate boundaries. *In* Orogenic andesites and related rocks (Thorpe, R.S.; editor). Wiley, Chichester: 525-548. U.K.

Pillans, B. 2004. Proposal to redefine the Quaternary. Episodes 27: 127.

Ramos, V.A.; Cegarra, M.; Cristallini, E. 1996. Cenozoic tectonics of the High Andes of west-central Argentina (30-36ºS latitude). Tectonophysics 259: 185-200.

Ramos, V.A.; Kay, S.M. 2006. Overview of the tectonic evolution of the southern Central Andes of Mendoza and Neuquén (35º-39ºS latitude). *In* Evolution of an Andean margin: A tectonic and magmatic view from the Andes to the Neuquén basin (35º-39ºS lat) (Kay, S.M.; Ramos, V.A.; editors). Geological Society of America Special Paper 407: 1-17.

Renne, P.R.; Swisher, C.C.; Deino, A.L.; Karner, D.B.; Owens, T.L.; DePaolo, D.J. 1998. Intercalibration of standards, absolute ages and uncertainties in $^{40}Ar/^{39}Ar$ dating. Chemical Geology 145: 117-152.

Rhodes, J.M. 1988. Geochemistry of the 1984 Mauna Loa eruption: Implications for magma storage and supply. Journal of Geophysical Research 93: 4453-4466.

Rhodes, J.M. 1996. Geochemical stratigraphy of lava flows sampled by the Hawaiian Scientific Drilling Project. Journal of Geophysical Research 101 (B5): 11729-11746.

Scott, K.M.; Gravlee, G.C. Jr. 1968. Flood surge on the Rubicon River, California-Hydrology, hydraulics and boulder transport. United States Geological Survey, Professional Paper 422-M, 38 p.

Silvestro, J.; Kraemer, P.; Achilli, F.; Brinkworth, W. 2005. Evolución de las cuencas sinorogénicas de la Cordillera Principal entre 35º-36ºS, Malargüe. Revista de la Asociación Geológica Argentina 60 (4): 627-643.

Singer, B.S.; Thompson, R.A.; Dungan, M.A.; Feeley, T.C.; Nelson, S.T.; Pickens, J.C.; Brown, L.L.; Wulff, A.W.; Davidson, J.P.; Metzger, J. 1997. Volcanism and erosion during the past 930 k.y. at the Tatara-San Pedro complex, Chilean Andes. Geological Society of America Bulletin 109: 127-142.

Singer, B.S.; Hoffman, K.A.; Chauvin, A.; Coe, R.S.; Pringle, M.S. 1999. Dating transitionally magnetized lavas of the late Matuyama Chron: Toward a new $^{40}Ar/^{39}Ar$ timescale of reversals and events. Journal of Geophysical Research 104 (B1): 679-693.

Singer, B.S.; Hildreth, W.; Vincze, Y. 2000. $^{40}Ar/^{39}Ar$ evidence for early deglaciation of the central Chilean Andes. Geophysical Research Letters 27: 1663-1666.

Singer, B.S.; Brown, L.L.; Rabassa, J.O.; Guillou, H. 2004a. $^{40}Ar/^{39}Ar$ chronology of late Pliocene and early Pleistocene geomagnetic and glacial events in southern Argentina. American Geophysical Union, Geophysical Monograph Series 145: 175-190.

Singer, B.S.; Ackert, R.P.; Jr.; Guillou, H. 2004b. $^{40}Ar/^{39}Ar$ and K-Ar chronology of Pleistocene glaciations in Patagonia. Geological Society of America Bulletin 116: 434-450.

Singer, B.S.; Jicha, B.R.; Harper, M.A.; Naranjo, J.A.; Lara, L.E.; Moreno-Roa, H. 2008. Eruptive history, geochronology, and magmatic evolution of the Puyehue-Cordón Caulle volcanic complex, Chile. Geological Society of America Bulletin 120: 599-618.

Stern, C.R.; Amini, H.; Charrier, R.; Godoy, E.; Hervé, F.; Varela, J. 1984. Petrochemistry and age of rhyolitic pyroclastic flows which occur along the drainage valleys of the Río Maipo and Río Cachapoal (Chile) and the Río Yaucha and Río Papagayos (Argentina). Revista Geológica de Chile 23: 39-52.

Sun, S.; McDonough, W.F. 1989. Chemical and isotopic systematics of oceanic basalts: Implications for mantle composition and processes. *In* Magmatism in the Ocean Basins (Saunders, A.D.; Norry, M.J.; editors). Geological Society, Special Publication 42: 313-345.

Taggart, J.E., Jr.; Lindsay, J.R.; Scott, B.A.; Vivit, D.V.; Bartel, A.J.; Stewart, K.C. 1987. Analysis of geologic materials by wavelength-dispersive x-ray fluorescence spectrometry. *In* Methods for geochemical analysis (Baedecker, P.A.; editor). United States Geological Survey Bulletin 1770: E1-E19.

Vergara, M.; Muñoz, J. 1982. La Formación Cola de Zorro en la Alta Cordillera Andina Chilena (36º-39º Lat.S), sus características petrográficas y petrológicas: Una revisión. Revista Geológica de Chile 17: 31-46.

Watt, S.F.L.; Pyle, D.M.; Mather, T.A.; Martin, R.S.; Matthews, N.E. 2009. Fallout and distribution of volcanic ash over Argentina following the May 2008 explosive eruption of Chaitén, Chile. Journal of Geophysical Research 114, B04207. doi: 10.1029/2008JB006219.

Yuan, X.; Asch, G.; Bataille, K.; Bock, G.; Bohm, M.; Echtler, H.; Kind, R.; Oncken, O.; Wölbern, I. 2006. Deep seismic images of the Southern Andes. *In* Evolution of an Andean margin: A tectonic and magmatic view from the Andes to the Neuquén basin (35º-39ºS lat) (Kay, S.M.; Ramos, V.A.; editors). Geological Society of America Special Paper 407: 61-72.

APPENDIX 1. ERUPTIVE UNITS OF THE LAGUNA DEL MAULE VOLCANIC FIELD.

Code*	Grid E/N †	% SiO_2	Unit Name and Notes
Postglacial eruptive units			
bhc	473/042	50-51	Basalt of Cerro Hoyo Colorado (small scoria and spatter cone along Arroyo de Rodríguez)
mcp	560/030	53-62	Andesite of Crater 2657 (cinder-spatter linear vent overlies till)
mct	570/030	53-54	Andesite of Arroyo Cabeceras de Troncoso (scoria/spatter of fissure vent and 3 small craters)
mnp	564/068	56-60	Andesite north of Estero Piojo (scoria ring and spatter-fed flow; intruded by rhyodacite unit **rdnp**)
aan	608/059	59	Andesite of Arroyo Las Nieblas (cinders and lava buried by lake sedment)
acn	593/073	57-58	Andesite of Crater Negro (pre-highstand scoria cone)
anc	593/084	59	Andesite north of Crater Negro (phreatomagmatic ejecta ring)
apj	610/085	59	Younger andesite of West Peninsula (pre-highstand lava flow into LdM)
apo	675/063	59.5	Andesite of Playa Oriental (blocky lava largely buried by beach deposits)
ars	480/055	59-61	Andesite of Río Saso (10-km-long lava flow with vent-scoria ramparts)
asm	577/090	61	Andesite south of Arroyo Los Mellicos (scoria vent 2,484; linear vent for thin deposit of coarse ejecta; see **dsm**, below)
asp	567/111	59	Andesite of Laguna Sin Puerto (scoria ring intruded by dome **rdsp**)
dcr	520/045	65	Dacite of Cordón Rodríguez (4 km-long-lava flow from ridgecrest vents)
dsm	577/091	66	Dacite south of Arroyo Los Mellicos (cerrillo 2,484 only; 25-m-wide window of blocky glassy lava mantled by scoria of unit **asm**, which erupted through and ejected abundant blocks of the dacite)
rdac	680/035	71.6	Rhyodacite of Arroyo de la Calle (lower of 2 pre-highstand coulees; upper is unit **ras**)
rdam	583/105	69-72	Rhyodacite of Arroyo Los Mellicos (pre-highstand coulee 1.2 km long)
rdcd	573/080	69-71	Rhyodacite of Colada Dendriforme (multilobate lava complex and 2 vent domes W of LdM)
rdcn	580/130	68-69	Rhyodacite of Northwest Coulee (large coulee at NW side of LdM)
rdep	565/045	68-69	Rhyodacite south of Estero Piojo (chain of 3 pre-highstand domes)
rdne	620/165	69	Rhyodacite northeast of Loma Los Espejos (small pumice-covered flow)
rdno	603/158	69-70	Rhyodacite northwest of Loma Los Espejos (overrun by **rle** coulee)
rdnp	561/071	68-69	Rhyodacite north of Estero Piojo (2 small domes intrude unit **mnp**)
rdsp	562/112	71	Rhyodacite of Laguna Sin Puerto (dome intrudes scoria cone **asp**)
ram	588/110	73	Rhyolite of Arroyo Los Mellicos (minidome intrudes **aam**)
rap	610/010	76	Rhyolite of Arroyo de Palacios (pumice-covered coulee SW of **rln**)
ras	685/020	73.6	Rhyolite of Arroyo de Sepúlveda (upper of 2 flows; overlies **rdac**)
rcb	700/965	74	Rhyolite of Cerro Barrancas (multi-coulee edifice with pumice cones)
rcd	730/064	74	Rhyolite of Colada Divisoria (divergent coulees from pumice cone)
rcl	718/110	74	Rhyolite of Cari Launa (multi-coulee edifice with pumice cone)
rle	620/140	76	Rhyolite of Loma de Los Espejos (coulee and pumice cone; impounded Laguna del Maule)

Appendix 1. continued.

Code*	Grid E/N †	% SiO_2	Unit Name and Notes
rln	625/021	74	Rhyolite of Colada Las Nieblas (coulee with pumice-ringed vent dome)
rng	737/955	73.5	Rhyolite of Laguna Negra (pumice cone and pumice-covered lava flows; earliest unit of Barrancas complex; impounds Laguna Negra)
rpp	721/141	74.4	Rhyolite of Paso Pehuenche (minidome 4 km SW of Paso Pehuenche)
rsl	733/107	75	Rhyolite south of Laguna Cari Launa (pumice-covered flow beneath **rcl**)
Late Pleistocene eruptive units			
bec	587/148	51-53	Basalt of El Candado (failure of cone flanks drained LdM highstand)
mcr	500/990	53-54	Andesite south of Cajón Rodríguez (pair of shallow craters; agglutinate and spatter-fed lavas limited to glaciated ejecta rings)
meb	558/224 548/220 564/206 618/192	53-55	Andesite of Estero Bobadilla (top flow on Maule-Campanario nose; flow remnant SW of confluence; banked-in remnant on rim at road; and flows on banks of Estero Bobadilla that issue from Crater Bobadilla scoria cone)
mls	538/025	55	Andesite of Cráter Las Salinas (thin phreatomagmatic ejecta ring)
mlt	590/015	53-54	Andesite of Laguna Turbia (scoria rings around two phreatomagmatic craters on north rim of Laguna Fea)
mpl	608/118	56-57	Andesite of Volcán Puente de la Laguna (glaciated scoria and spatter cone partly overrun by coulee **rle**)
mpn	550/130	51-54	Basalt and andesite of Vega Piedras Negras (lava plateau and scoria cone)
msm	587/206	51-57	Basalt and andesite of Salto del Maule (plateau-forming stack of lava flows extending from beneath coulee **rle** to eroded scarp at 570/210; proximal scoria fall crops out between flows at 601/160)
aam	590/110	58-59	Andesite of Arroyo Los Mellicos (spatter-ringed crater and lava-flow remnants along NW shore of LdM)
acr	504/024	61	Andesite of Cajón Rodríguez (intracanyon flow and vent scoria)
alc	559/222 543/230 562/207	59	Andesite of Cuesta los Cóndores (middle flow on Maule-Campanario nose; most distal 1,500 m remnant on valley floor; and 1,750 m rim remnant along roadgrade)
alm	596/134	61-62	Andesite of Presa Laguna del Maule (heterogeneous mixed lavas beneath **rdop** dome 2,367 just W of LdM dam)
alp	573/055	61	Andesite west of Laguna del Piojo (scoria mound overlapped by till)
als	547/021	60	Andesite northeast of Las Salinas (blocky orphan lava flow in upper headwaters of Cajón Rodríguez)
apñ	435/138	56-58	Andesite of Puntilla Los Ñirales (scoria cone and lavas atop obsidian **roz**)
apv	600/093	58	Older andesite of West Peninsula (glaciated lava under N edge of **apj**)
asd	586/107	62.5	Andesite south of Domo del Maule (small window of glassy lava under snout of Mellicos rhyodacite **rdam**)
avc	430/170	58-62	Andesite of Cabeceras del Valle Chico (lavas from Volcán Pellado capping ridge 2,630 on divide between Río de La Plata and Valle Chico)
avm	556/217	61-62	Andesite of Vacas Muertas (lowest flow on Maule-Campanario nose and remnant at Vacas Muertas)
avr	520/020	62	Andesite of Vega Rodríguez (intracanyon lava on floor of upper valley of Cajón Rodríguez)

Appendix 1. continued.

Code*	Grid E/N †	% SiO_2	Unit Name and Notes
dcc	561/208	63-66	Dacite of Cuesta Los Cóndores (lava flow drapes SW wall of canyon from above road to valley floor, where it underlies cliff of mafic lavas between Río Maule and Arroyo Arenas Blancas. Remnant is 10 m thick at road, 70 m at toe of scarp) [K-Ar dated at 100-180 ka by R.E. Drake]
dlp	597/051	63-64	Dacite of Laguna del Piojo (lava exposed in series of windows extending 4 km NE to terminus at Laguna del Piojo)
rddm	580/120	71	Rhyodacite of Domo del Maule (250-m-high glassy dome rises above eroded scarp of comagmatic lava-flow platform >50 m thick)
rdop	593/139	71	Rhyodacite west of Presa Laguna del Maule (two twin domes; dome 2,367 forms W wall of LdM outlet)
reb	705/202	75	Rhyolite of Estero de Bobadilla (dome 2,667 on floor of headwaters)
rep	601/137	73.5	Rhyolite east of Presa Laguna del Maule (lava flow forms E wall of LdM outlet from dam for 1.5 km N; underlies coulee **rle**)
ret	482/143	74	Rhyolite of Estero Terneros (coulee S of Cerro San Pedro)
rez	440/138	74	Rhyolite of Estero El Zorro (obsidian coulee E of Puntilla Los Ñirales)
Middle Pleistocene eruptive units			
bbc	660/160	52-53	Basalt of Volcán Bobadilla Chica (small mafic lava cone)
bcf	518/095	51-52	Basalt of Cajón Filume (intracanyon flow remnants extend 3 km southward to valley floor)
mcb	512/171	53-59	Andesite of Cerro Bahamondes (scoria cone 2,667 and lava apron on E side of Cerro San Pedro)
mcc	770/240	54	Andesite of Cerro Campanario (3,943-m mafic stratovolcano on divide; small peripheral cone east of edifice is unsampled.
mcs	486/166	49-58	Basalt and andesite of Cerro San Pedro (spatter and lava cone and shield apron extending 10 km N)
mlc	560/208	53-59	Andesitic dike of Cuesta los Cóndores (cuts Miocene rocks in roadcut; dike is compositionally heterogeneous)
mlp	585/165	53	Andesite of La Poza (glacially ravaged scoria and lava cone)
mor	685/215	54	Andesite west of Cerro Risco Bayo (stack of 3 phenocryst-poor lavas on Campanario-Bobadilla divide; overlies units **lbcb** and **lgbc**; chemically different from products of nearby V. Munizaga and Cerro Campanario)
mpc	723/229	54-58	Andesite of Paso Campanario (lava cone and vent breccia at crag 2,985; lavas fill pass between Río Campanario and [Argentine] Cajón Grande)
mrb	568/233 564/227	54	Andesite of Río Blanco (two lava-flow remnants NE of confluence of the Ríos Campanario and Maule)
mvc	717/047	53-56	Andesite of Volcán de la Calle (mafic lava cone on continental divide NW of Laguna Negra; crater rim at 2,954)
mvp	xxx/yyy 410/120 450/220	53-59	Andesite of Volcán Pellado (stratocone (~188-83 ka) centered W of map area; its valley-confined lava flows to S in Valle Chico and flows to NE capping Cordón Loma Seca frame W margin of LdM volcanic field)
aab	561/183	59-61	Andesite of Arroyo Arenas Blancas (lava flows bifurcate around hill of unit **rdla**; ice-contact terminus in valley to E; unglaciated scoria cone at source is more mafic [55% SiO_2] and either younger or above glaciers)
acp	485/027	59	Andesite of Casa de Piedra (250-m-thick intracanyon lava flow banked against N wall of Cajón Rodríguez)
aeb	500/260	54-62	Andesite of Estero Bahamondes (ridge-capping lava flows on both rims of lower canyon of Estero Bahamondes)

Appendix 1. continued.

Code*	Grid E/N †	% SiO_2	Unit Name and Notes
ans	584/213	62	Andesite north of Salto del Maule (100-m-thick flow remnant capping Cordón de Constanza at knob 2,003)
asb	574/218	60	Andesite south of Baños Campanario (130-m-thick flow remnant atop Cordón de Constanza at knob 2,046)
avz	454/154	52-61	Andesite of Volcán El Zorro (severely eroded stratocone centered at plug on divide between Esteros Terneros and Zorro)
dct	589/039	63	Dacite of Arroyo Cabeceras de Troncoso (small remnant of glassy lava on floor of the arroyo)
det	450/070	63-65	Dacite of Estero Tapia (thick lava flow drapes steep N wall of Río Saso from vent on Cordón Las Romazas)
rdcb	506/178	69	Rhyodacite west of Cajón Bahamondes (lower of 2 coulees between Cerros San Pedro and Bahamondes
rdcp	439/179	71	Rhyodacite of Cabeceras de La Plata (small dome at headwall of Río de La Plata)
rdct	585/033	71	Rhyodacite of Arroyo Cabeceras de Troncoso (coulee widely covered by scoria falls of units **mcp** and **mct**)
rdes	502/175	70	Rhyodacite east of Cerro San Pedro (upper of 2 coulees between Cerros San Pedro and Bahamondes
rdet	472/148	70	Rhyodacite of Estero Terneros (2 thick flows S of Cerro San Pedro)
rdez	450/145	70	Rhyodacite of Estero El Zorro (200-m-thick coulee beneath andesitic lava pile of **avz** cone)
rdpñ	435/125	70	Rhyodacite of Puntilla Los Ñirales (dome 2,603, 300 m thick exposure)
rdvc	432/154	70-71	Rhyodacite of Valle Chico (dome 2,583, 250-m-thick exposure)
rca	676/166	74	Rhyolite of Cajón Atravesado (vent tuff and glaciated coulee capping divide atop N wall of LdM basin)
rcn	710/130	75-77	Rhyolite of Cerro Negro (flow-dome complex 3,080, more than 900 m thick; forms steep NE wall of LdM basin)
rlm	480/200	73	Rhyolite of Los Murciélagos (thick glaciated lava flow ~10 km long preserved as several remnants along both rims of Río de La Plata)
igcc	565/218 502/275	74-75	Ignimbrite of Cordón de Constanza (remnants of nonwelded to sintered, pink to orange-brown ignimbrite, originally >250 m thick, preserved on Maule-Campanario divide and on Maule–La Plata divide)
igcg	600/260	75-76	Ignimbrite of Cerro Galaz (subhorizontal sheet of vitric, nonwelded to moderately sintered, biotite-rhyolite ash-flow tuff as thick as 40 m; rests on deformed dike-ridden Miocene fragmental strata of andesitic edifice)
Early Pleistocene eruptive units (≤1.5 Ma)			
mas	473/093	54	Andesite of Arroyo Santuario (stack of subhorizontal lava flows capping Botacura-Saso divide around Peak 2,844; unsampled vitrophyre along W wall of stack suggests wider range of compositions); source uncertain but probably an outlier of apron lavas from nearby unit **mcf**
mcf	505/087	53-59	Andesite of Cordón Filume (plug and surrounding stack of lava flows capping Botacura-Filume divide; underlies **igsp** on E wall Cajón Filume)
mqf	600/245	53	Andesite of Quebrada Fiera (orphan lava-flow remnant 3.5 km NE of Baños Campanario, at 2,300 m on S slope of Cerro Galaz)

Appendix 1. continued.

Code*	Grid E/N †	% SiO_2	Unit Name and Notes
msp	539/101	53-56	Andesite of Volcán Sin Puerto (ravaged edifice W of Laguna Sin Puerto; 300-m-wide plug and surrounding stacks of lavas and scoria)
mva	543/177	51-56	Basalt and andesite of Volcán Aguirre (ice-ravaged mafic stratocone; remnant >7 km long caps Bahamondes-Aguirre divide)
mvb	525/125	53-56	Andesite of Volcán Botacura (mafic lava and scoria cone centered near Peak 2,920 on Botacura-Filume divide)
mvm	725/193	50-55	Basalt and andesite of Volcán Munizaga (gutted stratovolcano on NW side of Paso Pehuenche; centered near Peak 3,132)
mvñ	424/110	53-57	Andesite of Volcán Ñirales (remnants of modest mafic edifice cap divide between Río Botacura and Valle Chico; many dikes near Peak 2,623)
acc	595/213	62	Andesite of Cordón de Constanza (remnant of single lava flow as thick as 130 m, atop Maule-Campanario divide)
alz	720/170	58	Andesite of Volcán La Zorra (widely altered intermediate lava pile centered 3 km SW of Paso Pehuenche)
ams	557/077	61-63	Andesite of Mellicos-Saso Divide (lava flows on Saso-LdM divide, along crest and/or downfaulted to E, that overlie ignimbrite **igsp**)
apg	760/160	55-62	Andesite of Paso del Guanaco (gently dipping stack of lavas that cap the continental divide from Laguna Cari Launa to Paso Pehuenche; may have issued from unmapped Cerro Bayo center 5 km farther E)
arp	553/027	61-62	Andesite of Rodríguez-Piojo Divide (subhorizontal stack of lava flows, each 50-150 m thick, that caps SW rim of LdM basin)
ava	680/180	54-67	Andesite and dacite of Volcán Atravesado (apron of lavas and thick breccias that extend 8 km N from N shore of LdM; N-dipping to subhorizontal; fed by dikes now near or under the lake that cut unit **igcb**, which the lava stack directly overlies)
avf	620/930	nd	Andesite of Volcán Laguna Fea (intermediate stratocone centered 2-3 km S of Laguna Fea; some outflow lavas preserved on N rim of lake)
dab	500/145 512/144 532/149	62-69	Dacite and rhyodacite of Arroyo de Botacura (several separate lava flows on the floor and lower walls on both sides of upper Botacura drainage, W of Vega Piedras Negras)
dlf	588/006 655/963	62-65	Dacite of Laguna Fea (remnant stacks of lava flows that cap the divide between LdM and Laguna Fea; gently N-dipping flows are each 30-150 m thick; source probably Volcán Laguna Fea just S of lake)
dpr	510/010	63	Dacite of La Puerta de Rodríguez (single 250-m-thick ridge-capping lava flow S of Cajón Rodríguez, glassy, convolute, widely columnar)
dsp	551/118	66	Dacite northwest of Laguna Sin Puerto (glassy stratified breccia, >100 m thick, that underlies mafic lavas of unit **msp**)
dvñ	425/114	66	Dacite of Volcán Ñirales (lava-flow remnant that caps Peak 2,623, the summit of the otherwise mafic edifice)
rdap	620/003	69	Rhyodacite plug of Arroyo de Palacios (columnar cliff >75 m high, on NE slope of Peak 2,818)
rdcr	464/094	71	Rhyodacite of Cordón Las Romazas (series of remnants along the Botacura-Saso divide of a lava more than 150-m-thick that flowed at least 5 km westward from Peak 2,764 as far as nose 2,145)
rddp	600/044	71	Rhyodacite dike south of Laguna del Piojo (5-m-thick vertical dike of hornblende-biotite rhyodacite; strikes E-W and cuts stack of Tertiary andesites that forms SW wall of LdM basin)

Appendix 1. continued.

Code*	Grid E/N †	% SiO_2	Unit Name and Notes
rdla	572/192	64-69	Rhyodacite of Lo Aguirre (lava dome-flow >450 m thick; extends from hill 2,262 over the steep S wall of the Río Maule canyon, where it is pierced by the road tunnel)
rlf	646/974	73	Rhyolite of Laguna Fea (dome >300 m thick at Peak 3,104 on divide between LdM and Laguna Fea; convolutely foliated and eroded craggy)
rls	543/015	72-73	Rhyolite of Las Salinas (700-m-long shallow intrusion (cryptodome) at head of Cajón Rodríguez; ovoid in plan, columnar throughout)
rnf	621/997	75	Rhyolite north of Laguna Fea (small dome remnant at Peak 2,994 on divide between LdM and Laguna Fea)
igbc	670/215	69	Ignimbrite of Bobadilla-Campanario Divide (remnant of welded-tuff orphan as thick as 150 m that extends 2 km along the divide crest; source unknown; widely columnar; overlies contrasting ignimbrite **igcb**)
igcb	655/120 675/205	66-72	Ignimbrite of Cajones de Bobadilla (intracaldera welded tuff >500 m thick but base nowhere exposed; from north wall at Cajón Grande de Bobadilla, unit extends 13 km south to peninsulas, islets, and beneath LdM)
igeb	716/250	61.5	Ignimbrite of Estero Guanaco (remnant sheet of moderately to densely welded tuff > 50 m thick, capping continental divide 5 km W of Cerro Campanario; abundant glassy fiamme; another ignimbrite remnant 5 km farther NW, unsampled, may be correlative)
igsp	554/075 580/150 620/208 496/250	64-70	Ignimbrite of Laguna Sin Puerto (many remnants of two-pyroxene-plagioclase welded tuff, typically 100-200 m thick, mostly capping ridgecrests; identified for 16 km from west rim of LdM to Bobadilla-Campanario divide; source uncertain but distribution suggests north end of LdM)
Eruptive units older than 1.5 Ma			
acs	553/066 561/103	53-62	Andesite of Cabeceras del Saso (stack of lava flows that underlies 1.5 Ma ignimbrite **Igsp** along west wall of LdM basin: Saso-LdM divide)
QTad	-	55-66	Undifferentiated undated *undeformed* andesite-dacite lavas and tuffs; largely subhorizontal ridge-capping units; most probably 3 to 1.5 Ma). Similar to Cola de Zorro Formation of Vergara and Muñoz (1982).
Tv, Tvs	-	53-68	Undifferentiated undated *deformed* (and commonly altered) lavas, tuffs, and subordinate volcaniclastic sedimentary strata (Pliocene and mostly Miocene); predominant assemblage exposed beneath the Quaternary LdM volcanic field; mostly andesite-dacite). Designated Tvs where volcaniclastic sedimentary strata make up more than trivial fractions of sequences.
Tdcl	695/085	52	Diorite of Cari Launa (1-km² ovoid pluton Ar-dated at 3.6 Ma, near east shore of LdM; intrudes pile of Tertiary andesitic rocks that form east wall of LdM basin)
Tdvl	490/115	n.d.	Diorite of Vega Larga (1-km² pluton that intrudes Tertiary andesitic pile on S wall of Arroyo Botacura; mostly amphibole and plagioclase with abundant disseminated epidote and pyrite)
Tiga	573/170	75-76	Ignimbrite of Estero Aguirre (indurated but nonwelded white ignimbrite of quartz-biotite high-silica rhyolite along Cajones Aguirre; associated with and locally intruded by lavas of unit Trea. White ignimbrite benches isolated just north of Salto del Maule [581/210] are lithologically and compositionally similar to **Tiga**, not to **Tigh**)

Appendix 1. continued.

Code*	Grid E/N †	% SiO_2	Unit Name and Notes
Tigh	520/290	68-71	Ignimbrite of Cajón El Huemul (Miocene biotite-rhyodacite welded tuff >1 km thick that crops out as a NNW-striking belt 5-7 km wide and at least 23 km long, from Cajones Aguirre to N of Río Puelche; synclinally folded where it crosses Río Maule [530/248]; includes outcrops in LdM outlet gorge [600/165]. K-Ar dated at 12.9±0.7 Ma at outlet gorge by R.E. Drake)
Tigr	450/090	n.d.	Ignimbrite of Cordón Las Romazas (Pliocene intracaldera biotite-rhyodacite welded tuff >950 m thick on south wall of Arroyo Botacura where its lithologic zoning is subhorizontal and its base is not exposed; along Río Saso to S, apparent outflow equivalent is half as thick and its base exposed atop Miocene andesites. K-Ar dated at 3.4±0.8 Ma by Muñoz and Niemeyer, 1984; Fig. 8)
Tig	-	-	Silicic ignimbrites, undivided (undeformed or little deformed; one unit just south of area mapped gave Muñoz and Niemeyer, 1984, a K-Ar age of 6.1±0.5 Ma; Fig.8)
Trcf	515/110	75	Rhyolite of Cajón Filume (lava dome-flow as thick as 250 m and 2.5 km long; on Botacura-Filume divide)
Trea	570/180 590/180 603/203	75-77	Rhyolite of Estero Aguirre (four discrete domes and a lava flow; all are Pliocene biotite-bearing high-silica rhyolites, distributed 3-7 km north or northwest of LdM; two domes are in part intrusive at level of exposure)
Kgi	480/260 470/310 490/360	54-68	Granodiorite of Los Indios (large 80 Ma pluton that crops out along a north-south strip from 6 km south of confluence of Ríos de La Plata and Maule as far as 4 km north of Río Puelche, 15 km in all. Units **Tigh**, **Tvs**, and several Quaternary lavas bank against or overlie it)
Mzsv	-	-	Undifferentiated Mesozoic sedimentary and volcanic rocks (crop out only just beyond fringes of LdM volcanic field-in Arroyo Pehuenche, Cajón de Troncoso, upper Río Invernada, and west of Los Indios pluton)

Miscellaneous Surficial Deposits

al	alluvium (Holocene and Pleistocene), locally pumice-rich
cl	colluvium (Holocene and Pleistocene; mapped only where bedrock relations are extensively obscured; actually ubiquitous as talus, scree, and slope-mantling debris)
lm	lake mud (peripheral to Laguna del Maule; exposed at shoreline during seasonal drawdown; also deposited as high as 200 m above modern lake level during late Pleistocene highstand
ls	landslides, slumps (Holocene and Pleistocene)
s	surficial deposits, undivided (Holocene; generally mixed areas of till, colluvium, pumice scree); includes beach deposits predominantly of reworked rhyolitic pumice and crystal sand
t	till (Late Pleistocene and Neoglacial; includes moraines, formless glacial deposits, and subordinate reworked gravels.

* Units are listed by (generally 3- or 4-letter) code within each of the five main age groups, first by composition (b, m, a, d, rd, r, ig) and then alphabetically, where **b**=basalt, **m**=mafic andesite, **a**=silicic andesite, **d**=dacite, **rd**=rhyodacite, **r**=rhyolite, and **ig**=ignimbrite.

† Locations are simplified to 100 m using the Universal Transverse Mercator (UTM) grid, which is shown on the IGM topographic maps of the area. The first three digits are easting, and the second three are northing. For example, the dam at the outlet of Laguna del Maule would be approximated as 599/135; *i.e.,* 59.9 km east, 13.5 km north.

APPENDIX 2. MAJOR ELEMENT DATA BY XRF.

LdM-#	Unit Label	SiO_2	TiO_2	Al_2O_3	FeO*	MnO	MgO	CaO	Na_2O	K_2O	P_2O_5	LOI	Original total
Main data are in order of compositional groups (r, rd, d. a, m, ig, Tv)													
195	ram	73.3	0.30	13.99	1.60	0.07	0.43	1.35	4.24	4.26	0.07	2.08	97.56
398	ram	73.2	0.29	14.22	1.53	0.07	0.43	1.30	4.23	4.25	0.10	2.41	96.69
199	rap	75.7	0.18	13.27	0.88	0.06	0.11	0.66	4.26	4.43	0.05	1.10	98.29
212	ras	73.6	0.31	14.0	1.47	0.07	0.35	1.10	4.49	4.18	0.07	0.31	99.08
58	rca	74.1	0.22	13.95	1.16	0.07	0.10	0.55	4.42	5.02	0.05	0.31	99.25
301	rca	74.3	0.21	13.80	1.11	0.08	0.12	0.58	4.43	4.96	0.05	0.33	99.00
415	rca	74.3	0.21	14.00	0.90	0.03	0.12	0.55	4.35	5.08	0.06	0.51	98.68
206	rcb	74.1	0.23	14.08	1.07	0.08	0.18	0.75	4.88	4.14	0.05	0.27	99.03
208	rcb	74.1	0.23	14.08	1.09	0.08	0.20	0.75	4.84	4.15	0.05	0.33	99.03
210	rcb	74.0	0.24	14.14	1.10	0.08	0.19	0.77	4.87	4.13	0.06	0.33	99.31
358	rcb	73.8	0.25	14.17	1.13	0.08	0.27	0.83	4.87	4.06	0.09	0.29	99.50
360	rcb	74.0	0.23	14.14	1.05	0.08	0.24	0.76	4.91	4.11	0.09	0.31	99.51
500	rcb	73.9	0.25	14.18	1.11	0.08	0.21	0.83	4.88	4.08	0.06	0.30	99.45
249A	rcd	74.1	0.25	14.00	1.13	0.08	0.25	0.73	4.79	4.18	0.07	0.41	98.90
351	rcd	74.2	0.25	14.01	1.11	0.08	0.24	0.73	4.82	4.13	0.10	0.38	99.35
247B	rcl	73.6	0.26	14.30	1.18	0.08	0.28	0.89	4.86	4.07	0.07	0.30	98.91
253	rcl	73.7	0.26	14.28	1.15	0.08	0.25	0.87	4.84	4.08	0.07	0.44	98.37
254A	rcl	73.8	0.26	14.21	1.16	0.08	0.27	0.87	4.84	4.07	0.07	0.36	98.83
348	rcl	73.6	0.26	14.26	1.16	0.08	0.29	0.89	4.89	4.04	0.10	0.26	99.56
417 pum fall	rcl	73.5	0.26	14.59	1.17	0.08	0.22	0.84	4.83	4.03	0.04	2.65	97.19
48	rcn	76.0	0.19	13.00	0.91	0.06	0.13	0.66	3.94	4.70	0.05	1.01	98.87
49	rcn	76.9	0.17	12.51	0.78	0.03	0.10	0.54	3.62	4.91	0.05	0.30	99.49
50	rcn	75.5	0.20	13.26	1.01	0.06	0.13	0.70	4.08	4.60	0.05	0.45	99.18
52	rcn	77.6	0.13	12.24	0.59	0.04	0.10	0.48	3.58	4.82	0.05	0.34	99.25
350	rcn	75.3	0.20	13.30	1.03	0.05	0.17	0.71	4.11	4.58	0.09	0.32	99.40
352	rcn	75.4	0.21	13.21	0.99	0.06	0.22	0.75	4.14	4.58	0.08	0.34	99.56
279	reb	74.8	0.21	13.90	0.52	0.03	0.08	0.52	4.40	5.05	0.04	0.26	98.90
61	rep	73.5	0.31	14.08	1.50	0.07	0.38	1.28	4.31	4.04	0.08	1.10	98.32
62	rep	73.5	0.32	13.96	1.53	0.07	0.41	1.27	4.29	4.12	0.08	0.70	98.46
C84-4	rep	73.6	0.29	14.03	1.43	0.06	0.53	1.25	4.22	4.14	0.08	0.69	98.70
86	ret	79.2	0.20	11.05	1.03	0.05	0.25	0.90	3.63	3.27	0.03	-	99.82
102	ret	73.7	0.25	14.15	1.32	0.06	0.33	1.20	4.54	4.01	0.05	-	98.97
94	rez	73.8	0.24	13.95	1.30	0.06	0.33	1.15	4.68	4.00	0.05	-	99.74
119	rez	73.8	0.26	14.12	1.27	0.06	0.29	1.13	4.47	4.09	0.07	0.41	98.75
6	rle	75.6	0.15	13.28	0.79	0.05	0.24	0.62	4.41	4.42	0.05	0.45	98.97
60	rle	75.7	0.18	13.23	0.87	0.07	0.12	0.64	4.27	4.44	0.05	0.73	98.64

Appendix 2. continued.

LdM-#	Unit Label	SiO_2	TiO_2	Al_2O_3	FeO*	MnO	MgO	CaO	Na_2O	K_2O	P_2O_5	LOI	Original total
169	rle	75.8	0.18	13.15	0.87	0.07	0.11	0.65	4.30	4.45	0.05	0.46	99.23
257 pum	rle	75.7	0.17	13.25	0.85	0.06	0.14	0.66	4.22	4.48	0.05	1.14	97.74
272	rle	75.6	0.17	13.23	0.86	0.06	0.16	0.66	4.33	4.44	0.05	0.45	98.63
307 ig pum	rle	76.7	0.15	12.93	0.72	0.05	0.10	0.58	3.71	4.62	0.07	3.27	95.51
422 ig pum	rle	76.4	0.16	13.19	0.77	0.05	0.09	0.58	3.79	4.57	0.05	2.20	97.37
356	rlf	72.7	0.32	14.67	1.46	0.06	0.34	1.24	4.80	3.91	0.12	0.37	99.35
147	rlm	73.0	0.33	14.35	1.68	0.04	0.34	1.30	4.45	4.01	0.11	0.35	98.58
156	rlm	73.0	0.31	13.99	1.71	0.05	0.46	1.37	4.74	3.91	0.06	-	99.73
158	rlm	72.6	0.32	14.04	1.79	0.05	0.56	1.50	4.81	3.89	0.06	-	100.17
161	rlm	73.2	0.29	14.00	1.66	0.06	0.43	1.32	4.69	3.90	0.05	-	99.56
162	rlm	72.7	0.31	14.03	1.76	0.05	0.51	1.46	4.79	3.90	0.06	-	99.86
444	rlm	73.2	0.31	14.14	1.64	0.05	0.42	1.29	4.46	3.96	0.10	0.76	98.50
446	rlm	73.2	0.32	14.10	1.64	0.05	0.40	1.34	4.60	3.91	0.08	0.27	99.64
450	rlm	73.0	0.32	14.09	1.67	0.05	0.41	1.38	4.57	3.99	0.08	0.34	98.82
197	rln	74.0	0.26	14.09	1.21	0.08	0.23	0.79	4.78	4.14	0.06	0.35	98.99
200	rln	73.4	0.26	14.60	1.19	0.08	0.22	0.80	4.89	4.09	0.05	0.39	99.58
205	rln	73.9	0.26	14.18	1.16	0.08	0.21	0.81	4.76	4.12	0.06	1.30	98.33
224 pum	rln	73.8	0.26	14.12	1.18	0.08	0.23	0.85	4.88	4.10	0.06	0.60	98.74
384	rls	72.4	0.27	15.25	1.58	0.06	0.36	1.49	4.99	3.07	0.09	0.58	99.28
202	rnf	74.9	0.28	14.18	1.12	0.01	0.34	0.90	3.11	4.66	0.05	2.79	96.56
501	rng	73.5	0.26	14.41	1.15	0.08	0.22	0.92	4.88	4.06	0.08	1.22	98.42
236	rpp	74.4	0.21	14.00	0.99	0.07	0.20	0.66	4.79	4.22	0.05	0.22	98.92
248	rsl	75.1	0.18	13.69	0.85	0.07	0.16	0.54	4.63	4.36	0.05	1.33	97.52
209	rdac	71.7	0.39	14.80	1.88	0.08	0.51	1.46	4.71	3.98	0.09	0.24	99.60
213	rdac	71.6	0.41	14.75	1.95	0.08	0.54	1.49	4.68	3.96	0.10	0.30	99.28
196	rdam	69.7	0.45	15.45	2.54	0.08	0.78	2.20	4.47	3.82	0.15	2.06	97.36
309	rdam	72.5	0.32	14.41	1.71	0.06	0.46	1.50	4.32	4.18	0.10	1.65	97.86
400	rdam	71.9	0.35	14.80	1.81	0.06	0.56	1.58	4.30	4.09	0.13	2.20	97.10
204	rdap	68.8	0.66	16.07	2.70	0.11	0.86	2.08	5.41	2.67	0.18	4.59	94.36
151	rdcb	68.9	0.47	15.67	2.94	0.07	0.72	2.44	4.84	3.39	0.13	-	98.98
1	rdcd	69.4	0.44	15.41	2.58	0.07	0.97	2.33	4.69	3.57	0.14	0.45	98.87
215	rdcd	70.6	0.41	15.13	2.25	0.08	0.65	1.97	4.64	3.79	0.12	0.31	99.38
216 (W dome)	rdcd	69.4	0.47	15.59	2.53	0.09	0.76	2.22	4.93	3.41	0.17	0.48	99.00
402	rdcd	69.7	0.45	15.31	2.52	0.08	0.84	2.25	4.66	3.60	0.19	0.59	99.14
392	rdcd(i)	53.6	1.22	18.10	8.57	0.14	4.69	8.21	3.72	0.97	0.34	0.35	98.55
402i	rdcd (i)	56.4	1.24	17.59	7.91	0.14	3.38	6.73	4.22	1.56	0.43	1.34	97.77

Appendix 2. continued.

LdM-#	Unit Label	SiO_2	TiO_2	Al_2O_3	FeO*	MnO	MgO	CaO	Na_2O	K_2O	P_2O_5	LOI	Original total
3	rdcn	69.1	0.53	15.43	2.71	0.09	0.92	2.38	5.02	3.29	0.16	0.31	100.07
187	rdcn	68.2	0.59	15.84	2.98	0.10	0.96	2.60	4.95	3.18	0.21	0.40	99.34
329	rdcn	68.7	0.55	15.68	2.82	0.10	0.91	2.40	4.94	3.27	0.19	0.58	98.49
438	rdcp	71.0	0.38	15.09	2.31	0.06	0.57	1.93	4.52	3.70	0.08	0.28	99.01
68	rdcr	71.0	0.37	15.09	1.84	0.08	0.52	1.36	5.33	3.91	0.08		99.91
110	rdcr	70.6	0.39	14.89	2.35	0.08	0.67	1.82	4.68	4.04	0.09		99.58
226	rdct	68.6	0.59	15.63	2.82	0.09	0.96	2.50	4.79	3.44	0.23	0.46	98.80
227	rdct	67.1	0.66	16.14	3.35	0.10	1.16	2.95	4.70	3.21	0.20	1.46	97.50
335	rdct	67.9	0.62	15.94	2.97	0.10	1.06	2.71	4.86	3.26	0.23	1.23	98.16
2	rddm	70.6	0.44	14.94	2.29	0.07	0.76	2.08	4.64	3.68	0.13	0.70	98.67
188	rddm	71.6	0.43	14.67	1.98	0.08	0.58	1.71	4.55	3.84	0.12	1.60	97.76
189	rddm	71.2	0.45	14.87	2.08	0.08	0.60	1.82	4.58	3.76	0.12	0.36	99.13
334	rddp	70.8	0.41	15.70	1.60	0.05	0.27	1.02	5.77	3.81	0.13	0.39	98.59
232	rdep-S	68.7	0.58	15.83	2.71	0.09	0.87	2.38	4.72	3.50	0.18	1.65	97.52
234	rdep-M	67.9	0.63	15.78	3.08	0.09	1.06	2.75	4.82	3.32	0.20	0.84	98.48
389	rdep-N	68.7	0.63	15.78	2.47	0.09	0.98	2.58	4.83	3.30	0.21	0.76	98.73
152	rdes	69.7	0.47	15.48	2.48	0.08	0.78	2.13	4.91	3.42	0.14	0.65	98.44
82	rdet	69.6	0.46	15.85	2.35	0.09	0.56	1.74	5.45	3.43	0.11		99.15
87	rdet	70.0	0.43	15.55	2.22	0.10	0.54	1.65	5.50	3.55	0.10		99.48
89	rdez	69.9	0.47	15.83	2.45	0.06	0.50	1.71	4.54	4.07	0.09		99.23
10	rdla	68.9	0.49	15.85	2.71	0.09	0.78	2.41	5.04	3.18	0.14		99.10
11	rdla	64.3	0.67	16.26	4.38	0.09	2.00	4.21	4.72	2.76	0.18	1.25	98.01
39	rdla	68.9	0.51	15.73	2.75	0.08	0.82	2.30	5.17	3.26	0.14	0.46	98.80
333	rdla	67.3	0.57	15.88	3.40	0.09	1.32	3.10	4.72	3.09	0.18	1.15	98.16
290	rdne	68.7	0.54	15.48	2.95	0.09	1.12	2.68	4.50	3.36	0.17	1.77	97.59
290i	rdne(i)	53.7	1.19	18.61	8.43	0.15	4.13	8.00	3.77	1.28	0.35	1.35	97.61
273	rdno	69.1	0.53	15.30	2.82	0.09	1.01	2.56	4.61	3.38	0.18	1.97	96.98
275	rdno	69.9	0.49	15.28	2.45	0.08	0.83	2.22	4.67	3.54	0.18	0.13	98.51
217	rdnp	68.3	0.54	15.82	2.90	0.10	0.95	2.61	4.89	3.26	0.20	1.14	98.24
220	rdnp	69.0	0.50	15.68	2.62	0.10	0.84	2.37	4.98	3.34	0.17	0.89	98.44
4	rdop	71.3	0.41	14.81	1.93	0.07	0.71	1.70	4.74	3.76	0.11	0.65	98.83
63	rdop	71.6	0.42	14.72	1.98	0.08	0.58	1.73	4.57	3.83	0.12	0.41	98.82
64	rdop	71.6	0.43	14.75	2.02	0.08	0.57	1.72	4.51	3.81	0.12	1.44	97.93
101	rdpñ	70.4	0.39	14.88	2.32	0.08	0.68	1.82	4.91	4.02	0.10		99.57
116	rdpñ	70.4	0.41	15.02	2.35	0.07	0.68	1.81	4.69	4.09	0.11	0.30	98.80
185	rdsp	70.6	0.43	15.13	2.24	0.09	0.65	1.89	4.88	3.55	0.10	0.20	99.40

Appendix 2. continued.

LdM-#	Unit Label	SiO_2	TiO_2	Al_2O_3	FeO*	MnO	MgO	CaO	Na_2O	K_2O	P_2O_5	LOI	Original total
192 pum	rdsp	70.1	0.44	15.90	2.11	0.09	0.56	1.88	4.87	3.50	0.13	3.08	96.46
123	rdvc	70.3	0.46	14.98	2.43	0.07	0.64	1.73	4.81	4.12	0.09	-	99.27
124	rdvc	71.2	0.38	15.08	1.98	0.03	0.45	1.45	4.70	4.28	0.06	-	99.43
103	dab	65.1	0.64	16.69	3.81	0.10	1.49	3.48	4.99	3.09	0.18	-	99.21
104	dab	67.7	0.53	15.73	3.34	0.08	1.15	2.73	4.70	3.46	0.14	-	99.43
107	dab	64.5	0.78	16.63	4.12	0.10	1.49	3.56	5.04	3.11	0.23	-	99.71
108	dab	62.4	0.87	16.92	4.98	0.11	2.01	4.50	4.75	2.75	0.27	-	99.13
491	dab	69.3	0.42	15.79	2.70	0.07	0.98	2.60	4.38	3.22	0.15	2.29	97.38
7	dcc	65.5	0.60	16.26	4.03	0.09	1.74	4.22	4.26	2.78	0.16	-	99.09
453	dcc	64.9	0.64	16.38	4.10	0.09	1.89	4.35	4.39	2.70	0.18	0.28	99.00
457	dcc	63.4	0.67	16.64	4.42	0.09	2.37	5.08	4.16	2.54	0.17	0.94	98.62
319	dcr	65.1	0.86	16.57	3.84	0.10	1.36	3.28	5.32	2.84	0.30	0.11	99.05
319i	dcr(i)	53.0	1.13	18.66	8.71	0.15	4.81	8.15	3.61	1.14	0.26	0.16	99.15
345	dct	63.2	0.98	16.41	5.04	0.10	1.89	4.41	4.54	2.64	0.39	0.15	99.28
374	det	65.5	0.66	16.73	3.78	0.12	1.21	3.19	5.28	2.95	0.22	0.40	99.09
375	det	63.9	0.71	17.10	4.25	0.11	1.73	3.79	5.01	2.74	0.26	0.65	98.63
198	dlf	61.7	0.93	16.63	5.92	0.12	2.19	4.61	4.53	2.70	0.23	-	99.06
338-B	dlf	65.1	0.63	16.90	3.92	0.15	1.32	3.64	5.28	2.32	0.33	1.35	98.24
357	dlf	63.0	1.12	16.13	5.57	0.13	1.83	4.15	4.53	2.78	0.38	2.44	97.63
359	dlf	64.1	0.91	16.51	5.02	0.10	1.35	3.63	4.69	2.97	0.32	0.86	98.55
225	dlp	64.3	0.85	16.80	4.04	0.11	1.53	3.83	5.03	2.78	0.30	-	99.28
229	dlp	63.0	0.92	16.95	4.53	0.12	1.82	4.30	4.98	2.60	0.35	-	99.29
235	dlp	63.4	0.94	16.92	4.49	0.11	1.69	4.27	4.82	2.63	0.37	0.27	98.89
343	dlp	61.8	1.01	17.09	5.07	0.11	2.13	4.74	4.79	2.45	0.43	0.05	99.55
344	dlp	64.1	0.87	16.86	4.16	0.11	1.61	3.89	4.89	2.76	0.35	0.41	99.27
383	dpr	62.8	0.96	17.06	4.67	0.11	1.87	4.41	4.83	2.57	0.35	0.00	99.82
261	dsm	66.0	0.78	16.21	3.72	0.10	1.30	3.20	4.78	3.29	0.26	0.19	98.91
180	dsp	65.6	0.59	16.46	3.91	0.09	1.53	3.61	4.12	3.50	0.19	1.41	97.68
115	dvñ	65.7	0.59	16.63	3.65	0.08	1.36	3.38	4.39	3.67	0.16	0.79	98.24
38	aab	59.3	0.83	17.63	5.91	0.12	2.93	6.31	4.37	1.99	0.21	0.08	99.42
164	aab	55.0	1.05	17.80	7.50	0.13	4.93	7.50	3.88	1.42	0.37		99.41
420	aab	61.4	0.81	17.41	5.33	0.12	2.42	5.20	4.51	2.23	0.21	0.55	99.59
193	aam	57.9	1.00	16.92	6.79	0.12	3.80	7.46	3.60	1.83	0.20	< 0.01	99.46
194	aam	58.8	1.17	16.90	6.83	0.13	2.85	6.12	4.35	2.05	0.39	-	98.95
223	aan	57.0	1.11	17.56	6.89	0.12	3.63	7.33	3.88	1.68	0.39	0.37	98.69
346	aan	59.3	1.03	17.06	6.23	0.11	3.11	6.30	4.06	2.03	0.41	0.65	98.95

Appendix 2. continued.

LdM-#	Unit Label	SiO_2	TiO_2	Al_2O_3	FeO*	MnO	MgO	CaO	Na_2O	K_2O	P_2O_5	LOI	Original total
268	acc	62.2	0.78	17.23	5.24	0.12	2.36	4.96	4.06	2.42	0.22	-	99.55
214	acn	57.1	1.24	16.97	7.61	0.13	3.33	6.77	4.22	1.81	0.40	-	99.18
393	acn	57.5	1.17	17.85	6.69	0.13	3.05	6.61	4.41	1.75	0.46	0.03	99.45
394	acn	57.7	1.18	17.86	6.60	0.13	3.01	6.46	4.38	1.83	0.50	0.74	98.56
401	acn	57.5	1.17	17.88	6.70	0.13	3.06	6.63	4.38	1.74	0.44	0.20	99.54
380	acp	59.0	0.91	17.79	6.47	0.14	3.12	6.85	3.34	1.77	0.19	4.55	95.05
381	acp	59.6	0.90	17.65	6.20	0.12	2.88	6.41	3.45	2.24	0.18	2.50	97.23
379	acr	61.1	0.98	17.47	5.23	0.11	2.31	5.12	4.60	2.33	0.35	0.10	99.43
181	acs	54.1	1.51	16.80	9.81	0.17	3.78	7.28	4.11	1.67	0.33	-	99.18
219	acs	53.2	1.36	17.67	10.20	0.21	3.89	7.74	3.98	1.10	0.25	0.66	98.66
316	acs	56.2	0.95	18.68	7.47	0.18	3.27	6.78	4.19	1.52	0.31	0.66	98.53
317	acs	61.1	0.62	18.24	5.26	0.09	2.04	5.32	4.53	1.96	0.44	1.35	98.23
143	aeb	61.6	1.04	16.79	5.68	0.10	1.97	4.61	4.35	3.11	0.33	0.79	98.46
157	aeb	59.4	0.80	17.59	5.95	0.11	3.29	6.53	3.68	2.13	0.15	0.38	98.50
9	alc	59.6	1.17	16.70	6.98	0.14	2.37	5.48	4.79	2.04	0.34	-	98.92
426	alc	59.3	1.19	16.99	7.02	0.13	2.42	5.51	4.73	2.00	0.34	0.14	99.33
461	alc	59.2	1.17	16.84	7.00	0.14	2.55	5.57	4.66	2.05	0.38	0.74	98.81
5	alm	61.8	0.97	16.70	5.39	0.10	2.34	4.91	4.41	2.62	0.31	0.68	98.41
37	alm	61.2	1.03	16.76	5.65	0.11	2.35	5.04	4.67	2.45	0.35	0.27	99.27
390	alp	60.7	1.03	17.27	5.54	0.11	2.36	5.43	4.46	2.41	0.34	0.30	97.89
386	als	59.6	1.08	17.40	5.91	0.11	2.80	5.66	4.47	2.14	0.44	0.39	99.22
56	alz	62.2	0.95	17.10	5.47	0.20	1.41	4.94	4.38	2.60	0.31	0.81	98.42
255	alz	57.7	1.04	17.19	7.81	0.19	2.93	6.70	3.92	1.82	0.27	1.65	97.32
419	alz	59.5	1.07	17.38	6.69	0.10	2.31	5.80	4.24	2.23	0.26	1.54	98.29
184	ams	61.9	1.13	16.89	5.37	0.12	1.63	4.39	4.82	2.88	0.45	0.19	99.09
191	ams	62.9	1.10	16.47	5.14	0.12	1.56	3.95	4.89	3.08	0.44	0.21	99.20
263	ams	62.2	1.10	16.82	5.30	0.11	1.57	4.22	4.84	2.96	0.45	0.59	98.28
314	ams	62.5	1.17	16.57	5.63	0.12	1.47	4.02	4.80	2.79	0.50	0.82	98.32
315	ams	62.8	1.15	16.41	5.23	0.13	1.62	3.86	4.94	3.00	0.48	0.31	98.75
318	ams	61.0	1.28	16.71	6.04	0.12	1.92	4.57	4.86	2.56	0.58	0.66	98.51
403	anc	59.4	1.06	17.30	6.05	0.11	2.82	6.19	4.20	2.05	0.37	0.28	98.80
430	ans	62.0	0.81	17.03	5.27	0.11	2.44	4.84	4.54	2.31	0.22	0.18	99.53
238	apg	62.3	0.87	16.95	5.23	0.15	1.83	4.28	5.16	2.44	0.40	-	99.33
244	apg	59.4	0.85	18.16	6.38	0.11	2.05	5.30	4.63	2.42	0.31	-	99.39
256	apg	54.9	1.11	17.83	8.21	0.16	3.32	8.46	3.73	1.57	0.30	2.85	96.10
221	apj	58.5	1.04	18.20	5.91	0.13	2.75	6.47	4.36	1.89	0.38	-	99.31

Appendix 2. continued.

LdM-#	Unit Label	SiO_2	TiO_2	Al_2O_3	FeO*	MnO	MgO	CaO	Na_2O	K_2O	P_2O_5	LOI	Original total
222	apj	58.8	0.97	18.09	5.75	0.12	2.80	6.45	4.33	1.92	0.35	0.71	98.55
395	apj	58.1	1.01	18.32	5.95	0.12	2.89	6.77	4.20	1.83	0.40	1.02	98.19
C84-5	apj	58.7	0.97	17.78	6.03	0.11	3.14	6.59	4.05	1.94	0.29	0.70	98.59
117	apñ	57.9	0.90	16.99	6.70	0.12	4.49	6.52	3.66	1.98	0.28	0.56	98.49
118	apñ	56.2	0.98	17.36	7.26	0.12	4.90	7.16	3.66	1.71	0.29	0.04	99.07
353	apo	59.5	1.14	16.90	6.46	0.11	2.76	5.90	4.32	2.10	0.43	-0.05	99.49
C84-6	apv	57.9	1.14	17.85	6.56	0.12	3.08	6.56	4.20	1.78	0.44	0.04	99.32
340	arp	61.9	0.88	17.29	5.27	0.15	1.85	4.44	5.16	2.20	0.50	0.34	99.15
341	arp	60.6	1.17	16.89	6.33	0.13	2.27	4.94	4.72	2.15	0.39	0.79	98.72
342	arp	61.9	0.87	17.29	5.24	0.15	1.96	4.40	5.11	2.21	0.50	0.42	98.17
111	ars	61.4	0.98	16.92	5.37	0.11	2.26	4.87	4.98	2.38	0.34	-	99.37
372-A	ars	59.6	0.95	17.10	6.00	0.11	3.21	5.89	4.30	2.15	0.28	0.21	99.18
372-B	ars	59.3	0.97	17.15	6.14	0.11	3.32	6.03	4.22	2.09	0.29	0.04	99.46
429	asb	60.4	0.82	17.21	5.71	0.11	3.13	5.59	4.31	2.10	0.23	0.19	98.90
399	asd	62.5	1.04	16.66	5.29	0.11	1.94	4.44	4.64	2.64	0.39	0.85	98.76
262	asm	61.3	0.88	16.74	5.79	0.11	2.72	5.13	4.25	2.39	0.28	0.85	98.15
186	asp	59.1	1.21	16.29	7.65	0.15	2.81	5.77	4.45	1.94	0.23	-	99.23
34	ava	56.8	1.19	17.98	7.59	0.15	2.48	7.14	4.11	1.89	0.29	0.85	98.59
55	ava	57.0	1.14	17.86	7.59	0.15	2.78	7.60	3.87	1.35	0.30	1.63	97.57
55	ava	56.9	1.12	17.88	7.56	0.15	2.75	7.58	4.06	1.35	0.28	-	99.58
57	ava	64.0	1.00	16.51	4.19	0.12	1.60	4.17	4.42	3.21	0.38	1.55	97.74
170	ava	59.3	1.21	16.96	6.69	0.14	2.38	5.95	4.29	2.38	0.33	1.17	98.66
280	ava	59.6	1.01	16.85	6.93	0.14	2.70	5.91	4.03	2.16	0.28	1.36	98.20
281	ava	67.1	0.43	17.23	3.67	0.10	0.55	3.28	4.32	2.71	0.25	3.15	96.49
297	ava	60.2	1.02	16.90	6.20	0.14	2.73	5.98	3.82	2.32	0.26	1.79	97.48
298	ava	60.3	0.98	16.79	6.57	0.14	2.55	5.70	3.94	2.33	0.26	1.65	97.29
300	ava	53.5	1.04	17.43	8.98	0.21	5.01	8.46	3.46	1.30	0.26	1.20	97.84
302	ava	60.5	1.01	16.84	6.45	0.15	2.41	5.50	3.98	2.46	0.29	1.30	97.96
303	ava	64.0	0.91	16.94	4.51	0.10	1.40	3.88	4.98	2.55	0.36	0.55	99.18
304	ava	64.6	0.79	16.54	4.20	0.08	1.48	3.89	4.58	3.16	0.28	0.30	99.48
305	ava	63.2	0.85	16.59	4.58	0.12	1.96	4.67	4.35	2.95	0.30	1.62	97.99
367	ava	64.1	0.95	16.48	4.99	0.11	1.67	3.79	4.85	2.33	0.37	3.25	95.47
411	ava	58.7	1.06	17.02	7.47	0.12	2.70	6.02	4.13	2.05	0.33	0.62	98.68
412	ava	56.6	1.15	17.44	7.75	0.14	2.94	7.27	4.01	1.97	0.35	1.64	98.03
413	ava	62.1	0.96	17.01	5.60	0.11	1.75	4.89	4.04	2.84	0.29	2.40	97.66
414	ava	59.4	0.89	17.09	6.92	0.16	2.53	6.01	3.43	2.85	0.28	3.10	96.26
C84-3	ava	60.5	1.13	16.24	6.72	0.14	2.31	5.16	4.50	2.52	0.36	0.19	99.38
131	avc	58.6	1.19	16.80	7.53	0.15	2.58	5.63	4.67	2.13	0.36	-	99.24
433	avc	61.0	0.99	16.80	6.19	0.11	2.15	4.89	4.56	2.58	0.33	-0.11	99.88

Appendix 2. continued.

LdM-#	Unit Label	SiO_2	TiO_2	Al_2O_3	FeO*	MnO	MgO	CaO	Na_2O	K_2O	P_2O_5	LOI	Original total
423	avm	62.0	0.76	16.79	5.17	0.11	2.58	5.16	4.39	2.39	0.22	1.25	98.29
427	avm	60.6	0.75	17.08	5.22	0.10	3.33	6.26	3.93	2.18	0.15	1.11	98.43
382	avr	61.9	0.94	17.15	4.95	0.11	2.23	4.82	4.65	2.46	0.37	0.14	99.02
72	avz	60.8	0.81	17.28	5.23	0.11	2.90	5.36	4.42	2.50	0.19	-	99.82
74	avz	56.5	0.98	17.59	6.72	0.12	3.95	7.30	4.28	1.99	0.22	-	99.39
75	avz	59.0	1.07	17.01	6.93	0.13	2.76	5.98	4.38	2.12	0.25	-	99.24
83	avz	53.9	0.87	18.08	7.38	0.14	5.40	8.66	3.73	1.33	0.13	-	99.87
84	avz	53.4	1.10	18.47	7.69	0.13	4.85	8.60	3.86	1.29	0.21	-	99.56
88	avz	61.0	0.88	17.60	5.19	0.10	2.26	5.19	4.64	2.51	0.26	-	99.54
90	avz	57.2	0.89	17.95	6.57	0.13	3.67	7.01	4.16	1.79	0.20	-	99.35
91	avz	54.0	1.08	18.06	7.42	0.13	4.88	8.57	3.78	1.45	0.21	-	99.38
92	avz	57.4	1.05	17.70	7.03	0.13	3.22	6.40	4.38	2.06	0.25	-	99.46
93	avz	59.0	0.94	17.48	6.26	0.12	3.00	5.88	4.43	2.30	0.23	-	99.65
96	avz	57.3	1.00	17.44	6.53	0.12	3.49	6.99	4.47	1.90	0.33	-	99.57
98	avz	57.7	0.91	17.21	6.76	0.12	4.26	6.54	3.81	1.94	0.30	-	99.59
100	avz	59.1	1.08	16.92	6.88	0.14	2.73	5.80	4.51	2.17	0.25	-	99.96
113	avz	54.1	1.07	18.53	7.96	0.14	4.16	7.84	3.87	1.67	0.21	-	98.13
130	avz	57.2	1.06	17.46	7.13	0.12	4.03	6.48	3.97	1.82	0.31	0.67	98.68
155	avz	58.4	0.92	17.26	6.58	0.12	3.49	6.01	4.36	2.25	0.24	-	99.07
163	avz	54.2	1.06	18.55	7.64	0.13	4.43	8.08	3.58	1.65	0.24	0.34	98.78
434	avz	56.4	1.02	18.23	7.09	0.12	3.69	6.93	3.95	1.93	0.23	0.94	98.30
435	avz	52.4	1.13	19.11	8.32	0.14	4.82	8.58	3.61	1.27	0.22	-0.05	99.39
436	avz	54.7	1.07	18.52	7.48	0.13	4.25	7.95	3.74	1.52	0.28	0.51	98.80
441	avz	54.8	1.07	18.37	7.47	0.13	4.27	7.88	3.86	1.53	0.26	-0.10	99.61
442	avz	54.0	1.06	17.55	7.70	0.13	5.51	8.39	3.62	1.44	0.25	0.00	99.20
443	avz	58.1	0.96	17.60	6.49	0.12	3.22	6.92	3.92	1.94	0.30	-0.01	99.20
445	avz	53.6	1.17	17.72	8.42	0.14	5.33	7.80	3.72	1.40	0.33	-0.13	99.40
449	avz	56.2	1.01	16.37	7.36	0.12	5.51	7.08	3.62	2.01	0.35	0.10	98.99
69	mas	53.8	1.07	18.82	8.46	0.15	3.87	8.25	3.94	1.07	0.19	-	99.36
150	mcb	53.5	1.11	17.68	8.39	0.13	5.55	7.85	3.81	1.21	0.33	-	98.75
490	mcb	59.3	0.91	17.19	6.08	0.11	3.47	6.38	3.93	1.99	0.27	0.01	99.46
239	mcc	54.2	1.23	18.00	8.20	0.14	4.55	7.60	3.83	1.48	0.37	0.24	99.06
240	mcc	54.1	1.18	17.85	8.22	0.15	4.16	7.74	4.22	1.56	0.36	-	99.35
241	mcc	54.4	1.20	18.00	8.04	0.14	4.46	7.63	3.88	1.48	0.36	< 0.01	99.05
76	mcf	52.8	0.81	18.95	7.95	0.14	4.97	9.25	3.49	1.08	0.16	-	99.33
77	mcf	55.2	1.08	17.87	8.35	0.16	3.77	7.51	4.13	1.35	0.23	-	99.43
79	mcf	58.8	0.95	17.96	6.08	0.13	2.75	6.25	4.41	2.03	0.23	-	99.32
322	mcf	58.1	1.12	17.89	7.05	0.14	2.71	5.88	4.54	1.74	0.43	0.26	98.95
228	mcp	55.8	1.03	17.93	7.25	0.13	4.15	7.55	3.99	1.51	0.29	-	99.46
231	mcp	53.7	1.06	18.29	7.85	0.14	4.91	8.32	3.82	1.19	0.33	-	99.60
233	mcp	55.5	1.00	17.98	7.18	0.12	4.25	7.60	3.97	1.49	0.27	-	99.47
385	mcp	53.5	1.23	18.13	8.51	0.14	4.45	8.24	3.93	1.20	0.30	-0.14	99.80
388	mcp	55.7	1.03	18.03	7.25	0.12	4.23	7.63	3.79	1.49	0.32	0.29	99.24

Appendix 2. continued.

LdM-#	Unit Label	SiO_2	TiO_2	Al_2O_3	FeO*	MnO	MgO	CaO	Na_2O	K_2O	P_2O_5	LOI	Original total
497	mcr	54.2	1.26	17.25	8.78	0.15	4.56	7.42	3.67	1.92	0.40	0.15	99.27
498	mcr	52.6	1.09	18.39	8.11	0.13	5.87	8.52	3.46	1.08	0.33	0.35	99.20
85	mcs	50.8	1.01	18.52	8.41	0.14	6.15	9.68	3.65	1.11	0.17	-	99.63
105	mcs	57.5	0.96	17.28	6.91	0.12	4.22	6.56	3.83	1.92	0.32	-	99.80
106	mcs	58.2	0.95	17.31	6.52	0.12	3.75	6.46	3.98	2.00	0.33	-	99.49
145	mcs	55.3	1.01	17.68	7.15	0.13	4.80	7.90	3.92	1.44	0.24	-	99.57
146	mcs	49.3	1.03	18.19	9.46	0.16	7.19	10.04	3.25	0.80	0.15	-	99.72
148	mcs	55.0	1.10	18.72	7.23	0.13	3.41	8.10	4.28	1.35	0.26	-	100.10
149	mcs	58.1	0.90	17.67	6.30	0.12	3.59	6.51	4.33	1.80	0.29	-	99.72
153	mcs	54.3	1.09	17.88	7.75	0.14	4.90	8.28	3.63	1.35	0.27	-	99.55
154	mcs	53.0	1.51	18.02	8.19	0.14	4.77	8.36	3.87	1.49	0.28	-	99.36
159	mcs	55.6	1.13	18.66	7.29	0.13	3.07	7.73	4.27	1.44	0.27	-	99.02
447	mcs	54.4	1.03	18.61	7.77	0.13	4.48	7.75	3.82	1.38	0.26	-0.15	99.71
448	mcs	53.7	1.00	18.48	8.12	0.13	5.13	7.79	3.66	1.30	0.26	0.00	99.51
456	mcs	54.8	1.10	19.04	7.23	0.12	3.56	8.26	3.97	1.27	0.28	0.59	98.72
230	mct	53.6	1.06	18.28	7.90	0.14	4.98	8.36	3.76	1.18	0.33	-	99.20
339	mct	53.8	1.07	18.23	7.97	0.14	4.98	8.31	3.55	1.18	0.39	0.28	99.64
35	meb	53.0	1.07	19.57	7.49	0.12	3.94	9.20	3.74	1.18	0.29	0.42	99.25
265	meb	54.9	1.17	17.71	8.14	0.14	4.10	7.68	4.06	1.45	0.30	-	99.19
270	meb	53.2	1.06	19.68	7.41	0.13	3.74	8.98	3.95	1.19	0.27	-	99.34
406	meb	53.1	1.06	19.56	7.43	0.12	4.05	9.16	3.62	1.25	0.27	0.41	99.52
407	meb	53.4	1.06	19.65	7.29	0.13	3.87	8.99	3.72	1.23	0.28	0.04	99.80
425	meb	53.9	1.14	18.74	7.79	0.13	3.96	8.47	3.87	1.31	0.28	-0.10	99.67
454	meb	53.0	1.08	19.45	7.60	0.12	4.35	8.93	3.65	1.14	0.31	0.23	98.90
462	meb	53.6	1.12	18.90	7.71	0.13	4.05	8.64	3.79	1.30	0.32	-0.06	99.29
8	mlc	53.4	1.05	19.23	7.56	0.13	4.15	8.90	3.75	1.19	0.27	-	99.32
455	mlc	59.4	1.19	16.78	7.00	0.13	2.53	5.51	4.69	2.01	0.34	-0.03	99.13
25	mlp	53.1	1.11	18.40	8.17	0.13	4.60	8.76	3.87	1.17	0.30	<.01	99.62
387	mls	56.0	1.18	18.05	7.47	0.13	3.56	7.15	4.15	1.54	0.38	0.47	97.78
336	mlt	52.8	1.24	18.44	8.70	0.15	4.52	8.50	3.85	1.10	0.30	-0.05	99.45
337	mlt	54.3	1.22	17.89	8.35	0.14	4.19	7.91	3.99	1.30	0.32	-0.03	99.21
218	mnp	57.9	1.05	17.20	7.00	0.13	3.49	6.35	4.34	1.83	0.28	-	99.11
218B	mnp	60.3	0.90	16.95	6.04	0.11	3.07	5.70	4.07	2.18	0.26	0.41	98.73
391	mnp	57.6	1.07	17.34	7.16	0.13	3.52	6.42	4.29	1.76	0.30	-0.08	97.59
282	mor	54.2	1.51	17.55	9.28	0.16	3.63	6.97	4.37	1.47	0.43	-0.20	99.07
283	mor	54.1	1.50	17.59	9.28	0.16	3.66	7.02	4.33	1.49	0.44	-0.05	98.41
510	mor	53.7	1.53	17.54	9.59	0.16	3.76	7.14	4.30	1.42	0.40	-0.25	99.36
506	mpc	58.1	0.93	18.03	6.94	0.13	2.98	6.31	3.96	1.89	0.31	0.86	98.52
508	mpc	54.0	1.01	16.28	8.20	0.16	6.62	8.03	3.12	1.97	0.25	0.95	98.31

Appendix 2. continued.

LdM-#	Unit Label	SiO_2	TiO_2	Al_2O_3	FeO*	MnO	MgO	CaO	Na_2O	K_2O	P_2O_5	LOI	Original total
59	mpl	57.2	1.22	17.49	6.94	0.12	3.44	7.05	3.94	1.81	0.41	0.05	99.10
397	mpl	56.3	1.20	17.74	6.98	0.12	3.74	7.44	3.96	1.70	0.43	0.09	99.20
44	mpn	52.2	1.19	18.49	9.15	0.14	4.30	8.87	3.99	0.96	0.27	0.35	99.13
175	mpn	53.2	1.01	18.83	8.01	0.15	4.77	8.27	3.78	1.30	0.22	-	99.30
176	mpn	54.1	1.21	17.70	8.91	0.15	4.02	7.97	4.08	1.22	0.26	-	99.02
326	mpn	53.4	1.14	18.33	8.61	0.14	4.23	8.45	3.91	1.12	0.29	-0.10	99.61
327	mpn	52.9	1.00	19.19	7.99	0.14	4.79	8.42	3.78	1.10	0.27	-0.04	99.78
488	mqf	53.7	1.25	17.96	8.43	0.14	4.75	8.09	3.75	1.16	0.36	0.67	98.91
459	mrb	54.4	1.21	17.53	7.97	0.13	4.88	7.78	3.84	1.47	0.42	-0.06	99.45
460	mrb	54.1	1.16	18.20	7.98	0.13	4.23	8.51	3.61	1.38	0.29	1.45	97.65
28	msm	53.7	1.34	17.57	9.31	0.17	3.98	7.94	4.08	1.24	0.28	<0.01	99.22
36	msm	55.6	1.17	17.75	8.08	0.13	3.54	7.42	4.11	1.56	0.29	0.55	98.78
65	msm	54.9	1.27	17.64	8.59	0.16	3.76	7.45	4.18	1.40	0.29	-	99.67
65	msm	54.9	1.29	17.64	8.71	0.16	3.76	7.43	3.97	1.39	0.30	0.19	98.80
271	msm	55.3	1.19	17.77	8.25	0.14	3.63	7.38	4.15	1.48	0.30	-	99.31
274	msm	51.8	1.12	19.37	8.58	0.16	4.64	9.13	3.61	0.97	0.22	-	99.23
291	msm	57.0	1.04	17.77	7.22	0.14	3.42	7.09	3.97	1.69	0.29	0.66	98.56
292	msm	55.3	1.07	18.24	7.73	0.12	3.89	7.67	3.89	1.42	0.28	0.14	99.32
306	msm	54.8	1.23	17.97	8.39	0.14	3.71	7.49	4.03	1.45	0.35	0.16	99.43
408	msm	54.5	1.19	18.34	8.34	0.13	3.96	7.59	3.88	1.36	0.35	0.67	98.66
409	msm	56.4	1.27	17.32	8.11	0.16	3.42	6.81	4.27	1.53	0.36	-0.11	99.63
458	msm	53.3	1.19	18.38	8.41	0.14	4.32	8.51	3.89	1.12	0.30	-0.14	99.22
177	msp	55.9	1.11	17.18	8.56	0.16	3.62	7.20	3.94	1.58	0.29	0.10	99.12
178	msp	55.9	1.10	17.15	8.51	0.17	3.62	7.26	3.91	1.76	0.23	-	99.08
179	msp	54.0	1.06	18.80	8.25	0.14	4.27	7.49	4.04	1.29	0.26	< 0.01	99.60
311	msp	53.2	0.92	17.86	9.01	0.17	4.94	9.11	3.16	1.07	0.19	0.01	99.21
312	msp	55.0	1.04	18.54	7.87	0.14	3.97	7.13	4.01	1.57	0.28	0.23	98.96
325	msp	56.7	1.00	18.12	7.36	0.13	3.30	6.89	4.18	1.69	0.27	0.71	98.49
40	mva	53.9	1.11	18.26	8.30	0.14	4.27	8.05	3.88	1.44	0.28	0.49	98.73
42	mva	51.4	0.77	15.09	8.10	0.14	10.96	9.36	2.73	0.84	0.19	0.16	99.02
43	mva	54.3	1.00	18.09	8.14	0.14	4.30	8.20	3.98	1.26	0.21	0.44	99.08
45	mva	54.8	1.11	18.31	8.06	0.14	3.80	7.18	4.29	1.57	0.30	0.57	98.46
165	mva	56.1	1.31	16.86	8.87	0.16	3.32	6.81	4.16	1.70	0.29	0.35	98.68
166	mva	54.8	1.36	16.75	9.78	0.18	3.48	7.15	4.47	1.36	0.26	-	99.55
492	mva	53.9	1.04	18.94	8.08	0.14	4.39	7.51	3.93	1.36	0.28	0.72	98.35
80	mvb	53.4	0.97	18.83	7.81	0.14	4.81	8.84	3.42	1.22	0.15	-	99.50
81	mvb	56.2	0.93	18.25	7.39	0.13	3.97	6.82	3.94	1.75	0.23	-	99.71
328	mvb	55.1	0.99	18.58	7.78	0.14	4.10	7.23	3.90	1.49	0.24	0.41	98.27
211	mvc	54.6	1.04	16.93	8.12	0.16	5.09	8.49	3.67	1.28	0.17	-	99.40
354	mvc	56.1	1.00	16.72	7.71	0.14	4.60	8.05	3.61	1.48	0.21	-0.19	99.82
355	mvc	53.5	1.12	18.57	8.25	0.14	4.69	7.75	3.90	1.42	0.32	0.30	99.33

Appendix 2. continued.

LdM-#	Unit Label	SiO_2	TiO_2	Al_2O_3	FeO*	MnO	MgO	CaO	Na_2O	K_2O	P_2O_5	LOI	Original total
237	mvm	54.0	1.06	17.96	8.80	0.16	4.51	7.72	3.56	1.57	0.27	0.40	98.71
242	mvm	53.1	1.20	19.04	8.57	0.15	3.65	8.66	3.78	1.18	0.28	0.31	98.87
243	mvm	50.3	1.03	18.45	9.45	0.16	6.77	9.49	3.06	0.71	0.22	1.60	97.71
277	mvm	53.8	1.08	17.72	8.77	0.16	4.40	8.44	3.54	1.41	0.28	0.66	98.75
278	mvm	54.7	1.16	17.92	8.67	0.15	4.14	7.23	3.84	1.52	0.30	0.32	98.85
369	mvm	54.1	1.13	17.76	8.72	0.16	4.48	7.75	3.77	1.39	0.30	1.19	98.21
95	mvñ	55.0	1.17	17.75	8.01	0.14	4.19	7.68	3.94	1.42	0.33	-	99.50
109	mvñ	51.3	1.23	17.81	8.84	0.15	6.26	8.98	3.51	1.18	0.28	-	99.17
114	mvñ	53.2	0.93	19.85	7.19	0.13	3.79	9.47	3.74	1.15	0.19	-	99.53
122	mvñ	57.0	0.93	17.17	6.97	0.12	4.77	6.79	3.69	1.83	0.29	<0.01	99.18
132	mvñ	54.8	1.00	17.42	7.63	0.13	5.62	7.50	3.70	1.48	0.29	-	99.53
112	mvp	57.3	0.93	17.28	6.68	0.12	4.14	7.01	3.96	1.86	0.28	-	99.29
112	mvp	57.5	0.96	17.23	6.64	0.11	4.24	6.99	3.77	1.84	0.32	<0.01	99.43
120	mvp	55.0	1.06	17.81	7.77	0.13	4.74	7.43	3.84	1.51	0.29	< 0.01	99.01
121	mvp	55.1	1.00	17.99	7.67	0.13	4.77	7.61	3.74	1.35	0.25	< 0.01	99.08
125	mvp	54.8	1.14	17.59	8.26	0.14	4.02	8.16	3.98	1.28	0.24	0.33	98.55
126	mvp	52.7	1.22	18.13	8.28	0.14	5.64	8.25	3.77	1.18	0.31	<0.01	99.45
127	mvp	56.8	1.05	18.16	7.24	0.13	3.03	7.13	4.28	1.51	0.24	0.08	99.76
128	mvp	54.9	1.07	17.78	8.01	0.13	4.93	7.16	3.88	1.44	0.27	-0.21	99.98
129	mvp	59.4	1.17	16.88	6.97	0.13	2.49	5.51	4.73	2.00	0.34	-0.18	99.37
134	mvp	56.8	0.97	18.00	6.92	0.13	3.70	7.24	3.85	1.70	0.24	0.61	98.48
137	mvp	53.0	1.14	18.20	8.15	0.14	5.57	8.15	3.75	1.17	0.29	-	99.29
139	mvp	58.8	1.17	17.06	7.06	0.13	2.56	5.89	4.67	1.90	0.35	<0.01	99.25
140	mvp	53.1	1.13	18.03	8.26	0.14	5.69	8.04	3.84	1.11	0.29	-	99.36
160	mvp	55.3	0.82	17.56	7.18	0.13	5.41	8.07	3.49	1.52	0.12	-	99.30
432	mvp	58.6	0.76	17.17	6.11	0.11	4.35	6.75	3.57	2.01	0.18	0.16	99.01
437	mvp	58.2	0.98	17.67	6.50	0.12	3.16	6.57	4.05	2.02	0.29	0.01	99.32
439	mvp	57.3	1.09	17.63	7.23	0.13	3.46	6.51	4.26	1.72	0.30	-0.26	99.56
440	mvp	58.4	1.05	17.52	6.99	0.12	2.70	6.42	4.43	1.72	0.29	0.11	99.13
33	bbc	52.0	1.21	18.68	8.71	0.14	5.05	8.55	3.83	1.07	0.33	0.11	99.16
294	bbc	52.7	1.20	18.32	8.67	0.14	5.19	8.16	3.77	1.13	0.35	-0.05	98.97
502	bbc	52.3	1.19	18.24	8.80	0.15	5.52	8.37	3.68	1.05	0.31	-0.08	99.05
320	bcf	52.4	1.05	19.40	7.89	0.13	4.87	9.09	3.44	1.06	0.28	-0.15	99.42
321	bcf	52.1	1.02	19.60	7.73	0.13	5.08	9.11	3.45	1.05	0.31	0.00	99.52
324	bcf	51.1	1.01	19.34	8.69	0.15	5.63	9.08	3.55	0.80	0.25	-0.13	99.63
16	bec	51.4	1.06	18.36	9.15	0.14	5.72	9.08	3.58	0.90	0.24	<0.01	99.83
404	bec	52.5	1.16	19.53	8.37	0.13	3.77	9.12	3.65	1.04	0.31	0.19	99.30
405	bec	52.2	1.07	18.42	8.80	0.14	5.35	8.75	3.52	1.02	0.31	0.86	98.68
396C	bec	52.9	1.17	18.20	9.08	0.14	4.56	8.56	3.63	1.09	0.27	0.24	98.90
396E	bec	52.8	1.27	18.48	9.45	0.15	4.44	7.94	3.75	1.08	0.26	1.71	97.28
371	bhc	50.0	1.00	16.59	9.58	0.14	10.30	7.88	3.02	0.83	0.26	-0.07	99.25
377	bhc	51.3	1.05	19.88	7.95	0.12	5.05	10.07	3.13	0.87	0.21	0.12	99.55

Appendix 2. continued.

LdM-#	Unit Label	SiO_2	TiO_2	Al_2O_3	FeO*	MnO	MgO	CaO	Na_2O	K_2O	P_2O_5	LOI	Original total
Quaternary Ignimbrites													
286	igbc	68.9	0.78	15.91	2.85	0.12	0.48	1.81	5.23	3.33	0.20	1.45	97.52
30	igcb	66.2	0.63	16.49	3.33	0.10	1.01	3.04	5.28	3.46	0.18	1.46	97.84
31	igcb	68.3	0.57	15.94	2.79	0.09	0.80	2.17	4.84	3.95	0.16	2.18	96.85
32	igcb	71.4	0.43	14.64	1.77	0.08	0.52	1.18	3.87	5.57	0.09	3.26	95.91
51	igcb?	67.1	0.77	18.51	1.57	0.06	0.27	2.42	5.13	3.49	0.24	1.69	97.93
53A	igcb	70.1	0.55	16.26	1.92	0.03	0.31	1.36	4.75	4.17	0.09	1.31	97.40
54	igcb	71.8	0.47	15.14	1.47	0.03	0.27	0.99	4.51	4.84	0.09	0.76	98.66
284	igcb	72.2	0.39	14.77	1.79	0.09	0.37	0.90	5.05	3.97	0.09	0.48	98.51
C84-2	igcb	70.6	0.51	15.87	2.06	0.02	0.54	1.39	4.15	4.33	0.11	2.32	96.62
428A	igcc	74.2	0.23	13.88	1.15	0.07	0.24	0.85	3.86	5.08	0.07	3.91	95.41
428B	igcc	74.4	0.23	13.76	1.12	0.07	0.20	0.81	4.14	4.76	0.07	3.93	94.93
428C	igcc	74.0	0.25	13.91	1.20	0.07	0.24	0.90	4.43	4.50	0.09	0.80	98.30
485	igcg	74.8	0.19	13.75	1.18	0.09	0.85	0.78	3.60	4.30	0.05	5.06	94.56
486	igcg	75.5	0.17	13.27	1.03	0.08	0.39	0.69	3.95	4.44	0.05	3.86	95.57
509B	igeb	61.6	1.43	16.69	5.54	0.13	1.38	4.28	5.39	2.55	0.66	1.24	97.99
15	igsp	70.2	0.49	15.27	2.31	0.04	0.36	1.48	5.01	4.39	0.09	0.60	98.51
17	igsp	68.1	0.58	17.17	2.35	0.08	0.55	1.39	4.52	4.72	0.10	5.27	93.98
18	igsp	66.0	0.63	16.36	3.95	0.10	1.13	3.27	4.80	3.10	0.22	0.50	98.64
26	igsp	64.3	0.69	16.89	4.43	0.12	1.56	3.81	4.85	2.72	0.23	1.44	97.89
41	igsp	64.8	0.67	16.82	4.27	0.11	1.39	3.53	4.90	2.84	0.22	0.51	98.92
46	igsp	64.6	0.66	16.74	4.26	0.12	1.46	3.80	4.97	2.72	0.23	1.15	98.15
46A	igsp	65.7	0.61	16.62	3.76	0.10	1.28	3.38	4.81	3.08	0.22	2.11	97.11
47	igsp	67.9	0.58	16.02	2.93	0.07	0.86	2.43	4.69	3.98	0.11	2.65	96.34
182	igsp	67.4	0.78	15.64	3.58	0.10	0.75	2.28	4.78	4.10	0.23	0.30	99.36
264A	igsp	67.6	0.79	15.83	3.57	0.09	0.67	2.07	4.86	3.89	0.22	0.79	98.12
264B	igsp	67.5	0.78	15.71	3.50	0.10	0.70	2.28	4.79	4.03	0.21	0.60	98.29
266	igsp	69.9	0.52	15.63	2.53	0.03	0.29	1.38	4.69	4.49	0.10	0.86	98.12
310	igsp	67.3	0.80	15.74	3.64	0.11	0.90	2.37	5.03	3.48	0.24	0.56	98.45
524	igsp	67.7	0.60	16.90	3.11	0.04	0.59	2.29	3.97	4.18	0.17	2.18	97.22
The following are in approximate order of age													
13	QTad	65.9	0.70	16.91	3.72	0.04	0.87	3.09	4.84	3.21	0.30	1.60	98.15
173	QTad	54.5	1.38	17.26	9.34	0.18	3.09	7.75	4.01	1.73	0.36	1.24	98.11
332	QTad	59.9	0.89	17.12	6.16	0.12	2.99	5.77	4.21	2.19	0.25	0.61	98.26
503	QTad	58.4	1.02	17.46	7.18	0.12	2.94	6.26	3.71	2.27	0.26	0.90	98.23
515	QTad	55.0	1.07	17.29	7.53	0.14	5.12	7.62	3.55	1.96	0.29	0.46	98.66
78	Trcf	74.8	0.24	13.42	1.27	0.05	0.24	0.88	4.13	4.59	0.03	-	100.09
323	Trcf	74.8	0.26	13.71	1.07	0.02	0.09	0.86	4.08	4.64	0.06	0.46	98.98

Appendix 2. continued.

LdM-#	Unit Label	SiO_2	TiO_2	Al_2O_3	FeO*	MnO	MgO	CaO	Na_2O	K_2O	P_2O_5	LOI	Original total
12	Trea	76.9	0.17	12.61	0.27	0.02	0.13	0.46	3.14	5.86	0.05	0.56	98.72
23	Trea	76.4	0.17	13.02	0.85	0.02	0.23	0.55	3.55	4.73	0.05	1.40	97.88
27	Trea	72.2	0.21	15.52	1.51	0.09	0.24	1.05	5.40	3.22	0.11	0.99	98.17
168	Trea	75.3	0.20	13.46	1.05	0.06	0.12	0.66	4.46	4.22	0.05	0.31	99.18
269	Trea	75.7	0.20	13.36	0.96	0.02	0.22	0.56	3.33	5.18	0.05	1.66	97.63
330	Trea	77.2	0.16	12.68	0.68	0.02	0.08	0.51	3.41	4.86	0.04	0.60	98.63
331-c	Trea	76.4	0.19	13.22	0.48	0.01	0.10	0.60	3.86	4.72	0.04	0.44	98.80
431	Tiga	76.0	0.19	13.11	1.27	0.07	0.50	0.87	1.48	5.99	0.08	2.72	96.53
525	Tiga	74.7	0.23	14.21	1.70	0.05	0.75	1.11	2.82	3.92	0.13	3.94	95.35
526	Tiga	76.2	0.16	13.12	0.88	0.04	0.13	0.52	3.30	5.19	0.08	1.01	97.92
347	Tdcl	52.4	1.10	18.87	8.59	0.14	4.87	8.47	3.62	1.23	0.28	0.84	98.41
245	Tv	57.2	1.22	17.98	6.94	0.14	2.46	6.48	4.33	2.45	0.37	-	99.01
246	Tv	60.5	0.83	17.81	5.95	0.12	2.28	5.08	4.40	2.33	0.31	0.65	98.45
250	Tv	54.7	1.25	17.76	8.23	0.14	3.68	7.71	3.90	1.89	0.31	-	99.47
487	Tv	52.5	1.16	18.26	9.07	0.15	4.62	9.19	3.46	0.93	0.27	1.85	97.01
496	Tv	59.0	1.00	17.31	7.23	0.13	2.63	5.89	3.91	2.23	0.28	1.27	97.77
C91-8	Tv	64.1	0.63	17.15	5.54	0.22	0.35	4.51	4.22	2.47	0.36	2.72	96.43
22	Tigh	70.7	0.54	15.30	2.49	0.03	0.21	1.65	3.87	4.65	0.11	1.04	98.28
24	Tigh	68.1	0.58	16.50	2.77	0.02	0.41	2.57	4.42	4.06	0.13	1.67	97.78
308	Tigh	67.5	0.81	16.64	3.53	0.03	0.35	2.22	4.43	3.81	0.24	2.33	97.32
483	Tigh	70.3	0.45	15.80	2.10	0.06	0.69	1.64	4.18	4.24	0.11	5.16	93.66
484	Tigh	70.4	0.39	15.28	2.72	0.06	0.39	1.18	4.71	4.39	0.08	1.40	98.11
528A	Tigh	69.8	0.53	15.29	2.58	0.07	0.42	2.21	3.88	4.68	0.14	1.81	97.04
531	Tigh	67.9	0.61	15.68	3.42	0.11	0.87	1.86	4.07	4.87	0.19	1.19	97.82
480	Kgi	58.1	0.66	18.51	5.75	0.12	3.83	5.96	5.75	0.64	0.23	1.45	97.08
481	Kgi	69.1	0.58	15.38	2.96	0.07	0.77	2.10	4.37	4.08	0.17	1.25	97.43
511	Kgi	63.6	0.51	17.27	4.79	0.08	1.85	5.31	4.12	1.85	0.19	0.89	98.35
512	Kgi	54.9	0.84	18.62	7.80	0.17	3.89	8.36	3.66	1.16	0.24	0.66	98.27

All data in weight percent. Determinations in U.S. Geological Survey laboratory at Lakewood, Colorado, supervised by J.E. Taggart. Methods and precision discussed by Taggart *et al.* (1987). **LOI**= weight loss on ignition at 900o C. **FeO***= total iron calculated as FeO (as analyzed): values are mutiplied by 1.03 to better approximate added weight of unanalyzed Fe_2O_3 (in order not to exaggerate SiO_2 content). All values normalized to volatile-free total of 99.6% (leaving 0.4% for trace oxides and halogens). Data are ordered numerically within map units, which are ordered alphabetically within compositional groups-- in sequence rhyolite **(r)**, rhyodacite **(rd)**, dacite **(d)**, andesite **(a)**, mafic andesite **(m)**, basalt **(b)**, ignimbrites **(ig)**, followed by miscellaneous pre-Quaternary units.

APPENDIX 3A. TRACE ELEMENTS BY XRF.

Part A. WDXRF analyses at Universities of Massachusetts and Lausanne.

LdM-#	Unit Label	Rb	Sr	Ba	Y	Zr	Nb	V	Cr	Ni	Zn	Ga	La	Ce	Pb	Th	U
3	rdcn	124.1	283	680	18.3	246	10.6	34	<2	<2	59	18	30	55	15	15	2
4	rdop	150.7	229	723	16.6	217	11.8	20	<2	<2	46	18	32	58	15	18	3
6	rle	181.7	66	662	15.8	132	11.9	4	<2	<2	33	16	32	56	17	22	6
7	dcc	99.6	403	545	15.4	189	6.2	68	18	14	56	18	21	40	17	12	3
8	mlc	30.5	681	368	16.0	135	5.6	183	48	20	74	20	14	33	8	3	0
9	alc	56.6	504	494	22.6	198	7.3	145	3	7	88	20	19	42	12	7	3
10	rdla	93.2	297	647	15.4	249	7.7	27	2	5	49	17	19	39	17	13	4
15	igsp	142.9	164	755	33.3	382	13.1	23	9	<2	39	19	33	67	18	15	3
16	bec	18.8	563	293	16.0	121	4.3	209	82	30	85	21	13	24	4	5	<2
25	mlp	30.1	563	348	16.9	145	5.5	200	60	19	86	21	17	30	8	5	<2
31	igcb	136.8	230	801	35.6	318	13.7	30	<2	<2	65	19	38	72	21	14	2
32	igcb	163.7	127	710	37.4	305	14.8	14	15	<2	51	17	38	72	14	17	4
33	bbc	24.1	606	346	18.3	145	5.8	194	92	47	88	22	16	31	7	4	<2
42	mva	13.2	635	214	13.1	77	2.1	203	654	218	73	18	10	18	5	4	<2
44	mpn	22.2	580	337	17.1	125	4.5	243	40	18	84	22	14	27	7	5	<2
49	rcn	207.7	46	560	16.4	105	12.2	4	2	<2	17	15	33	53	16	26	7
55	ava	54.0	536	476	25.4	150	7.4	180	13	14	81	19	19	42	11	5	2
61	rep	172.2	159	681	15.1	179	11.7	14	<2	<2	34	17	30	54	13	20	5
65	msm	36.2	562	364	23.2	128	5.4	205	7	9	86	20	13	32	8	4	2
68	rdcr	139.6	163	1038	15.2	354	11.1	12	0	3	46	16	37	56	17	18	5
69	mas	21.9	583	321	18.8	95	2.8	197	20	14	75	22	10	26	8	3	1
72	avz	74.6	402	515	20.9	211	5.9	114	23	15	69	18	19	38	17	9	3
74	avz	55.2	616	402	18.6	161	5.5	162	35	23	74	20	20	42	16	10	4
75	avz	64.0	479	462	22.4	181	5.9	180	10	9	88	20	19	39	15	8	3
76	mcf	26.2	643	264	16.4	87	2.7	237	45	35	77	20	11	22	9	4	2
77	mcf	31.3	545	403	20.1	121	4.3	215	22	5	89	19	14	36	10	5	2
78	Trcf	179.9	90	595	14.6	130	10.0	9	0	5	34	13	24	47	23	23	6
79	mcf	58.3	553	430	21.8	156	4.4	137	10	9	73	20	18	33	3	7	4
80	mvb	34.3	627	298	17.0	94	2.8	227	41	31	79	21	10	21	10	5	2
81	mvb	43.2	554	405	17.4	130	5.1	158	1	18	83	20	19	35	12	4	2
82	rdet	105.6	224	692	23.7	287	8.5	13	2	5	57	17	29	57	29	12	4
83	avz	33.4	599	259	15.2	91	3.1	204	73	42	78	19	9	24	10	5	1
84	avz	31.2	741	333	17.3	110	3.4	204	31	26	72	20	16	34	10	6	2
85	mcs	21.7	817	264	16.0	89	2.5	236	73	46	82	21	10	26	11	5	2
86	ret	150.1	156	687	11.0	203	8.4	8	0	3	36	13	19	47	20	18	5

Appendix 3, Part A. continued.

LdM-#	Unit Label	Rb	Sr	Ba	Y	Zr	Nb	V	Cr	Ni	Zn	Ga	La	Ce	Pb	Th	U
87	rdet	109.0	210	692	25.9	290	8.1	13	0	3	54	17	28	54	22	13	4
88	avz	78.1	425	547	24.3	230	6.0	95	18	17	58	18	24	49	12	10	4
89	rdez	148.1	197	675	16.2	278	6.5	30	6	3	35	16	22	39	18	18	6
90	avz	48.5	511	368	19.2	141	4.5	173	33	23	81	19	15	31	12	6	2
91	avz	37.0	766	358	15.7	120	3.4	200	58	36	73	20	17	39	13	8	3
92	avz	62.5	529	459	20.1	173	5.7	138	11	13	66	19	22	43	14	8	3
93	avz	72.7	532	457	21.0	196	6.2	125	8	13	64	19	20	47	15	10	3
94	rez	144.4	156	654	11.8	199	8.5	7	0	4	39	15	20	48	21	17	5
95	mvñ	37.4	606	450	18.6	163	7.7	184	40	22	88	20	27	50	10	4	1
96	avz	60.7	601	538	18.3	200	8.6	147	30	25	72	20	28	55	11	8	3
98	avz	64.6	542	525	18.7	180	7.7	136	77	39	72	19	30	49	11	8	3
100	avz	67.3	479	483	22.3	190	6.7	173	7	6	83	19	18	40	15	9	3
101	rdpñ	146.3	191	630	15.8	272	7.9	23	0	4	49	15	20	48	24	19	6
102	ret	144.7	163	660	12.6	200	7.7	9	0	3	39	14	22	46	20	17	5
103	dab	99.3	335	660	20.9	264	6.4	48	5	3	43	19	22	45	19	13	4
104	dab	115.2	281	636	18.6	274	7.1	43	4	8	45	17	22	44	20	15	5
105	mcs	63.3	535	530	17.1	187	7.9	138	69	34	82	20	25	57	11	8	3
106	mcs	62.6	560	515	17.9	194	8.3	134	53	34	82	19	27	53	13	7	3
107	dab	103.3	348	655	26.5	273	7.6	62	1	11	56	18	34	55	17	13	4
108	dab	85.2	404	626	22.0	247	7.0	88	7	5	55	19	26	51	15	11	4
109	mvñ	22.6	648	356	18.1	110	5.5	209	168	64	91	19	18	36	8	3	1
110	rdcr	146.5	194	633	16.0	277	7.2	22	1	5	47	14	23	45	23	18	6
111	ars	80.3	517	660	21.2	259	10.4	95	14	9	75	19	30	60	13	11	2
112	mvp	61.3	600	506	15.8	170	7.4	124	55	32	64	20	22	47	10	8	2
113	avz	41.7	712	335	18.4	141	4.3	190	14	22	76	20	16	35	13	7	2
114	mvñ	27.0	674	309	18.5	89	2.4	203	31	26	78	20	12	28	11	4	1
123	rdvc	146.6	178	678	23.0	307	7.5	27	5	3	46	17	17	49	27	18	5
124	rdvc	145.4	157	710	18.7	319	6.8	16	3	4	44	15	19	41	29	19	6
131	avc	58.5	480	500	29.8	223	6.6	143	5	6	78	20	22	49	19	6	2
132	mvñ	41.4	601	431	16.4	162	7.2	155	174	69	79	20	22	43	10	6	1
137	mvp	25.2	643	361	15.9	128	6.9	175	102	60	77	21	19	39	6	3	1
140	mvp	32.9	579	395	16.3	125	5.7	155	89	44	68	20	12	31	8	4	1
145	mcs	32.4	577	394	16.5	125	5.3	153	88	47	68	20	19	36	7	5	2
146	mcs	13.7	713	198	15.0	60	2.6	219	81	50	73	20	15	20	7	3	1
148	mcs	33.1	610	360	17.2	133	5.0	175	31	16	72	21	13	33	8	4	1
149	mcs	49.9	587	495	15.5	163	6.8	134	32	24	74	20	21	44	12	6	2
150	mcb	29.9	586	359	15.5	140	6.4	174	128	59	87	18	17	40	6	3	1

Appendix 3, Part A. continued.

LdM-#	Unit Label	Rb	Sr	Ba	Y	Zr	Nb	V	Cr	Ni	Zn	Ga	La	Ce	Pb	Th	U
151	rdcb	117.2	278	665	15.0	239	6.4	32	5	2	37	17	24	44	18	15	5
153	mcs	35.9	540	373	17.4	133	5.1	176	64	39	78	19	15	36	8	5	2
154	mcs	24.5	668	487	18.3	162	7.6	166	46	32	72	21	23	47	8	5	1
155	avz	72.7	463	494	23.0	213	6.8	114	49	30	62	20	23	48	12	9	3
156	rlm	135.0	150	643	12.6	220	7.4	17	0	3	37	14	18	38	20	17	5
158	rlm	132.9	157	630	12.6	218	7.7	22	2	4	39	14	20	39	19	17	5
159	mcs	37.9	591	402	18.2	147	5.5	188	22	17	69	21	17	34	11	5	2
160	mvp	43.4	525	294	15.2	129	3.1	179	95	52	64	18	10	22	6	6	1
161	rlm	133.3	149	641	12.4	217	7.7	14	1	4	38	13	19	39	20	17	5
162	rlm	132.4	153	632	12.8	216	7.4	18	0	5	39	14	21	44	20	17	5
164	aab	37.3	676	484	16.7	188	8.3	163	90	44	86	20	25	55	9	4	2
166	mva	31.8	498	397	24.7	116	4.1	228	0	8	78	23	16	33	11	5	1
175	mpn	26.3	617	329	16.9	101	3.6	201	26	27	82	20	11	26	8	3	1
176	mpn	29.7	549	353	18.5	124	4.9	245	23	13	94	20	14	33	8	4	1
178	msp	44.6	435	416	25.5	149	5.7	208	16	5	82	20	17	41	8	4	3
181	acs	46.9	505	428	26.8	163	6.6	274	19	20	100	20	21	44	11	5	1
186	asp	61.5	396	460	22.7	179	7.4	200	2	11	84	20	33	41	10	8	4
194	aam	62.5	566	575	20.8	222	11.2	164	11	6	93	20	33	63	11	8	3
198	dlf	86.5	383	653	28.3	237	8.8	109	4	5	64	19	26	59	15	11	3
202	rnf	193.5	118	797	14.8	209	10.4	10	15	<2	41	16	33	59	16	21	4
211	mvc	44.0	362	305	20.2	109	4.2	176	102	40	71	17	13	27	6	7	2
214	acn	53.4	593	523	19.1	216	10.9	198	14	15	98	20	30	61	12	7	2
218	mnp	56.4	522	436	18.4	163	6.7	167	19	11	86	20	20	42	11	7	2
221	apj	56.3	574	496	20.7	183	7.9	112	16	7	78	19	25	53	10	7	2
225	dlp	93.5	473	691	21.6	246	10.5	51	5	5	73	19	31	59	14	12	4
228	mcp	44.5	608	459	16.2	149	6.0	181	49	27	91	19	21	42	12	5	2
229	dlp	86.4	504	661	21.3	235	10.2	63	3	2	78	19	29	60	13	10	4
230	mct	29.7	613	391	17.9	140	6.7	183	65	33	88	20	20	39	8	4	1
231	mcp	29.8	617	390	18.4	141	7.2	185	66	35	89	17	20	40	8	4	1
233	mcp	43.6	598	440	15.7	144	6.0	179	51	27	88	19	21	42	10	5	2
238	apg	88.9	469	533	27.6	245	11.4	49	4	4	74	19	27	57	14	10	4
240	mcc	46.2	561	427	20.7	186	8.4	185	58	28	85	20	21	50	9	6	1
243	mvm	10.3	521	231	17.3	93	3.3	230	37	54	88	20	10	19	4	4	<2
244	apg	74.0	504	613	25.8	237	9.6	83	4	7	67	19	30	55	13	7	2
245	Tv	88.6	491	479	28.4	255	10.5	152	8	5	78	21	25	50	14	10	4
249A	rcd	163.4	93	713	18.6	193	13.2	4	<2	<2	45	17	33	65	16	20	5
250	Tv	68.7	514	404	24.5	214	9.2	218	36	15	83	21	21	46	10	9	3

Appendix 3, Part A. continued.

LdM-#	Unit Label	Rb	Sr	Ba	Y	Zr	Nb	V	Cr	Ni	Zn	Ga	La	Ce	Pb	Th	U
253	rcl	157.6	114	712	18.1	204	12.7	7	<2	<2	44	16	31	62	15	19	5
265	meb	37.7	594	437	18.5	157	7.2	202	34	24	84	19	19	44	8	5	2
268	acc	61.2	424	532	19.4	203	6.7	97	20	14	68	18	23	42	15	9	2
270	meb	27.5	685	371	16.0	137	6.0	180	36	13	74	21	17	37	8	4	1
271	msm	42.9	567	418	18.3	144	5.7	185	18	10	75	21	18	40	7	5	2
274	msm	21.7	640	309	18.6	98	3.8	199	30	23	67	20	11	22	8	3	2
279	reb	209.3	44	619	21.4	181	15.2	3	<2	<2	26	17	37	66	19	24	7
286	igbc	93.1	256	757	31.7	310	11.3	33	<2	<2	64	19	28	60	20	11	<2
311	msp	27.0	453	297	20.6	111	4.1	261	34	2	83	21	10	24	5	4	<2
320	bcf	27.7	607	349	16.1	135	5.2	181	47	28	75	22	17	30	5	4	<2
324	bcf	9.4	598	274	17.3	95	3.1	248	32	41	85	21	9	17	5	4	<2
335	rdct	118.2	336	721	20.3	252	12.1	37	<2	<2	60	19	33	66	15	15	<2
336	mlt	25.0	596	344	18.7	143	6.3	236	44	14	92	22	15	28	6	5	<2
356	rlf	136.1	164	907	19.2	263	11.2	8	<2	<2	44	17	36	65	19	17	3
360	rcb	162.5	94	730	18.9	187	13.2	4	<2	<2	45	17	33	64	17	19	5
369	mvm	37.5	486	372	23.1	136	5.9	205	41	18	81	21	16	31	7	5	<2
371	bhc	18.3	562	288	12.9	118	5.1	178	332	202	94	19	13	24	6	4	<2
384	rls	95.3	275	792	13.9	186	9.5	6	<2	<2	54	18	30	58	16	10	<2
387	mls	44.7	576	439	20.6	167	7.6	184	22	6	90	21	21	41	9	7	<2
397	mpl	49.1	651	506	18.3	206	12.0	167	42	16	83	21	27	54	8	8	<2
398	ram	168.5	141	697	15.8	187	11.4	16	<2	<2	38	17	30	55	17	21	5
404	bec	27.2	611	314	17.2	130	4.6	238	23	7	85	22	14	26	5	5	<2
415	rca	205.5	46	660	30.3	184	15.4	2	<2	<2	34	17	44	79	22	23	6
428C	igcc	171.1	100	756	16.7	204	11.5	7	<2	<2	42	16	32	60	21	18	4
446	rim	137.8	154	663	11.9	222	7.4	16	<2	<2	40	16	22	41	21	17	3
460	mrb	42.6	618	395	17.0	156	6.6	207	39	17	84	21	17	34	7	5	<2
486	igcg	146.9	51	638	16.2	104	12.5	6	<2	<2	34	16	20	42	17	13	4
488	mqf	22.5	611	321	16.5	141	5.6	202	48	29	95	21	15	30	6	4	<2
497	mcr	69.5	478	444	30.0	223	7.7	196	65	32	98	22	27	52	13	8	<2
498	mcr	26.3	649	391	15.3	145	6.6	188	133	71	83	21	17	34	6	5	<2
500	rcb	159.6	107	708	18.1	201	12.6	6	3	<2	43	17	32	63	16	19	5
508	mpc	74.4	426	316	23.5	172	7.5	191	271	120	74	19	16	32	10	8	<2
510	mor	32.2	560	419	22.4	186	8.1	215	<2	<2	97	23	20	42	7	6	<2

All abundances in ppm. Determinations at University of Massachusetts and Université de Lausanne by XRF methods of Rhodes (1988). Precision quantified by Rhodes (1996).

APPENDIX 3B. TRACE ELEMENTS BY XRF.

Part B. WDXRF analyses at U.S. Geological Survey laboratories.

LdM-#	Unit Label	Rb	Sr	Ba	Y	Zr	Nb	Cr	Ni	Cu	Zn
37	alm	80	480	590	20	200	10	< 20	< 10	10	70
42	mva	14	640	210	13	65	< 10	640	192	43	69
45	mva	38	590	415	22	136	< 10	< 20	13	50	81
48	rcn	196	70	670	27	140	16	< 10	< 10	< 10	26
49	rcn	220	55	610	26	120	17	< 10	< 10	< 10	18
50	rcn	182	75	740	27	160	15	< 10	< 10	< 10	22
51	igcb?	128	350	820	46	335	15	< 10	< 10	10	42
52	rcn	315	25	66	32	114	21	< 10	< 10	< 10	11
53A	igcb	154	210	750	43	330	12	< 20	< 10	< 10	47
54	igcb	182	138	820	44	320	16	< 10	< 10	< 10	80
55	ava	59	550	480	33	164	10	26	12	43	70
56	ava	92	405	600	38	205	12	< 10	< 10	26	65
57	ava	110	350	690	41	260	15	< 10	< 10	14	113
58	rca	210	58	680	34	190	19	< 10	< 10	< 10	38
59	mpl	62	620	540	28	205	14	39	19	32	79
60	rle	186	72	660	26	136	16	< 10	< 10	< 10	34
61	rep	174	170	670	27	188	16	< 10	< 10	< 10	33
62	rep	174	166	680	26	188	14	< 10	< 10	< 10	38
63	rdop	156	235	700	27	220	15	< 10	< 10	< 10	44
64	rdop	156	230	690	27	218	15	< 10	< 10	< 10	42
65	msm	43	560	400	31	142	10	16	15	22	76
112	mvp	60	590	-	18	174	<10				
115	dvñ	150	340	570	26	270	10	< 20	< 10	12	50
116	rdpñ	152	200	630	20	265	< 10	< 20	< 10	< 10	52
119	rez	150	160	660	18	194	10	< 20	< 10	< 10	38
120	mvp	45	530	425	22	158	< 10	63	39	53	75
121	mvp	40	570	370	20	124	< 10	66	36	50	65
127	mvp	40	541	373	15	145	-	-	-	-	-
128	mvp	40	555	376	13	133	-	-	-	-	-
129	mvp	53	485	448	18	188	-	-	-	-	-
130	avz	57	540	440	20	184	< 10	49	30	36	70
134	mvp	50	600	-	24	148	<10	-	-	-	-
139	mvp	60	520	-	26	180	<10	-	-	-	-
143	aeb	100	405	570	31	295	10	< 20	< 10	35	69
152	rdes	126	270	650	19	255	< 10	< 20	< 10	< 10	49
157	aeb	68	480	415	20	156	< 10	36	15	35	52
163	avz	42	690	360	17	140	< 10	32	21	68	70
165	mva	40	485	415	27	140	< 10	< 20	< 10	19	92
168	Trea	156	68	650	16	140	< 10	< 20	< 10	< 10	31
169	rle	176	62	670	19	126	13	< 20	< 10	< 10	33
170	ava	68	405	540	28	188	< 10	< 20	< 10	42	83
173	Qtad	44	500	440	30	176	< 10	< 20	< 10	35	80
179	msp	30	590	390	20	124	< 10	< 20	13	44	61
182	igsp	126	240	860	39	285	15	< 20	< 10	< 10	68
184	ams	93	405	710	34	240	< 10	< 20	< 10	< 10	59
185	rdsp	132	230	710	19	230	12	< 20	< 10	< 10	50
187	rdcn	114	300	670	21	230	11	< 20	< 10	< 10	62

Appendix 3, Part B. continued.

LdM-#	Unit Label	Rb	Sr	Ba	Y	Zr	Nb	Cr	Ni	Cu	Zn
188	rddm	148	215	700	19	200	12	< 20	< 10	< 10	40
189	rddm	142	225	730	22	205	11	< 20	< 10	< 10	42
191	ams	100	360	740	40	255	10	< 20	< 10	< 10	73
192	rdsp	124	265	710	22	250	12	< 20	< 10	< 10	56
193	aam	63	460	395	21	120	< 10	56	13	40	52
195	ram	162	140	700	21	176	12	< 20	< 10	< 10	33
196	rdam	138	240	720	20	255	12	< 20	< 10	< 10	43
197	rln	152	104	760	22	196	12	< 20	< 10	< 10	43
199	rap	178	68	670	21	132	14	< 20	< 10	< 10	35
200	rln	156	106	740	22	188	12	< 20	< 10	< 10	42
205	rln	154	108	730	20	186	12	< 20	< 10	< 10	41
206	rcb	160	92	750	22	176	11	< 20	< 10	< 10	42
208	rcb	156	93	750	23	182	14	< 20	< 10	< 10	43
209	rdac	160	184	810	20	260	12	< 20	< 10	< 10	43
210	rcb	156	94	750	23	178	13	< 20	< 10	< 10	44
212	ras	170	128	760	22	200	12	< 20	< 10	< 10	38
213	rdac	156	188	820	21	270	12	< 20	< 10	< 10	44
215	rdcd	148	230	760	21	270	10	< 20	< 10	< 10	43
216	rdcd	122	280	730	20	260	11	< 20	< 10	< 10	56
217	rdnp	120	315	700	22	250	11	< 20	< 10	< 10	56
218B	mnp	75	450	475	20	176	< 10	< 20	12	36	66
219	acs	26	530	370	21	104	< 10	22	11	16	74
220	rdnp	124	300	720	20	260	10	< 20	< 10	< 10	53
222	apj	63	550	-	20	186	<10	-	-	-	-
223	aan	52	610	530	21	194	11	50	16	49	75
224	rln	154	110	750	23	118	14	< 20	< 10	< 10	44
226	rdct	124	300	750	23	235	11	< 20	< 10	< 10	52
227	rdct	110	325	710	23	225	12	< 20	< 10	< 10	48
232	rdep	120	295	730	22	235	12	< 20	< 10	< 10	47
234	rdep	118	325	720	23	225	10	< 20	< 10	< 10	52
235	dlp	90	475	680	23	225	< 10	< 20	< 10	< 10	74
236	rpp	168	87	720	24	166	13	< 20	< 10	< 10	33
237	mvm	42	490	385	23	126	< 10	26	26	42	87
239	mcc	35	570	415	21	188	10	82	30	27	73
241	mcc	40	580	425	26	182	< 10	75	31	23	90
242	mvm	20	560	360	27	124	< 10	25	13	36	76
243	mvm	13	520	230	20	87	< 10	43	46	52	73
246	Tv	64	550	590	25	205	< 10	< 20	< 10	14	70
247B	rcl	168	120	710	23	200	14	< 20	< 10	< 10	50
248	rsl	182	60	680	24	132	13	< 20	< 10	< 10	45
249A	rcd	166	90	690	21	188	13	< 20	< 10	< 10	46
253	rcl	162	116	700	23	200	14	< 20	< 10	< 10	47
254A	rcl	164	120	730	22	200	12	< 20	< 10	< 10	50
256	apg	42	480	405	23	136	< 10	41	22	45	72
257	rle	178	65	640	20	128	12	< 20	< 10	< 10	36
261	dsm	126	375	710	25	260	11	< 20	< 10	< 10	46
262	asm	85	430	520	20	190	< 10	< 20	< 10	29	74
263	ams	100	400	710	40	250	< 10	< 20	< 10	10	81

Appendix 3, Part B. continued.

LdM-#	Unit Label	Rb	Sr	Ba	Y	Zr	Nb	Cr	Ni	Cu	Zn
264A	igsp	126	235	840	41	290	14	< 20	< 10	< 10	80
264B	igsp	122	240	790	37	285	11	< 20	< 10	< 10	80
266	igsp	148	156	690	38	365	13	< 20	< 10	< 10	37
269	Trea	230	69	640	20	154	13	< 20	< 10	< 10	30
272	rle	190	70	650	24	130	12	< 20	< 10	< 10	34
273	rdno	126	290	640	20	210	10	< 20	< 10	< 10	61
371	bhc	20	550	283	15	106	-	-	-	-	-
372-A	ars	72	491	567	26	279	11	-	-	-	-
372-B	ars	76	500	574	14	265	13	-	-	-	-
374	det	73	327	892	25	350	-	-	-	-	-
377	bhc	27	655	263	13	104	-	-	-	-	-
379	acr	75	513	593	17	213	13	-	-	-	-
380	acp	49	465	519	25	157	-	-	-	-	-
381	acp	59	392	500	26	158	10	-	-	-	-
383	dpr	87	473	653	22	231	10	-	-	-	-
384	rls	83	263	773	16	174	10	-	-	-	-
387	mls	52	564	414	23	160	15	-	-	-	-
390	mcp	82	491	601	19	226	11	-	-	-	-
391	mnp	57	516	417	22	167	-	-	-	-	-
399	asd	90	441	634	23	250	12	-	-	-	-
401	acn	59	580	472	20	183	-	-	-	-	-
403	anc	70	542	538	19	217	11	-	-	-	-
406	meb	38	661	347	15	134	-	-	-	-	-
407	meb	31	655	353	16	133	-	-	-	-	-
413	ava	83	362	546	30	200	12	-	-	-	-
417	rcl	153	110	694	20	197	12	-	-	-	-
419	ava	68	417	505	36	181	-	-	-	-	-
420	aab	56	439	520	22	180	-	-	-	-	-
422	rle	201	54	558	21	90	11	-	-	-	-
423	avm	81	417	476	14	175	-	-	-	-	-
425	meb	39	629	372	15	141	-	-	-	-	-
426	alc	58	491	469	21	188	11	-	-	-	-
427	avm	78	462	414		144	-	-	-	-	-
429	asb	68	448	463	17	181	-	-	-	-	-
430	ans	62	417	504	20	189	-	-	-	-	-
433	avc	81	437	525	28	249	10	-	-	-	-
434	avz	62	595	359	16	170	-	-	-	-	-
435	avz	36	743	300	15	121	-	-	-	-	-
437	mvp	63	483	439	18	185	-	-	-	-	-
438	rdcp	131	219	626	18	222	-	-	-	-	-
439	mvp	45	526	403	21	170	11	-	-	-	-

All abundances in ppm. Determinations in U.S. Geological Survey laboratories at Menlo Park, California, and Reston, Virginia; principal analyst B.-S. L. King. Methods and precision discussed in Taggart *et al.* (1987).

APPENDIX 3C. TRACE ELEMENTS BY XRF.

Part C. EDXRF analyses at U.S. Geological Survey, Menlo Park, California.

LdM-#	Unit Label	Rb	Sr	Ba	Y	Zr	Nb
1	rdcd	136	269	704	24	260	12
2	rddm	143	250	678	23	208	11
3	rdcn	122	273	655	22	223	10
4	rdop	145	224	679	22	201	11
5	alm	87	454	591	22	199	6
6	rle	179	70	661	22	126	9
11	rdla	76	356	526	19	193	5
12	Trea	251	52	574	18	136	8
15	igsp	130	154	723	33	345	8
16	bec	18	549	269	16	113	4
18	igsp	105	314	734	33	240	9
22	Tigh	171	182	693	27	297	11
23	Trea	183	59	595	20	140	8
24	Tigh	147	263	674	32	327	12
25	mlp	30	554	319	19	134	3
26	igsp	78	401	718	31	229	9
27	Trea	99	184	730	21	220	10
28	msm	41	555	316	24	128	4
30	igcb	111	304	747	33	277	8
31	igcb	130	229	752	37	285	10
32	igcb	165	119	694	34	274	12
33	bbc	30	599	309	20	138	3
34	ava	58	469	450	30	159	8
35	meb	28	646	342	15	141	7
36	msm	42	544	388	18	148	5
38	aab	59	501	458	24	167	5
39	rdla	95	280	642	18	227	8
40	mva	36	573	363	19	125	5
41	igsp	103	349	680	28	237	9
43	mva	21	567	289	19	99	2
44	mpn	19	578	323	20	119	3
46	igsp	89	361	675	26	231	6
46A	igsp	106	329	640	26	242	9
47	igsp	122	230	687	29	309	6
118	apñ	59	541	433	17	164	-
127	mvp	40	541	373	15	145	-
128	mvp	40	555	376	13	133	-
129	mvp	53	485	448	18	188	-
147	rlm	131	149	686	12	203	-
180	dsp	92	327	-	-	194	-
202	rnf	179	123	805	19	198	11
204	rdap	76	211	818	40	318	10
258	gr erratic	217	123	625	29	229	-
275	rdno	125	269	704	19	205	11
283	mor	36	552	-	-	174	-
290i	rdne (i)	38	587	-	-	138	-
307	rle	192	52	538	19	87	14
314	acs	80	407	-	-	253	-

Appendix 3, Part C. continued.

LdM-#	Unit Label	Rb	Sr	Ba	Y	Zr	Nb
315	ams	81	360	-	-	246	-
329	rdcn	113	281	-	-	224	-
334	rddp	123	161	-	-	357	-
342	arp	64	482	-	-	173	-
367	ava	75	368	-	-	222	-
371	bhc	20	550	283	15	106	-
372-A	ars	72	491	567	26	279	11
372-B	ars	76	500	574	14	265	13
374	det	73	327	892	25	350	-
375	det	71	329	837	22	336	12
377	bhc	27	655	263	13	104	-
379	acr	75	513	593	17	213	13
380	acp	49	465	519	25	157	-
381	acp	59	392	500	26	158	10
382	avr	83	476	609	16	219	10
383	dpr	87	473	653	22	231	10
384	rls	83	263	773	16	174	10
385	mcp	34	578	316	18	145	-
386	als	74	525	545	19	192	-
387	mls	52	564	414	23	160	15
388	mcp	48	563	429	15	147	-
389	rdep	113	318	711	22	235	12
390	alp	82	491	601	19	226	11
391	mnp	57	516	417	22	167	-
392	rdcd (i)	23	610	307	16	115	-
393	acn	57	557	455	16	174	-
394	acn	59	554	487	20	174	7
395	apj	57	562	477	20	173	9
396C	bec	30	535	313	17	109	-
396E	bec	28	513	318	18	121	-
397	mpl	51	651	486	19	194	13
398	ram	166	143	696	17	175	10
399	asd	90	441	634	23	250	12
400	rdam	159	188	750	18	242	9
401	acn	59	580	472	20	183	-
402	rdcd	135	248	712	20	259	7
402i	rdcd (i)	42	565	394	18	141	10
403	anc	70	542	538	19	217	11
404	bec	32	605	304	15	112	7
405	bec	29	553	290	13	111	10
406	meb	38	661	347	15	134	-
407	meb	31	655	353	16	133	-
408	msm	37	568	415	20	140	9
409	msm	43	527	424	20	129	5
411	ava	65	425	503	27	172	6
412	ava	55	444	715	23	147	9
413	ava	83	362	546	30	200	12
414	ava	84	399	483	31	186	11

Appendix 3, Part C. continued.

LdM-#	Unit Label	Rb	Sr	Ba	Y	Zr	Nb
415	rca	187	44	661	30	168	13
417	rcl pum	153	110	694	20	197	12
419	ava	68	417	505	36	181	-
420	aab	56	439	520	22	180	-
422	rle pum	201	54	558	21	90	11
423	avm	81	417	476	14	175	-
425	meb	39	629	372	15	141	-
426	alc	58	491	469	21	188	11
427	avm	78	462	414	<10 (9)	144	-
428A	igcc	174	95	690	21	175	11
428B	igcc	155	80	698	17	161	8
428C	igcc	162	100	755	16	191	11
429	asb	68	448	463	17	181	-
430	ans	62	417	504	20	189	-
431	Tiga	103	116	612	16	111	11
432	mvp	65	440	354	15	145	8
433	avc?	81	437	525	28	249	10
434	avz	62	595	359	16	170	-
435	avz	36	743	300	15	121	-
436	avz	45	689	330	16	139	3
437	mvp	63	483	439	18	185	-
438	rdcp	131	219	626	18	222	-
439	mvp	45	526	403	21	170	11
440	mvp	46	509	402	20	145	10
441	avz	50	688	323	19	140	-
442	avz	43	722	351	17	127	6
443	avz	67	486	414	16	185	-
444	rlm	137	149	671	13	208	7
445	avz	29	541	371	22	166	11
446	rlm	128	152	654	17	208	-
447	mcs	38	576	341	18	138	-
448	mcs	40	572	323	12	135	-
449	avz	63	463	407	21	198	8
450	rlm	132	150	696	14	213	-
453	dcc	97	396	525	10	180	10
454	meb	29	642	351	13	144	10
455	mlc	62	498	497	26	190	-
456	mcs	35	603	329	22	137	-
457	dcc	89	408	494	18	136	-
458	msm	32	586	344	17	134	-
459	mrb	49	633	450	18	196	11
460	mrb	46	601	374	18	136	-
461	alc	57	486	458	27	193	-
462	meb	37	632	362	17	145	11
480	Kgi	25	485	157	17	130	-
481	Kgi	131	207	717	29	287	12
483	Tigh	119	132	729	31	313	13
484	Tigh	136	134	804	38	342	10

Appendix 3, Part C. continued.

LdM-#	Unit Label	Rb	Sr	Ba	Y	Zr	Nb
485	igcg	138	67	628	18	98	15
486	igcg	138	55	618	19	88	11
488	baqf	31	590	290	17	123	-
490	mcb	61	536	498	11	154	-
491	dab	107	298	631	18	187	-
492	mva	36	601	357	14	122	-
497	mcr	75	478	411	29	219	-
498	mcr	31	649	363	13	142	-
500	rcb	145	102	715	23	194	12
501	rng	142	124	752	15	212	-
502	bbc	24	568	321	18	121	-
503	Qtad	86	406	410	28	202	11
506	bapc	52	582	529	20	179	13
508	bapc	70	413	288	23	164	10
509B	igeb	65	405	552	32	185	-
510	mor	36	560	398	23	172	10
511	Kgi	30	488	578	14	160	-
512	Kgi	37	438	330	21	127	11
515	QTad	65	498	358	25	186	-
522	Tiga	90	361	575	28	230	9
524	igsp	155	240	728	35	340	14
525	Tiga	142	159	437	33	80	24
526	Tiga	211	58	634	18	115	11
528A	Tigh	181	193	740	30	323	14
531	Tigh	160	211	853	26	280	11
C84-2	igcb	156	177	734	35	289	13
C84-3	ava	77	378	529	31	205	6
C84-4	rep	169	157	652	20	169	10
C84-5	apj	59	529	496	24	185	7
C84-6	apv	53	556	455	25	184	5

All abundances in ppm. Determinations by energy-dispersive x-ray fluorescence spectrometry at U.S. Geological Survey, Menlo Park, California; P. Bruggman, analyst. Methods and precision discussed by Johnson and King (1987) and Bacon and Druitt (1988).

IENT DATA BY INAA FOR LAGUNA DEL MAULE VOLCANIC FIELD.

Ba	Co	Cr	Cs	Hf	Rb	Sb	Ta	Th	U	Zn	Zr	Sc	La	Ce	Nd	Sm	Eu	Gd	Tb
699	3.4	2	4.80	6.2	132	0.33	0.96	18.6	4.5	49	300	4.6	28.3	54.1	21.0	3.74	0.83	3.8	0.4
712	2.8	3	4.08	5.3	140	0.25	1.07	17.9	4.2	51	260	5.2	31.9	61.2	24.7	4.44	0.95	5.7	0.4
694	2.9	-	3.70	5.6	120	0.31	0.95	16.0	3.9	54	240	5.6	30.2	57.0	23.0	4.40	0.98	4.2	0.4
689	1.6	-	4.20	5.3	142	0.25	1.11	18.2	4.6	43	180	3.7	32.0	61.8	23.2	4.24	0.85	4.8	0.4
600	11.1	10	2.46	4.7	84	0.20	0.71	10.9	2.4	77	270	13.2	28.6	56.1	26.1	5.33	1.25	3.1	0.6
692	0.2	1	5.63	4.0	179	0.36	1.29	23.8	5.8	28	110	2.4	32.2	60.7	20.7	3.68	0.53	4.9	0.3
580	9.8	21	5.33	4.8	87	0.55	0.55	11.0	2.8	59	209	9.9	21.3	42.5	18.7	3.92	0.95	4.3	0.4
723	2.2	1	1.96	8.6	133	0.47	0.95	15.9	4.0	35	348	6.1	32.0	66.3	30.7	6.91	1.04	-	0.9
267	35.5	78	0.67	2.6	22	0.22	0.28	2.8	0.5	88	85	22.8	13.5	28.9	15.7	3.72	1.08	-	0.5
319	27.8	58	0.53	3.3	30	-	0.28	3.6	-	-	-	22.3	17.1	39.5	20.9	4.44	1.29	-	0.5
710	2.6	-	2.40	8.1	176	0.24	1.13	19.9	2.7	35	276	5.2	32.2	64.0	28.8	6.30	1.16	5.2	0.6
696	7.3	3	4.00	6.0	89	0.22	0.74	10.6	2.4	74	203	9.5	30.1	59.7	25.8	5.59	1.26	-	0.7
690	1.3	-	7.31	7.8	168	0.32	1.19	18.6	4.6	46	280	6.0	38.1	73.9	32.4	7.34	1.16	5.9	0.9
309	29.5	92	0.93	3.0	30	-	0.29	3.2	-	-	-	20.2	16.3	38.4	21.4	4.45	1.35	-	0.5
367	22.9	39	0.77	3.1	30	0.21	0.41	3.9	0.9	76	107	20.4	17.6	36.3	18.4	4.25	1.20	-	0.5
210	40.4	655	0.63	1.8	14	-	0.20	1.7	-	-	-	28.3	9.2	21.8	12.9	2.82	0.88	-	0.4
323	29.7	41	0.59	2.7	19	-	0.18	3.4	-	-	-	24.5	14.0	33.1	18.5	3.75	1.18	-	0.4
66	0.2	-	9.30	3.8	315	-	1.58	39.2	-	-	-	1.7	31.4	65.9	22.2	3.84	0.24	-	0.4
264	27.0	53	0.63	2.2	26	-	0.15	4.0	-	-	-	28.4	10.3	25.7	14.0	3.25	1.04	-	0.4
264	27.6	67	0.85	3.6	22	-	0.41	3.7	-	-	-	24.2	22.1	51.2	25.7	5.33	1.47	-	0.7
356	33.6	173	0.71	2.7	23	-	0.25	2.7	-	-	-	26.7	15.1	36.8	19.7	4.04	1.30	-	0.5
309	21.8	26	2.30	2.5	27	-	0.19	3.9	-	-	-	26.1	12.8	30.5	17.5	4.01	1.21	-	0.4
395	31.4	113	0.24	2.9	33	-	0.30	2.6	-	-	-	21.2	15.2	37.8	20.0	4.22	1.21	-	0.6
198	20.6	36	0.52	3.3	14	-	0.22	4.2	-	-	-	22.0	15.1	35.8	19.9	4.09	1.24	-	0.5
305	30.5	106	1.14	2.8	44	-	0.31	6.7	-	-	-	27.1	13.5	29.8	15.3	3.61	1.14	-	0.5
415	26.2	90	1.20	4.4	35	-	0.61	4.9	-	-	-	19.1	23.6	55.1	27.8	5.87	1.56	-	0.6
230	37.1	36	0.28	2.0	13	-	0.23	1.6	-	-	-	26.4	10.5	25.3	14.6	3.47	1.09		0.4
679	1.1	2	5.12	4.7	169	-	1.17	20.9	5.3	35	147	3.1	30.2	57.0	19.9	3.71	0.67	3.0	0.4
495	16.3	30	1.76	4.2	60	0.27	0.58	7.2	1.6	77	185	16.7	24.0	49.7	27.9	5.04	1.27	4.5	0.6

1 samples analyzed at Massachusetts Institute of Technology under supervision of F.A. Frey.
ological Survey, Reston, Virginia, under supervision of C.A. Palmer and G.A. Wandless.
icussed by López-Escobar *et al.* (1981) and Baedecker and McKown (1987).
samples analyzed at MIT were reported by Frey *et al.* (1984); in our stratigraphic framework, they are as follows: LM-1 = unit **mlc**; LM-4, 5, 6, 7, 8 all = unit **msm**; L
= unit **meb**; FM-67a = unit **rpp**; FM-78 = unit **rcb**; FM-94 = unit **bec**; and FM-205 = unit **rdno**.